Non-local conservation laws for traffic flow modeling

Felisia Angela Chiarello

UNIVERSITÉ CÔTE D'AZUR

ÉCOLE DOCTORALE
SCIENCES FONDAMENTALES ET APPLIQUÉES

THÈSE DE DOCTORAT

Lois de conservation avec flux non-local pour la modélisation du trafic routier

Non-local conservation laws for traffic flow modeling

Felisia Angela CHIARELLO

LJAD- Inria ACUMES Project-Team

Présentée en vue de l'obtention du grade de docteur en Mathématiques **d'Université Côte d'Azur**

Dirigée par : Paola GOATIN

Soutenue le : 6 Décembre 2019

Devant le jury, composé de :

Raimund Bürger, Pr, UdeC
Christophe Chalons, Pr, UVSQ
Giuseppe M. Coclite, Pr, Politecnico di Bari
Paola Goatin, Dr, Inria Acumes EPI
Simone Göttlich, Pr, Universität Mannheim
Christian Rohde, Pr, Universität Stuttgart

Inria

Lois de conservation avec flux non-local pour la modélisation du trafic routier

Non-local conservation laws for traffic flow modeling

Jury :

Président du jury
Christophe Chalons, Pr, Université de Versailles Saint-Quentin-en-Yvelines

Rapporteurs
Raimund Bürger, Pr, Universidad de Concepción
Giuseppe Maria Coclite, Pr, Politecnico di Bari
Christian Rohde, Pr, Stuttgart Universität

Examinateurs
Paola Goatin, Dr, Inria Sophia Antipolis-Méditerranée
Simone Göttlich, Pr, Mannheim Universität

To my future husband Giovanni,
to my parents Cosimo and Maria,
to my grandfather Giuseppe.

Acknowledgments

I would like to thank my supervisor, Paola Goatin, because she drove me with enthusiasm and dedication in this journey. She allowed me to discover and appreciate the profession of researcher, contributing to my scientific and human growth. I show my gratitude to Raimund Bürger, Giuseppe Maria Coclite and Christian Rohde for accepting to be the reviewers of this manuscript. I thank Christophe Chalons and Simone Göttlich to be part of the jury. I am also grateful to all the Acumes team at Inria. They have been my family during these years. I am grateful to Luis Miguel Villada and Jan Friedrich for the nice scientific collaborations. A very special gratitude goes out to my parents, Cosimo and Maria. They have provided me through moral and emotional support in my life. They taught me the true love. And finally, I wish to give my heartfelt thanks to my future husband, Giovanni, whose unconditional love, patience, and continual support of my academic endeavours enabled me to complete this thesis. He has made my life so much better.

I would like to dedicate this work to Giovanni, my parents and my late grandfather, Giuseppe.

Lois de conservation avec flux non-local pour la modélisation du trafic routier

Résumé: Le but principal de cette thèse est de fournir des modèles mathématiques de trafic routier avec flux non-locaux, et des schémas numériques adaptés pour analyser numériquement ce type de modèles. D'abord, nous considérons une classe d'équations scalaires, où le support du noyau de convolution est proportionnel à la distance d'anticipation des conducteurs. Nous prouvons la stabilité des solutions par rapport aux données initiales et en déduisons l'existence par un argument d'approximation basé sur un schéma de type Lax-Friedrichs. Nous fournissons également la première preuve de convergence quand le support du noyau tend vers $+\infty$, ainsi que quelques simulations numériques. Ensuite, nous nous concentrons sur une classe spécifique d'équations scalaires, en considérant des noyaux reguliers. Le but est l'étude de problèmes d'optimisation concernant la gestion du trafic et, pour cette raison, nous sommes intéressés par l'étude de la dépendance des solutions en fonction du noyau de convolution et de la vitesse. En appliquant soigneusement la technique de doublement des variables de Kružkov, nous dérivons la dépendance $\mathbf{L^1}$ -Lipschitz des solutions par rapport à la donnée initiale, au noyau et á la vélocité. Nous montrons des simulations numériques illustrant le comportement des solutions d'un modèle non-local de trafic, lorsque la taille et la position du support du noyau ou la vélocité varient. En outre, nous considérons une classe de systèmes de M lois de conservation non-locales dans une dimension d'espace. Nous considérons un noyau anisotrope différent pour chaque équation du système. Le modèle prend en compte la distribution de conducteurs et de véhicules hétérogènes caractérisés par leurs vitesses maximales et leur horizon de vue dans un flux de trafic. Nous prouvons des estimations $\mathbf{L}^\infty$ et BV uniformes sur les solutions approchées obtenues par un schéma numérique de type Godunov et nous montrons l'existence en temps petits de solutions faibles. Nous présentons également quelques simulations numériques pour $M = 2$. En particulier, nous considérons le cas d'un flux mixte de voitures et de poids lourds sur un tronçon de route et d'un flux de véhicules mixtes autonomes et non autonomes sur une route circulaire. L'approximation numérique des solutions de ce modèle est difficile en raison de la grande non-linéarité du système et de la dépendance de la fonction flux du terme de convolution. Nous présentons une généralisation des schémas de Lagrangian-Antidiffusive Remap (L-AR). Nous derivons certaines propriétés des schémas dans les cas scalaires et multi-classe. Dans le cas scalaire, nous obtenons des estimations uniformes $\mathbf{L}^\infty$ et BV sur les solutions approchées calculées à l'aide des schémas L-AR afin de prouver l'existence de solutions faibles. Nous introduisons une version du second ordre d'un schéma numérique de type Godunov et nous présentons quelques simulations numériques, en analysant l'erreur $\mathbf{L^1}$ des solutions approchées calculées avec différents schémas. Nous proposons aussi un schéma WENO (FV-WENO) aux volumes finis d'ordre élevé pour résoudre le système multi-classe non-local.
Enfin, nous proposons un modèle scalaire unidimensionnel pour une jonction de deux routes. Ce modèle est basé sur la vitesse moyenne non-locale en aval. Il est destiné à décrire le comportement des conducteurs sur deux segments de route qui diffèrent par leur loi de vitesse et leur densité maximale autorisée. Nous approchons la solution en utilisant un schéma upwind adapté. En dérivant plusieurs propriétés du schéma, nous sommes en mesure de prouver le

caractére bien posé du modèle.

Mots clés: lois de conservation non-locales, schémas de volumes finis, modèles de trafic macroscopiques.

Non-local conservation laws for traffic flow modeling

Abstract: In this thesis, we provide mathematical traffic flow models with non-local fluxes and adapted numerical schemes to compute approximate solutions to such kind of equations. More precisely, we consider flux functions depending on an integral evaluation of the conserved variables through a convolution product. First of all, we prove the well-posedness of entropy weak solutions for a class of scalar conservation laws with non-local flux arising in traffic modeling. This model is intended to describe the reaction of drivers that adapt their velocity with respect to what happens in front of them. Here, the support of the convolution kernel is proportional to the look-ahead distance of drivers. We approximate the problem by a Lax-Friedrichs scheme and we provide some estimates for the sequence of approximate solutions. Stability with respect to the initial data is obtained through the doubling of variable technique. We study also the limit model as the kernel support tends to infinity. After that, we prove the stability of entropy weak solutions of a class of scalar conservation laws with non-local flux under higher regularity assumptions. We obtain an estimate of the dependence of the solution with respect to the kernel function, the speed and the initial datum. We also prove the existence for small times of weak solutions for non-local systems in one space dimension, given by a non-local multi-class model intended to describe the behaviour of different groups of drivers or vehicles. We approximate the problem by a Godunov-type numerical scheme and we provide uniform $\mathbf{L}^\infty$ and BV estimates for the sequence of approximate solutions, locally in time. We present some numerical simulations illustrating the behavior of different classes of vehicles and we analyze two cost functionals measuring the dependence of congestion on traffic composition. Furthermore, we propose alternative simple schemes to numerically integrate non-local multi-class systems in one space dimension. We obtain these schemes by splitting the non-local conservation laws into two different equations, namely, the Lagrangian and the remap steps. We provide some estimates recovered by approximating the problem with the Lagrangian-Antidiffusive Remap (L-AR) schemes, and we prove the convergence to weak solutions in the scalar case. We show some numerical simulations illustrating the efficiency of the L-AR schemes in comparison with classical first and second order numerical schemes. Moreover, we recover the numerical approximation of the non-local multi-class traffic flow model proposed, presenting the multi-class version of the Finite Volume WENO (FV-WENO) schemes, in order to obtain higher order of accuracy. Simulations using FV-WENO schemes for a multi-class model for autonomous and human-driven traffic flow are presented. Finally, we introduce a traffic model for a class of non-local conservation laws at road junctions. Instead of a single velocity function for the whole road, we consider two different road segments, which may differ for their speed law and number of lanes. We use an upwind type numerical scheme to construct a sequence of approximate solutions and we provide uniform $\mathbf{L}^\infty$ and BV estimates. Using a Lax-Wendroff type argument, we prove the well-posedness of the proposed model. Some numerical simulations are compared with the corresponding (discontinuous) local model.

Keywords: non-local conservation laws, finite-volume schemes, macroscopic traffic models.

Contents

List of Figures

List of Tables

Introduction

The aim of this thesis is to study mathematical traffic flow models with non-local fluxes and to provide adapted numerical schemes to compute approximate solutions of these models. The general form of non-local conservation laws considered here is

$$\partial_t u + \operatorname{div}_x F(t, x, u, \omega * u) = 0,$$

with $t \in \mathbb{R}^+$, $x \in \mathbb{R}^d$, $u(t,x) \in \mathbb{R}^N$, $\omega(t,x) \in \mathbb{R}^{m \times N}$. The term "non-local" refers to the dependence of the flux function F on the convolution term $\omega * u$, where ω is a properly chosen matrix of kernel functions and u is the vector of conserved quantities. It is worth noticing that conservation laws with non-local flux received growing attention in the recent years because they are suitable to describe several phenomena arising in many fields of application, for example: sedimentation [10], conveyor belts [51], granular flows [3], crowd dynamics [32], supply chains [31], gradient constraint [4], etc. In this thesis we will consider the application of this class of equations to traffic flow models.
Macroscopic traffic flow models based on fluid-dynamics equations have been introduced in transport literature since the mid-fifties of last century, with the Lighthill, Whitham and Richards (LWR) model [65, 67]. The LWR model consists in one scalar equation that expresses the conservation of cars:

$$\partial_t \rho + \partial_x (\rho\, v(\rho)) = 0,$$

with $\rho = \rho(t,x)$ representing the mean traffic density, i.e. the number of vehicles per unit length and v denoting the mean velocity. Since then, several approaches have been developed during the years, addressing the need for more sophisticated models better describing traffic flow. Indeed, traffic is not so easy to simulate due to the formation of traffic jams. In particular, the classical LWR model is based on the assumption that the mean traffic velocity is a function of the traffic density, which is not realistic in congested regimes because it does not match the experimental data. In order to overcome these drawbacks, researchers have started studying the so-called "second order" models, considering the two quantities as independent, consisting in a mass conservation equation for the density and an acceleration balance law for the speed, see the Payne-Whitham [66, 75] and the Aw-Rascle-Zhang [7, 76] models. Recently, "non-local" versions of the LWR model have been proposed in [11, 72]. In this type of models, the speed is assumed to depend on a weighted mean of the downstream traffic density. As a consequence, the speed becomes a Lipschitz function with respect to space and time variables, ensuring bounded acceleration and overcoming the limitations of classical macroscopic models that allows for speed discontinuities. Non-local traffic models are intended to describe the behaviour of drivers that adapt their velocity with respect to what happens in front of them. For this reason, the flux function depends on a "downstream" convolution term between the density of vehicles and a kernel function supported on the negative axis. The last assumption expresses the fact that drivers only look forward, not backward. As in classical (local) models, the speed is a monotone non-increasing function, because the higher the density of cars on a road, the lower their speed.

There are general existence and uniqueness results for non-local equations in [5, 55] for scalar equations in one-space dimension, in [31, 57] for multi-dimensional scalar equations, and in [2] for the multi-dimensional system case. There are mainly two different approaches to prove the existence of solutions for these non-local models. One is providing suitable compactness estimates on a sequence of approximate solutions constructed through finite volume schemes, as in [5, 2]. Another approach relies on characteristics and fixed-point theorems, as proposed in [55, 57]. In [5], Kružkov-type entropy conditions are used to prove the $\mathbf{L^1}-$stability with respect to the initial data through the doubling of variable technique, while in [55, 57], the uniqueness of weak solutions is obtained directly from the fixed point theorem, without prescribing any kind of entropy condition.

The numerical approximation of the solutions of non-local models is challenging due to the high non-linearity of the system and the dependence of the flux function on convolution terms, which highly impacts the computational cost. There are different ways to numerically integrate non-local conservation laws. In [2, 5, 10, 11, 49] a first order Lax-Friedrichs-type numerical scheme is used to approximate the problem and to prove the existence of solutions. Indeed, in this setting, the numerical scheme is not just a tool for numerically investigating the behaviour of solutions, but it is important from the analytical point of view, because it allows to construct a sequence of approximate solutions in order to apply an adapted version of Helly's theorem, see [44]. Another first order numerical scheme is proposed in [46], where a Godunov-type numerical scheme for a specific class of non-local flux problems is presented. This scheme allows for physically reasonable solutions, meaning that negative velocities as well as negative fluxes are avoided. Moreover, in comparison with Lax-Friedrichs scheme, Godunov scheme is less diffusive. Concerning high-order numerical schemes, it is worth citing the papers [19, 45]. In [19], the authors propose discontinuous Galerkin and finite volume WENO schemes to obtain high-order approximations of non-local scalar conservation laws in one space dimension, where the velocity function depends on a weighted mean of the conserved quantity. The discontinuos Galerkin schemes give the best results, but under a very restrictive Courant-Friedrichs-Lewy (CFL) condition. On the contrary, finite volume WENO schemes can be implemented on larger time steps. In [45], central WENO schemes are proposed, which, in contrast to the other high-order schemes for non-local conservation laws, neither require a restrictive CFL condition nor an additional reconstruction step.

Non-local equations are used to model various physical phenomena and sometimes those models might be defined in a bounded domain. The main difficulty lies in the fact that the non-local operator may need to evaluate the unknown outside the boundaries of the spatial domain, where it is not defined. The Initial boundary value problem for one-dimensional scalar non-local conservation laws has been studied in [40, 47, 58], and in [38] for multiD non-local systems. In [40], the solution is set outside the domain constantly equal to the corresponding boundary condition values, instead in [58] a kind of right-hand-side boundary datum is considered, which represents the external impact on the outflow. In [38, 47], the non-local operator is modified to take into account the presence of boundaries. In the one-

dimensional scalar case, the usual convolution product is replaced by

$$\mathcal{I}(\rho(t))(x) = \frac{1}{z(x)} \int_a^b \rho(t,y)\omega(y-x)dy,$$
$$z(x) = \int_a^b \omega(y-x)dy,$$

where ω is the kernel function and $]a,b[\subset \mathbb{R}$ is the open bounded interval considered, see [47].

Another interesting point regarding non-local conservation laws is the singular local limit, which is defined as follows. In the multi-dimensional scalar case, a parameter $\eta > 0$ related to the support of the kernel is fixed and the re-scaled kernel function is considered

$$\omega_\eta(x) = \frac{1}{\eta^d}\omega\left(\frac{x}{\eta}\right).$$

Owing to the assumption $\int_{\mathbb{R}^d} \omega_\eta(x)dx = 1$, when $\eta \to 0^+$ the family ω_η converges weakly* in the sense of measures to the Dirac delta and we formally obtain the corresponding local conservation law:

$$\textbf{Non-local:} \begin{cases} \partial_t u_\eta + \operatorname{div}\left(u_\eta v(u_\eta * \omega_\eta)\right) = 0, \\ u_\eta(0,x) = \bar{u}(x), \end{cases} \to \textbf{Local:} \begin{cases} \partial_t u + \operatorname{div}\left(uv(u)\right) = 0, \\ u(0,x) = \bar{u}(x), \end{cases}$$

with $v : \mathbb{R} \to \mathbb{R}^d$ a Lipschitz continuous vector-valued function. The above derivation is just formal and it has to be rigorously justified. The question is whether the solution u_η of the non-local Cauchy problem converges to the entropy admissible solution of the local Cauchy problem in some suitable topology. The rigorous derivation of this limit was initially posed in [5] for the one-dimensional scalar case motivated by numerical evidence, later corroborated in [11]. The answer is positive if we consider an even kernel function and a smooth compactly supported initial datum, as proved in [77]. The solution of one-dimensional scalar non-local conservation laws converges to the entropy solution of the corresponding local conservation laws also in the case of monotone initial data, see [56]. Nevertheless, in general, the solution of the non-local Cauchy problem does not converge to the solution of the local one and in [27] the authors show three counterexamples in this sense, while in [26], the role of numerical viscosity in the numerical investigation of such non-local-to-local limit is highlighted.

Finally, it is worth citing the papers [68, 69] for the analysis of traveling wave profiles for conservation laws with non-local flux in both the microscopic and the macroscopic case. In [68], the authors consider a constant road condition $k(x) := 1$, which denotes the speed limit of the road at point x. They derive delay differential equations satisfied by the profiles for the microscopic Follow-the-Leader models, and delay integro-differential equations for the traveling waves of the non-local PDE models, and they prove the existence and uniqueness of the stationary wave profiles. In [69], the author considers a piecewise constant road condition

$$k(x) := \begin{cases} k^-, & x < 0, \\ k^+, & x > 0, \end{cases}$$

and stationary traveling wave profiles crossing $x = 0$ are analyzed, depending on the cases $k^- > k^+$ and $k^- < k^+$. The author proves that there could be infinitely many profiles, a unique profile or no profiles at all.

Available non-local traffic models

Equations with non-local flux have been introduced in traffic flow modeling to account for the reaction of drivers or pedestrians to the surrounding density of other individuals [5, 28, 39, 72]. We give here a brief overview.

Non-local models for pedestrian traffic

In [28], the authors present a class of macroscopic models for crowd motion, in which each individual is assumed to move towards a fixed target, deviating from the desired path according to the instantaneous local crowd distribution. The equation reads

$$\partial_t \rho + \operatorname{div}\Big(\rho\, v(\rho)\,\big(\nu(x) + \mathcal{I}(\rho(t))(x)\big)\Big) = 0.$$

In this context, v is the pedestrians' speed and the vector $\nu(x)+\mathcal{I}(\rho(t))(x)$ describes the direction that the individual located at x follows. In particular, the vector $\mathcal{I}(\rho(t))(x)$ describes the deviation from the desired direction $\nu(x)$ due to the density distribution $\rho(t,\cdot)$. The operator $\mathcal{I}$ is non-local and $\mathcal{I}(\rho(t))(x)$ depends on the values of $\rho(t,\cdot)$ in a neighborhood of x. It is set as

$$\mathcal{I}(\rho(t)) = -\varepsilon \frac{\nabla(\rho * \omega)}{\sqrt{1 + \big\|\nabla(\rho * \omega)\big\|^2}},$$

where ω is a smooth kernel function. Numerical simulations show the phenomenon of pattern formation. Indeed, in the case of a crowd walking along a corridor, the solution self-organizes into lanes and the width of these lanes depends on the size of the support of the kernel function ω. The authors prove the existence of weak entropy solutions for this model and stability results. In particular, the present model accounts for the possibility of reducing the exit time from a room by carefully positioning obstacles that direct the crowd flow. A very similar model is introduced in [51] for conveyor belts. Here, the authors start from a microscopic model which, through a phenomenological study, yields a macroscopic model.
In [31], the authors consider the following model

$$\partial_t \rho + \operatorname{div}\left(\rho v(\rho * \omega)\nu(x)\right) = 0,$$

where ω is a smooth kernel function and $\nu(x)$ is the pedestrians' direction. This model is based on the non-local dependence of the speed function v on the density. In [31], the authors prove the existence of weak solutions locally in time and the differentiability of solutions of this model with respect to the initial datum. In [32], the authors generalize the models in [28, 31] to the multi-populations case. In particular, they prove the global well-posedness for the model in [31] and they provide numerical simulations showing that the formation of lanes is present also in the multi-populations setting [28].

The Arrhenius model for vehicular traffic flow

In [72], the authors introduce a traffic flow model based on Arrhenius stochastic microscopic dynamics. Using scaling and limit arguments they obtain a macroscopic description of the microscopic dynamics leading to higher-order dispersive partial differential equations. The dynamics includes interactions with other vehicles ahead. The non-local traffic flow model that derives from this stochastic process is

$$\partial_t \rho + \partial_x(\rho(1-\rho)\exp(-\omega_\eta * \rho)) = 0,$$

where the kernel acts only on the space variable x in this way

$$\omega_\eta * \rho(t,x) = \int_x^{x+\eta} \frac{J_0}{\eta}\rho(t,y)dy.$$

The kernel ω_η is an anisotropic short range inter-vehicle interaction potential, η is proportional to the look-ahead distance and J_0 is the interaction strength. In [64], the authors study the local classical solutions and show that the finite time blowup of solutions must occur at the level of the first order derivative of the solution. Indeed, for several types of physical initial data one has at some finite time $0 < T < +\infty$

$$\limsup_{t\to T} \left\|\partial_x \rho(t,\cdot)\right\|_\infty = +\infty$$

where ρ is the classical maximal-lifespan solution.

The Blandin-Goatin model for vehicular traffic flow

While pedestrians are likely to react to the presence of people all around them, drivers mostly adapt their velocity to the downstream traffic, assigning a greater importance to closer vehicles. In [11, 49], the authors consider the following mass conservation equation for traffic flow with non-local velocity depending on a mean downstream density:

$$\partial_t \rho(t,x) + \partial_x \left(\rho(t,x) v\left(\int_x^{x+\eta} \rho(t,y)\omega_\eta(y-x)dy\right)\right) = 0,$$

for $t \in \mathbb{R}^+$ and $x \in \mathbb{R}$, $\eta > 0$. The kernel function $\omega_\eta \in \mathbf{C^1}([0,\eta];\mathbb{R}^+)$ is non-increasing and the support η is proportional to the look-ahead visibility. The mean speed function v is continuous and decreasing. Considering BV initial data, the authors prove the well-posedness of entropy weak solutions for the corresponding Cauchy problem providing accurate $\mathbf{L^\infty}$, BV and $\mathbf{L^1}$ estimates on the sequence of approximate solutions constructed by an adapted Lax-Friedrichs scheme. In [9], the authors also study the regularity results for the solutions of this non-local model proving Sobolev estimates and the convergence of approximate solutions solving a viscous non-local equation. The Blandin-Goatin model belongs to the class of equations considered in [55].

The Friedrich-Kolb-Göttlich model for vehicular traffic flow

In [46], the authors propose a general non-local vehicular traffic flow model based on a mean downstream traffic velocity. This is the main difference with the models in [11, 21], where drivers adapt their velocity with respect to a mean downstream traffic density. The Friedrich-Kolb-Göttlich model reads

$$\partial_t \rho + \partial_x (g(\rho)(\omega_\eta * v(\rho))) = 0,$$

with

$$\omega_\eta * v(\rho)(t,x) := \int_x^{x+\eta} v(\rho(t,y))\omega_\eta(y-x)dy, \quad \eta > 0 \text{ and } g \in C^1([0,\rho_{max}],\mathbb{R}), \quad g' \geq 0.$$

The authors prove the well-posedness of entropy weak solutions approximating the problem through a Godunov-type numerical scheme and providing suitable estimates on the sequence of approximate solutions. Moreover, they show the better accuracy of the Godunov-type scheme in comparison to the Lax-Friedrichs scheme by a variety of numerical examples. If the velocity function v is linear, the Friedrich-Kolb-Göttlich model coincides with the one in [11, 21, 49].

Contribution and Structure of the thesis

- In Chapter 1, we consider a class of scalar equations that includes some vehicular traffic flow models [11, 49, 64, 72], where the support of the kernel function is proportional to the look-ahead distance of drivers. Unlike similar non-local equations [5, 10, 28, 33, 35, 51, 77], these models are characterized by the presence of an anisotropic discontinuous kernel, which makes general theoretical results [2, 5, 10] inapplicable as such. We prove the stability of solutions with respect to the initial data, based on a doubling of variable argument [59], and we derive the existence of solutions through an approximation argument based on a Lax-Friedrichs type scheme. In particular, we prove accurate $\mathbf{L}^\infty$ and BV estimates on the approximate solutions. Regarding the Arrhenius look-ahead model [72], our result allows to establish a global well-posedness result and more accurate $\mathbf{L}^\infty$ estimates with respect to previous studies [64]. We also provide the first convergence proof of a limiting procedure as the look-ahead distance tends to $+\infty$, and some numerical simulations.

- In Chapter 2, we focus on a specific class of scalar non-local equations, considering smooth kernel functions. Existence and uniqueness of solutions follows from [5], as well as some *a priori* estimates, namely $\mathbf{L^1}$, $\mathbf{L}^\infty$ and total variation estimates. The aim is the study of optimization problems concerning traffic management. For this reason, we are interested in analysing the dependence of solutions on the convolution kernel and on the velocity function. While controlling the speed may seem more straightforward, varying the interaction kernel could be of interest in applications to connected autonomous vehicles. Estimates of the dependence of solutions of a general balance law on the flux function can be found in [34, 62]. However, those estimates turn out to be implicit when applied to our setting. Carefully applying the Kružkov's doubling of variables technique, on the lines of [10, 52], we derive the $\mathbf{L^1}$-Lipschitz continuous dependence of solutions on the initial datum, the kernel and the velocity. We show some numerical simulations

illustrating the behaviour of the solutions of a non-local traffic flow model, when the size and the position of the kernel support or the velocity function vary. In particular, we analyze the impact on two cost functionals, measuring traffic congestion.

- In Chapter 3, we consider a system of M non-local conservation laws in one space dimension, given by a non-local multi-class model obtained as a generalization of the M-populations model for traffic flow described in [8]. This is a multi-class version of the one dimensional scalar conservation law with non-local flux proposed in [11]. We allow different anisotropic kernels for each equation of the system. The model takes into account the distribution of heterogeneous drivers and vehicles characterized by their maximal speeds and look-ahead visibility in a traffic stream. The main result of this chapter is the existence of weak solutions locally in time. We remark that, since the convolution kernels are not smooth on $\mathbb{R}$, the results in [2] cannot be applied due to the lack of $\mathbf{L}^\infty$-bounds on their derivatives. We do not address the question of uniqueness of solutions. Indeed, even if discrete entropy inequalities can be derived as in [11, Proposition 3], in the case of systems this is in general not sufficient to single out a unique solution. We prove uniform $\mathbf{L}^\infty$ and BV estimates on the approximate solutions obtained through an approximation argument based on a Godunov-type numerical scheme, see [46], and we prove the existence for small time of weak solutions applying Helly's theorem and a Lax-Wendroff type argument, see [63]. We also present some numerical simulations for $M = 2$. In particular, we consider the case of a mixed flow of cars and trucks on a stretch of road, and the flow of mixed autonomous and non-autonomous vehicles on a circular road.

- In Chapter 4, we study the computation of numerical solutions for the multi-class model proposed in Chapter 3. In [22, 21], the authors proposed first-order schemes, however it is well known that these schemes are very diffusive. In the scalar case, high-order Discontinuous Galerkin and Finite-Volume WENO schemes were constructed in [19]. In this chapter, we present a generalization of the Lagrangian-Antidiffusive Remap (L-AR) schemes introduced in [15, 16] and a Finite-Volume WENO scheme, in order to compute approximate solutions of the non-local multi-class model proposed in [22]. In [15], one step L-AR schemes were applied to (local) multi-class traffic models and in [16] these schemes were extended to polydisperse sedimentation models. L-AR schemes do not rely on spectral (characteristics) information and their implementation is as easy as that one of first- and second-order of accuracy schemes introduced in [17]. Nevertheless, the L-AR are more accurate and efficient. We recover some properties of the schemes in both the scalar and the multi-class cases. In the scalar case, we obtain uniform $\mathbf{L}^\infty$ and BV estimates on the approximate solutions computed through the L-AR schemes, which give an alternative proof of existence of weak solutions. We show a second-order version of a Godunov-type numerical scheme and we present some numerical simulations, analyzing the $\mathbf{L^1}$-error of the approximate solutions computed with different schemes and considering smooth and discontinuous initial data. Finally, we propose a high-order Finite-Volume WENO (FV-WENO) scheme to solve the non-local multi-class system. The procedure proposed in [19] is used and extended to the multi-class case in order to evaluate the non-local term that appears in the flux functions.

- In Chapter 5, we propose a one-dimensional scalar model for a 1-to-1 junction. This model is based on the non-local mean downstream velocity as the model [46], and it is intended to describe the behavior of drivers on two road segments that differ for their speed law and capacity. This model can be seen as a first step towards a non-local network formulation. We approximate the solution using an upwind type scheme. Deriving several properties of the scheme, such as the maximum principle and uniform total variation (BV) estimates, and relying on a Kružkov type entropy condition, we are able to prove the well-posedness of the model. In particular, we prove the Lipschitz continuous dependence of weak entropy solutions with respect to the initial data, which implies their uniqueness. Since it is still an open question whether the solution of the non-local model tends to the solution of the corresponding local equation when the support of the kernel function tends to zero, see the introduction of this thesis for an overview, we investigate this issue from the numerical point of view. We show numerical simulations fixing the support of the kernel function and we present some results regarding the limit model as the support tends to zero.

Publications

During the Ph.D. course the following articles have been published or submitted to journals.

Articles in Journals

- F. A. Chiarello, P. Goatin. Global entropy weak solutions for general non-local traffic flow models with anisotropic kernel. *ESAIM: M2AN*, Volume 52, Number 1, January-February 2018.
- F. A. Chiarello, P. Goatin, E. Rossi. Stability estimates for non-local scalar conservation laws. *Nonlinear Analysis Series B: Real World Applications*, Volume 45, 668-687, 2019.
- F. A. Chiarello, P. Goatin. Non-local multi-class traffic flow models. *Networks & Heterogeneous Media*, 14(2): 371-387, June 2019.
- F. A. Chiarello, P. Goatin, L. M. Villada. Lagrangian-Antidiffusive Remap schemes for non-local multi-class traffic flow models. *Computational and Applied Mathematics*, 2020.
- F. A. Chiarello, J. Friedrich, P. Goatin, S. Göttlich, O. Kolb. A non-local traffic flow model for 1-to-1 junctions. *European Journal of Applied Mathematics*, 1-21, 2019.

Conference Proceedings

- F. A. Chiarello, P. Goatin, L. M. Villada. High-order Finite Volume WENO schemes for non-local multi-class traffic flow models. Proceedings HYP conference 2018.
- F. A. Chiarello. Non-local traffic flow models. *Oberwolfach Rep. No. 24/2019,* DOI: 10.4171/OWR/2019/24, 2019.

Meetings, Conferences and Schools

During the Ph.D. course the following conferences, workshops and schools have been attended.

With Talk or Poster presentation

- *EDP e dintorni, III Meeting around PDE.*
  Department of Mathematics, Università degli Studi di Bari (Italy), December 18, 2017.
  Talk's title: *Global entropy weak solutions for general non-local traffic flow models with anisotropic kernel.*

- *Le Monde des Mathématiques Industrielles (MOMI2018).*
  Inria Sophia Antipolis (France), February 26-27, 2018.
  Poster's title: *Non-local traffic flow models.*

- *XVII International Conference on Hyperbolic Problem Theory, Numerics, Applications.*
  University Park, Pennsylvania (USA), June 25-29, 2018.
  Talk's title: *General non-local traffic flow models.*

- *Interactive workshop on hyperbolic equations.*
  Università degli Studi di Ferrara (Italy), September 10-12, 2018.
  Talk's title: *Non-local multi-class traffic flow models.*

- *Nonlinear Hyperbolic Problems: modeling, analysis, and numerics.*
  MFO Oberwolfach (Germany), May 19-25, 2019.
  Talk's title: *Non-local traffic flow models.*

- *9th International Congress on Industrial and Applied Mathematics (ICIAM 2019).*
  Valencia (Spain), July 15-19, 2019.
  Talk's title: *Non-local vehicular traffic flow models.*

Without Talk

- *The Finite volumes schemes and traffic modeling in Besançon.*
  Besançon (France), November 22-23, 2017.

- *Le Monde des Mathématiques Industrielles (MOMI2019).*
  Inria Sophia Antipolis (France), February 25-26, 2019.

Schools

- *Summer school on DDM.*
  Laboratoire Dieudonné, Nice (France), June 19-21, 2018.

- *Fall school: Hyperbolic Conservation Laws and Mathematical Fluid Dynamics.*
  Würzburg (Germany), October 1-5, 2018.
  Poster's title: *Non-local multi-class traffic flow models.*

Chapter 1

Global entropy weak solutions for general non-local traffic flow models with anisotropic kernel

This chapter is devoted to present the results obtained in [21].

1.1 Modeling

We consider the following scalar conservation law with non-local flux

$$\partial_t \rho + \partial_x \left(f(\rho) v(\omega_\eta * \rho) \right) = 0, \qquad x \in \mathbb{R},\ t > 0, \tag{1.1.1}$$

where

$$\omega_\eta * \rho(t,x) := \int_x^{x+\eta} \omega_\eta(y-x)\rho(t,y)dy, \qquad \eta > 0. \tag{1.1.2}$$

In (1.1.1), (1.1.2), we assume the following hypotheses:

$$\textbf{(H)} \quad \begin{array}{ll} f \in \mathbf{C^1}(I;\mathbb{R}^+), & I = [a,b] \subseteq \mathbb{R}^+, \\ v \in \mathbf{C^2}(I;\mathbb{R}^+) \text{ s.t.} & v' \leq 0, \\ \omega_\eta \in \mathbf{C^1}([0,\eta];\mathbb{R}^+) \text{ s.t.} & \omega_\eta' \leq 0 \\ \int_0^\eta \omega_\eta(x)dx := J_0,\ \forall \eta > 0, & \lim\limits_{\eta \to \infty} \omega_\eta(0) = 0. \end{array}$$

This class of equations includes in particular some vehicular traffic flow models [11, 49, 64, 72], where $\eta > 0$ is proportional to the look-ahead distance and the integral J_0 is the interaction strength (here assumed to be independent of η). In this setting, the non-local dependence of the speed function v can be interpreted as the reaction of drivers to a weighted mean of the downstream traffic density. The specific monotonicity assumptions on the speed function v and the kernel ω_η ensure nice properties of the corresponding solutions, such as a strong maximum principle (both from below and above) and the absence of unphysical oscillations due to a sort of monotonicity preservation, which make the choice (1.1.2) interesting and justified from the modeling perspective.

Adding an initial condition

$$\rho(0,x) = \rho_0(x), \qquad x \in \mathbb{R}, \tag{1.1.3}$$

with $\rho_0 \in \mathrm{BV}(\mathbb{R};I)$, entropy weak solutions of problem (1.1.1), (1.1.3), are intended the following sense [5, 10, 59].

Definition 1. *A function*

$$\rho \in (\mathbf{L^1} \cap \mathbf{L}^\infty \cap BV)(\mathbb{R}^+ \times \mathbb{R}; I)$$

is an entropy weak solution of (1.1.1), (1.1.3), *if*

$$\int_0^{+\infty} \int_{\mathbb{R}} \Big\{ |\rho - \kappa| \varphi_t + \operatorname{sgn}(\rho - \kappa)(f(\rho) - f(\kappa)) v(\omega_\eta * \rho) \varphi_x \\ - \operatorname{sgn}(\rho - \kappa) f(\kappa) v'(\omega_\eta * \rho) \partial_x(\omega_\eta * \rho) \varphi \Big\} dx dt + \int_{\mathbb{R}} |\rho_0(x) - \kappa| \varphi(0, x) dx \geq 0 \quad (1.1.4)$$

for all $\varphi \in \mathbf{C_c^1}(\mathbb{R}^2; \mathbb{R}^+)$ *and* $\kappa \in \mathbb{R}$.

Our aim is to prove the following results.

Theorem 1. *Let hypotheses* **(H)** *hold and* $\rho_0 \in BV(\mathbb{R}; I)$. *Then the Cauchy problem* (1.1.1), (1.1.3), *admits a unique weak entropy solution* ρ^η *in the sense of Definition 1, such that*

$$\min_{\mathbb{R}} \{\rho_0\} \leq \rho^\eta(t, x) \leq \max_{\mathbb{R}} \{\rho_0\}, \quad \text{for a.e. } x \in \mathbb{R},\ t > 0. \quad (1.1.5)$$

Moreover, for any $T > 0$ *and* $\tau > 0$, *the following estimates hold:*

$$TV(\rho^\eta(T, \cdot)) \leq e^{C(\omega_\eta)T} TV(\rho_0), \quad (1.1.6a)$$

$$\left\| \rho^\eta(T, \cdot) - \rho^\eta(T - \tau, \cdot) \right\|_{\mathbf{L^1}} \leq \tau e^{C(\omega_\eta)T} \left(\left\| f' \right\| \|v\| + J_0 \|f\| \left\| v' \right\| \right) TV(\rho_0), \quad (1.1.6b)$$

with $C(\omega_\eta) := \omega_\eta(0) \left(\left\| v' \right\| \left(\left\| f' \right\| \|\rho_0\| + 2\|f\| \right) + \frac{7}{2} J_0 \|f\| \left\| v'' \right\| \right)$.

Above, and in the sequel, we use the compact notation $\|\cdot\|$ for $\|\cdot\|_{\mathbf{L}^\infty}$.

Corollary 2. *Let hypotheses* **(H)** *hold and* $\rho_0 \in BV(\mathbb{R}; I)$. *As* $\eta \to \infty$, *the solution* ρ^η *of* (1.1.1), (1.1.3) *converges in the* $\mathbf{L^1_{loc}}$*-norm to the unique entropy weak solution of the classical Cauchy problem*

$$\begin{cases} \partial_t \rho + \partial_x \left(f(\rho) v(0) \right) = 0, & x \in \mathbb{R}, t > 0 \\ \rho(0, x) = \rho_0(x), & x \in \mathbb{R}. \end{cases} \quad (1.1.7)$$

In particular, we observe that $C(\omega_\eta) \to 0$ *in* (1.1.6a) *and* (1.1.6b), *allowing to recover the classical estimates.*

Section 1.2 is devoted to the proof of the stability of solutions with respect to the initial data, based on a doubling of variable argument [59].

In Section 1.3 we derive existence of solutions through an approximation argument based on a Lax-Friedrichs type scheme. In particular, we prove accurate $\mathbf{L}^\infty$ and BV estimates on the approximate solutions, which allow to derive (1.1.5) and (1.1.6). We remark once again that these estimates heavily rely on the monotonicity properties of ω_η, and do not hold for general kernels, see [5, 11]. To our knowledge, Corollary 2 provides the first convergence proof of a limiting procedure on the kernel support. Besides the mathematical implications of such result, Corollary 2 may give information on connected autonomous vehicle traffic flow characteristics. Indeed, large kernel supports could account for the information transmission range between connected vehicles. We present some numerical tests illustrating this convergence in Section 1.4.

1.2 Uniqueness and stability of entropy solutions

The Lipschitz continuous dependence of entropy solutions with respect to initial data can be derived using Kružkov's doubling of variable technique [59] as in [10, 11, 49].

Theorem 3. *Under hypotheses* **(H)**, *let* ρ, σ *be two entropy solutions to* (1.1.1) *with initial data* ρ_0, σ_0 *respectively. Then, for any* $T > 0$ *there holds*

$$\big\|\rho(t,\cdot) - \sigma(t,\cdot)\big\|_{\mathbf{L^1}} \leq e^{KT}\|\rho_0 - \sigma_0\|_{\mathbf{L^1}} \quad \forall t \in [0,T], \tag{1.2.1}$$

with K *given by* (1.2.5).

Proof. The functions ρ and σ are respectively entropy solutions of

$$\begin{aligned}
&\partial_t \rho(t,x) + \partial_x(f(\rho(t,x))V(t,x)) = 0, \quad V := v(\rho * \omega_\eta), \quad \rho(0,x) = \rho_0(x),\\
&\partial_t \sigma(t,x) + \partial_x(f(\sigma(t,x))U(t,x)) = 0, \quad U := v(\sigma * \omega_\eta), \quad \sigma(0,x) = \sigma_0(x).
\end{aligned}$$

V and U are bounded measurable functions and are Lipschitz continuous w.r. to x, since $\rho, \sigma \in (L^1 \cap L^\infty \cap \mathrm{BV})(\mathbb{R}^+ \times \mathbb{R}; \mathbb{R})$. In particular, we have

$$\|V_x\| \leq 2\omega_\eta(0)\big\|v'\big\|\|\rho\|, \quad \|U_x\| \leq 2\omega_\eta(0)\big\|v'\big\|\|\sigma\|.$$

Using the classical doubling of variables technique introduced by Kruzkov, we obtain the following inequality:

$$\begin{aligned}
\big\|\rho(T,\cdot) - \sigma(T,\cdot)\big\|_{\mathbf{L^1}} \leq{}& \|\rho_0 - \sigma_0\|_{\mathbf{L^1}}\\
&+ \big\|f'\big\| \int_0^T \int_{\mathbb{R}} \big|\rho_x(t,x)\big|\big|U(t,x) - V(t,x)\big| dxdt\\
&+ \int_0^T \int_{\mathbb{R}} \big|f(\rho(t,x))\big|\big|U_x(t,x) - V_x(t,x)\big| dxdt.
\end{aligned} \tag{1.2.2}$$

We observe that

$$\big|U(t,x) - V(t,x)\big| \leq \omega_\eta(0)\big\|v'\big\|\big\|\rho(t,\cdot) - \sigma(t,\cdot)\big\|_{\mathbf{L^1}}, \tag{1.2.3}$$

and that for a.e. $x \in \mathbb{R}$

$$\begin{aligned}
\big|U_x(t,x) - V_x(t,x)\big| \leq{}& \left(2(\omega_\eta(0))^2\big\|v''\big\|\big\|\rho(t,\cdot)\big\| + \big\|v'\big\|\big\|\omega_\eta'\big\|\right)\big\|\rho(t,\cdot) - \sigma(t,\cdot)\big\|_{\mathbf{L^1}}\\
&+ \omega_\eta(0)\big\|v'\big\|(|\rho - \sigma|(t,x+\eta) + |\rho - \sigma|(t,x).
\end{aligned} \tag{1.2.4}$$

Plugging (1.2.3) and (1.2.4) into (1.2.2), we get

$$\big\|\rho(T,\cdot) - \sigma(T,\cdot)\big\|_{\mathbf{L^1}} \leq \|\rho_0 - \sigma_0\|_{\mathbf{L^1}} + K\int_0^T \big\|\rho(t,\cdot) - \sigma(t,\cdot)\big\|_{\mathbf{L^1}} dt$$

with

$$\begin{aligned}
K = \omega_\eta(0)\big\|v'\big\|&\left(\big\|f'\big\| \sup_{t\in[0,T]} \big\|\rho(t,\cdot)\big\|_{\mathrm{BV}(\mathbb{R})} + 2\sup_{t\in[0,T]}\big\|f(\rho(t,\cdot))\big\|\right)\\
&+ \sup_{t\in[0,T]}\big\|f(\rho(t,\cdot))\big\|_{\mathbf{L^1}}\left(2(\omega_\eta(0))^2\big\|v''\big\| \sup_{t\in[0,T]}\big\|\rho(t,\cdot)\big\| + \big\|v'\big\|\big\|\omega_\eta'\big\|\right).
\end{aligned} \tag{1.2.5}$$

By Gronwall's lemma, we get the statement. □

1.3 Existence

1.3.1 Lax-Friedrichs numerical scheme

We discretize (1.1.1) on a fixed grid given by the cells interfaces $x_{j+\frac{1}{2}} = j\Delta x$ and the cells centers $x_j = (j-1/2)\Delta x$ for $j \in \mathbb{Z}$, taking a space step Δx such that $\eta = N\Delta x$ for some $N \in \mathbb{N}$, and $t^n = n\Delta t$ the time mesh. Our aim is to construct a finite volume approximate solution $\rho_{\Delta x}(t,x) = \rho_j^n$ for $(t,x) \in C_j^n = [t^n, t^{n+1}[\times]x_{j-1/2}, x_{j+1/2}]$. We approximate the initial datum ρ_0 with the piecewise constant function

$$\rho_j^0 = \frac{1}{\Delta x}\int_{x_{j-1/2}}^{x_{j+1/2}} \rho_0(x)dx.$$

We denote $\omega_\eta^k := \omega_\eta(k\Delta x)$ for $k = 0, ..., N-1$ and set

$$V_j^n := v(c_j^n),$$

where

$$c_j^n := \Delta x \sum_{k=0}^{N-1} \omega_\eta^k \rho_{j+k}^n.$$

The Lax-Friedrichs flux adapted to (1.1.1) is given by

$$F_{j+1/2}^n := \frac{1}{2}f(\rho_j^n)V_j^n + \frac{1}{2}f(\rho_{j+1}^n)V_{j+1}^n + \frac{\alpha}{2}(\rho_j^n - \rho_{j+1}^n), \tag{1.3.1}$$

$\alpha \geq 0$ being the viscosity coefficient. In this way, we obtain the $N+2$ points finite volume scheme

$$\rho_j^{n+1} = H(\rho_{j-1}^n, ..., \rho_{j+N}^n), \tag{1.3.2}$$

where

$$\begin{aligned} H(\rho_{j-1}, ..., \rho_{j+N}) := \rho_j + \frac{\lambda}{2}\alpha(\rho_{j-1} - 2\rho_j + \rho_{j+1}) \\ + \frac{\lambda}{2}\left(f(\rho_{j-1})V_{j-1}^n - f(\rho_{j+1})V_{j+1}^n\right), \end{aligned} \tag{1.3.3}$$

with $\lambda = \Delta t/\Delta x$.
Assume $\rho_i \in I$ for $i = j-1, ..., j+N$, we can compute:

$$\frac{\partial H}{\partial \rho_{j-1}} = \frac{\lambda}{2}\left(\alpha + V_{j-1}f'(\rho_{j-1}) + \Delta x\, v'(c_{j-1})\omega_\eta^0 f(\rho_{j-1})\right), \tag{1.3.4a}$$

$$\begin{aligned} \frac{\partial H}{\partial \rho_j} &= 1 - \lambda\left(\alpha - \frac{1}{2}\Delta x f(\rho_{j-1})v'(c_{j-1})\omega_\eta^1\right) \\ &\geq 1 - \lambda\left(\alpha + \frac{1}{2}\Delta x\omega_\eta(0)\left\|f\right\|\left\|v'\right\|\right), \end{aligned} \tag{1.3.4b}$$

$$\frac{\partial H}{\partial \rho_{j+1}} = \frac{\lambda}{2}\left(\alpha + \Delta x f(\rho_{j-1})v'(c_{j-1})\omega_\eta^2 - f'(\rho_{j+1})V_{j+1} - \Delta x f(\rho_{j+1})v'(c_{j+1})\omega_\eta^0\right), \tag{1.3.4c}$$

$$\frac{\partial H}{\partial \rho_{j+k}} = -\frac{\lambda}{2}\Delta x \left(f(\rho_{j+1})v'(c_{j+1})\omega_\eta^{k-1} - f(\rho_{j-1})v'(c_{j-1})\omega_\eta^{k+1} \right), \quad k = 2, \dots, N-2, \tag{1.3.4d}$$

$$\frac{\partial H}{\partial \rho_{j+N-1}} = -\frac{\lambda}{2}\Delta x f(\rho_{j+1})v'(c_{j+1})\omega_\eta^{N-2}, \tag{1.3.4e}$$

$$\frac{\partial H}{\partial \rho_{j+N}} = -\frac{\lambda}{2}\Delta x f(\rho_{j+1})v'(c_{j+1})\omega_\eta^{N-1}. \tag{1.3.4f}$$

We have that (1.3.4e) and (1.3.4f) are non-negative. The positivity of (1.3.4b) follows assuming

$$\Delta t \leq \frac{2}{2\alpha + \Delta x \omega_\eta(0)\, \|f\| \|v'\|} \Delta x, \tag{1.3.5}$$

which gives the CFL condition. Moreover, the bound

$$\alpha \geq \|f'\| \|v\| + \Delta x \omega_\eta(0) \|f\| \|v'\| \tag{1.3.6}$$

guarantees the increasing monotonicity w.r.t. ρ_{j-1} and ρ_{j+1}, respectively in (1.3.4a) and in (1.3.4c). The sign of (1.3.4d) cannot be a priori determined and for this reason the numerical scheme (1.3.2), (1.3.3) is not monotone.

1.3.2 Maximum principle

Proposition 1. *Let hypotheses* **(H)** *hold. Given an initial datum* ρ_j^0, $j \in \mathbb{Z}$, *such that* $\rho_m = \min_{j\in\mathbb{Z}} \rho_j^0 \in I$ *and* $\rho_M = \max_{j\in\mathbb{Z}} \rho_j^0 \in I$, *the finite volume approximation* ρ_j^n, $j \in \mathbb{Z}$ *and* $n \in N$, *constructed using the scheme* (1.3.2), (1.3.3), *satisfies the bounds*

$$\rho_m \leq \rho_j^n \leq \rho_M,$$

for all $j \in \mathbb{Z}$ *and* $n \in \mathbb{N}$, *under the CFL condition* (1.3.5).

Proof. We follow closely the idea in [11]. We start observing that

$$H(\rho_m, \rho_m, \rho_m, \rho_{j+2}, ..., \rho_{j+N-2}, \rho_m, \rho_m) \geq \rho_m, \tag{1.3.7}$$

$$H(\rho_M, \rho_M, \rho_M, \rho_{j+2}, ..., \rho_{j+N-2}, \rho_M, \rho_M) \leq \rho_M. \tag{1.3.8}$$

Indeed, we get

$$H(\rho_m, \rho_m, \rho_m, \rho_{j+2}, ..., \rho_{j+N-2}, \rho_m, \rho_m) = \rho_m + \frac{\lambda}{2} f(\rho_m)(V_{j-1}^n - V_{j+1}^n),$$

and we have that

$$V_{j-1}^n - V_{j+1}^n = v(c_{j-1}^n) - v(c_{j+1}^n) = -v'(\xi)\Delta x \sum_{k=0}^{N-1} \omega_\eta^k (\rho_{j+k+1} - \rho_{j+k-1}) \geq 0,$$

for some ξ is between c_{j-1}^n and c_{j+1}^n. Indeed, due to the non-increasing monotonicity of ω_η, we observe that

$$\sum_{k=0}^{N-1} \omega_\eta^k (\rho_{j+k+1} - \rho_{j+k-1}) = \rho_m(\omega_\eta^{N-2} + \omega_\eta^{N-1} - \omega_\eta^0 - \omega_\eta^1) + \sum_{k=1}^{N-2} \rho_{j+k}(\omega_\eta^{k-1} - \omega_\eta^{k+1})$$

$$\geq \rho_m \sum_{k=1}^{N-2} \left(\omega_\eta^{k-1} - \omega_\eta^{k+1}\right) \geq 0.$$

In this way we have the inequality (1.3.7) and the same procedure leads to (1.3.8).

Consider now the points

$$R_j^n = (\rho_{j-1}^n, ..., \rho_{j+N}^n)$$

and

$$R_m^n = (\rho_m, \rho_m, \rho_m, \rho_{j+2}^n, ..., \rho_{j+N-2}^n, \rho_m, \rho_m).$$

Applying the mean value theorem and using (1.3.7) one has

$$\begin{aligned} \rho_j^{n+1} = H(R_j^n) &= H(R_m^n) + \nabla H(R_\xi) \cdot (R_j^n - R_m^n) \\ &\geq \rho_m + \nabla H(R_\xi) \cdot (R_j^n - R_m^n), \end{aligned} \tag{1.3.9}$$

for $R_\xi = (1-\xi)R_m^n + \xi R_j^n$, for some $\xi \in [0,1]$. We note that

$$\frac{\partial H}{\partial \rho_{j+k}}(R_\xi)(R_j^n - R_m^n)_k = 0, \qquad k = 2, \ldots, N-2,$$

since $(R_j^n - R_m^n)_k = 0$ for $k = 2, \ldots, N-2$. Assuming (1.3.5) and (1.3.6), we conclude

$$\nabla H(R_\xi) \cdot (R_j^n - R_m^n) \geq 0,$$

which by (1.3.9) implies that $\rho_j^{n+1} \geq \rho_m$.
Similarly we can prove the upper bound by considering

$$R_M^n = (\rho_M, \rho_M, \rho_M, \rho_{j+2}^n, ..., \rho_{j+N-2}^n, \rho_M, \rho_M)$$

and (1.3.8). □

1.3.3 BV estimates

The approximate solutions constructed using adapted Lax-Friedrichs numerical scheme have uniformly bounded total variation.

Proposition 2. *Let hypotheses* **(H)** *hold,* $\rho_0 \in BV(\mathbb{R}; I)$*, and let* $\rho_{\Delta x}$ *be constructed using* (1.3.2), (1.3.3)*. If*

$$\begin{aligned} \alpha &\geq \left\|f'\right\|\|v\| + \Delta x \omega_\eta(0)\left\|v'\right\|(\|f\| + \left\|f'\right\|\|\rho_0\|), \\ \Delta t &\leq \frac{2\Delta x}{2\alpha + \Delta x \omega_\eta(0)\|v'\|(\|f\| + \|f'\|\|\rho_0\|)}, \end{aligned}$$

then for every $T > 0$ *the following discrete space* BV *estimate holds*

$$TV(\rho_{\Delta x})(T, \cdot) \leq e^{C(\omega_\eta)T}\, TV(\rho_0), \tag{1.3.10}$$

where $C(\omega_\eta) := \omega_\eta(0)\left(\left\|v'\right\|\left(\left\|f'\right\|\|\rho_0\| + 2\|f\|\right) + \frac{7}{2}J_0\|f\|\left\|v''\right\|\right)$.

Proof. At the mesh cell C_j^n there holds

$$\rho_j^{n+1} = \rho_j + \frac{\lambda\alpha}{2}(\rho_{j-1} - 2\rho_j + \rho_{j+1}) + \frac{\lambda}{2}(f(\rho_{j-1})V_{j-1} - f(\rho_{j+1})V_{j+1}),$$

and at C_{j+1}^n

$$\rho_{j+1}^{n+1} = \rho_{j+1} + \frac{\lambda\alpha}{2}(\rho_j - 2\rho_{j+1} + \rho_{j+2}) + \frac{\lambda}{2}(f(\rho_j)V_j - f(\rho_{j+2})V_{j+2}),$$

where we omitted the index n to simplify the notation. Computing the difference between ρ_{j+1}^{n+1} and ρ_j^{n+1} and setting $\Delta_{j+k-1/2}^n = \rho_{j+k}^n - \rho_{j+k-1}^n$ for $k = 0, \dots, N+1$ we get:

$$\begin{aligned}\Delta_{j+1/2}^{n+1} &= \Delta_{j+1/2} + \frac{\lambda\alpha}{2}[\Delta_{j-1/2} - 2\Delta_{j+1/2} + \Delta_{j+3/2}] \\ &+ \frac{\lambda}{2}[f(\rho_j)V_j \pm f(\rho_{j-1})V_j - f(\rho_{j-1})V_{j-1} - f(\rho_{j+2})V_{j+2} \pm f(\rho_{j+1})V_{j+2} + f(\rho_{j+1})V_{j+1}]\end{aligned} \tag{1.3.11}$$

Applying the mean value theorem we can rewrite (1.3.11) as:

$$\begin{aligned}\Delta_{j+1/2}^{n+1} = \Delta_{j+1/2} &+ \frac{\lambda\alpha}{2}\left[\Delta_{j-1/2} - 2\Delta_{j+1/2} + \Delta_{j+3/2}\right] \\ &+ \frac{\lambda}{2}\Big[V_j f'(\zeta_{j-1/2})\Delta_{j-1/2} + f(\rho_{j-1})(V_j - V_{j-1}) \\ &- V_{j+2} f'(\zeta_{j+3/2})\Delta_{j+3/2} + f(\rho_{j+1})(V_{j+1} - V_{j+2})\Big].\end{aligned} \tag{1.3.12}$$

where $\zeta_{j-1/2}$ is between ρ_{j-1} and ρ_j. Applying the mean value theorem we have

$$V_j - V_{j-1} = v'(\xi_{j-1/2})\Delta x \sum_{k=0}^{N-1} \omega_\eta^k \Delta_{j+k-\frac{1}{2}},$$

$$V_{j+2} - V_{j+1} = v'(\xi_{j+3/2})\Delta x \sum_{k=0}^{N-1} \omega_\eta^k \Delta_{j+k+\frac{3}{2}},$$

where $\xi_{j+3/2}$ is between $\sum_{k=0}^{N-1} \omega_\eta^k \rho_{j+k+1}$ and $\sum_{k=0}^{N-1} \omega_\eta^k \rho_{j+k+2}$. In this way we obtain

$$\Delta_{j+1/2}^{n+1} = \frac{\lambda}{2}[\alpha + V_j f'(\zeta_{j-1/2}) + \Delta x\, \omega_\eta^0\, v'(\xi_{j-1/2}) f(\rho_{j-1})]\Delta_{j-1/2} \tag{1.3.13a}$$

$$+ [1 - \lambda\alpha + \frac{\lambda}{2}\Delta x\, \omega_\eta^1\, v'(\xi_{j-1/2}) f(\rho_{j-1})]\Delta_{j+1/2} \tag{1.3.13b}$$

$$+ \frac{\lambda}{2}\Big[\alpha - V_{j+2} f'(\zeta_{j+3/2}) - \Delta x\, \omega_\eta^0\, f(\rho_{j+1}) v'(\xi_{j+3/2}) + \Delta x\, \omega_\eta^2 v'(\xi_{j-1/2}) f(\rho_{j-1})\Big]\Delta_{j+3/2} \tag{1.3.13c}$$

$$+ \frac{\lambda}{2}\Delta x\, f(\rho_{j-1}) v'(\xi_{j-1/2}) \sum_{k=3}^{N-1} \omega_\eta^k \Delta_{j+k-1/2} \tag{1.3.13d}$$

$$- \frac{\lambda}{2}\Delta x\, f(\rho_{j+1}) v'(\xi_{j+3/2}) \sum_{k=1}^{N-1} \omega_\eta^k \Delta_{j+k+3/2}. \tag{1.3.13e}$$

Rearranging the indexes in (1.3.13d) and (1.3.13e) we obtain

$$\begin{aligned}(1.3.13d)+(1.3.13e) = \frac{\lambda}{2}\Delta x \sum_{k=2}^{N-2}\Big[f(\rho_{j-1})v'(\xi_{j-1/2})\omega_\eta^{k+1} - f(\rho_{j+1})v'(\xi_{j+3/2})\omega_\eta^{k-1}\Big]\Delta_{j+k+1/2}\\ -\frac{\lambda}{2}\Delta x\, f(\rho_{j+1})v'(\xi_{j+3/2})\omega_\eta^{N-2}\Delta_{j+N-1/2}\\ -\frac{\lambda}{2}\Delta x\, f(\rho_{j+1})v'(\xi_{j+3/2})\omega_\eta^{N-1}\Delta_{j+N+1/2}.\end{aligned}$$

Noting that adding and subtracting $f(\rho_{j-1})\omega_\eta^{k-1}v'(\xi_{j-1/2})$ in the sum we have

$$\begin{aligned}&f(\rho_{j-1})v'(\xi_{j-1/2})\omega_\eta^{k+1} - f(\rho_{j+1})v'(\xi_{j+3/2})\omega_\eta^{k-1}\\ &= f(\rho_{j-1})v'(\xi_{j-1/2})(\omega_\eta^{k+1}-\omega_\eta^{k-1})\\ &\quad+\omega_\eta^{k-1}\Big(f(\rho_{j-1})v'(\xi_{j-1/2}) \pm f(\rho_{j-1})v'(\xi_{j+3/2}) - f(\rho_{j+1})v'(\xi_{j+3/2})\Big)\\ &= f(\rho_{j-1})v'(\xi_{j-1/2})(\omega_\eta^{k+1}-\omega_\eta^{k-1}) + \omega_\eta^{k-1}f(\rho_{j-1})(v'(\xi_{j-1/2})-v'(\xi_{j+3/2}))\\ &\quad-\omega_\eta^{k-1}v'(\xi_{j+3/2})f'(\zeta_j)\Big(\Delta_{j-1/2}+\Delta_{j+1/2}\Big),\end{aligned}$$

with ζ_j is between ρ_{j-1} and ρ_{j+1}. Therefore we get

$$\Delta_{j+1/2}^{n+1} = \frac{\lambda}{2}\Big[\alpha + V_j f'(\zeta_{j-1/2}) + \Delta x\,\omega_\eta^0 v'(\xi_{j-1/2})f(\rho_{j-1}) \tag{1.3.14a}$$

$$\qquad - \Delta x\, v'(\xi_{j+3/2})f'(\zeta_j)\sum_{k=2}^{N-2}\omega_\eta^{k-1}\Delta_{j+k+1/2}\Big]\Delta_{j-1/2}$$

$$+\Big[1-\lambda\alpha+\frac{\lambda}{2}\Delta x\omega_\eta^1 v'(\xi_{j-1/2})f(\rho_{j-1}) \tag{1.3.14b}$$

$$\qquad -\frac{\lambda}{2}\Delta x\, v'(\xi_{j+3/2})f'(\zeta_j)\sum_{k=2}^{N-2}\omega_\eta^{k-1}\Delta_{j+k+1/2}\Big]\Delta_{j+1/2}$$

$$+\frac{\lambda}{2}\Big[\alpha - V_{j+2}f'(\zeta_{j+3/2}) - \Delta x\omega_\eta^0 f(\rho_{j+1})v'(\xi_{j+3/2}) \tag{1.3.14c}$$

$$\qquad +\Delta x\omega_\eta^2 f(\rho_{j-1})v'(\xi_{j-1/2})\Big]\Delta_{j+3/2}$$

$$+\frac{\lambda}{2}\Delta x\sum_{k=2}^{N-2}\Big[f(\rho_{j-1})v'(\xi_{j-1/2})(\omega_\eta^{k+1}-\omega_\eta^{k-1}) \tag{1.3.14d}$$

$$\qquad +\omega_\eta^{k-1}f(\rho_{j-1})\Big(v'(\xi_{j+1/2})-v'(\xi_{j+3/2})\Big)\Big]\Delta_{j+k+1/2}$$

$$-\frac{\lambda}{2}\Delta x\, f(\rho_{j+1})v'(\xi_{j+3/2})\omega_\eta^{N-2}\Delta_{j+N-1/2} \tag{1.3.14e}$$

$$-\frac{\lambda}{2}\Delta x\, f(\rho_{j+1})v'(\xi_{j+3/2})\omega_\eta^{N-1}\Delta_{j+N+1/2}. \tag{1.3.14f}$$

Observe that the assumption $\alpha \geq \|f'\|\|v\| + \Delta x\omega_\eta(0)\|v'\|(\|f\| + \|f'\|\|\rho_0\|)$ guarantees the positivity of (1.3.14a). Similarly for (1.3.14c) we get $\alpha \geq \|f'\|\|v\| + \Delta x\omega_\eta(0)\|f\|\|v'\|$ and for

(1.3.14b) we have the following CFL condition

$$\Delta t \leq \frac{2\Delta x}{2\alpha + \Delta x \omega_\eta(0)\|v'\|(\|f\| + \|f'\|\|\rho_0\|)}. \tag{1.3.15}$$

Rearranging the indexes and taking the absolute values

$$\sum_j \left|\Delta_{j+1/2}^{n+1}\right| \tag{1.3.16a}$$

$$\leq \sum_j \left|\Delta_{j+1/2}\right| \tag{1.3.16b}$$

$$\times \left[\frac{\lambda}{2}\Big(\alpha + V_{j+1}f'(\zeta_{j+1/2}) + \Delta x\, \omega_\eta^0 v'(\xi_{j+1/2})\, f(\rho_j)\right. \tag{1.3.16c}$$

$$\left. - \Delta x v'(\xi_{j+5/2}) f'(\zeta_{j+1}) \sum_{k=2}^{N-2} \omega_\eta^{k-1} \Delta_{j+k+3/2}\Big)\right. \tag{1.3.16d}$$

$$+ 1 - \lambda\alpha + \frac{\lambda}{2}\Delta x\, \omega_\eta^1 v'(\xi_{j-1/2}) f(\rho_{j-1}) - \frac{\lambda}{2}\Delta x\, v'(\xi_{j+3/2}) f'(\zeta_j) \sum_{k=2}^{N-2} \omega_\eta^{k-1}\Delta_{j+k+1/2} \tag{1.3.16e}$$

$$+ \frac{\lambda}{2}\Big(\alpha - V_{j+1}f'(\zeta_{j+1/2}) - \Delta x\, \omega_\eta^0 f(\rho_j) v'(\xi_{j+1/2}) + \Delta x\, \omega_\eta^2 v'(\xi_{j-3/2}) f(\rho_{j-2})\Big) \tag{1.3.16f}$$

$$+ \frac{\lambda}{2}\Delta x \Bigg(\sum_{k=2}^{N-2} f(\rho_{j-k-1}) v'(\xi_{j-k-1/2})(\omega_\eta^{k+1} - \omega_\eta^{k-1}) \tag{1.3.16g}$$

$$+ \omega_\eta^{k-1} f(\rho_{j-k-1}) \Big| v'(\xi_{j-k-1/2}) - v'(\xi_{j-k+3/2}) \Big| \Bigg)$$

$$- \frac{\lambda}{2}\Delta x\, f(\rho_{j-N+2}) v'(\xi_{j-N+5/2}) \omega_\eta^{N-2} - \frac{\lambda}{2}\Delta x\, f(\rho_{j-N+1}) v'(\xi_{j-N+3/2}) \omega_\eta^{N-1}\Bigg]. \tag{1.3.16h}$$

Due to some cancellations, the coefficient of the right-hand side of (1.3.16) becomes

$$1 + \frac{\Delta t}{2}\Bigg[- v'(\xi_{j+5/2}) f'(\zeta_{j+1}) \sum_{k=2}^{N-2} \omega_\eta^{k-1}\Delta_{j+k+3/2} - v'(\xi_{j+3/2}) f'(\zeta_j) \sum_{k=2}^{N-2} \omega_\eta^{k-1}\Delta_{j+k+1/2}$$

$$+ \omega_\eta^1 v'(\xi_{j-1/2}) f(\rho_{j-1}) + \omega_\eta^2 v'(\xi_{j-3/2}) f(\rho_{j-2})$$

$$+ \Bigg(\sum_{k=2}^{N-2} f(\rho_{j-k-1}) v'(\xi_{j-k-1/2})(\omega_\eta^{k+1} - \omega_\eta^{k-1}) \tag{1.3.17}$$

$$+ \omega_\eta^{k-1} f(\rho_{j-k-1}) \Big| v'(\xi_{j-k-1/2}) - v'(\xi_{j-k+3/2}) \Big| \Bigg)$$

$$- f(\rho_{j-N+2}) v'(\xi_{j-N+5/2}) \omega_\eta^{N-2} - f(\rho_{j-N+1}) v'(\xi_{j-N+3/2}) \omega_\eta^{N-1}\Bigg]. \tag{1.3.18}$$

Following [48, pp. 11–12], applying the mean value theorem to v' and using the monotonicity of the kernel ω_η, we have

$$\left|v'(\xi_{j-k-1/2}) - v'(\xi_{j-k+3/2})\right| \leq 7\omega_\eta(0)\|v''\|\Delta x.$$

Therefore we have

$$(1.3.18) \leq 1+\frac{\Delta t}{2}\Bigg[2\omega_\eta(0)\|v'\|\|f'\|\|\rho_0\|+2\omega_\eta(0)\|v'\|\|f\| + \|v'\|\|f\|\underbrace{\sum_{k=2}^{N-2}(\omega_\eta^{k-1}-\omega_\eta^{k+1})}_{\sum_{k=1}^{N-3}\omega_\eta^k-\sum_{k=3}^{N-1}\omega_\eta^k}+7\omega_\eta(0)\|v''\|\|f\|\underbrace{\Delta x\sum_{k=2}^{N-2}\omega_\eta^{k-1}}_{\leq J_0}\Bigg].$$

Substituting in (1.3.16) we get

$$\sum_j\left|\Delta_{j+1/2}^{n+1}\right|\leq\left[1+\frac{\Delta t}{2}\left(2\omega_\eta(0)\|v'\|\left(\|f'\|\|\rho_0\|+2\|f\|\right)+7\omega_\eta(0)J_0\|f\|\|v''\|\right)\right]\sum_j\left|\Delta_{j+1/2}^{n}\right|,$$

therefore we recover the following estimate for the total variation

$$\begin{aligned}&\mathrm{TV}(\rho_{\Delta x}(T,\cdot))\leq\\&\quad\left[1+\frac{\Delta t}{2}\left(2\omega_\eta(0)\|v'\|\left(\|f'\|\|\rho_0\|+2\|f\|\right)+7\omega_\eta(0)J_0\|f\|\|v''\|\right)\right]^{T/\Delta t}\mathrm{TV}(\rho_{\Delta x}(0,\cdot))\\&\leq e^{\omega_\eta(0)\left(\|v'\|\left(\|f'\|\|\rho_0\|+2\|f\|\right)+\frac{7}{2}J_0\|f\|\|v''\|\right)T}\mathrm{TV}(\rho_0).\end{aligned}$$

□

From Proposition 2, the following space-time BVestimate can be derived (see [44, Corollary 5.1]).

Corollary 4. *Let hypotheses* **(H)** *hold,* $\rho_0\in BV(\mathbb{R};I)$*, and* $\rho_{\Delta x}$ *be given by* (1.3.2), (1.3.3). *If*

$$\begin{aligned}\alpha&\geq\|f'\|\|v\|+\Delta x\omega_\eta(0)\|v'\|(\|f\|+\|f'\|\|\rho_0\|),\\\Delta t&\leq\frac{2\Delta x}{2\alpha+\Delta x\omega_\eta(0)\|v'\|(\|f\|+\|f'\|\|\rho_0\|)},\end{aligned}$$

then, for every $T>0$, $\rho_{\Delta x}$ *satisfies the following Total Variation estimate in space and time*

$$\begin{aligned}&TV(\rho_{\Delta x};\mathbb{R}\times[0,T])\\&\leq T\,e^{C(\omega_\eta)T}\left(1+\|f'\|\|v\|+\frac{1}{2}\Delta x\,\omega_\eta(0)\|v'\|\left(5\|f\|+\|f'\|\|\rho_0\|\right)+J_0\|f\|\|v'\|\right)TV(\rho_0).\end{aligned}\tag{1.3.19}$$

Proof. Let us fix $T\in\mathbb{R}^+$. If $T\leq\Delta t$, then $\mathrm{TV}(\rho_{\Delta x};[0,T]\times\mathbb{R})\leq T\,\mathrm{TV}(\rho_0)$. Let us assume now that $T>\Delta t$. Let $M\in\mathbb{N}\backslash\{0\}$ such that $M\Delta t<T\leq(M+1)\Delta t$. Then

$$\mathrm{TV}(\rho_{\Delta x};\mathbb{R}\times[0,T])=\sum_{n=0}^{M-1}\sum_{j\in\mathbb{Z}}\Delta t\left|\rho_{j+1}^n-\rho_j^n\right|+(T-M\Delta t)\sum_{j\in\mathbb{Z}}\left|\rho_{j+1}^M-\rho_j^M\right|+\sum_{n=0}^{M-1}\sum_{j\in\mathbb{Z}}\Delta x\left|\rho_j^{n+1}-\rho_j^n\right|.$$

The spatial BV estimate yields

$$\sum_{n=0}^{M-1}\sum_{j\in\mathbb{Z}}\Delta t\Big|\rho_{j+1}^n-\rho_j^n\Big|+(T-M\Delta t)\sum_{j\in\mathbb{Z}}\Big|\rho_{j+1}^M-\rho_j^M\Big|\le T\,e^{C(\omega_\eta)T}\mathrm{TV}(\rho_0) \tag{1.3.20}$$

where $C(\omega_\eta)$ is the constant in Proposition 2. We are left to bound the term

$$\sum_{n=0}^{M-1}\sum_{j\in\mathbb{Z}}\Delta x\Big|\rho_j^{n+1}-\rho_j^n\Big|.$$

Let us make use of the definition of the numerical scheme (1.3.2), (1.3.3). Applying the mean value theorem to the function f we obtain

$$\begin{aligned}\rho_j^{n+1}-\rho_j^n=&\frac{\lambda}{2}(\alpha+V_{j+1}^nf'(\zeta_{j-1/2}))(\rho_{j-1}^n-\rho_j^n)\\&+\frac{\lambda}{2}(-\alpha+V_{j+1}^nf'(\zeta_{j+1/2}))(\rho_j^n-\rho_{j+1}^n)\\&+\frac{\lambda}{2}f(\rho_{j-1}^n)\left(V_{j-1}^n-V_j^n\right)+\frac{\lambda}{2}f(\rho_{j-1}^n)\left(V_j^n-V_{j+1}^n\right),\end{aligned}$$

where $\zeta_{j-1/2}$ is between ρ_{j-1}^n and ρ_j^n. Applying again the mean value theorem, we obtain

$$V_{j-1}^n-V_j^n=v'(\xi_{j-1/2})\Delta x\sum_{k=0}^{N-1}\omega_\eta^k(\rho_{j+k-1}^n-\rho_{j+k}^n)$$

and

$$V_j^n-V_{j+1}^n=v'(\xi_{j+1/2})\Delta x\sum_{k=0}^{N-1}\omega_\eta^k(\rho_{j+k}^n-\rho_{j+k+1}^n).$$

Therefore we can write

$$\begin{aligned}\rho_j^{n+1}-\rho_j^n=&\frac{\lambda}{2}\left(\alpha+V_{j+1}^nf'(\zeta_{j-1/2})+f(\rho_{j-1}^n)v'(\xi_{j-1/2})\Delta x\,\omega_\eta^0\right)(\rho_{j-1}^n-\rho_j^n)\\&+\frac{\lambda}{2}\Big(-\alpha+V_{j+1}^nf'(\zeta_{j+1/2})+f(\rho_{j-1}^n)v'(\xi_{j-1/2})\Delta x\omega_\eta^1\\&+f(\rho_{j-1}^n)v'(\xi_{j+1/2})\Delta x\omega_\eta^0\Big)(\rho_j^n-\rho_{j+1}^n)\\&+\frac{\lambda}{2}f(\rho_{j-1}^n)v'(\xi_{j-1/2})\Delta x\sum_{k=2}^{N-1}\omega_\eta^k(\rho_{j+k-1}^n-\rho_{j+k}^n)\\&+\frac{\lambda}{2}f(\rho_{j-1}^n)v'(\xi_{j+1/2})\Delta x\sum_{k=1}^{N-1}\omega_\eta^k(\rho_{j+k}^n-\rho_{j+k+1}^n).\end{aligned}$$

Rearranging the indexes of the last two terms, we can write

$$\begin{aligned}\rho_j^{n+1}-\rho_j^n=&\frac{\lambda}{2}\left(\alpha+V_{j+1}^nf'(\zeta_{j-1/2})+f(\rho_{j-1}^n)v'(\xi_{j-1/2})\Delta x\omega_\eta^0\right)(\rho_{j-1}^n-\rho_j^n)\\&-\frac{\lambda}{2}\Big(\alpha-V_{j+1}^nf'(\zeta_{j+1/2})-f(\rho_{j-1}^n)v'(\xi_{j-1/2})\Delta x\,\omega_\eta^1\end{aligned}\tag{1.3.21a}$$

$$-f(\rho_{j-1}^n)v'(\xi_{j+1/2})\Delta x\,\omega_\eta^0\Big)\,(\rho_j^n-\rho_{j+1}^n) \tag{1.3.21b}$$

$$+\frac{\lambda}{2}f(\rho_{j-1}^n)\Delta x\sum_{k=1}^{N-2}\Big(v'(\xi_{j-1/2})\,\omega_\eta^{k+1}+v'(\xi_{j+1/2})\,\omega_\eta^k\Big)\,(\rho_{j+k}^n-\rho_{j+k+1}^n) \tag{1.3.21c}$$

$$+\frac{\lambda}{2}f(\rho_{j-1}^n)v'(\xi_{j+1/2})\Delta x\,\omega_\eta^{N-1}(\rho_{j+N-1}^n-\rho_{j+N}^n). \tag{1.3.21d}$$

Observe that the coefficients in (1.3.21a) and (1.3.21b) are positive if $\alpha \geq \|f'\|\,\|v\| + \Delta x\omega_\eta(0)\|f\|\,\|v'\|$. Therefore, taking the absolute values in (1.3.21), summing on j and re-arranging the indexes we obtain

$$\begin{aligned}
\sum_{j\in\mathbb{Z}}\Delta x\Big|\rho_j^{n+1}-\rho_j^n\Big| \leq\ & \frac{\Delta t}{2}\sum_{j\in\mathbb{Z}}\Big|\rho_{j+1}^n-\rho_j^n\Big| \\
& \times\Bigg[2\alpha+f'(\zeta_{j+1/2})\left(V_{j+2}^n-V_{j+1}^n\right) \\
& +\Delta x\,f(\rho_j^n)v'(\xi_{j+1/2})\omega_\eta^0-\Delta x\,f(\rho_{j-1}^n)v'(\xi_{j-1/2})\omega_\eta^1 \\
& -\Delta x\,f(\rho_{j-1}^n)v'(\xi_{j+1/2})\omega_\eta^0 \\
& -\Delta x\sum_{k=1}^{N-2}f(\rho_{j-k-1}^n)\left(v'(\xi_{j-k-1/2})\omega_\eta^{k+1}+v'(\xi_{j-k+1/2})\omega_\eta^k\right) \\
& -\Delta x\,f(\rho_{j-N}^n)v'(\xi_{j-N+3/2})\omega_\eta^{N-1}\Bigg] \\
\leq\ & \frac{\Delta t}{2}\sum_{j\in\mathbb{Z}}\Big|\rho_{j+1}^n-\rho_j^n\Big|\left(2\alpha+\Delta x\,\omega_\eta(0)\|v'\|\left(3\|f\|+\|f'\|\|\rho_0\|\right)+2J_0\|f\|\|v'\|\right)
\end{aligned}$$

which yields

$$\begin{aligned}
&\sum_{n=0}^{M-1}\sum_{j\in\mathbb{Z}}\Delta x\Big|\rho_j^{n+1}-\rho_j^n\Big| \\
&\qquad\leq T\,e^{C(\omega_\eta)T}\left(\alpha+\frac{1}{2}\Delta x\,\omega_\eta(0)\|v'\|\left(3\|f\|+\|f'\|\|\rho_0\|\right)+J_0\|f\|\|v'\|\right)\mathrm{TV}(\rho_0),
\end{aligned} \tag{1.3.22}$$

since $M\Delta t < T$. Taking $\alpha = \|f'\|\,\|v\| + \Delta x\omega_\eta(0)\|f\|\,\|v'\|$, we obtain the bound (1.3.19) with

$$\tilde{C} = T\,e^{C(\omega_\eta)T}\left(1+\|f'\|\|v\|+\frac{1}{2}\Delta x\,\omega_\eta(0)\|v'\|\left(5\|f\|+\|f'\|\|\rho_0\|\right)+J_0\|f\|\|v'\|\right)\mathrm{TV}(\rho_0).$$

Note that (1.3.22) allows to recover (1.1.6b) as $\Delta x \to 0$. □

1.3.4 Discrete entropy inequalities

Following [5, 11, 49], we derive a discrete entropy inequality for the approximate solution generated by (1.3.2), (1.3.3), which is used to prove that the limit of Lax-Friedrichs approximations is indeed a weak entropy solution in the sense of Definition 1. We denote

$$G_{j+1/2}(u,w) := \frac{1}{2}f(u)V_j^n+\frac{1}{2}f(w)V_{j+1}^n+\frac{\alpha}{2}(u-w),$$

$$F^{\kappa}_{j+1/2}(u,w) := G_{j+1/2}(u\wedge\kappa, w\wedge\kappa) - G_{j+1/2}(u\vee\kappa, w\vee\kappa),$$

with $a\wedge b = \max(a,b)$ and $a\vee b = \min(a,b)$.

Proposition 3. *Under hypotheses* **(H)**, *let* ρ^n_j, $j\in\mathbb{Z}$, $n\in\mathbb{N}$, *be given by* (1.3.2), (1.3.3). *Then, if* $\alpha \geq \|f'\|\|v\|$ *and* $\lambda \leq 1/\alpha$, *we have*

$$\begin{aligned}\left|\rho^{n+1}_j - \kappa\right| - \left|\rho^n_j - \kappa\right| + \lambda\left(F^{\kappa}_{j+1/2}(\rho^n_j,\rho^n_{j+1}) - F^{\kappa}_{j-1/2}(\rho^n_{j-1},\rho^n_j)\right) \\ + \frac{\lambda}{2}\operatorname{sgn}(\rho^{n+1}_j - k)f(\kappa)(V^n_{j+1} - V^n_{j-1}) \leq 0,\end{aligned} \tag{1.3.23}$$

for all $j\in\mathbb{Z}$, $n\in\mathbb{N}$, *and* $\kappa\in\mathbb{R}$.

Proof. The proof follows closely [5, 11]. We detail it below for sake of completeness. We set

$$\tilde{H}_j(u,w,z) = w - \lambda\left(G_{j+1/2}(w,z) - G_{j-1/2}(u,w)\right).$$

The function $\tilde{H}_j$ is monotone non-decreasing with respect to each variable for $\alpha\lambda\leq 1$ and $\alpha\geq\|f'\|\|v\|$, which are guaranteed by (1.3.5) and (1.3.6). Indeed, we have

$$\tilde{H}_j(u,w,z) = w - \frac{\lambda}{2}\left(f(z)V^n_{j+1} - f(u)V^n_{j-1} + \alpha(2w-u-z)\right),$$

so the partial derivatives are

$$\begin{aligned}\frac{\partial\tilde{H}_j}{\partial u} &= \frac{\lambda}{2}\left(f'(u)V^n_{j-1} + \alpha\right),\\ \frac{\partial\tilde{H}_j}{\partial w} &= 1-\lambda\,\alpha,\\ \frac{\partial\tilde{H}_j}{\partial z} &= \frac{\lambda}{2}\left(\alpha - f'(z)V^n_{j+1}\right).\end{aligned}$$

Moreover, we have the identity

$$\begin{aligned}&\tilde{H}_j(\rho^n_{j-1}\wedge\kappa,\rho^n_j\wedge\kappa,\rho^n_{j+1}\wedge\kappa) - \tilde{H}_j(\rho^n_{j-1}\vee\kappa,\rho^n_j\vee\kappa,\rho^n_{j+1}\vee\kappa)\\ &\quad= |\rho^n_j-\kappa| - \lambda\left(F^{\kappa}_{j+1/2}(\rho^n_j,\rho^n_{j+1}) - F^{\kappa}_{j-1/2}(\rho^n_{j-1},\rho^n_j)\right).\end{aligned}$$

By monotonicity,

$$\begin{aligned}&\tilde{H}_j(\rho^n_{j-1}\wedge\kappa,\rho^n_j\wedge\kappa,\rho^n_{j+1}\wedge\kappa) - \tilde{H}_j(\rho^n_{j-1}\vee\kappa,\rho^n_j\vee\kappa,\rho^n_{j+1}\vee\kappa)\\ &\geq \tilde{H}_j(\rho^n_{j-1},\rho^n_j,\rho^n_{j+1})\wedge\tilde{H}_j(\kappa,\kappa,\kappa) - \tilde{H}_j(\rho^n_{j-1},\rho^n_j,\rho^n_{j+1})\vee\tilde{H}_j(\kappa,\kappa,\kappa)\\ &= \left|\tilde{H}_j(\rho^n_{j-1},\rho^n_j,\rho^n_{j+1}) - \tilde{H}_j(\kappa,\kappa,\kappa)\right|\\ &= \mathsf{sgn}\left(\tilde{H}_j(\rho^n_{j-1},\rho^n_j,\rho^n_{j+1}) - \tilde{H}_j(\kappa,\kappa,\kappa)\right)\times\left(\tilde{H}_j(\rho^n_{j-1},\rho^n_j,\rho^n_{j+1}) - \tilde{H}_j(\kappa,\kappa,\kappa)\right)\\ &= \mathsf{sgn}\left(\tilde{H}_j(\rho^n_{j-1},\rho^n_j,\rho^n_{j+1}) - \kappa + \frac{\lambda}{2}f(\kappa)(V^n_{j+1}-V^n_{j-1})\right)\\ &\quad\times\left(\tilde{H}_j(\rho^n_{j-1},\rho^n_j,\rho^n_{j+1}) - \kappa + \frac{\lambda}{2}f(\kappa)(V^n_{j+1}-V^n_{j-1})\right)\end{aligned}$$

$$
\begin{aligned}
&\geq \operatorname{sgn}\left(\tilde{H}_j(\rho_{j-1}^n,\rho_j^n,\rho_{j+1}^n)-\kappa\right)\times\left(\tilde{H}_j(\rho_{j-1}^n,\rho_j^n,\rho_{j+1}^n)-\kappa+\frac{\lambda}{2}f(\kappa)(V_{j+1}^n-V_{j-1}^n)\right)\\
&=\left|\tilde{H}_j(\rho_{j-1}^n,\rho_j^n,\rho_{j+1}^n)-\kappa\right|+\frac{\lambda}{2}\operatorname{sgn}\left(\tilde{H}_j(\rho_{j-1}^n,\rho_j^n,\rho_{j+1}^n)-\kappa\right)f(\kappa)\left(V_{j+1}^n-V_{j-1}^n\right)\\
&=\left|\rho_j^{n+1}-\kappa\right|+\frac{\lambda}{2}\operatorname{sgn}(\rho_j^{n+1}-\kappa)f(\kappa)\left(V_{j+1}^n-V_{j-1}^n\right),
\end{aligned}
$$

by definition of the scheme (1.3.2), (1.3.3), which gives (1.3.23). □

Proof of Theorem 1. Thanks to Proposition 1 and Corollary 4, we can apply Helly's theorem stating that there exists a subsequence $\rho_{\Delta x}$ that converges to some $\rho \in (L^1\cap L^\infty\cap \mathrm{BV})(\mathbb{R}^+\times\mathbb{R};I)$ in the $\mathbf{L^1_{loc}}$-norm. One can then follow a Lax-Wendroff type argument to show that the limit function ρ is a weak entropy solution of (1.1.1), (1.1.3), in the sense of Definition 1. We just observe that the numerical flux also depends on Δx, therefore the classical argument on flux consistency and Lipschitz dependence must be replaced by direct estimates, like in [11, 48]. □

Proof of Corollary 2. When the look-ahead distance $\eta\to\infty$, the non-local flux in (1.1.1) becomes a local one. Since the bounds (1.1.5), (1.1.6) are uniform as $\eta\to\infty$, the solution ρ^η of problem (1.1.1), (1.3.3), tends up to a subsequence to the solution ρ of the local problem (1.1.7) in the $\mathbf{L^1_{loc}}$-norm when $\eta\to\infty$. In fact, applying Lebesgue's dominated convergence theorem in (1.1.4), since

$$
\left|\operatorname{sgn}(\rho-\kappa)(f(\rho)-f(\kappa))v(\omega_\eta*\rho)\right|\leq 2|f|\,||v||
$$

and

$$
\left|\operatorname{sgn}(\rho-\kappa)f(\kappa)v'(\omega_\eta*\rho)\partial_x(\omega_\eta*\rho)\right|\leq 3|f|\,\|\rho\|\,\left\|\omega_\eta\right\|\,||v'||,
$$

we obtain

$$
\int_0^{+\infty}\int_{\mathbb{R}}\{|\rho-\kappa|\varphi_t+\operatorname{sgn}(\rho-\kappa)(f(\rho)-f(\kappa))v(0)\varphi_x+\int_{\mathbb{R}}|\rho_0(x)-\kappa|\varphi(0,x)dx\geq 0,
$$

which is the definition of entropy weak solution for the classical equation (1.1.7). □

1.4 Numerical tests

In this section, we perform some numerical simulations to illustrate the result of Corollary 2, taking two different choices for the speed law v, the convolution kernel ω_η and the function f. More precisely, we consider the models studied in [64, 72] and [11], which consist in the following equations:

$$
\partial_t\rho+\partial_x\left(\rho(1-\rho)e^{-(\omega_\eta*\rho)}\right)=0,\qquad x\in\mathbb{R},t>0, \tag{1.4.1}
$$

for the Arrhenius look-ahead dynamics [72], and

$$
\partial_t\rho+\partial_x\left(\rho(1-\omega_\eta*\rho)\right)=0,\qquad x\in\mathbb{R},t>0, \tag{1.4.2}
$$

for the Lighthill-Whitham-Richards (LWR) model with non-local velocity [11].
Equations (1.4.1) and (1.4.2) correspond to the following choices of $f \in \mathbf{C^1}([0,1];\mathbb{R}^+)$ and $v \in \mathbf{C^2}([0,1];\mathbb{R}^+)$:

$$f(\rho) = \rho\,(1-\rho)\,, \qquad v(\rho) = e^{-\rho}, \tag{1.4.3}$$

$$f(\rho) = \rho, \qquad v(\rho) = (1-\rho)\,, \tag{1.4.4}$$

respectively. Besides, we will consider the following kernels $\omega_\eta \in \mathbf{C^1}([0,\eta];\mathbb{R}^+)$, see [11, 60]:

$$\text{constant:} \qquad \omega_\eta(x) = \frac{1}{\eta},$$

$$\text{linear decreasing:} \qquad \omega_\eta(x) = \frac{2}{\eta}\left(1 - \frac{x}{\eta}\right).$$

For the tests, the space domain is given by the interval $[-1,1]$ and the space discretization mesh is $\Delta x = 0.001$. We impose absorbing conditions at the boundaries, adding $N = \eta/\Delta x$ ghost cells at the right boundary and just one at the left, where we extend the solution constantly equal to the last value inside the domain. Our aim is to investigate the convergence of (1.4.3) to the solution of the LWR model [65, 67]

$$\partial_t \rho + \partial_x(\rho(1-\rho)) = 0, \tag{1.4.5}$$

and the convergence of (1.4.4) to the solution of the transport equation

$$\partial_t \rho + \partial_x \rho = 0, \tag{1.4.6}$$

as $\eta \to \infty$. We study both problems with the initial datum

$$\rho_0(x) = \begin{cases} 0.8 & \text{for } -0.5 < x < -0.1, \\ 0 & \text{otherwise,} \end{cases} \tag{1.4.7}$$

that describes the case of a red traffic light located at $x = -0.1$, which turns green at the initial time $t = 0$. Figures 1.1 and 1.2 illustrate the behavior for models (1.4.1) and (1.4.2), respectively, in agreement with the theoretical results.

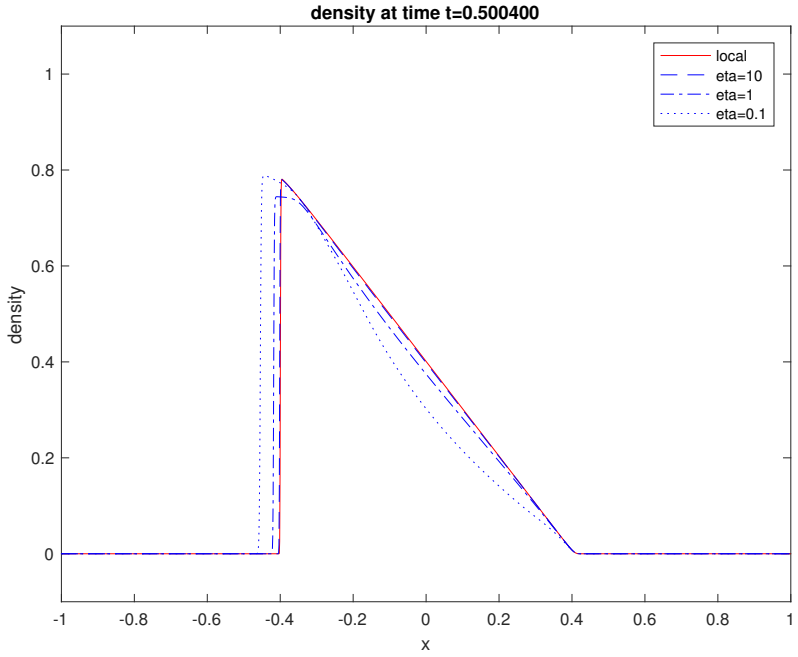

(a) ω_η constant

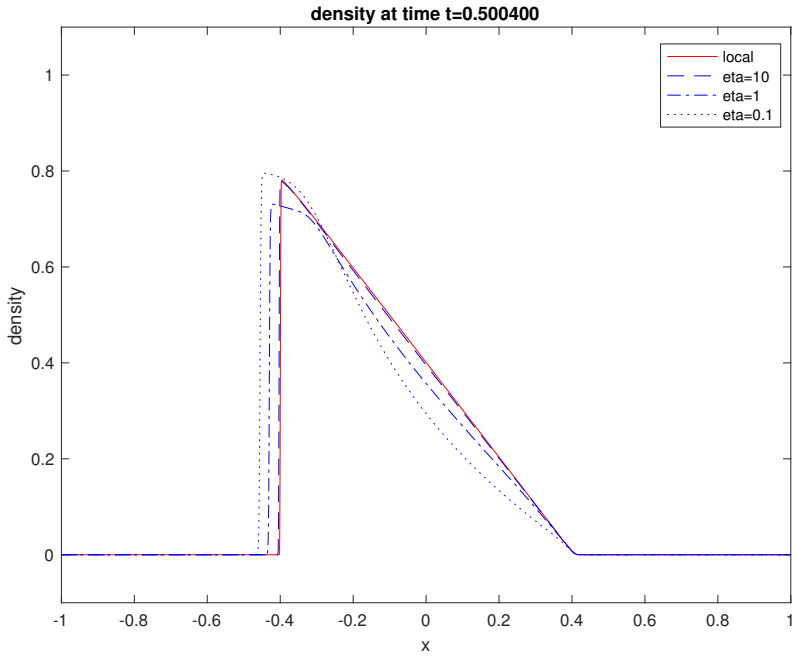

(b) ω_η linear decreasing

Figure 1.1: Density profiles corresponding to the non-local equation (1.4.1) with increasing values of $\eta = 0.1,\ 1,\ 10$. We can observe that the nonlocal solution tends to the solution of (1.4.5) (red line) as $\eta \to \infty$.

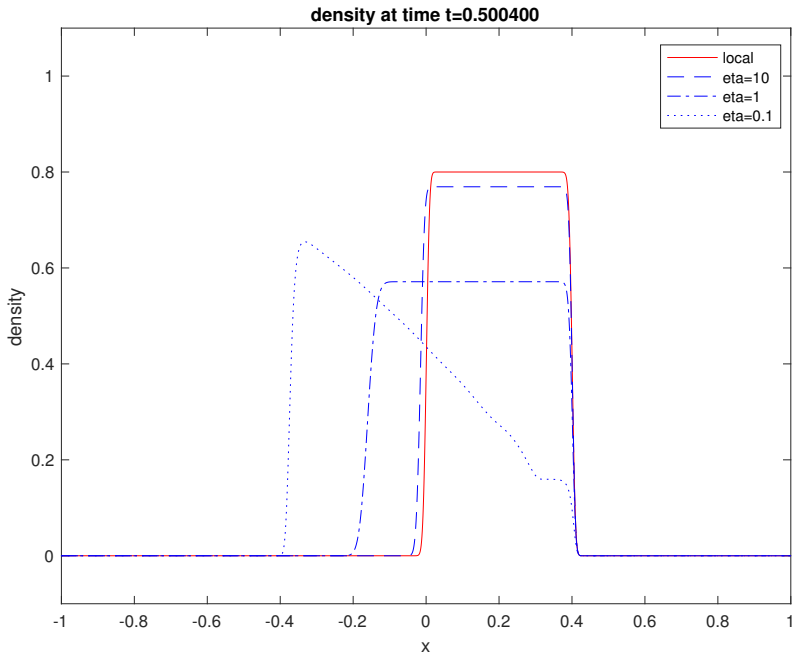

(a) ω_η constant

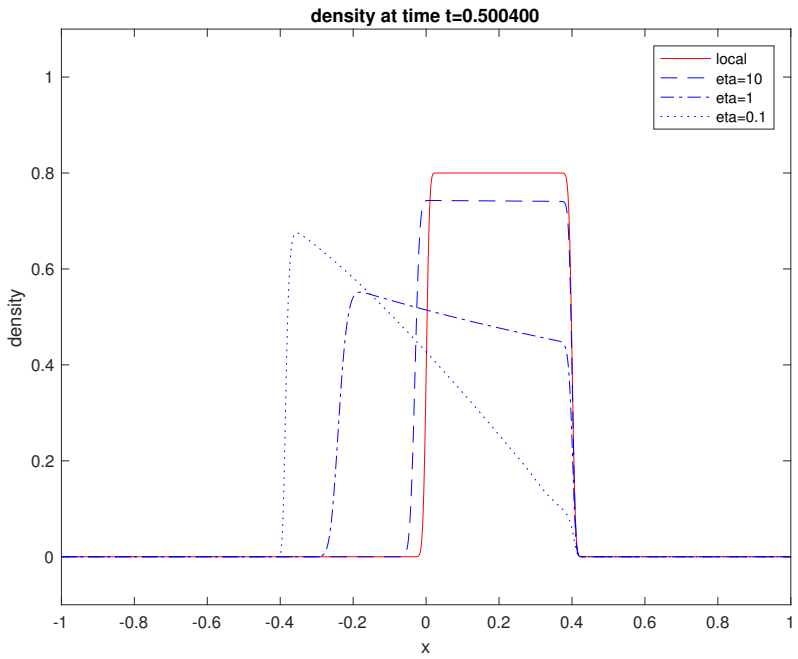

(b) ω_η linear decreasing

Figure 1.2: Density profiles corresponding to the non-local equation (1.4.2) with increasing values of $\eta = 0.1,\ 1,\ 10$. We can observe that the nonlocal solution tends to the solution of (1.4.6) (red line) as $\eta \to \infty$.

Chapter 2

Stability estimates for non-local scalar conservation laws

In this chapter, we focus on a specific class of non-local scalar equations. This study has been detailed in [23]. We consider the following Cauchy problem

$$\begin{cases} \partial_t \rho + \partial_x \big(f(t,x,\rho) V(t,x) \big) = 0 & t > 0,\ x \in \mathbb{R}, \\ \rho(0,x) = \rho_0(x), & x \in \mathbb{R}, \end{cases} \tag{2.0.1}$$

where $V(t,x) = v\big((\rho(t) * \omega)(x)\big)$, and ω is a smooth mollifier:

$$(\rho(t) * \omega)(x) = \int_{\mathbb{R}} \rho(t,y)\, \omega(x-y) dy.$$

Here and below, we set $\rho(t) := \rho(t,\cdot)$ the function $x \mapsto \rho(t,x)$.
In this setting, existence and uniqueness of solutions to (2.0.1) follows from [5], as well as some *a priori* estimates, namely $\mathbf{L^1}$, $\mathbf{L^\infty}$ and total variation estimates, see Section 2.1 below. Carefully applying the Kružkov's doubling of variables techniques, on the lines of [10, 52], we derive the $\mathbf{L^1}$-Lipschitz continuous dependence of solutions to (2.0.1) on the initial datum, the kernel (see Theorem 5) and the velocity (see Theorem 6). These results are collected in Section 2.1, while the technical proofs are deferred to Section 2.2. Finally, in Section 2.3 we show some numerical simulation illustrating the behaviour of the solutions of a non-local traffic flow model, when the size and the position of the kernel support or the velocity function vary. In particular, we analyse the impact on two cost functionals, measuring traffic congestion.

2.1 Main Results

The study of problem (2.0.1) is carried out in the same setting of [5], with slightly strengthened conditions. We recall here briefly the assumptions on the flux function f, on v and on w:

$$f \in \mathbf{C^2}(\mathbb{R}\times\mathbb{R}\times\mathbb{R};\mathbb{R}^+) \quad \text{and} \quad \begin{cases} \sup\limits_{t,x,\rho} \big|\partial_\rho f(t,x,\rho)\big| < +\infty \\ \sup\limits_{t,x} \big|\partial_x f(t,x,\rho)\big| < C|\rho| \\ \sup\limits_{t,x} \big|\partial^2_{xx} f(t,x,\rho)\big| < C|\rho| \\ \forall t,\ x \quad f(t,x,0) = 0 \end{cases} \tag{2.1.1}$$

$$v \in (\mathbf{C^2} \cap \mathbf{W^{2,\infty}})(\mathbb{R};\mathbb{R}) \quad \text{and} \quad \omega \in (\mathbf{C^2} \cap \mathbf{W^{1,1}} \cap \mathbf{W^{2,\infty}})(\mathbb{R};\mathbb{R}). \tag{2.1.2}$$

Throughout the chapter, we make use of the following definition of solution to problem (2.0.1), see also [5, Definition 2.1].

Definition 2. *Let $T > 0$. Fix $\rho_0 \in \mathbf{L}^\infty(\mathbb{R};\mathbb{R})$. A* weak entropy solution *to (2.0.1) on $[0,T]$ is a bounded measurable Kružkov solution $\rho \in \mathbf{C^0}([0,T];\mathbf{L^1_{loc}}(\mathbb{R};\mathbb{R}))$ to*

$$\begin{cases} \partial_t \rho + \partial_x \left(f(t,x,\rho)\, V(t,x) \right) = 0 \\ \rho(0,x) = \rho_0(x) \end{cases} \qquad \text{where} \quad V(t,x) = v((\rho(t) * \omega)(x)),$$

that is, for all $\varphi \in \mathbf{C^1_c}(\mathbb{R}^2;\mathbb{R}^+)$ and $k \in \mathbb{R}$,

$$\int_0^{+\infty} \int_{\mathbb{R}} \Big\{ |\rho - k|\, \partial_t \varphi(t,x) + \operatorname{sgn}(\rho - k) \left(f(t,x,\rho) - f(t,x,k) \right) V(t,x)\, \partial_x \varphi(t,x) \\ - \operatorname{sgn}(\rho - k)\, f(t,x,k)\, \partial_x V(t,x)\, \varphi(t,x) \Big\} dx dt + \int_{\mathbb{R}} |\rho_0(x) - k| \varphi(0,x) dx \geq 0.$$

The results in [5] ensure the existence and uniqueness of solution to (2.0.1) and provides the following *a priori* estimates on the solution.

Lemma 1 ([5, Lemma 2.2, Lemma 2.4, Lemma 2.5])**.** *Let conditions (2.1.1)-(2.1.2) hold. If $\rho_0(x) \geq 0$ for all $x \in \mathbb{R}$, then the solution to (2.0.1) is such that*

- *$\rho(t,x) \geq 0$ for all $(t,x) \in \mathbb{R}^+ \times \mathbb{R}$;*
- *for all $t \in \mathbb{R}^+$,*
$$\left\| \rho(t) \right\|_{\mathbf{L^1}(\mathbb{R};\mathbb{R})} \leq \|\rho_0\|_{\mathbf{L^1}(\mathbb{R};\mathbb{R})};$$
- *for all $t \in \mathbb{R}^+$,*
$$\left\| \rho(t) \right\|_{\mathbf{L}^\infty(\mathbb{R};\mathbb{R})} \leq \|\rho_0\|_{\mathbf{L}^\infty(\mathbb{R};\mathbb{R})}\, e^{\mathcal{L}t}, \tag{2.1.3}$$
where $\mathcal{L} = C\, \|v\|_{\mathbf{L}^\infty(\mathbb{R};\mathbb{R})} + \left\| \partial_\rho f \right\|_{\mathbf{L}^\infty([0,t]\times\mathbb{R}\times\mathbb{R};\mathbb{R})} \left\| v' \right\|_{\mathbf{L}^\infty(\mathbb{R};\mathbb{R})} \|\rho_0\|_{\mathbf{L^1}(\mathbb{R};\mathbb{R})} \left\| \omega' \right\|_{\mathbf{L}^\infty(\mathbb{R};\mathbb{R})}$.

Proposition 4 ([5, Proposition 2.6])**.** *Let conditions (2.1.1)-(2.1.2) hold. If $\rho_0(x) \geq 0$ for all $x \in \mathbb{R}$, then the solution to (2.0.1) satisfies the following total variation estimate: for all $t \in \mathbb{R}^+$*

$$TV(\rho(t)) \leq \left(\mathcal{K}_2\, t + TV(\rho_0) \right) e^{\mathcal{K}_1 t}, \tag{2.1.4}$$

where

$$\begin{aligned} \mathcal{K}_1 &= \left\| \partial^2_{\rho x} f \right\|_{\mathbf{L}^\infty(\Sigma_t;\mathbb{R})} \|v\|_{\mathbf{L}^\infty(\mathbb{R};\mathbb{R})}, \\ \mathcal{K}_2 &= \Bigg[\frac{3}{2} C + \left(\left\| \partial_\rho f \right\|_{\mathbf{L}^\infty(\Sigma_t;\mathbb{R})} + C \right) \left\| \omega' \right\|_{\mathbf{W}^{1,\infty}(\mathbb{R};\mathbb{R})} \|\rho_0\|_{\mathbf{L^1}(\mathbb{R};\mathbb{R})} \\ &\quad + \frac{1}{2} \left(C + \left\| \partial_\rho f \right\|_{\mathbf{L}^\infty(\Sigma_t;\mathbb{R})} \left(2 + \|\rho_0\|_{\mathbf{L^1}(\mathbb{R};\mathbb{R})} \left\| \omega' \right\|_{\mathbf{L}^\infty(\mathbb{R};\mathbb{R})} \right) \right) \left\| \omega' \right\|_{\mathbf{W}^{1,\infty}(\mathbb{R};\mathbb{R})} \Bigg] \\ &\quad \times \|v\|_{\mathbf{W^{2,\infty}}(\mathbb{R};\mathbb{R})} \|\rho_0\|_{\mathbf{L^1}(\mathbb{R};\mathbb{R})}, \end{aligned} \tag{2.1.5}$$

with $\Sigma_t = [0,t] \times \mathbb{R} \times [0, M_t]$ and $M_t = \|\rho_0\|_{\mathbf{L}^\infty(\mathbb{R};\mathbb{R})}\, e^{\mathcal{L}t}$, as in (2.1.3).

Remark 1. The regularity assumptions required in [5] for the functions v and w, see [5, Formula (2.2)], are actually less restrictive than (2.1.2). Indeed, to guarantee the existence of solutions and to obtain the *a priori* estimates above, it is sufficient that

$$v \in (\mathbf{C^2} \cap \mathbf{W^{1,\infty}})(\mathbb{R};\mathbb{R}) \qquad \text{and} \qquad \omega \in (\mathbf{C^2} \cap \mathbf{W^{2,\infty}})(\mathbb{R};\mathbb{R}).$$

Aim of this chapter is to study the stability of solutions to (2.0.1) with respect to both the kernel ω and the velocity function v. The following Theorem states the $\mathbf{L^1}$–Lipschitz continuous dependence of solutions to (2.0.1) on both the initial datum and the kernel function.

Theorem 5. *Let $T > 0$. Fix f and v satisfying (2.1.1) and (2.1.2) respectively. Fix $\rho_0, \tilde{\rho}_0 \in \mathbf{L}^\infty(\mathbb{R};\mathbb{R})$. Let $\omega, \tilde{\omega} \in (\mathbf{C^2} \cap \mathbf{W^{1,1}} \cap \mathbf{W^{2,\infty}})(\mathbb{R};\mathbb{R})$. Call ρ and $\tilde{\rho}$ the solutions, in the sense of Definition 2, to the following problems respectively*

$$\begin{cases} \partial_t \rho + \partial_x (f(t,x,\rho)\, V(t,x)) = 0 \\ \rho(0,x) = \rho_0(x) \end{cases} \quad \text{where} \quad V(t,x) = v((\rho(t) * \omega)(x)), \tag{2.1.6}$$

$$\begin{cases} \partial_t \tilde{\rho} + \partial_x (f(t,x,\tilde{\rho})\, \tilde{V}(t,x)) = 0 \\ \tilde{\rho}(0,x) = \tilde{\rho}_0(x) \end{cases} \quad \text{where} \quad \tilde{V}(t,x) = v((\tilde{\rho}(t) * \tilde{\omega})(x)). \tag{2.1.7}$$

Then, for any $t \in [0,T]$, the following estimate holds

$$\left\|\rho(t) - \tilde{\rho}(t)\right\|_{\mathbf{L^1}(\mathbb{R};\mathbb{R})} \leq \left(\|\rho_0 - \tilde{\rho}_0\|_{\mathbf{L^1}(\mathbb{R};\mathbb{R})} + a(t)\, \|\omega - \tilde{\omega}\|_{\mathbf{W^{1,1}}(\mathbb{R};\mathbb{R})}\right) \exp\left(\int_0^t b(r)dr\right), \tag{2.1.8}$$

where $a(t)$ and $b(t)$ depend on various norms of the initial data and of the functions f, v, ω and $\tilde{\omega}$, see (2.2.54) and (2.2.55).

The $\mathbf{L^1}$–Lipschitz continuous dependence of solutions to (2.0.1) on the velocity function v is ensured by the following Theorem.

Theorem 6. *Let $T > 0$. Fix f and ω satisfying (2.1.1) and (2.1.2) respectively. Fix $\rho_0 \in \mathbf{L}^\infty(\mathbb{R};\mathbb{R})$. Let $v, \tilde{v} \in (\mathbf{C^2} \cap \mathbf{W^{2,\infty}})(\mathbb{R};\mathbb{R})$. Call ρ and $\tilde{\rho}$ the solutions, in the sense of Definition 2, to the following problems respectively*

$$\begin{cases} \partial_t \rho + \partial_x (f(t,x,\rho)\, V(t,x)) = 0 \\ \rho(0,x) = \rho_0(x) \end{cases} \quad \text{where} \quad V(t,x) = v((\rho(t) * \omega)(x)), \tag{2.1.9}$$

$$\begin{cases} \partial_t \tilde{\rho} + \partial_x (f(t,x,\tilde{\rho})\, \tilde{V}(t,x)) = 0 \\ \tilde{\rho}(0,x) = \rho_0(x) \end{cases} \quad \text{where} \quad \tilde{V}(t,x) = \tilde{v}((\tilde{\rho}(t) * \omega)(x)). \tag{2.1.10}$$

Then, for any $t \in [0,T]$, the following estimate holds

$$\left\|\rho(t) - \tilde{\rho}(t)\right\|_{\mathbf{L^1}(\mathbb{R};\mathbb{R})} \leq \left(c_1(t)\, \|v - \tilde{v}\|_{\mathbf{L}^\infty(\mathbb{R};\mathbb{R})} + c_2(t)\, \left\|v' - \tilde{v}'\right\|_{\mathbf{L}^\infty(\mathbb{R};\mathbb{R})}\right) \exp\left(\int_0^t c_3(s)ds\right), \tag{2.1.11}$$

where the $c_i(t)$, $i = 1,2,3$, depend on various norms of the initial data and of the functions f, v, $\tilde{v}$ and ω, see (2.2.60), (2.2.61) and (2.2.62).

2.2 Proofs

The Lemma below is the building block of both Theorem 5 and Theorem 6. We remark that we could also consider the multi-dimensional case, yet leading to a very involved proof.

Lemma 2. *Let $T > 0$. Fix f satisfying (2.1.1) and $V, \tilde{V} \in (\mathbf{C^2} \cap \mathbf{W^{2,\infty}})(\mathbb{R} \times \mathbb{R}; \mathbb{R})$. Fix $\rho_0, \tilde{\rho}_0 \in \mathbf{L}^\infty(\mathbb{R}; \mathbb{R})$. Call ρ and $\tilde{\rho}$ the solutions to the following problems*

$$\begin{cases} \partial_t \rho + \partial_x (f(t,x,\rho)\, V(t,x)) = 0 \\ \rho(0,x) = \rho_0(x) \end{cases} \quad \textit{and} \quad \begin{cases} \partial_t \tilde{\rho} + \partial_x (f(t,x,\tilde{\rho})\, \tilde{V}(t,x)) = 0 \\ \tilde{\rho}(0,x) = \tilde{\rho}_0(x). \end{cases} \tag{2.2.1}$$

Then, for any $\tau, t \in]0,T[$, with $\tau < t$, the following estimate holds

$$\int_{\mathbb{R}} \left|\rho(\tau,x) - \tilde{\rho}(\tau,x)\right| dx - \int_{\mathbb{R}} \left|\rho(t,x) - \tilde{\rho}(t,x)\right| dx \tag{2.2.2}$$

$$\begin{aligned} &+ \int_\tau^t \int_{\mathbb{R}} \Big\{ \left|\partial_x \tilde{V}(s,x) - \partial_x V(s,x)\right| \left| f\left(s,x,\rho(s,x)\right)\right| \\ &\qquad + \left|\tilde{V}(s,x) - V(s,x)\right| \left|\partial_x f\left(s,x,\rho(s,x)\right)\right| \\ &+ \left|\tilde{V}(s,x) - V(s,x)\right| \left|\partial_\rho f\left(s,x,\rho(s,x)\right)\right| \left|\partial_x \rho(s,x)\right| \Big\} dx\, ds \geq\ 0. \end{aligned} \tag{2.2.3}$$

Proof. The proof is based on the *doubling of variables method* introduced by Kružkov in [59]. In particular, we follow the lines of [52, Theorem 1.3], although there the flux function has the form $l(x)\, g(\rho)$, while here it is of the form $f(t,x,\rho)\, V(t,x)$. The dependence on time does not add any difficulties in the proof, while the dependence of f on the space variable x produces additional terms.

Let $\varphi \in \mathbf{C}^\infty_{\mathbf{c}}(]0;T[\times\mathbb{R}; \mathbb{R}^+)$ be a test function as in the definition of solution by Kružkov. Let $Y \in \mathbf{C}^\infty_{\mathbf{c}}(\mathbb{R}; \mathbb{R}^+)$ be such that

$$Y(z) = Y(-z), \qquad Y(z) = 0 \text{ for } |z| \geq 1, \qquad \int_{\mathbb{R}} Y(z) dz = 1,$$

and define $Y_h = \frac{1}{h} Y\left(\frac{z}{h}\right)$. Obviously $Y_h \in \mathbf{C}^\infty_{\mathbf{c}}(\mathbb{R}; \mathbb{R}^+)$, $Y_h(-z) = Y_h(z)$, $Y_h(z) = 0$ for $|z| \geq h$, $\int_{\mathbb{R}} Y_h(z) dz = 1$ and $Y_h \to \delta_0$ as $h \to 0$, where δ_0 is the Dirac delta in 0. Define, for $h > 0$,

$$\psi_h(t,x,s,y) = \varphi\left(\frac{t+s}{2}, \frac{x+y}{2}\right) Y_h(t-s)\, Y_h(x-y) = \varphi(\cdots)\ Y_h(t-s)\, Y_h(x-y). \tag{2.2.4}$$

Introduce the space $\Pi_T =]0,T[\times\mathbb{R}$. We derive the following entropy inequalities for the solutions $\rho = \rho(t,x)$ and $\tilde{\rho} = \tilde{\rho}(s,y)$ to (2.2.1):

$$\begin{aligned} \iiiint\limits_{\Pi_T \times \Pi_T} \Big\{ &|\rho - \tilde{\rho}|\, \partial_t \psi_h(t,x,s,y) + \operatorname{sgn}(\rho - \tilde{\rho}) V(t,x) \left(f(t,x,\rho) - f(t,x,\tilde{\rho})\right) \partial_x \psi_h(t,x,s,y) \\ &+ \operatorname{sgn}(\rho - \tilde{\rho})\, \partial_x \left[f(t,x,\tilde{\rho})\, V(t,x)\right] \psi_h(t,x,s,y) \Big\}\, dx\, dt\, dy\, ds \geq 0 \end{aligned}$$

and

$$\begin{aligned} \iiiint\limits_{\Pi_T \times \Pi_T} \Big\{ &|\tilde{\rho} - \rho|\, \partial_t \psi_h(t,x,s,y) + \operatorname{sgn}(\tilde{\rho} - \rho) \tilde{V}(s,y) \left(f(s,y,\tilde{\rho}) - f(s,y,\rho)\right) \partial_y \psi_h(t,x,s,y) \\ &+ \operatorname{sgn}(\tilde{\rho} - \rho)\, \partial_y \left[f(s,y,\rho)\, \tilde{V}(s,y)\right] \psi_h(t,x,s,y) \Big\}\, dx\, dt\, dy\, ds \geq 0. \end{aligned}$$

Summing the two inequalities above and rearranging the terms therein, relying on the explicit form of the function ψ_h (2.2.4), we obtain

$$\iiiint\limits_{\Pi_T\times\Pi_T}\Big\{\big|\rho(t,x)-\tilde\rho(s,y)\big|\,\partial_t\varphi\,(\cdots)\;Y_h(t-s)\,Y_h(x-y) \tag{2.2.5}$$

$$+\operatorname{sgn}(\rho-\tilde\rho)\Big(V(t,x)f(t,x,\rho)-\tilde V(s,y)f(s,y,\tilde\rho)\Big)\,\partial_x\varphi\,(\cdots)\;Y_h(t-s)\,Y_h(x-y) \tag{2.2.6}$$

$$+\operatorname{sgn}(\rho-\tilde\rho)\Big(\tilde V(s,y)f(s,y,\tilde\rho)-V(t,x)f(t,x,\tilde\rho)\Big)\,\partial_x\psi_h(t,x,s,y) \tag{2.2.7}$$

$$+\operatorname{sgn}(\rho-\tilde\rho)\Big(\tilde V(s,y)f(s,y,\rho)-V(t,x)f(t,x,\rho)\Big)\,\partial_y\psi_h(t,x,s,y) \tag{2.2.8}$$

$$+\operatorname{sgn}(\rho-\tilde\rho)\Big[\partial_y\Big(\tilde V(s,y)\,f(s,y,\rho)\Big)-\partial_x\Big(V(t,x)\,f(t,x,\tilde\rho)\Big)\Big]\,\psi_h(t,x,s,y)\Big\} \tag{2.2.9}$$

$$dx\,dt\,dy\,ds\geq 0.$$

Consider (2.2.7) and (2.2.8): explicit the function ψ_h to obtain

$$\begin{aligned}
&[(2.2.7)]+[(2.2.8)]\\
&=\frac{\operatorname{sgn}(\rho-\tilde\rho)}{2}\tilde V(s,y)\big(f(s,y,\tilde\rho)+f(s,y,\rho)\big)\,\partial_x\varphi(\cdots)\,Y_h(t-s)\,Y_h(x-y) && (2.2.10)\\
&\quad-\frac{\operatorname{sgn}(\rho-\tilde\rho)}{2}V(t,x)\big(f(t,x,\tilde\rho)+f(t,x,\rho)\big)\,\partial_x\varphi(\cdots)\,Y_h(t-s)\,Y_h(x-y) && (2.2.11)\\
&\quad-\operatorname{sgn}(\rho-\tilde\rho)\tilde V(s,y)\big(f(s,y,\tilde\rho)-f(s,y,\rho)\big)\,\varphi(\cdots)\,Y_h(t-s)\,Y_h'(x-y) && (2.2.12)\\
&\quad+\operatorname{sgn}(\rho-\tilde\rho)V(t,x)\big(f(t,x,\rho)-f(t,x,\tilde\rho)\big)\,\varphi(\cdots)\,Y_h(t-s)\,Y_h'(x-y). && (2.2.13)
\end{aligned}$$

In (2.2.9) compute

$$\begin{aligned}
[(2.2.9)]=\;&\operatorname{sgn}(\rho-\tilde\rho)\Big[\partial_y\tilde V(s,y)\,f(s,y,\rho)+\tilde V(s,y)\,\partial_y f(s,y,\rho)\\
&\qquad-\partial_x V(t,x)\,f(t,x,\tilde\rho)-V(t,x)\,\partial_x f(t,x,\tilde\rho)\Big]\psi_h(t,x,s,y).
\end{aligned}\tag{2.2.14}$$

Introduce the following notation

$$F\left(t,x,\rho(t,x),\tilde\rho(s,y)\right)=\operatorname{sgn}\left(\rho(t,x)-\tilde\rho(s,y)\right)\Big(f\left(t,x,\rho(t,x)\right)-f\left(t,x,\tilde\rho(s,y)\right)\Big), \tag{2.2.15}$$

so that (2.2.12) – (2.2.13) now reads

$$\begin{aligned}
&\iiiint\limits_{\Pi_T\times\Pi_T}[(2.2.12)]+[(2.2.13)]dx\,dt\,dy\,ds\\
&=\iiiint\limits_{\Pi_T\times\Pi_T}\Big(V(t,x)F(t,x,\rho,\tilde\rho)-\tilde V(s,y)F(s,y,\rho,\tilde\rho)\Big)\,\varphi(\cdots)\,Y_h(t-s)\,Y_h'(x-y)dx\,dt\,dy\,ds\\
&=-\iiiint\limits_{\Pi_T\times\Pi_T}\Big(V(t,x)\frac{\mathrm{d}}{dx}F(t,x,\rho,\tilde\rho)-\tilde V(s,y)\frac{\mathrm{d}}{dx}F(s,y,\rho,\tilde\rho)\Big)\,\psi_h(t,x,s,y)dx\,dt\,dy\,ds && (2.2.16)\\
&\quad-\iiiint\limits_{\Pi_T\times\Pi_T}\partial_x V(t,x)\,F(t,x,\rho,\tilde\rho)\,\psi_h(t,x,s,y)dx\,dt\,dy\,ds && (2.2.17)
\end{aligned}$$

$$-\iiiint_{\Pi_T\times\Pi_T}\frac{1}{2}\Big(V(t,x)F(t,x,\rho,\tilde\rho)-\tilde V(s,y)F(s,y,\rho,\tilde\rho)\Big)\,\partial_x\varphi(\cdots) \times Y_h(t-s)\,Y_h(x-y)dx\,dt\,dy\,ds, \tag{2.2.18}$$

where we also integrate by parts. Combine the integrand of (2.2.17) together with (2.2.14) to get

$$\begin{aligned}&-\partial_x V(t,x)\,F(t,x,\rho,\tilde\rho)\,\psi_h(t,x,s,y)+[(2.2.14)]\\ =\;&\operatorname{sgn}(\rho-\tilde\rho)\Big(\partial_y\tilde V(s,y)\,f(s,y,\rho)-\partial_x V(t,x)\,f(t,x,\rho)\Big)\,\psi_h(t,x,s,y) &(2.2.19)\\ &+\operatorname{sgn}(\rho-\tilde\rho)\Big(\tilde V(s,y)\,\partial_y f(s,y,\rho)-V(t,x)\partial_x f(t,x,\tilde\rho)\Big)\,\psi_h(t,x,s,y). &(2.2.20)\end{aligned}$$

Observe that the following equality holds

$$\begin{aligned}&\iiiint_{\Pi_T\times\Pi_T}[(2.2.6)]+[(2.2.10)]+[(2.2.11)]+[(2.2.18)]dx\,dt\,dy\,ds\\ =\;&\iiiint_{\Pi_T\times\Pi_T}\operatorname{sgn}(\rho-\tilde\rho)\,\tilde V(s,y)\big(f(s,y,\rho)-f(s,y,\tilde\rho)\big)\,\partial_x\varphi(\cdots)\,Y_h(t-s)\,Y_h(x-y)dx\,dt\,dy\,ds.\end{aligned} \tag{2.2.21}$$

We are therefore left with

$$\iiiint_{\Pi_T\times\Pi_T}[(2.2.5)]+[(2.2.16)]+[(2.2.19)]+[(2.2.20)]+[(2.2.21)]dx\,dt\,dy\,ds\geq 0. \tag{2.2.22}$$

Let now h go to 0. The terms in (2.2.5) and (2.2.21) can be treated exactly as in [59], leading to

$$\begin{aligned}&\lim_{h\to 0+}\iiiint_{\Pi_T\times\Pi_T}\big\{[(2.2.5)]+[(2.2.21)]\big\}\,dx\,dt\,dy\,ds\\ =\;&\iint_{\Pi_T}\Big\{\big|\rho(t,x)-\tilde\rho(t,x)\big|\partial_t\varphi(t,x) &(2.2.23)\\ &+\operatorname{sgn}\big(\rho(t,x)-\tilde\rho(t,x)\big)\,\tilde V(t,x)\Big(f\big(t,x,\rho(t,x)\big)-f\big(t,x,\tilde\rho(t,x)\big)\Big)\,\partial_x\varphi(t,x)\Big\}dx\,dt. &(2.2.24)\end{aligned}$$

Regarding (2.2.19), we simplify the notation by introducing the map

$$\Upsilon_1(t,x,s,y)=\operatorname{sgn}\big(\rho(t,x)-\tilde\rho(s,y)\big)\Big(\partial_y\tilde V(s,y)f\,(s,y,\rho)-\partial_x V(t,x)f\,(t,x,\rho)\Big)\,\varphi\bigg(\frac{t+s}{2},\frac{x+y}{2}\bigg),$$

so that

$$\begin{aligned}&[(2.2.19)]\\ =\;&\Upsilon_1(t,x,s,y)\,Y_h(t-s)\,Y_h(x-y)\end{aligned}$$

$$= \Upsilon_1(t,x,t,x)\, Y_h(t-s)\, Y_h(x-y) + \big(\Upsilon_1(t,x,s,y) - \Upsilon_1(t,x,t,x)\big)\; Y_h(t-s)\, Y_h(x-y)$$

$$= \operatorname{sgn}\big(\rho(t,x) - \tilde\rho(t,x)\big)\Big(\partial_x \tilde V(t,x) - \partial_x V(t,x)\Big)\, f\,(t,x,\rho)\, \varphi(t,x)\; Y_h(t-s)\, Y_h(x-y) \tag{2.2.25}$$

$$+ \big(\Upsilon_1(t,x,s,y) - \Upsilon_1(t,x,t,x)\big)\; Y_h(t-s)\, Y_h(x-y). \tag{2.2.26}$$

It is immediate to see that

$$\iiiint\limits_{\Pi_T\times\Pi_T} [(2.2.25)]\,dxdtdyds$$

$$= \iint\limits_{\Pi_T} \operatorname{sgn}\big(\rho(t,x) - \tilde\rho(t,x)\big)\Big(\partial_x \tilde V(t,x) - \partial_x V(t,x)\Big)\, f\,\big(t,x,\rho(t,x)\big)\; \varphi(t,x)\,dxdt. \tag{2.2.27}$$

Concerning (2.2.26), it vanishes as h goes to 0 when integrated over $\Pi_T \times \Pi_T$. Indeed, recall that $|Y_h| \le \big(Y(0)/h\big)\,\chi_{[-h,h]}$ (where χ_I denotes the characteristic function of the interval $I \subseteq \mathbb{R}$) and apply [36, Lemma 6.2], see also [59, Lemma 2], with $N = 3$, $X = (x,t,x)$, $Y = (x,t,y)$ and

$$w(s,Y) = \frac{\big(Y(0)\big)^2}{h^2}\,\Upsilon_1(t,x,s,y).$$

Focus the attention on (2.2.16). With abuse of notation, since the function F is only Lipschitz continuous with respect to ρ, we write

$$\frac{\mathrm{d}}{dx} F\,\big(t,x,\rho(t,x),\tilde\rho(s,y)\big)$$

$$= \partial_x F\,\big(t,x,\rho(t,x),\tilde\rho(s,y)\big) + \partial_\rho F\,\big(t,x,\rho(t,x),\tilde\rho(s,y)\big)\,\partial_x\rho(t,x)$$

$$= \operatorname{sgn}\big(\rho(t,x) - \tilde\rho(s,y)\big)\Big(\partial_x f\,\big(t,x,\rho(t,x)\big) - \partial_x f\,\big(t,x,\tilde\rho(s,y)\big)\Big) \tag{2.2.28}$$

$$+ \partial_\rho F\,\big(t,x,\rho(t,x),\tilde\rho(s,y)\big)\,\partial_x\rho(t,x) \tag{2.2.29}$$

and

$$\frac{\mathrm{d}}{dx} F\,\big(s,y,\rho(t,x),\tilde\rho(s,y)\big)$$

$$= \partial_\rho F\,\big(s,y,\rho(t,x),\tilde\rho(s,y)\big)\,\partial_x\rho(t,x)$$

$$= \partial_\rho F\,\big(t,x,\rho(t,x),\tilde\rho(t,x)\big)\,\partial_x\rho(t,x) \tag{2.2.30}$$

$$+ \Big(\partial_\rho F\,\big(s,y,\rho(t,x),\tilde\rho(s,y)\big) - \partial_\rho F\,\big(t,x,\rho(t,x),\tilde\rho(t,x)\big)\Big)\,\partial_x\rho(t,x). \tag{2.2.31}$$

Above, the derivatives $\partial_\rho F$ and $\partial_x\rho$ should be intended in the sense of measures, see [13, Lemma A2.1] and [52, Lemma 4.1] for further details. In particular observe that we can combine (2.2.20) with (2.2.28) to get

$$[(2.2.20)] - V(t,x)\operatorname{sgn}\big(\rho(t,x) - \tilde\rho(s,y)\big)\Big(\partial_x f\,\big(t,x,\rho(t,x)\big) - \partial_x f\,\big(t,x,\tilde\rho(s,y)\big)\Big)\,\psi_h(t,x,s,y)$$

$$= \operatorname{sgn}\big(\rho(t,x) - \tilde\rho(s,y)\big)\Big(\tilde V(s,y)\partial_y f\,(s,y,\rho) - V(t,x)\partial_x f\,(t,x,\rho)\Big)\,\psi_h(t,x,s,y). \tag{2.2.32}$$

An application of [36, Lemma 6.2] yields

$$\begin{aligned}&\lim_{h\to 0}\iiiint_{\Pi_T\times\Pi_T}[(2.2.32)]dx\,dt\,dy\,ds\\ &=\iint_{\Pi_T}\operatorname{sgn}\left(\rho(t,x)-\tilde\rho(t,x)\right)\left(\tilde V(t,x)-V(t,x)\right)\partial_x f\left(t,x,\rho(t,x)\right)\varphi(t,x)dx\,dt.\end{aligned}\tag{2.2.33}$$

In order to deal with the remaining terms, i.e. (2.2.29), (2.2.30) and (2.2.31), we need to introduce a regularisation of the sign function. In particular, for $\alpha>0$ set

$$s_\alpha(u)=\left(\operatorname{sgn}*Y_\alpha\right)(u).$$

Observe that $s'_\alpha(u)=\dfrac{2}{\alpha}\,Y\left(\dfrac{u}{\alpha}\right)$. Recall the definition of the map F (2.2.15) and compute

$$\begin{aligned}&\iiiint_{\Pi_T\times\Pi_T}-V(t,x)\times[(2.2.29)]\times\psi_h(t,x,s,y)dxdtdyds\\ &=\lim_{\alpha\to 0}\iiiint_{\Pi_T\times\Pi_T}\Big\{s'_\alpha\left(\rho(t,x)-\tilde\rho(s,y)\right)\left(f\left(t,x,\rho(t,x)\right)-f\left(t,x,\tilde\rho(s,y)\right)\right)&(2.2.34)\\ &\qquad+s_\alpha\left(\rho(t,x)-\tilde\rho(s,y)\right)\partial_\rho f\left(t,x,\rho(t,x)\right)\Big\}&(2.2.35)\\ &\qquad\times\left(-V(t,x)\right)\partial_x\rho(t,x)\psi_h(t,x,s,y)dx\,dt\,dy\,ds.&(2.2.36)\end{aligned}$$

By the Dominated Convergence Theorem, as α goes to 0, since

$$\begin{aligned}&\left|\frac{2}{\alpha}\,Y\left(\frac{\rho-\tilde\rho}{\alpha}\right)\left(f\left(t,x,\rho(t,x)\right)-f\left(t,x,\tilde\rho(s,y)\right)\right)V(t,x)\,\partial_x\rho(t,x)\,\psi_h(t,x,s,y)\right|\\ &\le\frac{2}{\alpha}\,Y\left(\frac{\rho-\tilde\rho}{\alpha}\right)\int_{\tilde\rho}^{\rho}\left|\partial_\rho f(s,y,r)\right|dr\,\|V\|_{\mathbf{L}^\infty(\Pi_T;\mathbb{R})}\left|\partial_x\rho(t,x)\right|\psi_h(t,x,s,y)\\ &\le 2\,\|Y\|_{\mathbf{L}^\infty(\mathbb{R};\mathbb{R})}\left\|\partial_\rho f\right\|_{\mathbf{L}^\infty(\Pi_T\times\mathbb{R};\mathbb{R})}\|V\|_{\mathbf{L}^\infty(\Pi_T;\mathbb{R})}\left|\partial_x\rho(t,x)\right|\psi_h(t,x,s,y)\quad\in\mathbf{L^1}(\Pi_T\times\Pi_T;\mathbb{R}),\end{aligned}$$

we get

$$\iiiint_{\Pi_T\times\Pi_T}[(2.2.34)]\times[(2.2.36)]dx\,dt\,dy\,ds\to 0.$$

Therefore we have

$$\begin{aligned}&\iiiint_{\Pi_T\times\Pi_T}-V(t,x)\times[(2.2.29)]\times\psi_h(t,x,s,y)dx\,dt\,dy\,ds\\ &=-\iiiint_{\Pi_T\times\Pi_T}\operatorname{sgn}\left(\rho(t,x)-\tilde\rho(s,y)\right)V(t,x)\,\partial_\rho f\left(t,x,\rho(t,x)\right)\partial_x\rho(t,x)\,\psi_h(t,x,s,y)dx\,dt\,dy\,ds.\end{aligned}\tag{2.2.37}$$

The term

$$\iiiint_{\Pi_T\times\Pi_T}\tilde V(s,y)\times[(2.2.30)]\times\psi_h(t,x,s,y)dx\,dt\,dy\,ds$$

can be treated exactly in the same way, leading to

$$\iiiint\limits_{\Pi_T\times\Pi_T} \operatorname{sgn}\big(\rho(t,x)-\tilde\rho(t,x)\big)\,\tilde V(s,y)\,\partial_\rho f\left(t,x,\rho(t,x)\right)\partial_x\rho(t,x)\,\psi_h(t,x,s,y)dx\,dt\,dy\,ds. \tag{2.2.38}$$

Introduce now the notation

$$\Upsilon_2(s,y)=\operatorname{sgn}\big(\rho(t,x)-\tilde\rho(t,x)\big)\,\tilde V(s,y)-\operatorname{sgn}\big(\rho(t,x)-\tilde\rho(s,y)\big)\,V(t,x)$$

and apply [36, Lemma 6.2]:

$$\begin{aligned}&\lim_{h\to0}[(2.2.38)]+[(2.2.37)]\\ &=\iint\limits_{\Pi_T}\operatorname{sgn}\big(\rho(t,x)-\tilde\rho(t,x)\big)\Big(\tilde V(t,x)-V(t,x)\Big)\,\partial_\rho f\left(t,x,\rho(t,x)\right)\,\partial_x\rho(t,x)\,\varphi(t,x)dx\,dt.\end{aligned} \tag{2.2.39}$$

In order to deal with the last term, i.e. (2.2.31), exploit the same regularisation of the sign function as above and compute

$$\iiiint\limits_{\Pi_T\times\Pi_T}\tilde V(s,y)\times[(2.2.31)]\times\psi_h(t,x,s,y)dx\,dt\,dy\,ds \tag{2.2.40}$$

$$=\lim_{\alpha\to0}\iiiint\limits_{\Pi_T\times\Pi_T}\Big[s'_\alpha\left(\rho(t,x)-\tilde\rho(s,y)\right)\Big(f\left(s,y,\rho(t,x)\right)-f\left(s,y,\tilde\rho(s,y)\right)\Big) \tag{2.2.41}$$

$$-s'_\alpha\left(\rho(t,x)-\tilde\rho(t,x)\right)\Big(f\left(t,x,\rho(t,x)\right)-f\left(t,x,\tilde\rho(t,x)\right)\Big) \tag{2.2.42}$$

$$+s_\alpha\left(\rho(t,x)-\tilde\rho(s,y)\right)\partial_\rho f\left(s,y,\rho(t,x)\right)$$

$$-s_\alpha\left(\rho(t,x)-\tilde\rho(t,x)\right)\partial_\rho f\left(t,x,\rho(t,x)\right)\Big]$$

$$\times\tilde V(s,y)\,\partial_x\rho(t,x)\,\psi_h(t,x,s,y)dx\,dt\,dy\,ds. \tag{2.2.43}$$

By the Dominated Convergence Theorem, as α goes to 0, we get

$$\iiiint\limits_{\Pi_T\times\Pi_T}[(2.2.41)]\times[(2.2.43)]dx\,dt\,dy\,ds\to0,\quad \iiiint\limits_{\Pi_T\times\Pi_T}[(2.2.42)]\times[(2.2.43)]dx\,dt\,dy\,ds\to0.$$

Indeed,

$$\begin{aligned}&\left|\frac{2}{\alpha}\,Y\left(\frac{\rho-\tilde\rho}{\alpha}\right)\Big(f\left(s,y,\rho(t,x)\right)-f\left(s,y,\tilde\rho(s,y)\right)\Big)\tilde V(s,y)\,\partial_x\rho(t,x)\,\psi_h(t,x,s,y)\right|\\ &\le\frac{2}{\alpha}\,Y\left(\frac{\rho-\tilde\rho}{\alpha}\right)\int_{\tilde\rho}^{\rho}\left|\partial_\rho f(s,y,r)\right|dr\left\|\tilde V\right\|_{\mathbf{L}^\infty(\Pi_T;\mathbb{R})}\left|\partial_x\rho(t,x)\right|\psi_h(t,x,s,y)\\ &\le2\left\|Y\right\|_{\mathbf{L}^\infty(\mathbb{R};\mathbb{R})}\left\|\partial_\rho f\right\|_{\mathbf{L}^\infty(\Pi_T\times\mathbb{R};\mathbb{R})}\left\|\tilde V\right\|_{\mathbf{L}^\infty(\Pi_T;\mathbb{R})}\left|\partial_x\rho(t,x)\right|\psi_h(t,x,s,y)\quad\in\mathbf{L^1}(\Pi_T\times\Pi_T;\mathbb{R}).\end{aligned}$$

Therefore we have

[(2.2.40)]

$$= \iiiint\limits_{\Pi_T\times\Pi_T} \Big[\operatorname{sgn}\big(\rho(t,x)-\tilde\rho(s,y)\big)\,\partial_\rho f\,\big(s,y,\rho(t,x)\big) - \operatorname{sgn}\big(\rho(t,x)-\tilde\rho(t,x)\big)\,\partial_\rho f\,\big(t,x,\rho(t,x)\big)\Big] \times \tilde V(s,y)\,\partial_x\rho(t,x)\,\psi_h(t,x,s,y)dx\,dt\,dy\,ds.$$

Introduce the notation $\Upsilon_3(s,y) = \operatorname{sgn}\big(\rho(t,x)-\tilde\rho(s,y)\big)\,\partial_\rho f\,\big(s,y,\rho(t,x)\big)$ and bound the above quantity as follows

$$[(2.2.40)] \le \left\|\tilde V\right\|_{\mathbf{L}^\infty(\Pi_T;\mathbb{R})} \iiiint\limits_{\Pi_T\times\Pi_T} \big|\Upsilon_3(s,y)-\Upsilon_3(t,x)\big|\big|\partial_x\rho(t,x)\big|\,\psi_h(t,x,s,y)dx\,dt\,dy\,ds,$$

the left hand side clearly vanishing as h goes to 0, thanks to [36, Lemma 6.2] and to the fact that ρ has bounded variation.

Collecting together all the estimates obtained in (2.2.23), (2.2.24), (2.2.27), (2.2.33) and (2.2.39), we get

$$\begin{aligned}
&\lim_{h\to0}[(2.2.22)]\\
&= \iint\limits_{\Pi_T} \Big\{\big|\rho(t,x)-\tilde\rho(t,x)\big|\partial_t\varphi(t,x) \qquad (2.2.44)\\
&\quad + \operatorname{sgn}\big(\rho(t,x)-\tilde\rho(t,x)\big)\,\tilde V(t,x)\,\Big(f\,\big(t,x,\rho(t,x)\big)-f\,\big(t,x,\tilde\rho(t,x)\big)\Big)\,\partial_x\varphi(t,x)\\
&\quad + \operatorname{sgn}\big(\rho(t,x)-\tilde\rho(t,x)\big)\,\Big(\partial_x\tilde V(t,x)-\partial_x V(t,x)\Big)\,f\,(t,x,\rho)\,\varphi(t,x)\\
&\quad + \operatorname{sgn}\big(\rho(t,x)-\tilde\rho(t,x)\big)\,\Big(\tilde V(t,x)-V(t,x)\Big)\,\partial_x f\,\big(t,x,\rho(t,x)\big)\,\varphi(t,x)\\
&\quad + \operatorname{sgn}\big(\rho(t,x)-\tilde\rho(t,x)\big)\Big(\tilde V(t,x)-V(t,x)\Big)\partial_\rho f\,\big(t,x,\rho(t,x)\big)\;\partial_x\rho(t,x)\,\varphi\,(t,x)\Big\}dx\,dt. \qquad (2.2.45)
\end{aligned}$$

Let now $h>0$ and $r>1$. Fix $0<\tau<t<T$, define

$$\Phi_h(s) = \alpha_h(s-\tau)-\alpha_h(s-t), \qquad \text{where} \quad \alpha_h(z) = \int_{-\infty}^{z} Y_h(\zeta)\,\mathrm{d}\zeta\,,$$

and

$$\Psi_r(x) = \int_{\mathbb{R}} Y(|x-y|)\,\chi_{\{|y|<r\}}(y)dy.$$

Observe that, as h goes to 0, $\Phi_h \to \chi_{[\tau,t]}$, and $\Phi_h' \to \delta_\tau-\delta_t$. Moreover, $\Psi_r'(x)=0$ for $|x|<r-1$ or $|x|>r+1$ and, as r tends to $+\infty$, $\Psi_r\to\chi_{\mathbb{R}}$. Choose $\varphi(t,x)=\Phi_h(t)\,\Psi_r(x)$ in $[(2.2.44)\cdots(2.2.45)]$ and pass to the limits $h\to0$ and $r\to+\infty$ to obtain the desired estimate [(2.2.2)–(2.2.3)]:

$$\begin{aligned}
&\int_{\mathbb{R}}\big|\rho(\tau,x)-\tilde\rho(\tau,x)\big|dx - \int_{\mathbb{R}}\big|\rho(t,x)-\tilde\rho(t,x)\big|dx\\
&+\int_\tau^t\int_{\mathbb{R}}\Big\{\Big|\partial_x\tilde V(s,x)-\partial_x V(s,x)\Big|\,\Big|f\,\big(s,x,\rho(s,x)\big)\Big|\\
&\qquad +\Big|\tilde V(s,x)-V(s,x)\Big|\,\Big|\partial_x f\,\big(s,x,\rho(s,x)\big)\Big|
\end{aligned}$$

$$+\Big|\tilde V(s,x)-V(s,x)\Big|\,\Big|\partial_\rho f\left(s,x,\rho(s,x)\right)\Big|\,\big|\partial_x\rho(s,x)\big|\Big\}dx\,ds\geq\ 0.$$

□

Proof of Theorem 5. We can apply Lemma 2 to problems (2.1.6) and (2.1.7). By Lemma 1, with obvious notation, for all $t\in[0,T]$ we have

$$\big\|\rho(t)\big\|_{\mathbf{L}^\infty(\mathbb{R};\mathbb{R})}\leq\|\rho_0\|_{\mathbf{L}^\infty(\mathbb{R};\mathbb{R})}\,e^{\mathcal{L}\,t}=M_t,\qquad\big\|\tilde\rho(t)\big\|_{\mathbf{L}^\infty(\mathbb{R};\mathbb{R})}\leq\|\tilde\rho_0\|_{\mathbf{L}^\infty(\mathbb{R};\mathbb{R})}\,e^{\tilde{\mathcal{L}}\,t}=\tilde M_t.$$

For the sake of simplicity introduce the space

$$\Sigma_t=[0,t]\times\mathbb{R}\times[0,\max\{M_t,\tilde M_t\}].\tag{2.2.46}$$

Let $\tau\to0$ in [(2.2.2)$\cdots$(2.2.3)]:

$$\begin{aligned}\big\|\rho(t)-\tilde\rho(t)\big\|_{\mathbf{L}^1(\mathbb{R};\mathbb{R})}&\leq\|\rho_0-\tilde\rho_0\|_{\mathbf{L}^1(\mathbb{R};\mathbb{R})}&(2.2.47)\\&+\int_0^t\|f\|_{\mathbf{L}^\infty(\Sigma_s;\mathbb{R})}\int_{\mathbb{R}}\Big|\partial_xV(s,x)-\partial_x\tilde V(s,x)\Big|dxds&(2.2.48)\\&+\int_0^t\|\partial_xf\|_{\mathbf{L}^\infty(\Sigma_s;\mathbb{R})}\int_{\mathbb{R}}\Big|\tilde V(s,x)-V(s,x)\Big|dxds&(2.2.49)\\&+\int_0^t\big\|\partial_\rho f\big\|_{\mathbf{L}^\infty(\Sigma_s;\mathbb{R})}\int_{\mathbb{R}}\big|\partial_x\rho(s,x)\big|\,\Big|V(s,x)-\tilde V(s,x)\Big|dxds.&(2.2.50)\end{aligned}$$

Consider (2.2.48). By the definitions of V and $\tilde V$, compute

$$\begin{aligned}&\int_{\mathbb{R}}\Big|\partial_xV(s,x)-\partial_x\tilde V(s,x)\Big|dx\\=&\int_{\mathbb{R}}\Big|v'((\rho(s)*\omega)(x))\ \big(\rho(s)*\partial_x\omega\big)(x)-v'((\tilde\rho(s)*\tilde\omega)(x))\ \big(\tilde\rho(s)*\partial_x\tilde\omega\big)(x)\Big|dx\\\leq&\big\|v'\big\|_{\mathbf{L}^\infty(\mathbb{R};\mathbb{R})}\left(\big\|\rho(s)-\tilde\rho(s)\big\|_{\mathbf{L}^1(\mathbb{R};\mathbb{R})}\ \min\Big\{\|\partial_x\omega\|_{\mathbf{L}^1(\mathbb{R};\mathbb{R})},\|\partial_x\tilde\omega\|_{\mathbf{L}^1(\mathbb{R};\mathbb{R})}\Big\}\right.\\&\qquad\left.+\|\partial_x\omega-\partial_x\tilde\omega\|_{\mathbf{L}^1(\mathbb{R};\mathbb{R})}\ \min\Big\{\big\|\rho(s)\big\|_{\mathbf{L}^1(\mathbb{R};\mathbb{R})},\big\|\tilde\rho(s)\big\|_{\mathbf{L}^1(\mathbb{R};\mathbb{R})}\Big\}\right)\\&+\ \big\|v''\big\|_{\mathbf{L}^\infty(\mathbb{R};\mathbb{R})}\min\Big\{\big\|\rho(s)\big\|_{\mathbf{L}^1(\mathbb{R};\mathbb{R})}\|\partial_x\omega\|_{\mathbf{L}^\infty(\mathbb{R};\mathbb{R})},\big\|\tilde\rho(s)\big\|_{\mathbf{L}^1(\mathbb{R};\mathbb{R})}\|\partial_x\tilde\omega\|_{\mathbf{L}^\infty(\mathbb{R};\mathbb{R})}\Big\}\\&\quad\times\left(\big\|\rho(s)-\tilde\rho(s)\big\|_{\mathbf{L}^1(\mathbb{R};\mathbb{R})}\ \min\Big\{\|\omega\|_{\mathbf{L}^1(\mathbb{R};\mathbb{R})},\|\tilde\omega\|_{\mathbf{L}^1(\mathbb{R};\mathbb{R})}\Big\}\right.\\&\qquad\left.+\|\omega-\tilde\omega\|_{\mathbf{L}^1(\mathbb{R};\mathbb{R})}\ \min\Big\{\big\|\rho(s)\big\|_{\mathbf{L}^1(\mathbb{R};\mathbb{R})},\big\|\tilde\rho(s)\big\|_{\mathbf{L}^1(\mathbb{R};\mathbb{R})}\Big\}\right)\\\leq&\left(\big\|v'\big\|_{\mathbf{L}^\infty(\mathbb{R};\mathbb{R})}+\big\|v''\big\|_{\mathbf{L}^\infty(\mathbb{R};\mathbb{R})}\min\Big\{\|\rho_0\|_{\mathbf{L}^1(\mathbb{R};\mathbb{R})}\|\partial_x\omega\|_{\mathbf{L}^\infty(\mathbb{R};\mathbb{R})},\|\tilde\rho_0\|_{\mathbf{L}^1(\mathbb{R};\mathbb{R})}\|\partial_x\tilde\omega\|_{\mathbf{L}^\infty(\mathbb{R};\mathbb{R})}\Big\}\right)\\&\quad\times\left(\big\|\rho(s)-\tilde\rho(s)\big\|_{\mathbf{L}^1(\mathbb{R};\mathbb{R})}\min\Big\{\|\omega\|_{\mathbf{W}^{1,1}(\mathbb{R};\mathbb{R})},\|\tilde\omega\|_{\mathbf{W}^{1,1}(\mathbb{R};\mathbb{R})}\Big\}\right.\\&\qquad\left.+\|\omega-\tilde\omega\|_{\mathbf{W}^{1,1}(\mathbb{R};\mathbb{R})}\ \min\Big\{\|\rho_0\|_{\mathbf{L}^1(\mathbb{R};\mathbb{R})},\|\tilde\rho_0\|_{\mathbf{L}^1(\mathbb{R};\mathbb{R})}\Big\}\right),\end{aligned}$$

where we exploit also Lemma 1. Therefore,

$$
\begin{aligned}
&[(2.2.48)]\\
\leq\ &\left(\left\|v'\right\|_{\mathbf{L}^\infty(\mathbb{R};\mathbb{R})}+\left\|v''\right\|_{\mathbf{L}^\infty(\mathbb{R};\mathbb{R})}\min\left\{\|\rho_0\|_{\mathbf{L^1}(\mathbb{R};\mathbb{R})}\|\partial_x\omega\|_{\mathbf{L}^\infty(\mathbb{R};\mathbb{R})},\|\tilde\rho_0\|_{\mathbf{L^1}(\mathbb{R};\mathbb{R})}\|\partial_x\tilde\omega\|_{\mathbf{L}^\infty(\mathbb{R};\mathbb{R})}\right\}\right)\\
&\times\left(\min\left\{\|\omega\|_{\mathbf{W^{1,1}}(\mathbb{R};\mathbb{R})},\|\tilde\omega\|_{\mathbf{W^{1,1}}(\mathbb{R};\mathbb{R})}\right\}\int_0^t\|f\|_{\mathbf{L}^\infty(\Sigma_s;\mathbb{R})}\left\|\rho(s)-\tilde\rho(s)\right\|_{\mathbf{L^1}(\mathbb{R};\mathbb{R})}ds\right.\qquad(2.2.51)\\
&\qquad\left.+\|\omega-\tilde\omega\|_{\mathbf{W^{1,1}}(\mathbb{R};\mathbb{R})}\|f\|_{\mathbf{L}^\infty(\Sigma_t;\mathbb{R})}\min\left\{\|\rho_0\|_{\mathbf{L^1}(\mathbb{R};\mathbb{R})},\|\tilde\rho_0\|_{\mathbf{L^1}(\mathbb{R};\mathbb{R})}\right\}t\right).
\end{aligned}
$$

Consider (2.2.49): compute

$$
\begin{aligned}
\int_{\mathbb{R}}\left|V(s,x)-\tilde V(s,x)\right|dx&\leq\left\|v'\right\|_{\mathbf{L}^\infty(\mathbb{R};\mathbb{R})}\min\left\{\|\omega\|_{\mathbf{L^1}(\mathbb{R};\mathbb{R})},\|\tilde\omega\|_{\mathbf{L^1}(\mathbb{R};\mathbb{R})}\right\}\left\|\rho(s)-\tilde\rho(s)\right\|_{\mathbf{L^1}(\mathbb{R};\mathbb{R})}\\
&\quad+\left\|v'\right\|_{\mathbf{L}^\infty(\mathbb{R};\mathbb{R})}\min\left\{\left\|\rho(s)\right\|_{\mathbf{L^1}(\mathbb{R};\mathbb{R})},\left\|\tilde\rho(s)\right\|_{\mathbf{L^1}(\mathbb{R};\mathbb{R})}\right\}\|\omega-\tilde\omega\|_{\mathbf{L^1}(\mathbb{R};\mathbb{R})}\\
&\leq\left\|v'\right\|_{\mathbf{L}^\infty(\mathbb{R};\mathbb{R})}\min\left\{\|\omega\|_{\mathbf{L^1}(\mathbb{R};\mathbb{R})},\|\tilde\omega\|_{\mathbf{L^1}(\mathbb{R};\mathbb{R})}\right\}\left\|\rho(s)-\tilde\rho(s)\right\|_{\mathbf{L^1}(\mathbb{R};\mathbb{R})}\\
&\quad+\left\|v'\right\|_{\mathbf{L}^\infty(\mathbb{R};\mathbb{R})}\min\left\{\|\rho_0\|_{\mathbf{L^1}(\mathbb{R};\mathbb{R})},\|\tilde\rho_0\|_{\mathbf{L^1}(\mathbb{R};\mathbb{R})}\right\}\|\omega-\tilde\omega\|_{\mathbf{L^1}(\mathbb{R};\mathbb{R})}.
\end{aligned}
$$

In this way we have

$$
\begin{aligned}
&[(2.2.49)]\leq\\
&\quad\left\|v'\right\|_{\mathbf{L}^\infty(\mathbb{R};\mathbb{R})}\min\left\{\|\omega\|_{\mathbf{L^1}(\mathbb{R};\mathbb{R})},\|\tilde\omega\|_{\mathbf{L^1}(\mathbb{R};\mathbb{R})}\right\}\int_0^t\|\partial_xf\|_{\mathbf{L}^\infty(\Sigma_s;\mathbb{R})}\left\|\rho(s)-\tilde\rho(s)\right\|_{\mathbf{L^1}(\mathbb{R};\mathbb{R})}ds\\
&\quad+\|\partial_xf\|_{\mathbf{L}^\infty(\Sigma_t;\mathbb{R})}\left\|v'\right\|_{\mathbf{L}^\infty(\mathbb{R};\mathbb{R})}\min\left\{\|\rho_0\|_{\mathbf{L^1}(\mathbb{R};\mathbb{R})},\|\tilde\rho_0\|_{\mathbf{L^1}(\mathbb{R};\mathbb{R})}\right\}\|\omega-\tilde\omega\|_{\mathbf{L^1}(\mathbb{R};\mathbb{R})}\,t.\qquad(2.2.52)
\end{aligned}
$$

Finally, consider (2.2.50) and compute

$$
\begin{aligned}
\left|V(s,x)-\tilde V(s,x)\right|&\leq\left\|v'\right\|_{\mathbf{L}^\infty(\mathbb{R};\mathbb{R})}\min\left\{\|\omega\|_{\mathbf{L}^\infty(\mathbb{R};\mathbb{R})},\|\tilde\omega\|_{\mathbf{L}^\infty(\mathbb{R};\mathbb{R})}\right\}\left\|\rho(s)-\tilde\rho(s)\right\|_{\mathbf{L^1}(\mathbb{R};\mathbb{R})}\\
&\quad+\left\|v'\right\|_{\mathbf{L}^\infty(\mathbb{R};\mathbb{R})}\min\left\{\left\|\rho(s)\right\|_{\mathbf{L}^\infty(\mathbb{R};\mathbb{R})},\left\|\tilde\rho(s)\right\|_{\mathbf{L}^\infty(\mathbb{R};\mathbb{R})}\right\}\|\omega-\tilde\omega\|_{\mathbf{L^1}(\mathbb{R};\mathbb{R})}\\
&\leq\left\|v'\right\|_{\mathbf{L}^\infty(\mathbb{R};\mathbb{R})}\min\left\{\|\omega\|_{\mathbf{L}^\infty(\mathbb{R};\mathbb{R})},\|\tilde\omega\|_{\mathbf{L}^\infty(\mathbb{R};\mathbb{R})}\right\}\left\|\rho(s)-\tilde\rho(s)\right\|_{\mathbf{L^1}(\mathbb{R};\mathbb{R})}\\
&\quad+\left\|v'\right\|_{\mathbf{L}^\infty(\mathbb{R};\mathbb{R})}\min\left\{M_s,\tilde M_s\right\}\|\omega-\tilde\omega\|_{\mathbf{L^1}(\mathbb{R};\mathbb{R})}.
\end{aligned}
$$

Hence,

$$
\begin{aligned}
[(2.2.50)]&\leq\left\|v'\right\|_{\mathbf{L}^\infty(\mathbb{R};\mathbb{R})}\min\left\{\|\omega\|_{\mathbf{L}^\infty(\mathbb{R};\mathbb{R})},\|\tilde\omega\|_{\mathbf{L}^\infty(\mathbb{R};\mathbb{R})}\right\}\\
&\quad\times\int_0^t\left\|\partial_\rho f\right\|_{\mathbf{L}^\infty(\Sigma_s;\mathbb{R})}\mathrm{TV}\left(\rho(s)\right)\left\|\rho(s)-\tilde\rho(s)\right\|_{\mathbf{L^1}(\mathbb{R};\mathbb{R})}ds\qquad(2.2.53)\\
&\quad+\left\|\partial_\rho f\right\|_{\mathbf{L}^\infty(\Sigma_t;\mathbb{R})}\mathrm{TV}\left(\rho(t)\right)\left\|v'\right\|_{\mathbf{L}^\infty(\mathbb{R};\mathbb{R})}\min\left\{M_t,\tilde M_t\right\}\|\omega-\tilde\omega\|_{\mathbf{L^1}(\mathbb{R};\mathbb{R})}\,t.
\end{aligned}
$$

Therefore, the inequality [(2.2.47)$\cdots$(2.2.50)] can be estimated as follows

$$
\left\|\rho(t)-\tilde\rho(t)\right\|_{\mathbf{L^1}(\mathbb{R};\mathbb{R})}
$$

$$\leq \|\rho_0 - \tilde{\rho}_0\|_{\mathbf{L^1}(\mathbb{R};\mathbb{R})} + a(t)\,\|\omega - \tilde{\omega}\|_{\mathbf{W^{1,1}}(\mathbb{R};\mathbb{R})} + \int_0^t b(s)\,\big\|\rho(s) - \tilde{\rho}(s)\big\|_{\mathbf{L^1}(\mathbb{R};\mathbb{R})} ds,$$

where, thanks to the total variation estimate provided by Proposition 4,

$$\begin{aligned}
&a(t) \qquad (2.2.54)\\
&= t\,\Bigg[\min\Big\{\|\rho_0\|_{\mathbf{L^1}(\mathbb{R};\mathbb{R})}, \|\tilde{\rho}_0\|_{\mathbf{L^1}(\mathbb{R};\mathbb{R})}\Big\}\,\|f\|_{\mathbf{L}^\infty(\Sigma_t;\mathbb{R})}\\
&\quad\times\Big(\big\|v'\big\|_{\mathbf{L}^\infty(\mathbb{R};\mathbb{R})} + \big\|v''\big\|_{\mathbf{L}^\infty(\mathbb{R};\mathbb{R})}\,\min\Big\{\|\rho_0\|_{\mathbf{L^1}(\mathbb{R};\mathbb{R})}\|\partial_x\omega\|_{\mathbf{L}^\infty(\mathbb{R};\mathbb{R})}, \|\tilde{\rho}_0\|_{\mathbf{L^1}(\mathbb{R};\mathbb{R})}\|\partial_x\tilde{\omega}\|_{\mathbf{L}^\infty(\mathbb{R};\mathbb{R})}\Big\}\Big)\\
&\quad+\min\Big\{\|\rho_0\|_{\mathbf{L^1}(\mathbb{R};\mathbb{R})}, \|\tilde{\rho}_0\|_{\mathbf{L^1}(\mathbb{R};\mathbb{R})}\Big\}\,\|\partial_x f\|_{\mathbf{L}^\infty(\Sigma_t;\mathbb{R})}\,\big\|v'\big\|_{\mathbf{L}^\infty(\mathbb{R};\mathbb{R})}\\
&\quad+\big\|\partial_\rho f\big\|_{\mathbf{L}^\infty(\Sigma_t;\mathbb{R})}\,\big(\mathcal{K}_2 t + \mathrm{TV}(\rho_0)\big)\,e^{\mathcal{K}_1 t}\,\big\|v'\big\|_{\mathbf{L}^\infty(\mathbb{R};\mathbb{R})}\,\min\Big\{M_t, \tilde{M}_t\Big\}\Bigg]
\end{aligned}$$

and

$$\begin{aligned}
&b(s) \qquad (2.2.55)\\
&= \|f\|_{\mathbf{L}^\infty(\Sigma_s;\mathbb{R})}\,\min\Big\{\|\omega\|_{\mathbf{W^{1,1}}(\mathbb{R};\mathbb{R})}, \|\tilde{\omega}\|_{\mathbf{W^{1,1}}(\mathbb{R};\mathbb{R})}\Big\}\\
&\quad\times\Big(\big\|v'\big\|_{\mathbf{L}^\infty(\mathbb{R};\mathbb{R})} + \big\|v''\big\|_{\mathbf{L}^\infty(\mathbb{R};\mathbb{R})}\,\min\Big\{\|\rho_0\|_{\mathbf{L^1}(\mathbb{R};\mathbb{R})}\|\partial_x\omega\|_{\mathbf{L}^\infty(\mathbb{R};\mathbb{R})}, \|\tilde{\rho}_0\|_{\mathbf{L^1}(\mathbb{R};\mathbb{R})}\|\partial_x\tilde{\omega}\|_{\mathbf{L}^\infty(\mathbb{R};\mathbb{R})}\Big\}\Big)\\
&\quad+\|\partial_x f\|_{\mathbf{L}^\infty(\Sigma_s;\mathbb{R})}\,\big\|v'\big\|_{\mathbf{L}^\infty(\mathbb{R};\mathbb{R})}\,\min\Big\{\|\omega\|_{\mathbf{L^1}(\mathbb{R};\mathbb{R})}, \|\tilde{\omega}\|_{\mathbf{L^1}(\mathbb{R};\mathbb{R})}\Big\}\\
&\quad+\big\|\partial_\rho f\big\|_{\mathbf{L}^\infty(\Sigma_s;\mathbb{R})}\,\big(\mathcal{K}_2 s + \mathrm{TV}(\rho_0)\big)\,e^{\mathcal{K}_1 s}\,\big\|v'\big\|_{\mathbf{L}^\infty(\mathbb{R};\mathbb{R})}\,\min\Big\{\|\omega\|_{\mathbf{L}^\infty(\mathbb{R};\mathbb{R})}, \|\tilde{\omega}\|_{\mathbf{L}^\infty(\mathbb{R};\mathbb{R})}\Big\},
\end{aligned}$$

$\mathcal{K}_1$ and $\mathcal{K}_2$ being specified in (2.1.5). An application of Gronwall Lemma yields

$$\begin{aligned}
\big\|\rho(t) - \tilde{\rho}(t)\big\|_{\mathbf{L^1}(\mathbb{R};\mathbb{R})} &\leq \|\rho_0 - \tilde{\rho}_0\|_{\mathbf{L^1}(\mathbb{R};\mathbb{R})} + a(t)\,\|\omega - \tilde{\omega}\|_{\mathbf{W^{1,1}}(\mathbb{R};\mathbb{R})}\\
&\quad+\int_0^t \Big(\|\rho_0 - \tilde{\rho}_0\|_{\mathbf{L^1}(\mathbb{R};\mathbb{R})} + a(s)\Big)\,b(s)\,\exp\left(\int_s^t b(r)dr\right)ds.
\end{aligned}$$

Since $a(s) \leq a(t)$ for any $s \in [0,t]$ and

$$\int_0^t b(s)\,\exp\left(\int_s^t b(r)dr\right)ds = \left[-\exp\left(\int_s^t b(r)dr\right)\right]_0^t = -1 + \exp\left(\int_0^t b(r)dr\right),$$

we obtain

$$\big\|\rho(t) - \tilde{\rho}(t)\big\|_{\mathbf{L^1}(\mathbb{R};\mathbb{R})} \leq \Big(\|\rho_0 - \tilde{\rho}_0\|_{\mathbf{L^1}(\mathbb{R};\mathbb{R})} + a(t)\,\|\omega - \tilde{\omega}\|_{\mathbf{W^{1,1}}(\mathbb{R};\mathbb{R})}\Big)\exp\left(\int_0^t b(r)dr\right), \qquad (2.2.56)$$

concluding the proof. □

Remark 2. Notice that, when $t = 0$, the right hand side of (2.2.56) is equal to $\|\rho_0 - \tilde{\rho}_0\|_{\mathbf{L^1}(\mathbb{R};\mathbb{R})}$, since $a(0) = 0$.

Remark 3. Compare our estimate (2.2.56) with the one in [10, Theorem 4.1]:

$$\left\|\rho(t) - \tilde{\rho}(t)\right\|_{\mathbf{L^1}(\mathbb{R};\mathbb{R})} \leq e^{C_2\, t} \|\rho_0 - \tilde{\rho}\|_{\mathbf{L^1}(\mathbb{R};\mathbb{R})},$$

where

$$\begin{aligned} C_2 = \ & \|f\|_{\mathbf{L}^\infty(\Sigma_t;\mathbb{R})} \Big(\left\|v'\right\|_{\mathbf{L}^\infty(\mathbb{R};\mathbb{R})} \|\partial_x \omega\|_{\mathbf{L^1}(\mathbb{R};\mathbb{R})} \\ & + \left\|v''\right\|_{\mathbf{L}^\infty(\mathbb{R};\mathbb{R})} \|\partial_x \omega\|_{\mathbf{L}^\infty(\mathbb{R};\mathbb{R})} \|\omega\|_{\mathbf{L^1}(\mathbb{R};\mathbb{R})} \min\left\{ \|\rho_0\|_{\mathbf{L^1}(\mathbb{R};\mathbb{R})}, \|\tilde{\rho}_0\|_{\mathbf{L^1}(\mathbb{R};\mathbb{R})} \right\} \Big) \\ & + \left\|f'\right\|_{\mathbf{L}^\infty(\Sigma_t;\mathbb{R})} \mathrm{TV}\left(\rho(t)\right) \left\|v'\right\|_{\mathbf{L}^\infty(\mathbb{R};\mathbb{R})} \|\omega\|_{\mathbf{L}^\infty(\mathbb{R};\mathbb{R})}. \end{aligned}$$

The main hypotheses there are the following:

- $f(t, x, \rho) = f(\rho)$;
- $\omega = \tilde{\omega}$, thus the kernel functions are the same;
- different initial data: $\rho_0 \neq \tilde{\rho}_0$.

It is immediate to see that, once the estimate for the total variation of $\rho(t)$ is inserted, the bound C_2 bears a strong resemblance with our $b(t)$ (2.2.55), provided the $\mathbf{L^1}$-norm of the kernel ω and of its derivative are controlled by $\|\omega\|_{\mathbf{W^{1,1}}(\mathbb{R};\mathbb{R})}$.

Remark 4. One may wonder why there is the need to exploit the doubling of variables method and to go through all the steps of the proof instead of using the available estimate provided in [62, Theorem 2.5 or Proposition 2.9]. The reason lies in the coefficient κ^* appearing in the estimates presented in that work. Indeed, with our notation, this coefficient reads

$$\kappa^* = \left\| \partial_\rho \partial_x \left(f(t, x, \rho) \left(V(t, x) - \tilde{V}(t, x) \right) \right) \right\|_{\mathbf{L}^\infty(\Sigma_t;\mathbb{R})}.$$

Computing the derivatives yields

$$\kappa^* \leq \left\|\partial_x \partial_\rho f\right\|_{\mathbf{L}^\infty(\Sigma_t;\mathbb{R})} \left\|V - \tilde{V}\right\|_{\mathbf{L}^\infty([0,t]\times\mathbb{R};\mathbb{R})} + \left\|\partial_\rho f\right\|_{\mathbf{L}^\infty(\Sigma_t;\mathbb{R})} \left\|\partial_x V - \partial_x \tilde{V}\right\|_{\mathbf{L}^\infty([0,t]\times\mathbb{R};\mathbb{R})}.$$

Substitute now the definitions of V and $\tilde{V}$, using also the estimates for (2.2.48) and (2.2.50) computed in the proof of Theorem 5: we obtain an estimate for κ^* depending on the term $\|\rho - \tilde{\rho}\|_{\mathbf{L^1}(\mathbb{R};\mathbb{R})}$. Going back to the estimate presented in [62], we see that the coefficient κ^* appears in the term $e^{\kappa^* t}\|\rho_0 - \tilde{\rho}_0\|_{\mathbf{L^1}(\mathbb{R};\mathbb{R})}$. Therefore, the authors get a dependence of the exponential function on the $\mathbf{L^1}$ norm of the difference $\rho - \tilde{\rho}$, which is clearly not what desired since the final goal is to control from above $\left\|\rho(t) - \tilde{\rho}(t)\right\|_{\mathbf{L^1}(\mathbb{R};\mathbb{R})}$.

Proof of Theorem 6. We can apply Lemma 2 to problems (2.1.9) and (2.1.10). Let us start from the inequality [(2.2.2)–(2.2.3)]. Introduce the following notation, based on Lemma 1:

$$\left\|\rho(t)\right\|_{\mathbf{L}^\infty(\mathbb{R};\mathbb{R})} \leq \|\rho_0\|_{\mathbf{L}^\infty(\mathbb{R};\mathbb{R})}\, e^{\mathcal{L}\, t} \qquad \left\|\tilde{\rho}(t)\right\|_{\mathbf{L}^\infty(\mathbb{R};\mathbb{R})} \leq \|\rho_0\|_{\mathbf{L}^\infty(\mathbb{R};\mathbb{R})}\, e^{\tilde{\mathcal{L}}\, t}.$$

Define $\mathcal{G}_t = \|\rho_0\|_{\mathbf{L}^\infty(\mathbb{R};\mathbb{R})}\, e^{\max\{\mathcal{L},\tilde{\mathcal{L}}\}\,t}$. Similarly to (2.2.46), introduce the space

$$\Sigma_t = [0,t]\times\mathbb{R}\times[0,\mathcal{G}_t].$$

Let $\tau\to 0$ in [(2.2.2)–(2.2.3)] and recall also the assumption $\sup_{t,x}\left|\partial_x f(t,x,\rho)\right| < C|\rho|$:

$$\begin{aligned}
\left\|\rho(t)-\tilde\rho(t)\right\|_{\mathbf{L^1}(\mathbb{R};\mathbb{R})} \le{}& \int_0^t \|f\|_{\mathbf{L}^\infty(\Sigma_s;\mathbb{R})}\int_{\mathbb{R}}\left|\partial_x V(s,x)-\partial_x\tilde V(s,x)\right|dx\,ds && (2.2.57)\\
&+\int_0^t\int_{\mathbb{R}} C|\rho(t,x)|\left|\tilde V(s,x)-V(s,x)\right|dx\,ds && (2.2.58)\\
&+\int_0^t \left\|\partial_\rho f\right\|_{\mathbf{L}^\infty(\Sigma_s;\mathbb{R})}\int_{\mathbb{R}}\left|\partial_x\rho(s,x)\right|\left|V(s,x)-\tilde V(s,x)\right|dx\,ds. && (2.2.59)
\end{aligned}$$

By the definitions of V and $\tilde V$, compute:

$$\begin{aligned}
&\left|V(s,x)-\tilde V(s,x)\right|\\
&= \left|v((\rho(s)*\omega)(x))-\tilde v((\tilde\rho(s)*\omega)(x))\right|\\
&\le \min\left\{\left\|v'\right\|_{\mathbf{L}^\infty(\mathbb{R};\mathbb{R})},\left\|\tilde v'\right\|_{\mathbf{L}^\infty(\mathbb{R};\mathbb{R})}\right\}\|\omega\|_{\mathbf{L}^\infty(\mathbb{R};\mathbb{R})}\left\|\rho(s)-\tilde\rho(s)\right\|_{\mathbf{L^1}(\mathbb{R};\mathbb{R})}+\|v-\tilde v\|_{\mathbf{L}^\infty(\mathbb{R};\mathbb{R})}
\end{aligned}$$

and

$$\begin{aligned}
&\int_{\mathbb{R}}\left|\partial_x V(s,x)-\partial_x\tilde V(s,x)\right|dx\\
&= \int_{\mathbb{R}}\left|v'((\rho(s)*\omega)(x))\,\left(\rho(s)*\partial_x\omega\right)(x)-\tilde v'((\tilde\rho(s)*\omega)(x))\,\left(\tilde\rho(s)*\partial_x\omega\right)(x)\right|dx\\
&\le \min\left\{\left\|v'\right\|_{\mathbf{L}^\infty(\mathbb{R};\mathbb{R})},\left\|\tilde v'\right\|_{\mathbf{L}^\infty(\mathbb{R};\mathbb{R})}\right\}\|\partial_x\omega\|_{\mathbf{L^1}(\mathbb{R};\mathbb{R})}\left\|\rho(s)-\tilde\rho(s)\right\|_{\mathbf{L^1}(\mathbb{R};\mathbb{R})}\\
&\quad+\left\|v'-\tilde v'\right\|_{\mathbf{L}^\infty(\mathbb{R};\mathbb{R})}\|\partial_x\omega\|_{\mathbf{L^1}(\mathbb{R};\mathbb{R})}\min\left\{\left\|\rho(s)\right\|_{\mathbf{L^1}(\mathbb{R};\mathbb{R})},\left\|\tilde\rho(s)\right\|_{\mathbf{L^1}(\mathbb{R};\mathbb{R})}\right\}\\
&\le \min\left\{\left\|v'\right\|_{\mathbf{L}^\infty(\mathbb{R};\mathbb{R})},\left\|\tilde v'\right\|_{\mathbf{L}^\infty(\mathbb{R};\mathbb{R})}\right\}\|\partial_x\omega\|_{\mathbf{L^1}(\mathbb{R};\mathbb{R})}\left\|\rho(s)-\tilde\rho(s)\right\|_{\mathbf{L^1}(\mathbb{R};\mathbb{R})}\\
&\quad+\left\|v'-\tilde v'\right\|_{\mathbf{L}^\infty(\mathbb{R};\mathbb{R})}\|\partial_x\omega\|_{\mathbf{L^1}(\mathbb{R};\mathbb{R})}\|\rho_0\|_{\mathbf{L^1}(\mathbb{R};\mathbb{R})},
\end{aligned}$$

where we exploit also Lemma 1. Therefore the inequality [(2.2.57)– (2.2.59)] can be estimated as follows:

$$\begin{aligned}
&\left\|\rho(t)-\tilde\rho(t)\right\|_{\mathbf{L^1}(\mathbb{R};\mathbb{R})}\\
&\le c_1(t)\,\|v-\tilde v\|_{\mathbf{L}^\infty(\mathbb{R};\mathbb{R})}+c_2(t)\left\|v'-\tilde v'\right\|_{\mathbf{L}^\infty(\mathbb{R};\mathbb{R})}+\int_0^t c_3(s)\left\|\rho(s)-\tilde\rho(s)\right\|_{\mathbf{L^1}(\mathbb{R};\mathbb{R})}ds,
\end{aligned}$$

where, thanks to the total variation estimate provided by Proposition 4,

$$\begin{aligned}
c_1(t) &= t\,\left(C\,\|\rho_0\|_{\mathbf{L^1}(\mathbb{R};\mathbb{R})}+(\mathcal{K}_2\,t+\mathrm{TV}(\rho_0))\,e^{\mathcal{K}_1\,t}\left\|\partial_\rho f\right\|_{\mathbf{L}^\infty(\Sigma_t;\mathbb{R})}\right), && (2.2.60)\\
c_2(t) &= t\,\|f\|_{\mathbf{L}^\infty(\Sigma_t;\mathbb{R})}\,\|\partial_x\omega\|_{\mathbf{L^1}(\mathbb{R};\mathbb{R})}\,\|\rho_0\|_{\mathbf{L^1}(\mathbb{R};\mathbb{R})}, && (2.2.61)\\
c_3(s) &= \|f\|_{\mathbf{L}^\infty(\Sigma_s;\mathbb{R})}\min\left\{\left\|v'\right\|_{\mathbf{L}^\infty(\mathbb{R};\mathbb{R})},\left\|\tilde v'\right\|_{\mathbf{L}^\infty(\mathbb{R};\mathbb{R})}\right\}\|\partial_x\omega\|_{\mathbf{L^1}(\mathbb{R};\mathbb{R})}\\
&\quad+\left(C\,\|\rho_0\|_{\mathbf{L^1}(\mathbb{R};\mathbb{R})}+(\mathcal{K}_2\,s+\mathrm{TV}(\rho_0))\,e^{\mathcal{K}_1\,s}\left\|\partial_\rho f\right\|_{\mathbf{L}^\infty(\Sigma_s;\mathbb{R})}\right) && (2.2.62)
\end{aligned}$$

$$\times \min\left\{\|v'\|_{\mathbf{L}^\infty(\mathbb{R};\mathbb{R})}, \|\tilde{v}'\|_{\mathbf{L}^\infty(\mathbb{R};\mathbb{R})}\right\} \|\omega\|_{\mathbf{L}^\infty(\mathbb{R};\mathbb{R})},$$

$\mathcal{K}_1$ and $\mathcal{K}_2$ being specified in (2.1.5). An application of Gronwall Lemma yields

$$\|\rho(t) - \tilde{\rho}(t)\|_{\mathbf{L^1}(\mathbb{R};\mathbb{R})} \leq \left(c_1(t)\,\|v - \tilde{v}\|_{\mathbf{L}^\infty(\mathbb{R};\mathbb{R})} + c_2(t)\,\|v' - \tilde{v}'\|_{\mathbf{L}^\infty(\mathbb{R};\mathbb{R})}\right) \exp\left(\int_0^t c_3(s)ds\right),$$

concluding the proof. □

2.3 Numerical Integrations

In this section, we investigate the dependence of solutions to (2.0.1) on the kernel and the velocity function via numerical integrations. To this end, we discretize (2.0.1) on a fixed grid given by the cells interfaces $x_{j+\frac{1}{2}} = j\Delta x$ and the cells centres $x_j = (j-\frac{1}{2})\Delta x$ for $j \in \mathbb{Z}$, taking a space step Δx and a time step Δt, so that $t^n = n\Delta t$ is the time mesh. The Lax-Friedrichs flux adapted to (2.0.1) is given by

$$F^n_{j+1/2} := \frac{1}{2}\left(f(t^n, x_j, \rho^n_j)v(R^n_j) + f(t^n, x_{j+1}, \rho^n_{j+1})v(R^n_{j+1})\right) - \frac{\alpha}{2}(\rho^n_{j+1} - \rho^n_j) \tag{2.3.1}$$

where $\alpha \geq 0$ is the viscosity coefficient and $R^n_j := \Delta x \sum_{k\in\mathbb{Z}} \rho^n_{j+k}\omega^k_\eta$, denoting $\omega^k_\eta := \omega_\eta(k\Delta x)$ for $k \in \mathbb{Z}$. In this way we have the finite volume scheme

$$\rho^{n+1}_j = \rho^n_j - \lambda\left[F^n_{j+1/2} - F^n_{j-1/2}\right], \tag{2.3.2}$$

with $\lambda = \Delta t/\Delta x$. A rigorous study of the convergence of Lax-Friedrichs type schemes for non-local conservation laws has been carried out in [2, 5, 11]. Here we limit the study to the derivation of sufficient conditions ensuring that the above discretization (2.3.1)–(2.3.2) is positivity preserving.

Lemma 3. *For any $T > 0$, under the CFL conditions*

$$\lambda\left(\alpha + \left(C\,\Delta x + 2\,\|\partial_\rho f\|_{\mathbf{L}^\infty(\Sigma_T;\mathbb{R})}\right)\|v\|_{\mathbf{L}^\infty(\mathbb{R};\mathbb{R})}\right) < 1, \tag{2.3.3}$$

$$\alpha \geq \|\partial_\rho f\|_{\mathbf{L}^\infty(\Sigma_T;\mathbb{R})}\|v\|_{\mathbf{L}^\infty(\mathbb{R};\mathbb{R})}, \tag{2.3.4}$$

the scheme (2.3.1)–(2.3.2) is positivity preserving on $[0,T]\times\mathbb{R}$.

Proof. Let us assume that $\rho^n_j \geq 0$ for all $j \in \mathbb{Z}$. It suffices to prove that ρ^{n+1}_j in (2.3.2) is non-negative. For the sake of simplicity, in the following we omit the dependence on n and introduce the notation $f_i(\rho_j) = f(t^n, x_i, \rho_j)$ and $v_j = v(R^n_j)$. Compute

$$\begin{aligned}\rho^{n+1}_j &= \rho_j + \frac{\lambda\,\alpha}{2}(\rho_{j+1} - 2\,\rho_j + \rho_{j-1}) - \frac{\lambda}{2}\left[f_{j+1}(\rho_{j+1})\,v_{j+1} - f_{j-1}(\rho_{j-1})\,v_{j-1}\right]\\ &= \rho_j(1 - \lambda\,\alpha) + \frac{\lambda\,\alpha}{2}(\rho_{j+1} + \rho_{j-1})\end{aligned}$$

$$
\begin{aligned}
&- \frac{\lambda}{2}\Big[\big(f_{j+1}(\rho_{j+1}) - f_{j+1}(\rho_j)\big)\, v_{j+1} + \big(f_{j-1}(\rho_j) - f_{j-1}(\rho_{j-1})\big)\, v_{j-1} \\
&\qquad + \big(f_{j+1}(\rho_j) - f_{j-1}(\rho_j)\big)\, v_{j+1} + f_{j-1}(\rho_j)\,\big(v_{j+1} - v_{j-1}\big)\Big] \\
&= \rho_j \left(1 - \lambda\,\alpha + \frac{\lambda}{2}\,\frac{f_{j+1}(\rho_{j+1}) - f_{j+1}(\rho_j)}{\rho_{j+1} - \rho_j}\, v_{j+1} - \frac{\lambda}{2}\,\frac{f_{j-1}(\rho_j) - f_{j-1}(\rho_{j-1})}{\rho_j - \rho_{j-1}}\, v_{j-1}\right) \\
&\quad + \rho_{j+1}\left(\frac{\lambda\,\alpha}{2} - \frac{\lambda}{2}\,\frac{f_{j+1}(\rho_{j+1}) - f_{j+1}(\rho_j)}{\rho_{j+1} - \rho_j}\, v_{j+1}\right) \\
&\quad + \rho_{j-1}\left(\frac{\lambda\,\alpha}{2} + \frac{\lambda}{2}\,\frac{f_{j-1}(\rho_j) - f_{j-1}(\rho_{j-1})}{\rho_j - \rho_{j-1}}\, v_{j-1}\right) \\
&\quad - \frac{\lambda}{2}\, v_{j+1}\big(f_{j+1}(\rho_j) - f_{j-1}(\rho_j)\big) - \frac{\lambda}{2}\, f_{j-1}(\rho_j)\,\big(v_{j+1} - v_{j-1}\big)\,.
\end{aligned}
$$

Observe that, thanks to the assumption (2.3.4) on α,

$$
\begin{aligned}
&\alpha + \frac{f_{j-1}(\rho_j) - f_{j-1}(\rho_{j-1})}{\rho_j - \rho_{j-1}}\, v_{j-1} = \alpha + \partial_\rho f_{j-1}(\zeta_{j-1/2})\, v_{j-1} \geq \alpha - \big\|\partial_\rho f\big\|_{\mathbf{L}^\infty(\Sigma_T;\mathbb{R})} \|v\|_{\mathbf{L}^\infty(\mathbb{R};\mathbb{R})} \geq 0, \\
&\alpha - \frac{f_{j+1}(\rho_{j+1}) - f_{j+1}(\rho_j)}{\rho_{j+1} - \rho_j}\, v_{j+1} = \alpha - \partial_\rho f_{j+1}(\zeta_{j+1/2})\, v_{j+1} \geq \alpha - \big\|\partial_\rho f\big\|_{\mathbf{L}^\infty(\Sigma_T;\mathbb{R})} \|v\|_{\mathbf{L}^\infty(\mathbb{R};\mathbb{R})} \geq 0.
\end{aligned}
$$

Moreover,

$$
v_{j+1}\big(f_{j+1}(\rho_j) - f_{j-1}(\rho_j)\big) \leq 2\,C\,\|v\|_{\mathbf{L}^\infty(\mathbb{R};\mathbb{R})}\,\Delta x\,\rho_j
$$

and

$$
f_{j-1}(\rho_j)\,\big(v_{j+1} - v_{j-1}\big) \leq 2\,\big\|\partial_\rho f\big\|_{\mathbf{L}^\infty(\Sigma_T;\mathbb{R})} \|v\|_{\mathbf{L}^\infty(\mathbb{R};\mathbb{R})} \rho_j.
$$

Hence,

$$
\begin{aligned}
&\rho_j \left(1 - \lambda\,\alpha + \frac{\lambda}{2}\,\frac{f_{j+1}(\rho_{j+1}) - f_{j+1}(\rho_j)}{\rho_{j+1} - \rho_j}\, v_{j+1} - \frac{\lambda}{2}\,\frac{f_{j-1}(\rho_j) - f_{j-1}(\rho_{j-1})}{\rho_j - \rho_{j-1}}\, v_{j-1}\right) \\
&\quad - \frac{\lambda}{2}\, v_{j+1}\big(f_{j+1}(\rho_j) - f_{j-1}(\rho_j)\big) - \frac{\lambda}{2}\, f_{j-1}(\rho_j)\,\big(v_{j+1} - v_{j-1}\big) \\
&\geq \rho_j \Big(1 - \lambda\,\alpha - 2\,\lambda\,\big\|\partial_\rho f\big\|_{\mathbf{L}^\infty(\Sigma_T;\mathbb{R})} \|v\|_{\mathbf{L}^\infty(\mathbb{R};\mathbb{R})} - \lambda\,C\,\|v\|_{\mathbf{L}^\infty(\mathbb{R};\mathbb{R})}\,\Delta x\Big) \geq 0,
\end{aligned}
$$

by the CFL condition (2.3.3). □

Fix $T = 0.5$. Let us now consider the following problem, describing traffic flow on a circular road with variable speed limit in space and time, starting from a constant initial density $\rho_0 \equiv 0.6$ (for simplicity, the maximal density is here normalised to 1):

$$
\begin{cases}
\partial_t \rho + \partial_x\big(f(t,x,\rho) v(\omega_{\eta,\delta} * \rho)\big) = 0, \quad t \in [0,T],\ x \in\,]-1,1[\,, \\
\rho(0,x) = 0.6,
\end{cases}
\tag{2.3.5}
$$

with periodic boundary conditions at $x = \pm 1$ and

$$
f(t,x,\rho) = V_{\max}(t,x)\rho(1-\rho), \qquad \rho \in [0,1], \tag{2.3.6}
$$

$$v(\rho) = (1-\rho)^{m-1}(1+\rho)^m, \qquad m \in \mathbb{N}^*, \tag{2.3.7}$$

$$\omega_{\eta,\delta}(x) = \frac{1}{\eta^6}\frac{16}{5\pi}(\eta^2 - (x-\delta)^2)^{\frac{5}{2}}\chi_{[-\eta+\delta,\eta+\delta]}, \qquad \eta \in]0,1],\ \delta \in [-\eta,\eta]. \tag{2.3.8}$$

In (2.3.6), $V_{\max}(t,x)$ is given by the convolution between the gaussian kernel $g(x) = \frac{1}{\sigma\sqrt{2\pi}}e^{-\frac{1}{2}(\frac{x}{\sigma})^2}$ with $\sigma = 10$ and the following piece-wise constant function:

$$\varphi(t,x) = \begin{cases} 7 & \text{if } x \in\ ]-1,-1/3] \cup\ ]1/3,1], \\ 3 & \text{if } x \in\ ]-1/3,1/3],\ t \in [0,1/6] \cup\ ]1/3,1/2], \\ 1.5 & \text{if } x \in\ ]-1/3,1/3],\ t \in]1/6,1/3], \end{cases}$$

see Figure 2.1. The function $V_{\max}(t,x)$ is chosen to mimic the presence of a slow speed sector, whose speed limit depends on the time of the day. In (2.3.7), m can be seen as a fitting parameter of the Greenshield fundamental diagram. In (2.3.8), we define a symmetric kernel function $\omega_{\eta,\delta}$: the parameter η represents the radius of the kernel support and describes the maximal interaction distance between vehicles, while δ is the point at which the maximum of the kernel function is attained and it determines the location of the kernel support. Note that assumptions (2.1.1)-(2.1.2) are fulfilled.

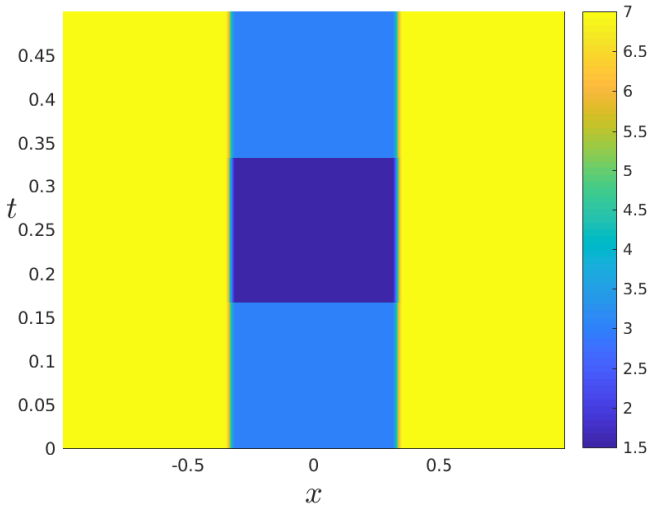

Figure 2.1: 2D plot of the function $V_{max}(t,x)$

As a metric of traffic congestion, we consider the two following functionals [29, 30, 37]:

$$J(T) = \int_0^T d\big|d_x\rho(t,\cdot)\big|dt, \tag{2.3.9}$$

$$\Psi(T;a,b) = \int_0^T \int_a^b \varphi(\rho(t,x))\,dx\,dt, \tag{2.3.10}$$

where

$$\varphi(r) = \begin{cases} 0 & r < 0.75, \\ 10\,r - 7.5 & 0.75 \le r \le 0.85, \\ 1 & 0.85 < r \le 1. \end{cases}$$

The functional J defined in (2.3.9) measures the integral with respect to time of the spatial total variation of the traffic density. The results of Theorems 5 and 6 apply to the present setting and ensure the continuous dependence of J on the parameters m, η and δ. Indeed, the map $\delta \to \omega_{\eta,\delta}$ is Lipschitz continuous with respect to the $\mathbf{W^{1,1}}$ distance, the map $\eta \to \omega_{\eta,\delta}$ is continuous with respect to the $\mathbf{W^{1,1}}$ distance and the map $m \to v$ is continuous with respect to the $\mathbf{W^{1,\infty}}$ distance. Theorem 5 then ensures that the map $\omega_{\eta,\delta} \to \rho$, where ρ solves (2.3.5)–(2.3.8), is continuous with respect to the $\mathbf{W^{1,1}}$ distance, while Theorem 6 ensures the continuity of the map $v \to \rho$. Finally, the map $\rho \to J$ is lower semicontinuous, as showed in [30, Lemma 2.1]. Therefore, any minimising sequence of solutions converges, guaranteeing the existence of optimal choices of the parameters η, δ and m.

The functional Ψ in (2.3.10) was introduced in [37] and it is obviously continuous with respect to ρ in the $\mathbf{L^1}$-distance. It measures the queue that forms in the space interval $[a, b]$, which is chosen equal to $[-4/5, -1/3]$ in the numerical simulations below to be located just upstream the lower speed limit region.

For the tests, we fix the space discretization mesh to $\Delta x = 0.001$. Figures 2.2–2.3 show the values of the functionals J and ψ when we vary the value of one of the parameters η, δ and m, keeping the other fixed. In particular, the functionals are evaluated on the following grids:

$$\eta = 0.1, 0.2, \dots, 0.9, 1, \qquad \delta = -0.1, -0.08, \dots, 0.08, 0.1, \qquad m = 1, 2, \dots, 9, 10.$$

We observe that the functionals are in general not monotone and display some extrema in the considered intervals. Figures 2.5, 2.6 and 2.7 show the behaviour of the solutions corresponding to some of these extremal values. More precisely, Figures 2.5a, 2.5b and 2.5c show the solutions corresponding to $\eta = 0.2,\ 0.5,\ 1$ for $m = 3$ and centered kernel ($\delta = 0$). In particular, the solutions displayed in 2.5a and 2.5c correspond to the minimum and maximum values of the functional J (2.3.9) for $\eta \in [0.1, 1]$ (see Figure 2.2, left). Figure 2.6a shows the solution obtained for $\delta = -0.04$ (and $m = 3$, $\eta = 0.1$) and corresponding to the point of minimum of both J and Ψ functionals, while Figures 2.6b and 2.6c correspond to the points of maximum of the functionals J and Ψ, respectively (see Figure 2.3). Finally, in Figures 2.7a and 2.7b we give the solutions corresponding to the maximum and minimum points of the functional J for $m \in \{1, \dots, 10\}$ for $\eta = 0.1$ and $\delta = 0$ (see Figure 2.4).

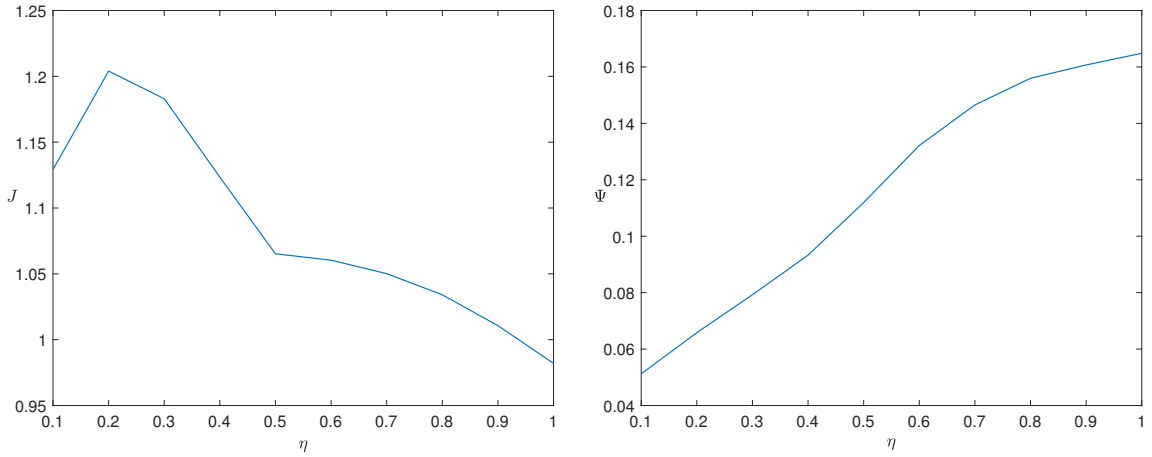

Figure 2.2: Functionals J (2.3.9) (left) and Ψ (2.3.10) (right) with $m = 3$, $\delta = 0$ and $\eta \in [0.1, 1]$.

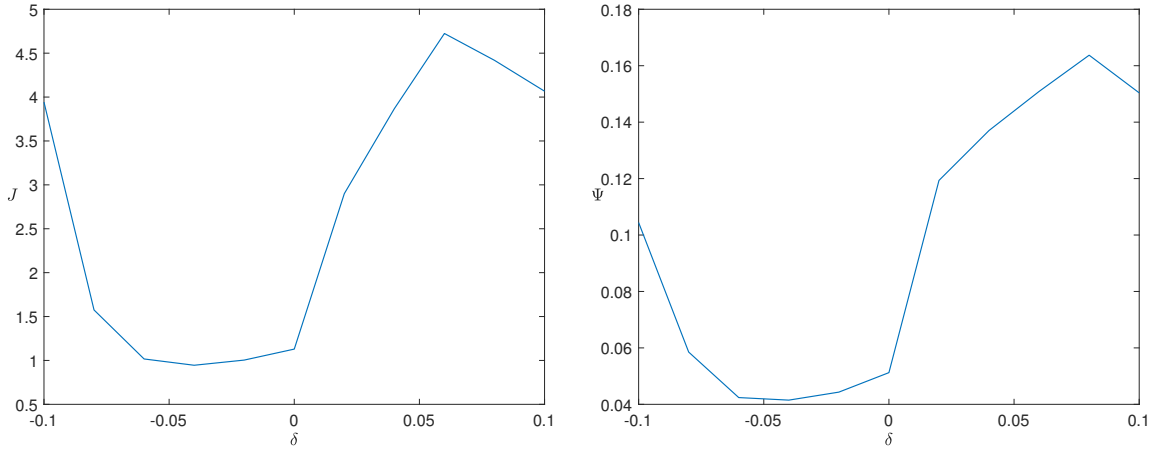

Figure 2.3: Functionals J (2.3.9) (left) and Ψ (2.3.10) (right) with $\eta = 0.1$, $m = 3$ and $\delta \in [-\eta, \eta]$.

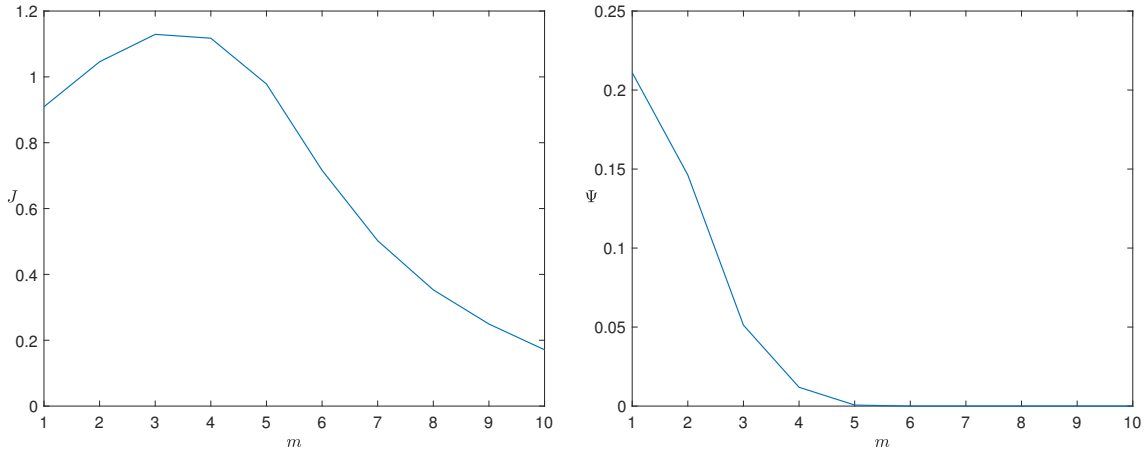

Figure 2.4: Functionals J (2.3.9) (left) and Ψ (2.3.10) (right) with $\eta = 0.1$, $\delta = 0$ and $m \in [1, 10]$.

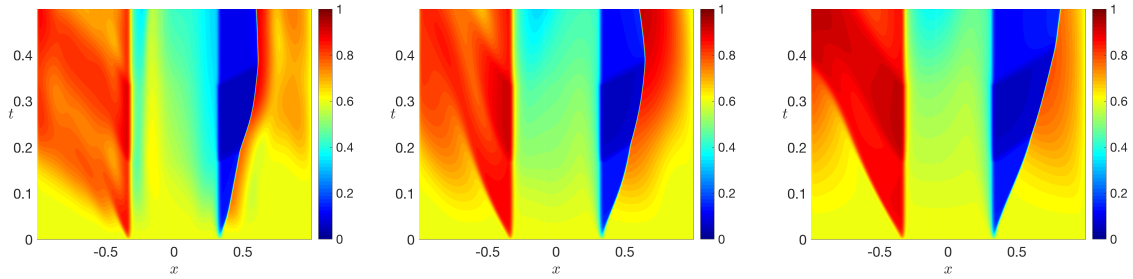

(a) (b) (c)

Figure 2.5: (t, x)-plots of the solution to (2.3.5)–(2.3.8), for $m = 3$ and $\delta = 0$, and, from the left, $\eta = 0.2, 0.5, 1$.

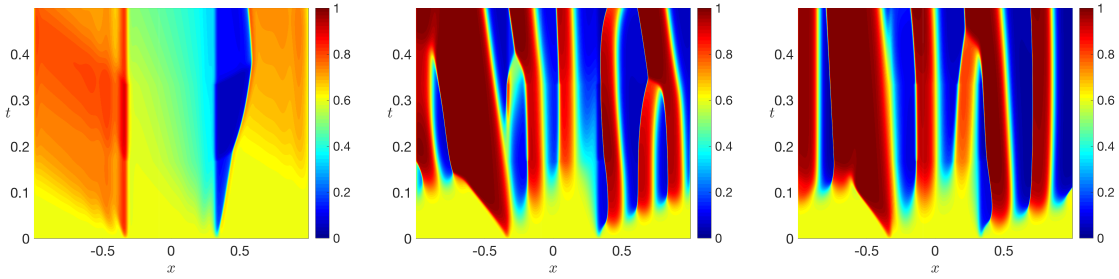

(a) (b) (c)

Figure 2.6: (t, x)-plots of the solution to (2.3.5)–(2.3.8), for $m = 3$ and $\eta = 0.1$, and, from the left, $\delta = -0.04, 0.06, 0.08$.

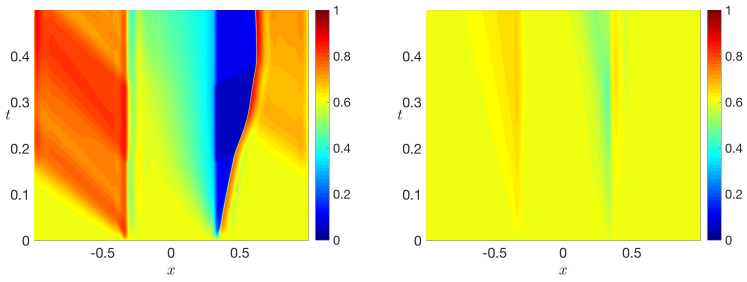

(a) (b)

Figure 2.7: (t, x)-plots of the solution to (2.3.5)–(2.3.8), for $\eta = 0.1$, $\delta = 0$, and $m = 3$ on the left, $m = 10$ on the right.

Chapter 3

Non-local multi-class traffic flow models

In this chapter, we present results obtained in [22].

3.1 Modeling

We consider the following class of non-local systems of M conservation laws in one space dimension:

$$\partial_t \rho_i(t,x) + \partial_x \left(\rho_i(t,x) v_i((r * \omega_i)(t,x))\right) = 0, \qquad i = 1, ..., M, \tag{3.1.1}$$

where

$$r(t,x) := \sum_{i=1}^{M} \rho_i(t,x), \tag{3.1.2}$$

$$v_i(\xi) := v_i^{\max} \psi(\xi), \tag{3.1.3}$$

$$(r * \omega_i)(t,x) := \int_x^{x+\eta_i} r(t,y)\omega_i(y-x)dy, \tag{3.1.4}$$

and we assume:

(H1) The convolution kernels $\omega_i \in \mathbf{C^1}([0,\eta_i];\mathbb{R}^+)$, $\eta_i > 0$, are non-increasing functions such that $\int_0^{\eta_i} \omega_i(y)dy = J_i$. We set $W_0 := \max_{i=1,...,M} \omega_i(0)$.

(H2) $v_i^{\max}$ are the maximal velocities, with $0 < v_1^{\max} \leq v_2^{\max} \leq \ldots \leq v_M^{\max}$.

(H3) $\psi : \mathbb{R}^+ \to \mathbb{R}^+$ is a smooth non-increasing function such that $\psi(0) = 1$ and $\psi(r) = 0$ for $r \geq 1$ (for simplicity, we can consider the function $\psi(r) = \max\{1 - r, 0\}$).

We couple (3.1.1) with an initial datum

$$\rho_i(0,x) = \rho_i^0(x), \qquad i = 1, \ldots, M. \tag{3.1.5}$$

Model (3.1.1) is obtained generalizing the n-populations model for traffic flow described in [8] and it is a multi-class version of the one dimensional scalar conservation law with non-local flux proposed in [11], where ρ_i is the density of vehicles belonging to the i-th class, η_i is proportional to the look-ahead distance and J_i is the interaction strength. In our setting, the non-local dependence of the speed functions v_i describes the reaction of drivers that adapt their velocity to the downstream traffic, assigning greater importance to closer vehicles, see also [21, 49]. We allow different anisotropic kernels for each equation of the system. The

model takes into account the distribution of heterogeneous drivers and vehicles characterized by their maximal speeds and look-ahead visibility in a traffic stream.

Due to the possible presence of jump discontinuities, solutions to (3.1.1), (3.1.5) are intended in the following weak sense.

Definition 3. *A function* $\boldsymbol{\rho} = (\rho_1, \dots, \rho_M) \in (\mathbf{L^1} \cap \mathbf{L^\infty})([0, T[\times\mathbb{R}; \mathbb{R}^M)$, $T > 0$, *is a weak solution of* (3.1.1), (3.1.5) *if*

$$\int_0^T \int_{-\infty}^{\infty} \left(\rho_i \partial_t \varphi + \rho_i v_i (r * \omega_i) \partial_x \varphi\right)(t,x) dx\, dt + \int_{-\infty}^{\infty} \rho_i^0(x) \varphi(0,x)\, dx = 0$$

for all $\varphi \in \mathbf{C_c^1}(]-\infty, T[\times\mathbb{R}; \mathbb{R})$, $i = 1, \dots, M$.

The main result of this chapter is the proof of existence of weak solutions to (3.1.1), (3.1.5), locally in time. We remark that, since the convolution kernels ω_i are not smooth on $\mathbb{R}$, the results in [2] cannot be applied due to the lack of $\mathbf{L}^\infty$-bounds on their derivatives.

Theorem 7. *Let* $\rho_i^0(x) \in (BV \cap \mathbf{L}^\infty)(\mathbb{R}; \mathbb{R}^+)$, *for* $i = 1, \dots, M$, *and assumptions* **(H1)** - **(H3)** *hold. Then the Cauchy problem* (3.1.1), (3.1.5) *admits a weak solution on* $[0, T[\times\mathbb{R}$, *for some* $T > 0$ *sufficiently small.*

We do not address the question of uniqueness of the solutions to (3.1.1). Indeed, even if discrete entropy inequalities can be derived as in [11, Proposition 3], in the case of systems this is in general not sufficient to single out a unique solution.

The chapter is organized as follows. Section 3.2 is devoted to prove uniform $\mathbf{L}^\infty$ and BV estimates on the approximate solutions obtained through an approximation argument based on a Godunov type numerical scheme, see [46]. In Section 3.3 we prove the existence in finite time of weak solutions applying Helly's theorem and a Lax-Wendroff type argument, see [63]. In Section 3.4 we present some numerical simulations for $M = 2$. In particular, we consider the case of a mixed flow of cars and trucks on a stretch of road, and the flow of mixed autonomous and non-autonomous vehicles on a circular road. In this latter case, we analyze two cost functionals measuring the traffic congestion, depending on the penetration ratio of autonomous vehicles. The final Section 3.5 contains alternative $\mathbf{L}^\infty$ and BV estimates, based on approximate solutions constructed via a Lax-Friedrichs type scheme, which is commonly used in the framework of non-local equations, see [2, 5, 11].

3.2 Godunov type approximate solutions

First of all, we extend $\omega_i(x) = 0$ for $x > \eta_i$. For $j \in \mathbb{Z}$ and $n \in \mathbb{N}$, let $x_{j+1/2} = j\Delta x$ be the cell interfaces, $x_j = (j - 1/2)\Delta x$ the cells centers and $t^n = n\Delta t$ the time mesh. We aim at constructing a finite volume approximate solution $\boldsymbol{\rho}^{\Delta x} = \left(\rho_1^{\Delta x}, \dots, \rho_M^{\Delta x}\right)$, with $\rho_i^{\Delta x}(t,x) = \rho_{i,j}^n$ for $(t,x) \in C_j^n = [t^n, t^{n+1}[\times]x_{j-1/2}, x_{j+1/2}]$ and $i = 1, ..., M$.
To this end, we approximate the initial datum ρ_i^0 for $i = 1, ..., M$ with a piecewise constant function

$$\rho_{i,j}^0 = \frac{1}{\Delta x} \int_{x_{j-1/2}}^{x_{j+1/2}} \rho_i^0(x)\, dx, \qquad j \in \mathbb{Z}.$$

Similarly, for the kernel, we set

$$\omega_i^k := \frac{1}{\Delta x}\int_{k\Delta x}^{(k+1)\Delta x} \omega_i(x)\,dx, \qquad k \in \mathbb{N},$$

so that $\Delta x \sum_{k=0}^{+\infty} \omega_i^k = \int_0^{\eta_i} \omega_i(x)\,dx = J_i$ (the sum is indeed finite since $\omega_i^k = 0$ for $k \geq N_i$ sufficiently large). Moreover, we set $r_{j+k}^n = \sum_{i=1}^{M} \rho_{i,j+k}^n$ for $k \in \mathbb{N}$ and

$$V_{i,j}^n := v_i^{\max}\psi\left(\Delta x \sum_{k=0}^{+\infty} \omega_i^k r_{j+k}^n\right), \qquad i = 1,\dots,M, \quad j \in \mathbb{Z}. \tag{3.2.1}$$

We consider the following Godunov-type scheme adapted to (3.1.1), which was introduced in [46] in the scalar case:

$$\rho_{i,j}^{n+1} = \rho_{i,j}^n - \lambda\left(\rho_{i,j}^n V_{i,j+1}^n - \rho_{i,j-1}^n V_{i,j}^n\right) \tag{3.2.2}$$

where we have set $\lambda = \frac{\Delta t}{\Delta x}$.

3.2.1 Compactness estimates

We provide here the necessary estimates to prove the convergence of the sequence of approximate solutions constructed via the Godunov scheme (3.2.2).

Lemma 4. (Positivity) *For any $T > 0$, under the CFL condition*

$$\lambda \leq \frac{1}{v_M^{\max}\|\psi\|_\infty}, \tag{3.2.3}$$

the scheme (3.2.2) is positivity preserving on $[0,T]\times\mathbb{R}$.

Proof. Let us assume that $\rho_{i,j}^n \geq 0$ for all $j \in \mathbb{Z}$ and $i \in 1,...,M$. It suffices to prove that $\rho_{i,j}^{n+1}$ in (3.2.2) is non-negative. We compute

$$\rho_{i,j}^{n+1} = \rho_{i,j}^n\left(1 - \lambda V_{i,j+1}^n\right) + \lambda\,\rho_{i,j-1}^n V_{i,j}^n \geq 0 \tag{3.2.4}$$

under assumption (3.2.3). □

Corollary 8. ($\mathbf{L^1}$-bound) *For any $n \in \mathbb{N}$, under the CFL condition (3.2.3) the approximate solutions constructed via the scheme (3.2.2) satisfy*

$$\left\|\rho_i^n\right\|_{\mathbf{L^1}} = \left\|\rho_i^0\right\|_{\mathbf{L^1}}, \qquad i = 1,\dots,M, \tag{3.2.5}$$

where $\left\|\rho_i^n\right\|_{\mathbf{L^1}} := \Delta x \sum_j \left|\rho_{i,j}^n\right|$ denotes the $\mathbf{L^1}$ norm of the i-th component of $\rho^{\Delta x}$.

Proof. Thanks to Lemma 4, for all $i \in \{1,...,M\}$ we have

$$\left\|\rho_i^{n+1}\right\|_{\mathbf{L^1}} = \Delta x \sum_j \rho_{i,j}^{n+1} = \Delta x \sum_j \left(\rho_{i,j}^n - \lambda\rho_{i,j}^n V_{i,j+1}^n + \lambda\,\rho_{i,j-1}^n V_{i,j}^n\right) = \Delta x \sum_j \rho_{i,j}^n,$$

proving (3.2.5). □

Lemma 5. ($\mathbf{L}^\infty$-bound) *If $\rho^0_{i,j} \geq 0$ for all $j \in \mathbb{Z}$ and $i = 1, ..., M$, and (3.2.3) holds, then the approximate solution $\boldsymbol{\rho}^{\Delta x}$ constructed by the algorithm (3.2.2) is uniformly bounded on $[0,T] \times \mathbb{R}$ for any T such that*

$$T < \left(M \left\| \boldsymbol{\rho}^0 \right\|_\infty v_M^{\max} \|\psi'\|_\infty W_0 \right)^{-1}.$$

Proof. Let $\bar{\rho} = \max\{\rho^n_{i,j-1}, \rho^n_{i,j}\}$. Then we get

$$\rho^{n+1}_{i,j} = \rho^n_{i,j} \left(1 - \lambda V^n_{i,j+1}\right) + \lambda \, \rho^n_{i,j-1} V^n_{i,j} \leq \bar{\rho} \left(1 + \lambda \left(V^n_{i,j} - V^n_{i,j+1}\right)\right) \tag{3.2.6}$$

and

$$\begin{aligned}
\left| V^n_{i,j} - V^n_{i,j+1} \right| &= v_i^{\max} \left| \psi \left(\Delta x \sum_{k=0}^{+\infty} \omega_i^k r^n_{j+k} \right) - \psi \left(\Delta x \sum_{k=0}^{+\infty} \omega_i^k r^n_{j+k+1} \right) \right| \\
&\leq v_i^{\max} \|\psi'\|_\infty \, \Delta x \left| \sum_{k=0}^{+\infty} \omega_i^k (r^n_{j+k+1} - r^n_{j+k}) \right| \\
&= v_i^{\max} \|\psi'\|_\infty \, \Delta x \left| -\omega_i^0 r^n_j + \sum_{k=1}^{+\infty} (\omega_i^{k-1} - \omega_i^k) r^n_{j+k} \right| \\
&\leq v_i^{\max} \|\psi'\|_\infty \Delta x M \|\boldsymbol{\rho}^n\|_\infty \omega_i(0)
\end{aligned} \tag{3.2.7}$$

where $\|\boldsymbol{\rho}\|_\infty = \|(\rho_1, \ldots, \rho_M)\|_\infty = \max_{i,j} |\rho_{i,j}|$. Let now $K > 0$ be such that $\left\| \boldsymbol{\rho}^\ell \right\|_\infty \leq K$, $\ell = 0, \ldots, n$. From (3.2.6) and (3.2.7) we get

$$\left\| \boldsymbol{\rho}^{n+1} \right\|_\infty \leq \|\boldsymbol{\rho}^n\|_\infty \left(1 + MK v_M^{\max} \|\psi'\|_\infty W_0 \Delta t\right),$$

which implies

$$\|\boldsymbol{\rho}^n\|_\infty \leq \left\| \boldsymbol{\rho}^0 \right\|_\infty e^{Cn\Delta t},$$

with $C = MK v_M^{\max} \|\psi'\|_\infty W_0$. Therefore we get that $\left\| \boldsymbol{\rho}(t, \cdot) \right\|_\infty \leq K$ for

$$t \leq \frac{1}{MK v_M^{\max} \|\psi'\|_\infty W_0} \ln \left(\frac{K}{\left\| \boldsymbol{\rho}^0 \right\|_\infty} \right) \leq \frac{1}{Me \left\| \boldsymbol{\rho}^0 \right\|_\infty v_M^{\max} \|\psi'\|_\infty W_0},$$

where the maximum is attained for $K = e \left\| \boldsymbol{\rho}^0 \right\|_\infty$.

Iterating the procedure, at time t^m, $m \geq 1$ we set $K = e^m \left\| \boldsymbol{\rho}^0 \right\|_\infty$ and we get that the solution is bounded by K until t^{m+1} such that

$$t^{m+1} \leq t^m + \frac{m}{Me^m \left\| \boldsymbol{\rho}^0 \right\|_\infty v_M^{\max} \|\psi'\|_\infty W_0}.$$

Therefore, the approximate solution remains bounded, uniformly in Δx, at least for $t \leq T$ with

$$T \leq \frac{1}{M \left\| \boldsymbol{\rho}^0 \right\|_\infty v_M^{\max} \|\psi'\|_\infty W_0} \sum_{m=1}^{+\infty} \frac{m}{e^m} \leq \frac{1}{M \left\| \boldsymbol{\rho}^0 \right\|_\infty v_M^{\max} \|\psi'\|_\infty W_0}.$$

□

Remark 5. Figure 3.1 shows that the simplex

$$\mathcal{S} := \left\{ \boldsymbol{\rho} \in \mathbb{R}^M : \sum_{i=1}^{M} \rho_i \leq 1,\ \rho_i \geq 0 \text{ for } i = 1, \ldots, M \right\}$$

is not an invariant domain for (3.1.1), unlike the classical multi-population model [8]. Indeed,

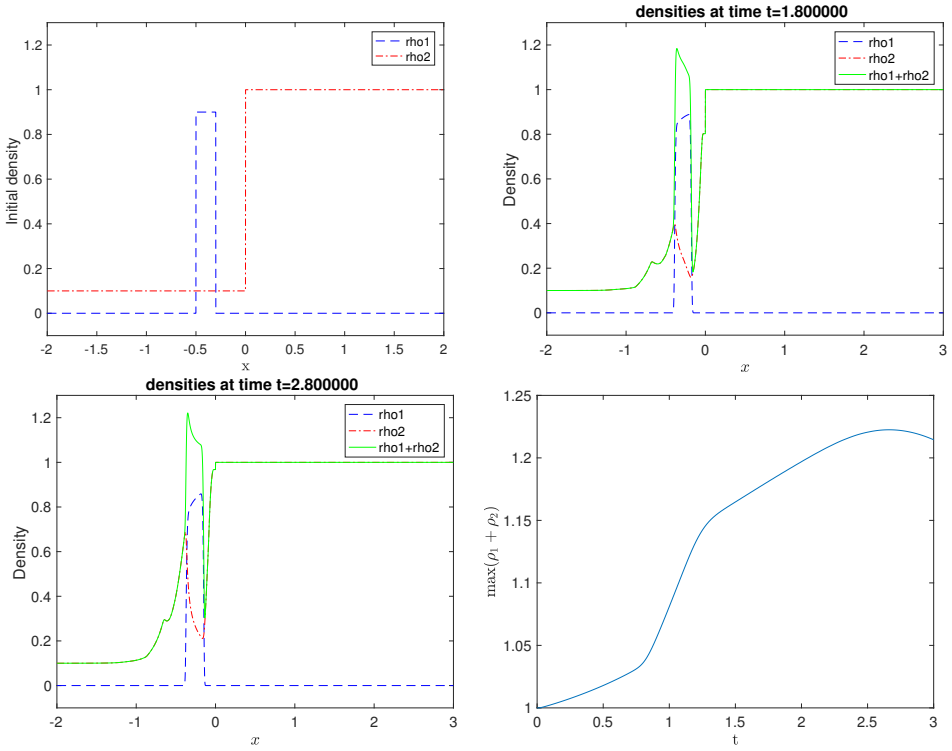

Figure 3.1: Numerical simulation illustrating that the simplex $\mathcal{S}$ is not an invariant domain for (3.1.1). We take $M = 2$ and we consider the initial conditions $\rho_1(0,x) = 0.9\chi_{[-0.5,-0.3]}$ and $\rho_2(0,x) = 0.1\chi_{]-\infty,0]} + \chi_{]0,+\infty[}$ depicted in (a), the constant kernels $\omega_1(x) = \omega_2(x) = 1/\eta$, $\eta = 0.5$, and the speed functions given by $v_1^{max} = 0.2$, $v_2^{max} = 1$, $\psi(\xi) = \max\{1-\xi, 0\}$ for $\xi \geq 0$. The space and time discretization steps are $\Delta x = 0.001$ and $\Delta t = 0.4\Delta x$. Plots (b) and (c) show the density profiles of ρ_1, ρ_2 and their sum r at times $t = 1.8,\ 2.8$. The function $\max_{x\in\mathbb{R}} r(t,x)$ is plotted in (d), showing that r can take values greater than 1, even if $r(0,x) = \rho_1(0,x) + \rho_2(0,x) \leq 1$.

let us consider the system

$$\partial_t \rho_i(t,x) + \partial_x \left(\rho_i(t,x) v_i(r(t,x)) \right) = 0, \qquad i = 1, ..., M, \tag{3.2.8}$$

where r and v_i are as in (3.1.2) and (3.1.3), respectively. We have the following:

Lemma 6. *Under the CFL condition*

$$\lambda \leq \frac{1}{v_M^{\max} \left(\|\psi\|_\infty + \|\psi'\|_\infty \right)},$$

for any initial datum $\boldsymbol{\rho}_0 \in \mathcal{S}$ *the approximate solutions to* (3.2.8) *computed by the upwind scheme*

$$\boldsymbol{\rho}_j^{n+1} = \boldsymbol{\rho}_j^n - \lambda \left[\mathbf{F}(\boldsymbol{\rho}_j^n, \boldsymbol{\rho}_{j+1}^n) - \mathbf{F}(\boldsymbol{\rho}_{j-1}^n, \boldsymbol{\rho}_j^n) \right], \tag{3.2.9}$$

with $\mathbf{F}(\boldsymbol{\rho}_j^n, \boldsymbol{\rho}_{j+1}^n) = \boldsymbol{\rho}_j^n \psi(r_{j+1}^n)$*, satisfy the following uniform bounds:*

$$\boldsymbol{\rho}_j^n \in \mathcal{S} \quad \forall j \in \mathbb{Z},\ n \in \mathbb{N}. \tag{3.2.10}$$

Proof. Assuming that $\boldsymbol{\rho}_j^n \in \mathcal{S}$ for all $j \in \mathbb{Z}$, we want to prove that $\boldsymbol{\rho}_j^{n+1} \in \mathcal{S}$. Rewriting (3.2.9), we get

$$\rho_{i,j}^{n+1} = \rho_{i,j}^n - \lambda \left[v_i^{\max} \rho_{i,j}^n \psi(r_{j+1}^n) - v_i^{\max} \rho_{i,j-1}^n \psi(r_j^n) \right].$$

Summing on the index $i = 1, \dots, M$, gives

$$\begin{aligned} r_j^{n+1} = \sum_{i=1}^M \rho_{i,j}^{n+1} &= \sum_{i=1}^M \rho_{i,j}^n - \lambda \sum_{i=1}^M \left[v_i^{\max} \rho_{i,j}^n \psi(r_{j+1}^n) - v_i^{\max} \rho_{i,j-1}^n \psi(r_j^n) \right] \\ &= r_j^n + \lambda \psi(r_j^n) \sum_{i=1}^M v_i^{\max} \rho_{i,j-1}^n - \lambda \psi(r_{j+1}^n) \sum_{i=1}^M v_i^{\max} \rho_{i,j}^n. \end{aligned}$$

Defining the following function of $\boldsymbol{\rho}_j^n$

$$\Phi(\rho_{1,j}^n, \dots, \rho_{M,j}^n) = r_j^n + \lambda \psi(r_j^n) \sum_{i=1}^M v_i^{\max} \rho_{i,j-1}^n - \lambda \psi(r_{j+1}^n) \sum_{i=1}^M v_i^{\max} \rho_{i,j}^n,$$

we observe that

$$\Phi(0, \dots, 0) = \lambda \psi(0) \sum_i^M v_i^{\max} \rho_{i,j-1}^n \le \lambda \|\psi\|_\infty v_M^{\max} \le 1$$

if $\lambda \le 1/v_M^{\max} \|\psi\|_\infty$ and

$$\Phi(\rho_{1,j}^n, ..., \rho_{M,j}^n) = 1 - \lambda \psi(r_{j+1}^n) \sum_{i=1}^M v_i^{\max} \rho_{i,j}^n \le 1$$

for $\boldsymbol{\rho}_j^n \in \mathcal{S}$ such that $r_j^n = \sum_{i=1}^M \rho_{i,j}^n = 1$. Moreover

$$\frac{\partial \Phi}{\partial \rho_{i,j}^n}(\boldsymbol{\rho}_j^n) = 1 + \lambda \psi'(r_j^n) \sum_{i=1}^M v_i^{\max} \rho_{i,j-1}^n - \lambda \psi(r_{j+1}^n) v_i^{\max} \ge 0$$

if $\lambda \le 1/v_M^{\max} \left(\|\psi\|_\infty + \|\psi'\|_\infty \right)$. This proves that $r_j^{n+1} \le 1$. To prove the positivity of (3.2.9), we observe that

$$\rho_{i,j}^{n+1} = \rho_{i,j}^n \left(1 - \lambda v_i^{\max} \psi(r_{j+1}^n) \right) + \lambda v_i^{\max} \rho_{i,j-1}^n \psi(r_j^n) \ge 0$$

if $\lambda \le 1/v_M^{\max} \|\psi\|_\infty$. □

Lemma 7. (Spatial BV-bound) *Let $\rho_i^0 \in (BV \cap \mathbf{L}^\infty)(\mathbb{R}, \mathbb{R}^+)$ for all $i = 1, ..., M$. If (3.2.3) holds, then the approximate solution $\boldsymbol{\rho}^{\Delta x}(t, \cdot)$ constructed by the algorithm (3.2.2) has uniformly bounded total variation for $t \in [0, T]$, for any T such that*

$$T \leq \min_{i=1,\dots,M} \frac{1}{\mathcal{H}\left(TV(\rho_i^0) + 1\right)}, \tag{3.2.11}$$

where $\mathcal{H} = \|\boldsymbol{\rho}\|_\infty v_M^{\max} W_0 M \left(6MJ_0\|\boldsymbol{\rho}\|_\infty \|\psi''\|_\infty + \|\psi'\|_\infty\right)$.

Proof. Subtracting the identities

$$\rho_{i,j+1}^{n+1} = \rho_{i,j+1}^n - \lambda\left(\rho_{i,j+1}^n V_{i,j+2}^n - \rho_{i,j}^n V_{i,j+1}^n\right), \tag{3.2.12}$$

$$\rho_{i,j}^{n+1} = \rho_{i,j}^n - \lambda\left(\rho_{i,j}^n V_{i,j+1}^n - \rho_{i,j-1}^n V_{i,j}^n\right), \tag{3.2.13}$$

and setting $\Delta_{i,j+1/2}^n = \rho_{i,j+1}^n - \rho_{i,j}^n$, we get

$$\Delta_{i,j+1/2}^{n+1} = \Delta_{i,j+1/2}^n - \lambda\left(\rho_{i,j+1}^n V_{i,j+2}^n - 2\,\rho_{i,j}^n V_{i,j+1}^n + \rho_{i,j-1}^n V_{i,j}^n\right).$$

Now, we can write

$$\begin{aligned}\Delta_{i,j+1/2}^{n+1} = &\left(1 - \lambda V_{i,j+2}^n\right)\Delta_{i,j+1}^n &(3.2.14)\\ &+ \lambda V_{i,j}^n \Delta_{i,j-1/2}^n \\ &- \lambda\rho_{i,j}^n\left(V_{i,j+2}^n - 2V_{i,j+1}^n + V_{i,j}^n\right). &(3.2.15)\end{aligned}$$

Observe that assumption (3.2.3) guarantees the positivity of (3.2.14). The term (3.2.15) can be estimated as

$$\begin{aligned}&V_{i,j+2}^n - 2V_{i,j+1}^n + V_{i,j}^n = \\ =&v_i^{\max}\left(\psi\left(\Delta x\sum_{k=0}^{+\infty}\omega_i^k r_{j+k+2}^n\right) - 2\,\psi\left(\Delta x\sum_{k=0}^{+\infty}\omega_i^k r_{j+k+1}^n\right) + \psi\left(\Delta x\sum_{k=0}^{+\infty}\omega_i^k r_{j+k}^n\right)\right)\\ =&v_i^{\max}\psi'(\xi_{j+1})\Delta x\left(\sum_{k=0}^{+\infty}\omega_i^k r_{j+k+2}^n - \sum_{k=0}^{+\infty}\omega_i^k r_{j+k+1}^n\right)\\ &+ v_i^{\max}\psi'(\xi_j)\Delta x\left(\sum_{k=0}^{+\infty}\omega_i^k r_{j+k}^n - \sum_{k=0}^{+\infty}\omega_i^k r_{j+k+1}^n\right)\\ =&v_i^{\max}\psi'(\xi_{j+1})\Delta x\left(\sum_{k=1}^{+\infty}(\omega_i^{k-1} - \omega_i^k) r_{j+k+1}^n - \omega_i^0 r_{j+1}^n\right)\\ &+ v_i^{\max}\psi'(\xi_j)\Delta x\left(\sum_{k=1}^{+\infty}(\omega_i^k - \omega_i^{k-1}) r_{j+k}^n + \omega_i^0 r_j^n\right)\end{aligned}$$

$$
\begin{aligned}
=&v_i^{\max}(\psi'(\xi_{j+1})-\psi'(\xi_j))\Delta x\left(\sum_{k=1}^{+\infty}(\omega_i^{k-1}-\omega_i^k)r_{j+k+1}^n-\omega_i^0 r_{j+1}^n\right)\\
&+v_i^{\max}\psi'(\xi_j)\Delta x\left(\sum_{k=1}^{+\infty}(\omega_i^{k-1}-\omega_i^k)(r_{j+k+1}^n-r_{j+k}^n)+\omega_i^0(r_j^n-r_{j+1}^n)\right)\\
=&v_i^{\max}\psi''(\tilde{\xi}_{j+1/2})(\xi_{j+1}-\xi_j)\Delta x\left(\sum_{k=1}^{+\infty}\sum_{\beta=1}^{M}\omega_i^k\Delta_{\beta,j+k+3/2}^n\right)\\
&+v_i^{\max}\psi'(\xi_j)\Delta x\left(\sum_{\beta=1}^{M}\sum_{k=1}^{N-1}(\omega_i^{k-1}-\omega_i^k)\Delta_{\beta,j+k+1/2}^n-\omega_i^0\Delta_{\beta,j+1/2}^n\right),
\end{aligned}
$$

with $\xi_j\in\mathcal{I}\left(\Delta x\sum_{k=0}^{+\infty}\omega_i^k r_{j+k}^n,\Delta x\sum_{k=0}^{+\infty}\omega_i^k r_{j+k+1}^n\right)$ and $\tilde{\xi}_{j+1/2}\in\mathcal{I}\left(\xi_j,\xi_{j+1}\right)$, where we set $\mathcal{I}(a,b)=\left[\min\{a,b\},\max\{a,b\}\right]$. For some $\vartheta,\mu\in[0,1]$, we compute

$$
\begin{aligned}
\xi_{j+1}-\xi_j=&\vartheta\Delta x\sum_{k=0}^{+\infty}\omega_i^k\sum_{\beta=1}^{M}\rho_{\beta,j+k+2}^n+(1-\vartheta)\Delta x\sum_{k=0}^{+\infty}\omega_i^k\sum_{\beta=1}^{M}\rho_{\beta,j+k+1}^n\\
&-\mu\Delta x\sum_{k=0}^{+\infty}\omega_i^k\sum_{\beta=1}^{M}\rho_{\beta,j+k+1}^n-(1-\mu)\Delta x\sum_{k=0}^{+\infty}\omega_i^k\sum_{\beta=1}^{M}\rho_{\beta,j+k}^n\\
=&\vartheta\Delta x\sum_{k=1}^{+\infty}\omega_i^{k-1}\sum_{\beta=1}^{M}\rho_{\beta,j+k+1}^n+(1-\vartheta)\Delta x\sum_{k=0}^{+\infty}\omega_i^k\sum_{\beta=1}^{M}\rho_{\beta,j+k+1}^n\\
&-\mu\Delta x\sum_{k=0}^{+\infty}\omega_i^k\sum_{\beta=1}^{M}\rho_{\beta,j+k+1}^n-(1-\mu)\Delta x\sum_{k=-1}^{+\infty}\omega_i^{k+1}\sum_{\beta=1}^{M}\rho_{\beta,j+k+1}^n\\
=&\Delta x\sum_{k=1}^{+\infty}\left[\vartheta\omega_i^{k-1}+(1-\vartheta)\omega_i^k-\mu\omega_i^k-(1-\mu)\omega_i^{k+1}\right]\sum_{\beta=1}^{M}\rho_{\beta,j+k+1}^n\\
&+(1-\vartheta)\Delta x\omega_i^0\sum_{\beta=1}^{M}\rho_{\beta,j+1}^n-\mu\Delta x\omega_i^0\sum_{\beta=1}^{M}\rho_{\beta,j+1}^n\\
&-(1-\mu)\Delta x\left(\omega_i^0\sum_{\beta=1}^{M}\rho_{\beta,j}^n+\omega_i^1\sum_{\beta=1}^{M}\rho_{\beta,j+1}^n\right).
\end{aligned}
$$

By monotonicity of ω_i we have

$$
\vartheta\omega_i^{k-1}+(1-\vartheta)\omega_i^k-\mu\omega_i^k-(1-\mu)\omega_i^{k+1}\geq 0\,.
$$

Taking the absolute values we get

$$
\left|\xi_{j+1}-\xi_j\right|\leq\Delta x\left\{\sum_{k=2}^{+\infty}\left[\vartheta\omega_i^{k-1}+(1-\vartheta)\omega_i^k-\mu\omega_i^k-(1-\mu)\omega_i^{k+1}\right]+4\omega_i^0\right\}M\|\boldsymbol{\rho}^n\|_\infty
$$

$$\leq \Delta x \left\{ \sum_{k=2}^{+\infty} \left[\omega_i^{k-1} - \omega_i^{k+1} \right] + 4\omega_i^0 \right\} M \|\boldsymbol{\rho}^n\|_\infty$$
$$\leq \Delta x \, 6 \, W_0 M \|\boldsymbol{\rho}^n\|_\infty .$$

Let now $K_1 > 0$ be such that $\sum_j \left|\Delta^\ell_{\beta,j}\right| \leq K_1$ for $\beta = 1, \dots, M$, $\ell = 0, \dots, n$. Taking the absolute values and rearranging the indexes, we have

$$\sum_j \left|\Delta^{n+1}_{i,j+1/2}\right| \leq \sum_j \left|\Delta^n_{i,j+1/2}\right| \left(1 - \lambda \left(V^n_{i,j+2} - V^n_{i,j+1}\right)\right) + \Delta t \, \mathcal{H} K_1,$$

where $\mathcal{H} = \|\boldsymbol{\rho}\|_\infty v_M^{\max} W_0 M \left(6 M J_0 \|\boldsymbol{\rho}\|_\infty \|\psi''\|_\infty + \|\psi'\|_\infty\right)$. Therefore, by (3.2.7) we get

$$\sum_j \left|\Delta^{n+1}_{i,j+1/2}\right| \leq \sum_j \left|\Delta^n_{i,j+1/2}\right| (1 + \Delta t \, \mathcal{G}) + \Delta t \, \mathcal{H} K_1,$$

with $\mathcal{G} = v_M^{\max} \|\psi'\|_\infty W_0 M \|\boldsymbol{\rho}\|_\infty$. We thus obtain

$$\sum_j \left|\Delta^n_{i,j+1/2}\right| \leq e^{\mathcal{G} n \Delta t} \sum_j \left|\Delta^0_{i,j+1/2}\right| + e^{\mathcal{H} K_1 n \Delta t} - 1,$$

that we can rewrite as

$$\begin{aligned} \mathrm{TV}(\rho_i^{\Delta x})(n\Delta t, \cdot) &\leq e^{\mathcal{G} n \Delta t} \mathrm{TV}(\rho_i^0) + e^{\mathcal{H} K_1 n \Delta t} - 1 \\ &\leq e^{\mathcal{H} K_1 n \Delta t} \left(\mathrm{TV}(\rho_i^0) + 1\right) - 1 , \end{aligned}$$

since $\mathcal{H} \geq \mathcal{G}$ and it is not restrictive to assume $K_1 \geq 1$. Therefore, we have that $\mathrm{TV}(\rho_i^{\Delta x}) \leq K_1$ for

$$t \leq \frac{1}{\mathcal{H} K_1} \ln \left(\frac{K_1 + 1}{\mathrm{TV}(\rho_i^0) + 1} \right),$$

where the maximum is attained for some $K_1 < e \left(\mathrm{TV}(\rho_i^0) + 1\right) - 1$ such that

$$\ln \left(\frac{K_1 + 1}{\mathrm{TV}(\rho_i^0) + 1} \right) = \frac{K_1}{K_1 + 1} .$$

Therefore the total variation is uniformly bounded for

$$t \leq \frac{1}{\mathcal{H} e \left(\mathrm{TV}(\rho_i^0) + 1\right)} .$$

Iterating the procedure, at time t^m, $m \geq 1$ we set $K_1 = e^m \left(\mathrm{TV}(\rho_i^0) + 1\right) - 1$ and we get that the solution is bounded by K_1 until t^{m+1} such that

$$t^{m+1} \leq t^m + \frac{m}{\mathcal{H} e^m \left(\mathrm{TV}(\rho_i^0) + 1\right)}. \tag{3.2.16}$$

Therefore, the approximate solution has bounded total variation for $t \leq T$ with

$$T \leq \frac{1}{\mathcal{H}\left(\mathrm{TV}(\rho_i^0)+1\right)}.$$

□

Corollary 9. *Let $\rho_i^0 \in (BV \cap \mathbf{L}^\infty)(\mathbb{R};\mathbb{R}^+)$. If (3.2.3) holds, then the approximate solution $\boldsymbol{\rho}^{\Delta x}$ constructed by the algorithm (3.2.2) has uniformly bounded total variation on $[0,T]\times\mathbb{R}$, for any T satisfying (3.2.11).*

Proof. If $T \leq \Delta t$, then $\mathrm{TV}(\rho_i^{\Delta x};[0,T]\times\mathbb{R}) \leq T\mathrm{TV}(\rho_i^0)$. Let us assume now that $T > \Delta t$. Let $n_T \in \mathbb{N}\backslash\{0\}$ such that $n_T\Delta t < T \leq (n_T+1)\Delta t$. Then

$$\begin{aligned}
&\mathrm{TV}(\rho_i^{\Delta x};[0,T]\times\mathbb{R}) \\
&= \underbrace{\sum_{n=0}^{n_T-1}\sum_{j\in\mathbb{Z}} \Delta t\left|\rho_{i,j+1}^n - \rho_{i,j}^n\right| + (T-n_T\Delta t)\sum_{j\in\mathbb{Z}}\left|\rho_{i,j+1}^{n_T} - \rho_{i,j}^{n_T}\right|}_{\leq T\,\sup_{t\in[0,T]}\mathrm{TV}(\rho_i^{\Delta x})(t,\cdot)} \\
&\qquad + \sum_{n=0}^{n_T-1}\sum_{j\in\mathbb{Z}}\Delta x\left|\rho_{i,j}^{n+1} - \rho_{i,j}^n\right|.
\end{aligned}$$

We then need to bound the term

$$\sum_{n=0}^{n_T-1}\sum_{j\in\mathbb{Z}}\Delta x\left|\rho_{i,j}^{n+1} - \rho_{i,j}^n\right|.$$

From the definition of the numerical scheme (3.2.2), we obtain

$$\begin{aligned}
\rho_{i,j}^{n+1} - \rho_{i,j}^n &= \lambda\left(\rho_{i,j-1}^n V_{i,j}^n - \rho_{i,j}^n V_{i,j+1}^n\right) \\
&= \lambda\left(\rho_{i,j-1}^n\left(V_{i,j}^n - V_{i,j+1}^n\right) + V_{i,j+1}^n\left(\rho_{i,j-1}^n - \rho_{i,j}^n\right)\right).
\end{aligned}$$

Taking the absolute values and using (3.2.7) we obtain

$$\left|\rho_{i,j}^{n+1} - \rho_{i,j}^n\right| \leq \lambda\left(v_i^{\max}\left\|\psi'\right\|_\infty M\|\boldsymbol{\rho}^n\|_\infty\omega_i(0)\Delta x\left|\rho_{i,j-1}^n\right| + v_i^{\max}\|\psi\|_\infty\left|\rho_{i,j-1}^n - \rho_{i,j}^n\right|\right).$$

Summing on j, we get

$$\begin{aligned}
\sum_{j\in\mathbb{Z}}\Delta x\left|\rho_{i,j}^{n+1} - \rho_{i,j}^n\right| &= v_i^{\max}\left\|\psi'\right\|_\infty M\|\boldsymbol{\rho}^n\|_\infty\omega_i(0)\,\Delta t\sum_{j\in\mathbb{Z}}\Delta x\left|\rho_{i,j-1}^n\right| \\
&\quad + v_i^{\max}\|\psi\|_\infty\Delta t\sum_{j\in\mathbb{Z}}\left|\rho_{i,j-1}^n - \rho_{i,j}^n\right|,
\end{aligned}$$

which yields

$$\sum_{n=0}^{n_T-1}\sum_{j\in\mathbb{Z}}\Delta x\left|\rho_{i,j}^{n+1} - \rho_{i,j}^n\right|$$

$$\leq v_M^{\max}\|\psi\|_\infty T \sup_{t\in[0,T]} \mathrm{TV}(\rho_i^{\Delta x})(t,\cdot)$$
$$+ v_M^{\max}\|\psi'\|_\infty MW_0 T \sup_{t\in[0,T]} \left\|\rho_i^{\Delta x}(t,\cdot)\right\|_{\mathbf{L^1}} \left\|\rho_i^{\Delta x}(t,\cdot)\right\|_\infty$$

that is bounded by Corollary 8, Lemma 5 and Lemma 7. □

3.3 Proof of Theorem 7

To complete the proof of the existence of solutions to the problem (3.1.1), (3.1.5), we follow a Lax-Wendroff type argument as in [11], see also [63], to show that the approximate solutions constructed by scheme (3.2.2) converge to a weak solution of (3.1.1). By Lemma 5, Lemma 7 and Corollary 9, we can apply Helly's theorem, stating that for $i = 1,\dots,M$, there exists a subsequence, still denoted by $\rho_i^{\Delta x}$, which converges to some $\rho_i \in (\mathbf{L^1}\cap \mathrm{BV})([0,T]\times\mathbb{R};\mathbb{R}^+)$ in the $\mathbf{L^1_{loc}}$-norm. Let us fix $i\in\{1,\dots,M\}$. Let $\varphi \in \mathbf{C_c^1}([0,T[\,\times\mathbb{R})$ and multiply (3.2.2) by $\varphi(t^n,x_j)$. Summing over $j\in\mathbb{Z}$ and $n\in\{0,\dots,n_T\}$ we get

$$\sum_{n=0}^{n_T-1}\sum_j \varphi(t^n,x_j)\left(\rho_{i,j}^{n+1}-\rho_{i,j}^n\right)$$
$$= -\lambda \sum_{n=0}^{n_T-1}\sum_j \varphi(t^n,x_j)\left(\rho_{i,j}^n V_{i,j+1}^n - \rho_{i,j-1}^n V_{i,j}^n\right).$$

Summing by parts we obtain

$$-\sum_j \varphi((n_T-1)\Delta t,x_j)\rho_{i,j}^{n_T} + \sum_j \varphi(0,x_j)\rho_{i,j}^0$$
$$+ \sum_{n=1}^{n_T-1}\sum_j \left(\varphi(t^n,x_j)-\varphi(t^{n-1},x_j)\right)\rho_{i,j}^n \tag{3.3.1}$$
$$+ \lambda \sum_{n=0}^{n_T-1}\sum_j \left(\varphi(t^n,x_{j+1})-\varphi(t^n,x_j)\right)V_{i,j+1}^n\rho_{i,j}^n = 0.$$

Multiplying by Δx we get

$$-\Delta x\sum_j \varphi((n_T-1)\Delta t,x_j)\rho_{i,j}^{n_T} + \Delta x\sum_j \varphi(0,x_j)\rho_{i,j}^0 \tag{3.3.2}$$
$$+\Delta x\Delta t\sum_{n=1}^{n_T-1}\sum_j \frac{\left(\varphi(t^n,x_j)-\varphi(t^{n-1},x_j)\right)}{\Delta t}\rho_{i,j}^n \tag{3.3.3}$$
$$+\Delta x\Delta t\sum_{n=0}^{n_T-1}\sum_j \frac{\left(\varphi(t^n,x_{j+1})-\varphi(t^n,x_j)\right)}{\Delta x}V_{i,j+1}^n\rho_{i,j}^n = 0. \tag{3.3.4}$$

By $\mathbf{L^1_{loc}}$ convergence of $\rho_i^{\Delta x}\to\rho_i$, it is straightforward to see that the terms in (3.3.2), (3.3.3) converge to

$$\int_{\mathbb{R}}\left(\rho_i^0(x)\varphi(0,x)-\rho_i(T,x)\varphi(T,x)\right)dx + \int_0^T\int_{\mathbb{R}}\rho_i(t,x)\partial_t\varphi(t,x)\,dx\,dt, \tag{3.3.5}$$

as $\Delta x \to 0$. Concerning the last term (3.3.4), we can rewrite

$$\begin{aligned}
&\Delta x\Delta t \sum_{n=0}^{n_T-1}\sum_{j} \frac{\varphi(t^n, x_{j+1}) - \varphi(t^n, x_j)}{\Delta x} V^n_{i,j+1}\rho^n_{i,j} \\
&= \Delta x\Delta t \sum_{n=0}^{n_T-1}\sum_{j} \frac{\varphi(t^n, x_{j+1}) - \varphi(t^n, x_j)}{\Delta x} \left(\rho^n_{i,j} V^n_{i,j+1} - \rho^n_{i,j} V^n_{i,j}\right) \\
&\quad + \Delta x\Delta t \sum_{n=0}^{n_T-1}\sum_{j} \frac{\varphi(t^n, x_{j+1}) - \varphi(t^n, x_j)}{\Delta x} \rho^n_{i,j} V^n_{i,j}.
\end{aligned} \tag{3.3.6}$$

By (3.2.7) we get the estimate

$$\rho^n_{i,j} V^n_{i,j+1} - \rho^n_{i,j} V^n_{i,j} \le v_i^{\max} \left\|\psi'\right\|_\infty \Delta x M \|\boldsymbol{\rho}\|^2_\infty \omega_i(0).$$

Set $R > 0$ such that $\varphi(t,x) = 0$ for $|x| > R$ and j_0, $j_1 \in \mathbb{Z}$ such that $-R \in]x_{j_0-\frac{1}{2}}, x_{j_0+\frac{1}{2}}]$ and $R \in]x_{j_1-\frac{1}{2}}, x_{j_1+\frac{1}{2}}]$, then

$$\begin{aligned}
&\Delta x\Delta t \sum_{n=0}^{n_T}\sum_{j} \frac{\varphi(t^n, x_{j+1}) - \varphi(t^n, x_j)}{\Delta x} (\rho^n_{i,j} V^n_{i,j+1} - \rho^n_{i,j} V^n_{i,j}) \\
&\le \Delta x\Delta t \|\partial_x \varphi\|_\infty \sum_{n=0}^{n_T}\sum_{j=j_0}^{j_1} v_i^{\max} \left\|\psi'\right\|_\infty M \|\boldsymbol{\rho}\|^2_\infty \omega_i(0)\, \Delta x \\
&\le \|\partial_x \varphi\|_\infty \; v_i^{\max} \left\|\psi'\right\|_\infty M \|\boldsymbol{\rho}\|^2_\infty \omega_i(0)\, \Delta x\, 2\, R\, T\,,
\end{aligned}$$

which goes to zero as $\Delta x \to 0$.

Finally, again by the $\mathbf{L^1_{loc}}$ convergence of $\rho_i^{\Delta x} \to \rho_i$, we have that

$$\Delta x\Delta t \sum_{n=0}^{n_T-1}\sum_{j} \frac{\big(\varphi(t^n, x_{j+1}) - \varphi(t^n, x_j)\big)}{\Delta x} \rho^n_{i,j} V^n_{i,j-\frac{1}{2}} \to \int_0^T \int_{\mathbb{R}} \partial_x \varphi(t,x) \rho_i(t,x) v_i(r * \omega_i)\, dx\, dt.$$

3.4 Numerical tests

In this section we perform some numerical simulations to illustrate the behaviour of solutions to (3.1.1) for $M = 2$ modeling two different scenarios. In the following, the space mesh is set to $\Delta x = 0.001$.

3.4.1 Cars and trucks mixed traffic

In this example, we consider a stretch of road populated by cars and trucks. The space domain is given by the interval $[-2, 3]$ and we impose absorbing conditions at the boundaries, adding $N_1 = \eta_1/\Delta x$ ghost cells for the first population and $N_2 = \eta_2/\Delta x$ for the second one at the right boundary, and just one ghost cell for both populations at the left boundary, where we

extend the solution constantly equal to the last value inside the domain. The dynamics is described by the following 2×2 system

$$\begin{cases} \partial_t \rho_1(t,x) + \partial_x \left(\rho_1(t,x) v_1^{\max} \psi((r * \omega_1)(t,x)) \right) = 0, \\ \partial_t \rho_2(t,x) + \partial_x \left(\rho_2(t,x) v_2^{\max} \psi((r * \omega_2)(t,x)) \right) = 0, \end{cases} \tag{3.4.1}$$

with

$$\begin{aligned} &\omega_1(x) = \frac{2}{\eta_1}\left(1 - \frac{x}{\eta_1}\right), && \eta_1 = 0.3, \\ &\omega_2(x) = \frac{2}{\eta_2}\left(1 - \frac{x}{\eta_2}\right), && \eta_2 = 0.1, \\ &\psi(\xi) = \max\{1 - \xi, 0\}, && \xi \geq 0, \\ &v_1^{max} = 0.8, \quad v_2^{max} = 1.3. \end{aligned}$$

In this setting, ρ_1 represents the density of trucks and ρ_2 is the density of cars on the road. Trucks moves at lower maximal speed than cars and have grater view horizon, but of the same order of magnitude. Figure 3.2 describes the evolution in time of the two population densities, correspondent to the initial configuration

$$\begin{cases} \rho_1(0,x) = 0.5 \chi_{[-1.1,-1.6]}, \\ \rho_2(0,x) = 0.5 \chi_{[-1.6,-1.9]}, \end{cases}$$

in which a platoon of trucks precedes a group of cars. Due to their higher speed, cars overtake trucks, in accordance with what observed in the local case [8].

3.4.2 Impact of connected autonomous vehicles

The aim of this test is to study the possible impact of the presence of Connected Autonomous Vehicles (CAVs) on road traffic performances. Let us consider a circular road modeled by the space interval $[-1, 1]$ with periodic boundary conditions at $x = \pm 1$. In this case, we assume that autonomous and non-autonomous vehicles have the same maximal speed, but the interaction radius of CAVs is two orders of magnitude grater than the one of human-driven cars. Moreover, we assume CAVs have constant convolution kernel, modeling the fact that they have the same degree of accuracy on information about surrounding traffic, independent from the distance. In this case, model (3.1.1) reads

$$\begin{cases} \partial_t \rho_1(t,x) + \partial_x \left(\rho_1(t,x) v_1^{\max} \psi((r * \omega_1)(t,x)) \right) = 0, \\ \partial_t \rho_2(t,x) + \partial_x \left(\rho_2(t,x) v_2^{\max} \psi((r * \omega_2)(t,x)) \right) = 0, \\ \rho_1(0,x) = \beta \left(0.5 + 0.3 \sin(5\pi x)\right), \\ \rho_2(0,x) = (1-\beta) \left(0.5 + 0.3 \sin(5\pi x)\right), \end{cases} \tag{3.4.2}$$

with

$$\omega_1(x) = \frac{1}{\eta_1}, \qquad \eta_1 = 1,$$

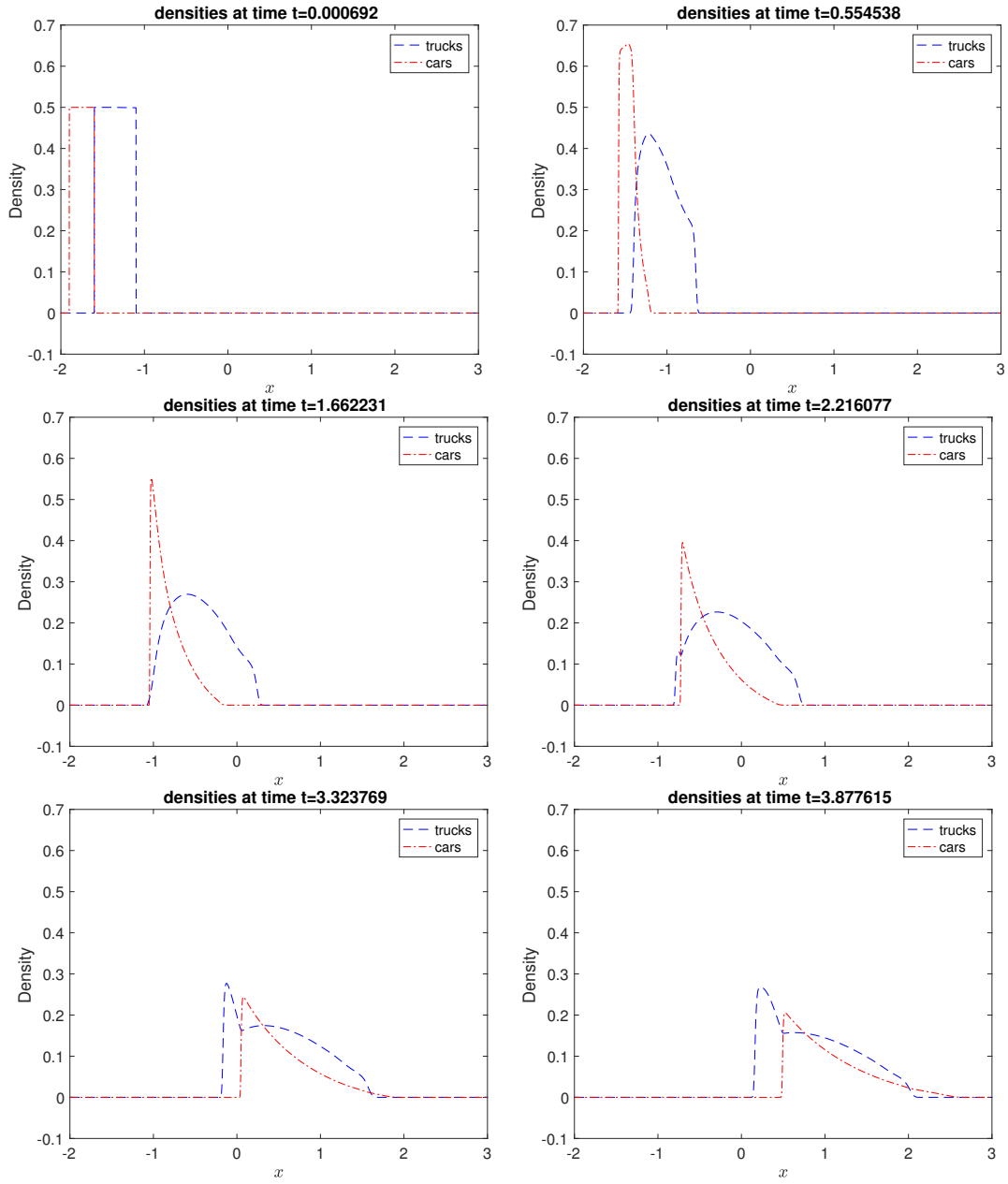

Figure 3.2: Density profiles of cars and trucks at increasing times corresponding to the non-local model (3.4.1).

$$\omega_2(x) = \frac{2}{\eta_2}\left(1 - \frac{x}{\eta_2}\right), \qquad \eta_2 = 0.01,$$
$$\psi(\xi) = \max\{1-\xi, 0\}, \qquad \xi \geq 0,$$
$$v_1^{max} = v_2^{max} = 1.$$

Above ρ_1 represents the density of autonomous vehicles, ρ_2 the density of non-autonomous vehicles and $\beta \in [0,1]$ is the penetration rate of autonomous vehicle. Figure 3.3 displays the traffic dynamics in the case $\beta = 0.9$.

As a metric of traffic congestion, given a time horizon $T > 0$, we consider the two following functionals:

$$J(\beta) = \int_0^T \mathrm{d}|\,\partial_x r|\,dt, \tag{3.4.3}$$
$$\Psi(\beta) = \int_0^T \left[\rho_1(t,\bar{x})v_1^{\max}\psi((r*\omega_1)(t,\bar{x})) + \rho_2(t,\bar{x})v_2^{\max}\psi((r*\omega_2)(t,\bar{x}))\right] dt, \tag{3.4.4}$$

where $\bar{x} = x_0 \approx 0$. The functional J measures the integral with respect to time of the spatial total variation of the total traffic density, see [30]. The functional Ψ measures the integral with respect to time of the traffic flow at a given point $\bar{x}$, corresponding to the number of cars that have passed through $\bar{x}$ in the studied time interval. Figure 3.4 displays the values of the functionals J and Ψ for different values of $\beta = 0,\ 0.1,\ 0.2, \ldots,\ 1$. We can notice that the functionals are not monotone and present minimum and maximum values. The traffic evolution patterns corresponding these stationary values are reported in Figure 3.5, showing the (t,x)-plots of the total traffic density $r(t,x)$ corresponding to these values of β.

3.5 Lax-Friedrichs numerical scheme

We provide here alternative estimates for (3.1.1), based on approximate solutions constructed via the following adapted Lax-Friedrichs scheme:

$$\rho_{i,j}^{n+1} = \rho_{i,j}^n - \lambda\left(F_{i,j+1/2}^n - F_{i,j-1/2}^n\right), \tag{3.5.1}$$

with

$$F_{i,j+1/2}^n := \frac{1}{2}\rho_{i,j}^n V_{i,j}^n + \frac{1}{2}\rho_{i,j+1}^n V_{i,j+1}^n + \frac{\alpha}{2}\left(\rho_{i,j}^n - \rho_{i,j+1}^n\right), \tag{3.5.2}$$

where $\alpha \geq 1$ is the viscosity coefficient and $\lambda = \frac{\Delta t}{\Delta x}$. The proofs are very similar to those exposed for Godunov approximations.

Lemma 8. *For any $T > 0$, under the CFL conditions*

$$\lambda\alpha < 1, \tag{3.5.3}$$
$$\alpha \geq v_M^{\max}\|\psi\|_\infty, \tag{3.5.4}$$

the scheme (3.5.2)-(3.5.1) is positivity preserving on $[0,T]\times\mathbb{R}$.

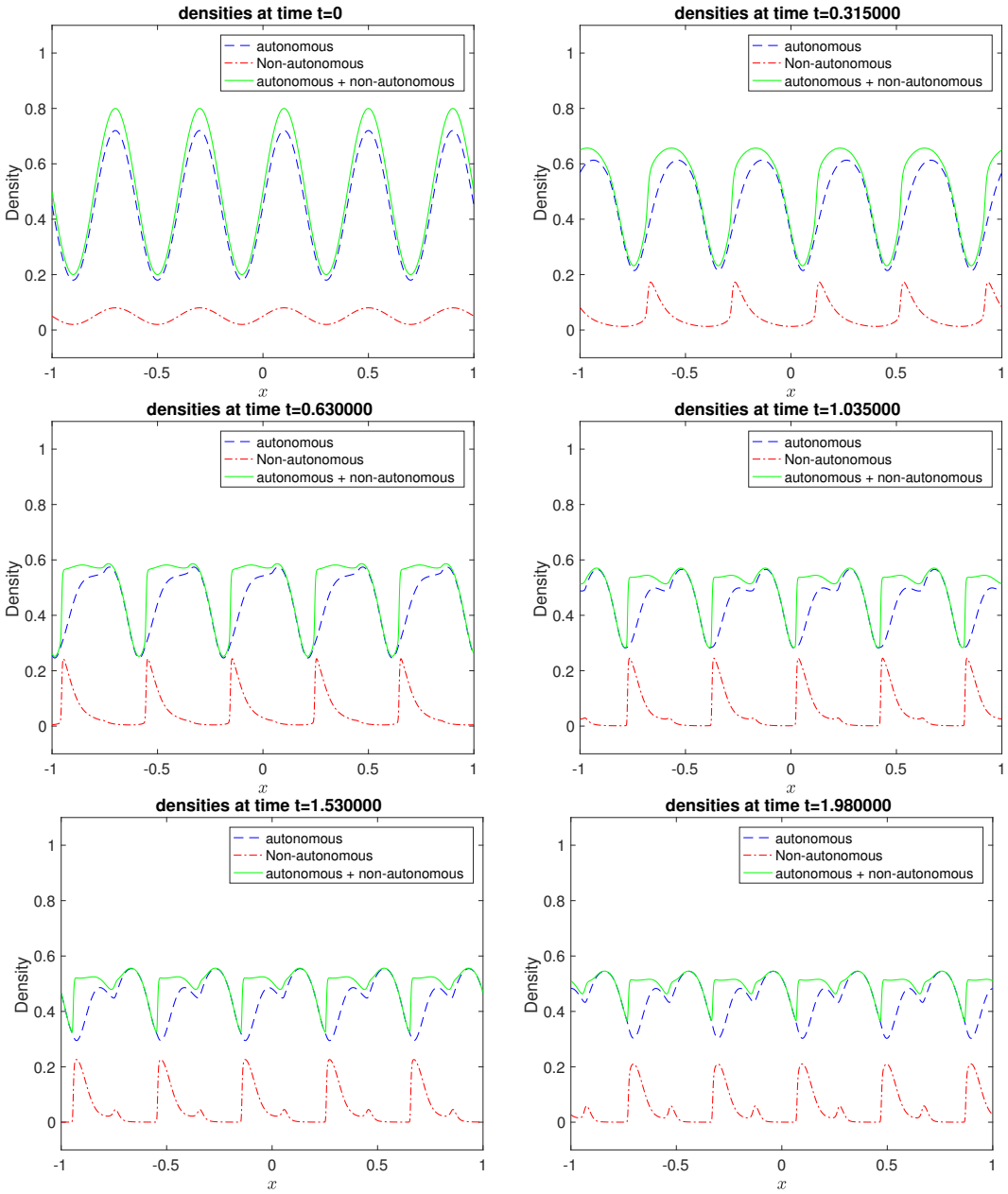

Figure 3.3: Density profiles corresponding to the non-local problem (3.4.2) with $\beta = 0.9$ at different times.

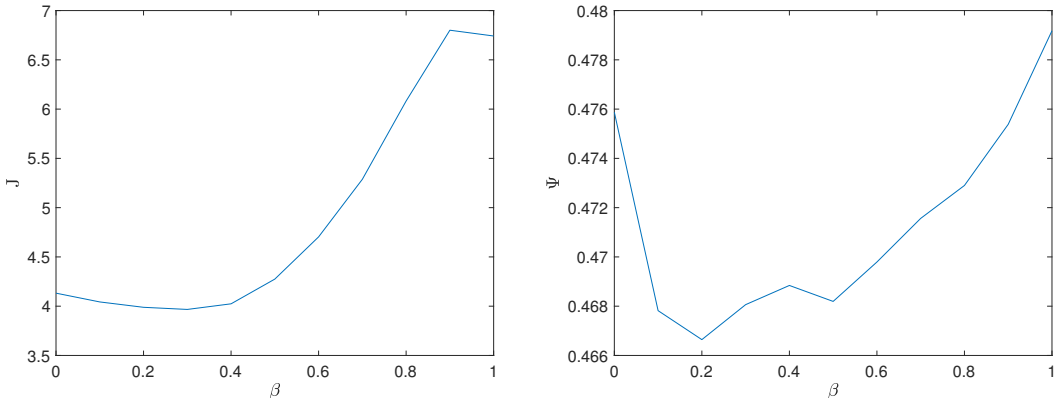

Figure 3.4: Functional J (left) and Ψ (right)

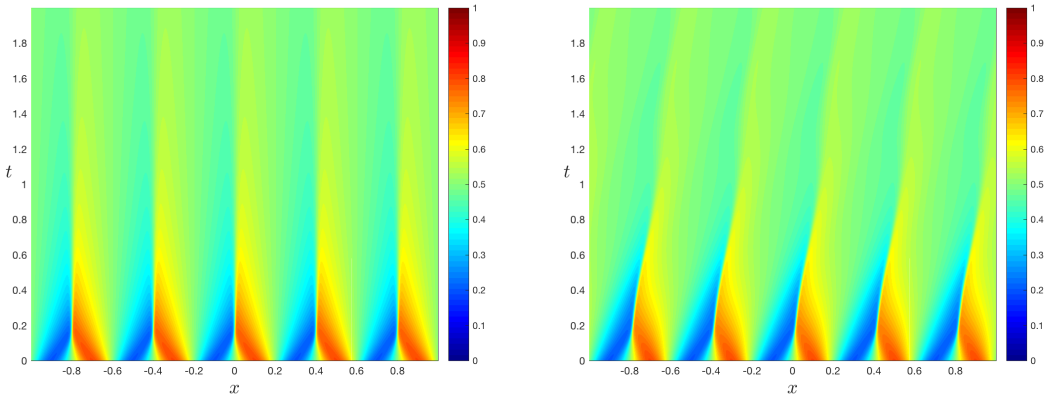

(a) $\beta = 0$

(b) $\beta = 0.2$

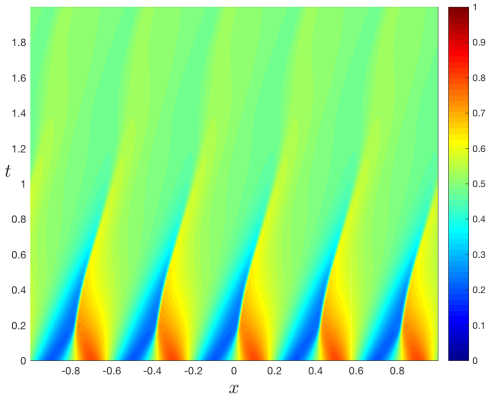

(c) $\beta = 0.3$

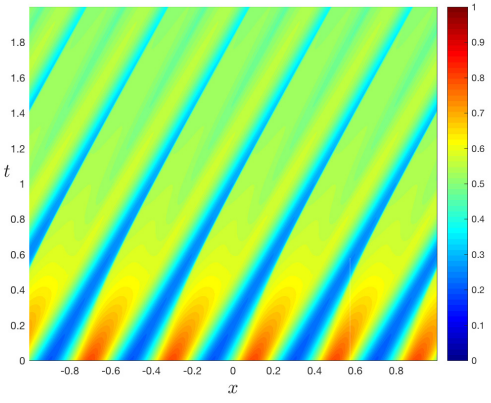

(d) $\beta = 0.9$

Figure 3.5: (t, x)-plots of the total traffic density $r(t, x) = \rho_1(t, x) + \rho_2(t, x)$ in (3.4.2) corresponding to different values of β: (a) no autonomous vehicles are present; (b) point of minimum for Ψ; (c) point of minimum for J; (d) point of maximum for J.

Proof. Let us assume that $\rho_{i,j}^n \geq 0$ for all $j \in \mathbb{Z}$ and $i \in 1, ..., M$. It suffices to prove that $\rho_{i,j}^{n+1}$ in (3.5.1) is non-negative. Compute

$$\rho_{i,j}^{n+1} = \rho_{i,j}^n + \frac{\lambda}{2}\alpha(\rho_{i,j+1}^n - 2\rho_{i,j}^n + \rho_{i,j-1}^n) + \frac{\lambda}{2}\left(\rho_{i,j-1}^n V_{i,j-1}^n - \rho_{i,j+1}^n V_{i,j+1}^n\right) \tag{3.5.5}$$

$$= \rho_{i,j-1}^n \frac{\lambda}{2}\left(\alpha + V_{i,j-1}^n\right) + \rho_{i,j}^n(1 - \lambda\alpha) + \rho_{i,j+1}^n \frac{\lambda}{2}\left(\alpha - V_{i,j+1}^n\right), \tag{3.5.6}$$

under assumptions (3.5.3) and (3.5.4), we obtain that $\rho_{i,j}^{n+1}$ is positive. □

Corollary 10. ($\mathbf{L^1}$ bound) *For any $T > 0$, under the CFL conditions (3.5.3)-(3.5.4) the scheme (3.5.2)-(3.5.1) preserves the $\mathbf{L^1}$ norm of the i-th component of $\rho^{\Delta x}$.*

Proof. See proof of Corollary 8. □

Lemma 9. ($\mathbf{L^\infty}$-bound) *If $\rho_{i,j}^0 \geq 0$ for all $j \in \mathbb{Z}$ and $i = 1, ..., M$, and the CFL conditions (3.5.3)-(3.5.4) hold, the approximate solution $\boldsymbol{\rho}^{\Delta x}$ constructed by the algorithm (3.5.2)-(3.5.1) is uniformly bounded on $[0, T] \times \mathbb{R}$ for any T such that*

$$T < \left(M \left\|\boldsymbol{\rho}^0\right\|_\infty v_M^{\max} \left\|\psi'\right\|_\infty W_0\right)^{-1}. \tag{3.5.7}$$

Proof. From (3.5.6) we can define

$$\rho_{i,j}^{n+1} = \frac{\lambda}{2}\rho_{i,j-1}^n \left(\alpha + V_{i,j-1}^n\right) + (1 - \lambda\alpha)\rho_{i,j}^n + \frac{\lambda}{2}\rho_{i,j+1}^n \left(\alpha - V_{i,j+1}^n\right)$$

Let $\bar{\rho} = \max\left\{\rho_{i,j-1}^n, \rho_{i,j}^n, \rho_{i,j+1}^n\right\}$. Then we get

$$\rho_{i,j}^{n+1} \leq \bar{\rho}\left[1 + \frac{\lambda}{2}\left(V_{i,j-1}^n - V_{i,j+1}^n\right)\right]$$

and by (3.2.7)

$$\left|V_{i,j-1}^n - V_{i,j+1}^n\right| = v_i^{\max}\left[\psi\left(\Delta x \sum_{k=0}^{+\infty} \omega_i^k r_{j-1+k}\right) - \psi\left(\Delta x \sum_{k=0}^{+\infty} \omega_i^k r_{j+1+k}\right)\right] \tag{3.5.8}$$

$$= -v_i^{\max}\Delta x\, \psi'(\xi_j)\left(\sum_{k=0}^{+\infty} \omega_i^k (r_{j+1+k} - r_{j-1+k})\right) \tag{3.5.9}$$

$$= -v_i^{\max}\Delta x\, \psi'(\xi_j)\left(\sum_{k=1}^{+\infty} \omega_i^{k-1} r_{j+k} - \sum_{k=-1}^{+\infty} \omega_i^{k+1} r_{j+k}\right) \tag{3.5.10}$$

$$= -v_i^{\max}\Delta x\, \psi'(\xi_j)\left(\sum_{k=1}^{+\infty} (\omega_i^{k-1} - \omega_\eta^{k+1}) r_{j+k} - \omega_i^0 r_{j-1} - \omega_i^1 r_j\right) \tag{3.5.11}$$

$$\leq 2v_M^{\max}\left\|\psi'\right\|_\infty \Delta x\, \omega_i(0) M \|\boldsymbol{\rho}\|_\infty. \tag{3.5.12}$$

where $\|\boldsymbol{\rho}\|_\infty = \|(\rho_1, \dots, \rho_M)\|_\infty = \max_i |\rho_i|$ and we have used the fact that $r_j \geq 0$ for $j \in \mathbb{Z}$, guaranteed by Lemma 8. Therefore, until $\|\boldsymbol{\rho}^n\|_\infty \leq K$, for some $K \geq \|\boldsymbol{\rho}^0\|_\infty$, we get

$$\left\|\boldsymbol{\rho}^{n+1}\right\|_\infty \leq \|\boldsymbol{\rho}^n\|_\infty \left(1 + MKv_M^{\max}\|\psi'\|_\infty W_0 \Delta t\right),$$

and we can reason as in the proof of Lemma 5, which implies

$$\|\boldsymbol{\rho}^n\|_\infty \leq \left\|\boldsymbol{\rho}^0\right\|_\infty e^{Cn\Delta t}, \tag{3.5.13}$$

where $C = MKv_M^{\max}\|\psi'\|_\infty W_0$ and $W_0 := \max_{i=1,\dots,M} \omega_i(0)$. Therefore we get that $\|\rho(t)\|_\infty \leq K$ for

$$t \leq \frac{1}{MKv_M^{\max}\|\psi'\|_\infty W_0} \ln\left(\frac{K}{\|\boldsymbol{\rho}^0\|_\infty}\right) \leq \frac{1}{Me\|\boldsymbol{\rho}^0\|_\infty v_M^{\max}\|\psi'\|_\infty W_0},$$

where the maximum is attained for $K = e\|\boldsymbol{\rho}^0\|_\infty$. Iterating the procedure, at time t^m, $m \geq 1$ we set $K = e^m\|\boldsymbol{\rho}^0\|_\infty$ and we get that the solution is bounded by K until t^{m+1} such that

$$t^{m+1} \leq t^m + \frac{1}{Me^m\|\boldsymbol{\rho}^0\|_\infty v_M^{\max}\|\psi'\|_\infty W_0}.$$

Therefore, the approximate solution satisfies the bound (3.5.13) for $t \leq T$ with

$$T \leq \frac{1}{M\|\boldsymbol{\rho}^0\|_\infty v_M^{\max}\|\psi'\|_\infty W_0} \sum_{m=1}^{+\infty} \frac{1}{e^m} = \frac{1}{M(e-1)\|\boldsymbol{\rho}^0\|_\infty v_M^{\max}\|\psi'\|_\infty W_0}.$$

□

Lemma 10. (BV estimates) *Let $\rho_i^0 \in (BV \cap \mathbf{L}^\infty)(\mathbb{R}, \mathbb{R}^+)$ for all $i = 1, ..., M$. If (3.5.4) holds and*

$$\Delta t \leq \frac{2}{2\alpha + \Delta x \|\psi'\|_\infty W_0 v_M^{\max}\|\boldsymbol{\rho}\|_\infty} \Delta x, \tag{3.5.14}$$

then the solution constructed by the algorithm (3.5.2)-(3.5.1) has uniformly bounded total variation for any T such that

$$T \leq \min_{i=1,\dots,M} \frac{1}{\mathcal{D}\left(TV(\rho_i^0) + 1\right)}, \tag{3.5.15}$$

where $\mathcal{D} = \|\boldsymbol{\rho}\|_\infty v_M^{\max} W_0 M \left(3MJ_0\|\boldsymbol{\rho}\|_\infty\|\psi''\|_\infty + 2\|\psi'\|_\infty\right)$.

Proof. Subtracting the following expressions

$$\rho_{i,j+1}^{n+1} = \rho_{i,j+1}^n + \frac{\lambda}{2}\alpha(\rho_{i,j}^n - 2\rho_{i,j+1}^n + \rho_{i,j+2}^n) + \frac{\lambda}{2}\left(\rho_{i,j}^n V_{i,j}^n - \rho_{i,j+2}^n V_{i,j+2}^n\right),$$
$$\rho_{i,j}^{n+1} = \rho_{i,j}^n + \frac{\lambda}{2}\alpha(\rho_{i,j-1}^n - 2\rho_{i,j}^n + \rho_{i,j+1}^n) + \frac{\lambda}{2}\left(\rho_{i,j-1}^n V_{i,j-1}^n - \rho_{i,j+1}^n V_{i,j+1}^n\right),$$

we get

$$\Delta_{i,j+1/2}^{n+1} = \frac{\lambda}{2}\alpha\Delta_{i,j-1/2}^{n+1} + (1 - \lambda\alpha)\Delta_{i,j+1/2}^n + \frac{\lambda}{2}\alpha\Delta_{i,j+3/2}^{n+1}$$

$$+\frac{\lambda}{2}\left[V_{i,j}^n\Delta_{i,j-1/2}^n+\rho_{i,j-1}^n\left(V_{i,j}^n-V_{i,j-1}^n\right)-V_{i,j+2}^n\Delta_{i,j+3/2}+\rho_{i,j+1}\left(V_{i,j+1}^n-V_{i,j+2}^n\right)\right].$$

Now, we can write

$$\begin{aligned}V_{i,j}^n-V_{i,j-1}^n&=v_i^{\max}\psi'(\xi_{j-1/2})\Delta x\sum_{k=0}^{+\infty}\omega_i^k\sum_{\beta=1}^{M}\rho_{\beta,j+k}^n-\rho_{\beta,j+k-1}^n\\&=v_i^{\max}\psi'(\xi_{j-1/2})\Delta x\sum_{k=0}^{+\infty}\omega_i^k\sum_{\beta=1}^{M}\Delta_{\beta,j+k-1/2}^n\\&=v_i^{\max}\psi'(\xi_{j-1/2})\Delta x\left(\sum_{\beta=1}^{M}\sum_{k=0}^{+\infty}(\omega_i^k-\omega_i^{k+1})\rho_{\beta,j+k}-\omega_i^0\rho_{\beta,j-1}\right),\end{aligned}$$

and

$$\begin{aligned}V_{i,j+2}^n-V_{i,j+1}^n&=v_i^{\max}\psi'(\xi_{j+3/2})\Delta x\sum_{k=0}^{+\infty}\omega_i^k\sum_{\beta=1}^{M}\Delta_{\beta,j+k+3/2}^n\\&=v_i^{\max}\psi'(\xi_{j+3/2})\Delta x\left(\sum_{\beta=1}^{M}\sum_{k=1}^{+\infty}(\omega_i^{k-1}-\omega_i^k)\rho_{\beta,j+k+1}-\omega_\eta^0\rho_{\beta,j+1}\right).\end{aligned}$$

We get

$$\begin{aligned}&\Delta_{i,j+1/2}^{n+1}=\\&=\frac{\lambda}{2}\left(\alpha+V_{i,j}^n\right)\Delta_{i,j-1/2}^n+(1-\lambda\alpha)\,\Delta_{i,j+1/2}^n+\frac{\lambda}{2}\left(\alpha-V_{i,j+2}^n\right)\Delta_{i,j+3/2}^n\\&\quad+\frac{\lambda}{2}\rho_{i,j-1}^n\left(v_i^{\max}\psi'(\xi_{j-1/2})\Delta x\left(\sum_{\beta=1}^{M}\sum_{k=0}^{+\infty}(\omega_i^k-\omega_\eta^{k+1})\rho_{\beta,j+k}^n-\omega_\eta^0\rho_{\beta,j-1}^n\right)\right)\\&\quad-\frac{\lambda}{2}\rho_{i,j+1}^n\left(v_i^{\max}\psi'(\xi_{j+3/2})\Delta x\left(\sum_{\beta=1}^{M}\sum_{k=1}^{+\infty}(\omega_i^{k-1}-\omega_i^k)\rho_{\beta,j+k+1}^n-\omega_i^0\rho_{\beta,j+1}^n\right)\right)\\&=\frac{\lambda}{2}\left(\alpha+V_{i,j}^n\right)\Delta_{i,j-1/2}^n+(1-\lambda\alpha)\,\Delta_{i,j+1/2}^n+\frac{\lambda}{2}\left(\alpha-V_{i,j+2}^n\right)\Delta_{i,j+3/2}^n\\&\quad+\frac{\lambda}{2}(\rho_{i,j-1}^n-\rho_{i,j+1}^n)\left(V_{i,j}^n-V_{i,j-1}^n\right)\\&\quad+\frac{\lambda}{2}\rho_{i,j+1}^n\left[v_i^{\max}\psi'(\xi_{j-1/2})\Delta x\left(\sum_{\beta=1}^{M}\sum_{k=0}^{+\infty}(\omega_i^k-\omega_i^{k+1})\rho_{\beta,j+k}^n-\omega_\eta^0\rho_{\beta,j-1}^n\right)\right.\\&\qquad\pm v_i^{\max}\psi'(\xi_{j+3/2})\Delta x\left(\sum_{\beta=1}^{M}\sum_{k=0}^{+\infty}(\omega_i^k-\omega_i^{k+1})\rho_{\beta,j+k}^n-\omega_i^0\rho_{\beta,j-1}^n\right)\\&\qquad\left.-v_i^{\max}\psi'(\xi_{j+3/2})\Delta x\left(\sum_{\beta=1}^{M}\sum_{k=1}^{+\infty}(\omega_i^{k-1}-\omega_i^k)\rho_{\beta,j+k+1}^n-\omega_i^0\rho_{\beta,j+1}^n\right)\right]\end{aligned}$$

$$
\begin{aligned}
&= \frac{\lambda}{2}\left(\alpha + V^n_{i,j}\right)\Delta^n_{i,j-1/2} + (1-\lambda\alpha)\,\Delta^n_{i,j+1/2} + \frac{\lambda}{2}\left(\alpha - V^n_{i,j+2}\right)\Delta^n_{i,j+3/2} \\
&\quad - \frac{\lambda}{2}\left(V^n_{i,j} - V^n_{i,j-1}\right)\left(\Delta^n_{i,j-1/2} + \Delta^n_{i,j+1/2}\right) \\
&\quad + \frac{\lambda}{2}\rho^n_{i,j+1}\left[v_i^{\max}\psi''(\xi_{j+1})(\xi_{j-1/2} - \xi_{j+3/2})\Delta x\left(\sum_{\beta=1}^{M}\sum_{k=0}^{+\infty}(\omega_i^k - \omega_i^{k+1})\rho^n_{\beta,j+k} - \omega_\eta^0\rho^n_{\beta,j-1}\right)\right. \\
&\qquad \left. + v_i^{\max}\psi'(\xi_{j+3/2})\Delta x\left(\sum_{\beta=1}^{M}\sum_{k=0}^{+\infty}(\omega_i^k - \omega_i^{k+1})(\rho^n_{\beta,j+k} - \rho^n_{\beta,j+k+2}) \;-\omega_i^0(\rho^n_{\beta,j-1} - \rho^n_{\beta,j+1})\right)\right] \\
&= \frac{\lambda}{2}\left(\alpha + V^n_{i,j-1}\right)\Delta^n_{i,j-1/2} \qquad (3.5.16) \\
&\quad + \left(1 - \lambda\alpha - \frac{\lambda}{2}\left(V^n_{i,j} - V^n_{i,j-1}\right)\right)\Delta^n_{i,j+1/2} \qquad (3.5.17) \\
&\quad + \frac{\lambda}{2}\left(\alpha - V^n_{i,j+2}\right)\Delta^n_{i,j+3/2} \qquad (3.5.18) \\
&\quad + \frac{\lambda}{2}\rho^n_{i,j+1}\left[v_i^{\max}\psi''(\tilde{\xi}_{j+1})(\xi_{j-1/2} - \xi_{j+3/2})\Delta x\left(\sum_{k=0}^{+\infty}\omega_i^k\sum_{\beta=1}^{M}\Delta^n_{\beta,j+k-1/2}\right)\right. \\
&\qquad + v_i^{\max}\psi'(\xi_{j+3/2})\Delta x\left(\sum_{k=0}^{+\infty}(\omega_i^{k+1} - \omega_i^k)\sum_{\beta=1}^{M}\left(\Delta^n_{\beta,j+k+1/2} + \Delta^n_{\beta,j+k+3/2}\right)\right. \\
&\qquad \left.\left. + \omega_i^0\sum_{\beta=1}^{M}\left(\Delta^n_{\beta,j-1/2} + \Delta^n_{\beta,j+1/2}\right)\right)\right].
\end{aligned}
$$

where $\tilde{\xi}_{j+1} \in \mathcal{I}(\xi_{j+1/2}, \xi_{j+3/2})$. For some $\vartheta, \mu \in [0,1]$, we compute

$$
\begin{aligned}
\xi_{j-1/2} - \xi_{j+3/2} &= \vartheta\Delta x\sum_{k=0}^{+\infty}\omega_i^k\sum_{\beta=1}^{M}\rho^n_{\beta,j+k} + (1-\vartheta)\Delta x\sum_{k=0}^{+\infty}\omega_i^k\sum_{\beta=1}^{M}\rho^n_{\beta,j+k-1} \\
&\quad - \mu\Delta x\sum_{k=0}^{+\infty}\omega_i^k\sum_{\beta=1}^{M}\rho^n_{\beta,j+k+2} - (1-\mu)\Delta x\sum_{k=0}^{+\infty}\omega_i^k\sum_{\beta=1}^{M}\rho^n_{\beta,j+k+1} \\
&= \vartheta\Delta x\sum_{k=0}^{+\infty}\omega_i^k\sum_{\beta=1}^{M}\rho^n_{\beta,j+k} + (1-\vartheta)\Delta x\sum_{k=-1}^{+\infty}\omega_i^{k+1}\sum_{\beta=1}^{M}\rho^n_{\beta,j+k} \\
&\quad - \mu\Delta x\sum_{k=2}^{+\infty}\omega_i^{k-2}\sum_{\beta=1}^{M}\rho^n_{\beta,j+k} - (1-\mu)\Delta x\sum_{k=1}^{+\infty}\omega_i^{k-1}\sum_{\beta=1}^{M}\rho^n_{\beta,j+k} \\
&= \Delta x\sum_{k=2}^{+\infty}\left[\vartheta\omega_i^k + (1-\vartheta)\omega_i^{k+1} - \mu\omega_i^{k-2} - (1-\mu)\omega_i^{k-1}\right]\sum_{\beta=1}^{M}\rho^n_{\beta,j+k} \\
&\quad + \vartheta\Delta x\left(\omega_i^0\sum_{\beta=1}^{M}\rho^n_{\beta,j} + \omega_i^1\sum_{\beta=1}^{M}\rho^n_{\beta,j+1}\right)
\end{aligned}
$$

$$+ (1-\vartheta)\Delta x \left(\omega_i^0 \sum_{\beta=1}^{M} \rho_{\beta,j-1}^n + \omega_i^1 \sum_{\beta=1}^{M} \rho_{\beta,j}^n + \omega_i^2 \sum_{\beta=1}^{M} \rho_{\beta,j+1}^n \right)$$
$$- (1-\mu)\Delta x \left(\omega_i^0 \sum_{\beta=1}^{M} \rho_{\beta,j+1}^n \right).$$

By monotonicity of ω_η we have

$$\vartheta\omega_i^k + (1-\vartheta)\omega_i^{k+1} - \mu\omega_i^{k-2} - (1-\mu)\omega_i^{k-1} \leq 0.$$

Taking the absolute values we get

$$\begin{aligned}
\left|\xi_{j-1/2} - \xi_{j+3/2}\right| &\leq \Delta x \left\{ \sum_{k=2}^{+\infty} \left[\mu\omega_i^{k-2} + (1-\mu)\omega_i^{k-1} - \vartheta\omega_i^k - (1-\vartheta)\omega_i^{k+1} \right] + 3\omega_i(0) \right\} M \|\boldsymbol{\rho}^n\|_\infty \\
&\leq \Delta x \left\{ \sum_{k=2}^{N-2} \left[\omega_i^{k-2} - \omega_i^{k+1} \right] + 3\omega_i(0) \right\} M \|\boldsymbol{\rho}^n\|_\infty \\
&\leq \Delta x \, 6\, \omega_i(0) M \|\boldsymbol{\rho}^n\|_\infty.
\end{aligned}$$

Observe that assumption (3.5.4) guarantees the positivity of (3.5.16) and (3.5.18). Similarly, (3.5.14) ensures the positivity of (3.5.17).

Until $\sum_j \left|\Delta_{\beta,j}^n\right| \leq K_1$ for $\beta = 1, ..., M$ for some $K_1 \geq \sum_j \left|\Delta_{\beta,j}^0\right|$, taking the absolute values and rearranging the indexes, we have

$$\sum_j \left|\Delta_{i,j+1/2}^{n+1}\right| \leq \sum_j \left|\Delta_{i,j+1/2}^{n}\right| \left(1 + \frac{\lambda}{2}\left(V_{i,j-1} - V_{i,j+1}\right)\right) + \Delta t\, \mathcal{D} K_1$$

where $\mathcal{D} = \|\boldsymbol{\rho}\|_\infty \, v_M^{\max} W_0 M \left(3MJ_0\|\boldsymbol{\rho}\|_\infty \left\|\psi''\right\|_\infty + 2\left\|\psi'\right\|_\infty\right)$. Therefore, by (3.5.8) we get

$$\sum_j \left|\Delta_{i,j+1/2}^{n+1}\right| \leq \sum_j \left|\Delta_{i,j+1/2}^{n}\right| (1 + \Delta t\, \mathcal{C}) + \Delta t\, \mathcal{D} K_1$$

with $\mathcal{C} = v_M^{\max}\left\|\psi'\right\|_\infty W_0 M \|\boldsymbol{\rho}\|_\infty$. In this way we obtain

$$\sum_j \left|\Delta_{i,j+1/2}^{n+1}\right| \leq e^{\mathcal{C}n\Delta t} \sum_j \left|\Delta_{i,j+1/2}^{0}\right| + e^{\mathcal{D}K_1 n\Delta t} - 1,$$

that we can rewrite as

$$\begin{aligned}
\mathrm{TV}(\rho_{i,\Delta x})(n\Delta t, \cdot) &\leq e^{\mathcal{C}n\Delta t}\mathrm{TV}(\rho_i^0) + e^{\mathcal{D}K_1 n\Delta t} - 1 \\
&\leq e^{\mathcal{D}K_1 n\Delta t}\left(\mathrm{TV}(\rho_i^0) + 1\right) - 1, \qquad (3.5.19)
\end{aligned}$$

since $\mathcal{D} \geq 2\mathcal{C}$ and it is not restrictive to assume $K_1 \geq \frac{1}{2}$. Therefore we have that $\mathrm{TV}(\rho_{i,\Delta x}) \leq K_1$ for

$$t \leq \frac{1}{\mathcal{D}K_1} \ln\left(\frac{K_1 + 1}{\mathrm{TV}(\rho_i^0) + 1}\right),$$

where the maximum is attained for some $K_1 \leq e\left(\mathrm{TV}(\rho_i^0)+1\right)-1$ such that

$$\ln\left(\frac{K_1+1}{TV(\rho_i^0)+1}\right)=\frac{K_1}{K_1+1}.$$

Therefore the total variation is uniformly bounded for

$$t \leq \frac{1}{\mathcal{D}e\left(\mathrm{TV}(\rho_i^0)+1\right)}.$$

Iterating the procedure, at time t^m, $m \geq 1$ we set $K_1 = e^m\left(\mathrm{TV}(\rho_i^0)+1\right)-1$ and we get that the solution is bounded by K_1 until t^{m+1} such that

$$t^{m+1} \leq t^m + \frac{m}{\mathcal{D}e^m\left(\mathrm{TV}(\rho_i^0)+1\right)}. \tag{3.5.20}$$

Therefore, the approximate solution satisfies the bound (3.5.19) for $t \leq T$ with

$$T \leq \frac{1}{\mathcal{D}\left(\mathrm{TV}(\rho_i^0)+1\right)}.$$

□

Corollary 11. *Let $\rho_i^0 \in BV(\mathbb{R};[0,1])$. If (2.3.3)-(2.3.4) holds, then the approximate solution $\boldsymbol{\rho}^{\Delta x}$ constructed by the algorithm (3.5.2)-(3.5.1) has uniformly bounded total variation on $[0,T]\times\mathbb{R}$, for any T satisfying (3.5.15).*

Proof. Let us fix $T \in \mathbb{R}^+$ such that (3.5.15) and (3.5.7) hold. If $T \leq \Delta t$, then $\mathrm{TV}(\rho_{i,\Delta x};\mathbb{R}\times[0,T]) \leq T\mathrm{TV}(\rho_{i,0})$. Let us assume now that $T \geq \Delta t$. Let $M \in \mathbb{N}\backslash\{0\}$ such that $n_T\Delta t < T \leq (n_T+1)\Delta t$. Then

$$\mathrm{TV}(\rho_{i,\Delta x};\mathbb{R}\times[0,T]) \tag{3.5.21}$$

$$= \underbrace{\sum_{n=0}^{n_T-1}\sum_{j\in\mathbb{Z}}\Delta t\left|\rho_{i,j+1}^n-\rho_{i,j}^n\right| + (T-n_T\Delta t)\sum_{j\in\mathbb{Z}}\left|\rho_{i,j+1}^{n_T}-\rho_{i,j}^{n_T}\right|}_{\leq T\sup_{t\in[0,T]}\mathrm{TV}(\rho_i^{\Delta x})(t,\cdot)} + \sum_{n=0}^{n_T-1}\sum_{j\in\mathbb{Z}}\Delta x\left|\rho_{i,j}^{n+1}-\rho_{i,j}^n\right| \tag{3.5.22}$$

The spatial BV estimate yields

$$\sum_{n=0}^{n_T-1}\sum_{j\in\mathbb{Z}}\Delta t\left|\rho_{i,j+1}^n-\rho_{i,j}^n\right| + (T-n_T\Delta t)\sum_{j\in\mathbb{Z}}\left|\rho_{i,j+1}^{n_T}-\rho_{i,j}^{n_T}\right| \leq Te^{\mathcal{C}_1 n\Delta t}\left(\mathrm{TV}(\rho_i^0)+1\right). \tag{3.5.23}$$

We then need to bound the term

$$\sum_{n=0}^{n_T-1}\sum_{j\in\mathbb{Z}}\Delta x\left|\rho_{i,j}^{n+1}-\rho_{i,j}^n\right|. \tag{3.5.24}$$

Let us make use of the definition of the numerical scheme (3.5.2)-(3.5.1), we obtain

$$\begin{aligned}\rho_{i,j}^{n+1}-\rho_{i,j}^{n}&\\ =&\frac{\lambda}{2}\left(\alpha+V_{i,j+1}\right)\left(\rho_{i,j-1}-\rho_{i,j}\right)-\frac{\lambda}{2}\left(\alpha-V_{i,j+1}\right)\left(\rho_{i,j}-\rho_{i,j+1}\right)\\ &+\frac{\lambda}{2}\rho_{i,j-1}\left(V_{i,j-1}-V_{i,j+1}\right).\end{aligned}$$

If (2.3.4) holds, we can take the absolute value

$$\begin{aligned}\left|\rho_{i,j}^{n+1}-\rho_{i,j}^{n}\right|&\\ =&\frac{\lambda}{2}\left(\alpha+V_{i,j+1}\right)\left|\rho_{i,j-1}-\rho_{i,j}\right|-\frac{\lambda}{2}\left(\alpha-V_{i,j+1}\right)\left|\rho_{i,j}-\rho_{i,j+1}\right|\\ &+\frac{\lambda}{2}\left|\rho_{i,j-1}\right|\left|V_{i,j-1}-V_{i,j+1}\right|.\end{aligned}$$

Summing on j and rearranging the indexes we get

$$\begin{aligned}\sum_{j\in\mathbb{Z}}\Delta x\left|\rho_{i,j}^{n+1}-\rho_{i,j}^{n}\right|&\\ =&\frac{\Delta t}{2}\sum_{j\in\mathbb{Z}}\left|\rho_{i,j+1}-\rho_{i,j}\right|\left(2\alpha+V_{i,j+2}-V_{i,j+1}\right)\\ &+\frac{\Delta t}{2}\sum_{j\in\mathbb{Z}}\left|\rho_{i,j-1}\right|\left|V_{i,j-1}-V_{i,j+1}\right|\\ =&\frac{\Delta t}{2}\sum_{j\in\mathbb{Z}}\left|\rho_{i,j+1}-\rho_{i,j}\right|\left(2\alpha+v_M^{\max}\left\|\psi'\right\|_\infty\Delta x\,\omega_\eta(0)M\|\boldsymbol{\rho}\|_\infty\right)\\ &+\Delta t\sum_{j\in\mathbb{Z}}\left|\rho_{i,j-1}\right|\Delta x\,v_M^{\max}\left\|\psi'\right\|_\infty W_0M\|\boldsymbol{\rho}\|_\infty\end{aligned}$$

which yields

$$\begin{aligned}&\sum_{n=0}^{n_T-1}\sum_{j\in\mathbb{Z}}\Delta x\left|\rho_{i,j}^{n+1}-\rho_{i,j}^{n}\right|\\ \leq&Te^{\mathcal{C}_1n\Delta t}\left(\mathrm{TV}(\rho_i^0)+1\right)\left(\alpha+\frac{1}{2}v_M^{\max}\left\|\psi'\right\|_\infty\Delta x\,W_0M\|\boldsymbol{\rho}\|_\infty\right)\\ &+T\sup_{t\in[0,T]}\left\|\rho_i^{\Delta x}(t,\cdot)\right\|_{\mathbf{L^1}}v_M^{\max}\left\|\psi'\right\|_\infty W_0M\left\|\rho_i^{\Delta x}(t,\cdot)\right\|_\infty.\end{aligned}$$

□

Proof of Theorem 7. Let us define

$$g(\rho_{i,j}^n,...,\rho_{i,j+N}^n):=\frac{1}{2}\rho_{i,j}^nV_{i,j}^n+\frac{1}{2}\rho_{i,j+1}^nV_{i,j+1}^n+\frac{\alpha}{2}\left(\rho_{i,j}^n-\rho_{i,j+1}^n\right).$$

Fix $i\in\{1,...,M\}$. Let $\varphi\in\mathbf{C_c^1}([0,T]\times\mathbb{R})$ and multiply (3.5.1) by $\varphi(t^n,x_j)$. Summing over $j\in\mathbb{Z}$ and $n\in\{0,1,...,n_T\}$ we get

$$\sum_{n=0}^{n_T-1}\sum_j\varphi(t^n,x_j)\left(\rho_{i,j}^{n+1}-\rho_{i,j}^n\right)$$

$$= -\lambda \sum_{n=0}^{n_T-1} \sum_j \varphi(t^n, x_j) \left(g(\rho^n_{i,j}, ..., \rho^n_{i,j+N}) - g(\rho^n_{i,j-1}, ..., \rho^n_{i,j+N-1}) \right).$$

Summing by parts we obtain

$$- \sum_j \varphi((n_T-1)\Delta t, x_j)\rho^{n_T}_{i,j} + \sum_j \varphi(0, x_j)\rho^0_{i,j} + \sum_{n=1}^{n_T-1} \sum_j \left(\varphi(t^n, x_j) - \varphi(t^{n-1}, x_j) \right) \rho^n_{i,j}$$
$$+ \lambda \sum_{n=0}^{n_T-1} \sum_j \left(\varphi(t^n, x_{j+1}) - \varphi(t^n, x_j) \right) g(\rho^n_{i,j}, ..., \rho^n_{i,j+N}) = 0. \tag{3.5.25}$$

Multiplying by Δx

$$- \Delta x \sum_j \varphi((n_T-1)\Delta t, x_j)\rho^{n_T}_{i,j} + \Delta x \sum_j \varphi(0, x_j)\rho^0_{i,j} + \Delta x \Delta t \sum_{n=1}^{n_T-1} \sum_j \frac{\left(\varphi(t^n, x_j) - \varphi(t^{n-1}, x_j) \right)}{\Delta t} \rho^n_{i,j} \tag{3.5.26}$$

$$+ \Delta x \Delta t \sum_{n=0}^{n_T-1} \sum_j \frac{\left(\varphi(t^n, x_{j+1}) - \varphi(t^n, x_j) \right)}{\Delta x} g(\rho^n_{i,j}, ..., \rho^n_{i,j+N}) = 0. \tag{3.5.27}$$

By $\mathbf{L^1_{loc}}$ convergence of $\rho_{i,\Delta x} \to \rho_i$, it is straightforward to see that the first two terms in (3.5.26) converge to

$$\int_{\mathbb{R}} (\rho^0_i(x)\varphi(0, x) - \rho_i(T, x)\varphi(T, x))\, dx + \int_0^T \int_{\mathbb{R}} \rho_i(t, x)\partial_t\varphi(t, x)\, dx\, dt \tag{3.5.28}$$

as $\Delta x \to 0$. Concerning the last term, we can observe that

$$\begin{aligned}
&\left| g(\rho^n_{i,j}, ..., \rho^n_{i,j+N}) - \rho^n_{i,j} V^n_{i,j} \right| \\
&\leq \frac{\alpha}{2} \left| \rho^n_{i,j+1} - \rho^n_{i,j} \right| + \frac{1}{2} \left| (\rho^n_{i,j+1} - \rho^n_{i,j}) V^n_{i,j+1} + \rho^n_{i,j} \left(V^n_{i,j+1} - V^n_{i,j} \right) \right| \\
&\leq \frac{\alpha + v^{\max}_M \|\psi\|_\infty}{2} \left| \rho^n_{i,j+1} - \rho^n_{i,j} \right| + \frac{1}{2} W_0 \Delta x \mathrm{TV}(\rho_{i,\Delta x}(t^n, \cdot)) v^{max}_M \left\| \psi' \right\|_\infty \\
&\leq \frac{\alpha + v^{\max}_M \|\psi\|_\infty}{2} \left| \rho^n_{i,j+1} - \rho^n_{i,j} \right| + \mathcal{J}\, \Delta x.
\end{aligned}$$

where $\mathcal{J} = \frac{1}{2} v^{\max}_M \left\| \psi' \right\|_\infty W_0 \mathrm{TV}(\rho_{i,\Delta x}(T, \cdot))$. Therefore, the last term in (3.5.25) can be rewritten as

$$\begin{aligned}
&\Delta x \Delta t \sum_{n=0}^{n_T-1} \sum_j \frac{\varphi(t^n, x_{j+1}) - \varphi(t^n, x_j)}{\Delta x} g(\rho^n_{i,j}, ..., \rho^n_{i,j+N}) \\
=&\Delta x \Delta t \sum_{n=0}^{n_T-1} \sum_j \frac{\varphi(t^n, x_{j+1}) - \varphi(t^n, x_j)}{\Delta x} \rho^n_{i,j} V^n_{i,j} \\
&+ \Delta x \Delta t \sum_{n=0}^{n_T-1} \sum_j \frac{\varphi(t^n, x_{j+1}) - \varphi(t^n, x_j)}{\Delta x} (g(\rho^n_{i,j}, ..., \rho^n_{i,j+N}) - \rho^n_j V^n_{i,j}).
\end{aligned}$$

By $\mathbf{L^1_{loc}}$ convergence of $\rho_{i,\Delta x} \to \rho_i$ and boundedness of ω_i, the first term in the above decomposition converges to

$$\int_0^T \int_{\mathbb{R}} \rho_i(t,x) v(r * \omega_\eta) \partial_x \varphi(t,x)\, dx\, dt.$$

Set $R > 0$ such that $\varphi(t,x) = 0$ for $|x| > R$ and j_0, $j_1 \in \mathbb{Z}$ such that $-R \in]x_{j_0-1/2}, x_{j_0+1/2}[$ and $R \in]x_{j_1-1/2}, x_{j_1+1/2}[$, then

$$\begin{aligned}
&\Delta x \Delta t \sum_{n=0}^{n_T-1} \sum_j \frac{\varphi(t^n, x_{j+1}) - \varphi(t^n, x_j)}{\Delta x} (g(\rho^n_{i,j}, ..., \rho^n_{i,j+N}) - \rho^n_{i,j} V^n_{i,j}) \\
&\leq \Delta x \Delta t \|\partial_x \varphi\|_\infty \sum_{n=0}^{n_T-1} \sum_{j=j_0}^{j_1} \left(\frac{\alpha + v_M^{\max} \|\psi\|_\infty}{2} \left| \rho^n_{i,j+1} - \rho^n_{i,j} \right| + \mathcal{J}\, \Delta x \right) \\
&= \frac{\alpha + v_M^{\max} \|\psi\|_\infty}{2} \|\partial_x \varphi\|_\infty \Delta x \Delta t \sum_{n=0}^{n_T-1} \sum_{j=j_0}^{j_1} \left| \rho^n_{i,j+1} - \rho^n_{i,j} \right| + \|\partial_x \varphi\|_\infty \mathcal{J}\, \Delta x\, 2\, R\, \tau \\
&\leq \frac{\alpha + v_M^{\max} \|\psi\|_\infty}{2} \|\partial_x \varphi\|_\infty \mathrm{TV}(\rho_{i,\Delta x}(T, \cdot)) \Delta x + \|\partial_x \varphi\|_\infty \mathcal{J}\, \Delta x\, 2\, R\, \tau
\end{aligned}$$

which goes to zero when $\Delta x \to 0$. Finally, again by the $\mathbf{L^1_{loc}}$ convergence of $\rho_i^{\Delta x} \to \rho_i$, we have that

$$\Delta x \Delta t \sum_{n=0}^{n_T-1} \sum_j \frac{\big(\varphi(t^n, x_{j+1}) - \varphi(t^n, x_j)\big)}{\Delta x} \rho^n_{i,j} V^n_{i,j} \to \int_0^T \int_{\mathbb{R}} \partial_x \varphi(t,x) \rho_i(t,x) v_i(r * \omega_i)\, dx\, dt.$$

Chapter 4

Numerical schemes for non-local traffic flow models

This chapter contains the results obtained in [25, 24].
We consider the class of non-local systems of M conservation laws in one space dimension [22], like in Chapter 3. We couple (3.1.1) with an initial datum (3.1.5). Due to the possible presence of jump discontinuities, solutions to (3.1.1), (3.1.5) are intended in the weak sense of Definition 3.
The computation of numerical solutions for (3.1.1) is challenging due to the dependence of the flux function on convolution terms. In this chapter, we present a generalization of the L-AR schemes introduced in [15, 16], and a high-order Finite-Volume WENO (FV-WENO) scheme, in order to compute approximate solutions of the non-local multi-class model (3.1.1) proposed in [22].The chapter is organized as follows. Section 4.1 presents the Lagrangian-Antidiffusive Remap schemes. We recover some properties of the L-AR schemes in both scalar and multi-class cases. In the scalar case, we obtain uniform $\mathbf{L}^\infty$, BV estimates on the approximate solutions computed through the L-AR schemes in order to prove the existence of weak solutions. In Section 4.2 we recall classical first-order schemes used to approximate the solutions of the non-local problem (3.1.1) and we show a second-order version of a Godunov type numerical scheme. In Section 4.3 we present some numerical simulations, analyzing the $\mathbf{L^1}$-error of the approximate solutions of (3.1.1) computed with different schemes and considering smooth and discontinuous initial data. In Section 4.4, we describe the implementation of the high-order FV-WENO scheme for the non-local system (3.1.1). Finally, in Section 4.5, we provide a couple of numerical tests in the case of three populations ($M = 3$) and convergence studies for third, fifth and seventh accuracy order.

4.1 Lagrangian-Antidiffusive Remap (L-AR) schemes

4.1.1 Discretization

First of all, we extend $\omega_i(x) = 0$ for $x > \eta_i$. For $j \in \mathbb{Z}$ and $n \in \mathbb{N}$, let $x_{j+1/2} = j\Delta x$ be the cells interfaces, $x_j = (j - 1/2)\Delta x$ the cells centers and $t^n = n\Delta t$ the time mesh. In the chapter, we will set $\lambda = \frac{\Delta t}{\Delta x}$. We aim at constructing a finite volume approximate solution $\boldsymbol{\rho}^{\Delta x} = \left(\rho_1^{\Delta x}, \dots, \rho_M^{\Delta x}\right)$, with $\rho_i^{\Delta x}(t, x) = \rho_{i,j}^n$ for $(t, x) \in C_j^n = [t^n, t^{n+1}[\times]x_{j-1/2}, x_{j+1/2}]$ and $i = 1, ..., M$.
To this end, we approximate the initial datum ρ_i^0 for $i = 1, ..., M$ with a piece-wise constant function

$$\rho_{i,j}^0 = \frac{1}{\Delta x} \int_{x_{j-1/2}}^{x_{j+1/2}} \rho_i^0(x)\, dx, \qquad j \in \mathbb{Z}. \tag{4.1.1}$$

Similarly, for the kernel, we set

$$\omega_i^k := \frac{1}{\Delta x}\int_{(k-1)\,\Delta x}^{k\,\Delta x} \omega_i(x)\,dx, \qquad k \in \mathbb{N}^*, \tag{4.1.2}$$

so that $\Delta x \sum_{k=1}^{+\infty} \omega_i^k = \int_0^{\eta_i} \omega_i(x)\,dx = J_i$ (the sum is indeed finite since $\omega_i^k = 0$ for $k \geq N_i$ sufficiently large). Moreover, we set $r_{j+k}^n = \sum_{i=1}^{M} \rho_{i,j+k}^n$ for $k \in \mathbb{N}$ and

$$V_{i,j+1/2}^n := v_i^{\max}\psi\left(\Delta x \sum_{k=1}^{+\infty} \omega_i^k r_{j+k}^n\right), \qquad i = 1,\dots,M, \quad j \in \mathbb{Z}. \tag{4.1.3}$$

We formally rewrite (3.1.1) as

$$\partial_t \rho_i + \rho_i \partial_x(v_i(r * \omega_i)) + v_i(r * \omega_i)\partial_x \rho_i = 0, \quad i = 1,\dots,M. \tag{4.1.4}$$

L-AR schemes are obtained splitting (4.1.4) into two different equations, which are solved successively for each time iteration. To advance the solution from time t to $t + \Delta t$, we first apply a Lagrangian method [50] to solve

$$\partial_t \rho_i + \rho_i \partial_x(v_i(r * \omega_i)) = 0, \tag{4.1.5}$$

and we use this solution, evolved over a time interval of length Δt, as initial condition for solving in a second step the transport equation [12]

$$\partial_t \rho_i + v_i(r * \omega_i)\partial_x \rho_i = 0, \tag{4.1.6}$$

whose solution, again evolved over a time interval of length Δt, provides the sought approximate solution of (3.1.1) valid for $t + \Delta t$.

4.1.2 Discretization of the Lagrangian step.

We observe that, defining $\tau_i := 1/\rho_i$, one obtains from (4.1.5) the conservation mass equation in Lagrangian coordinates

$$\rho_i \partial_t \tau_i - \partial_x(v_i(r * \omega_i)) = 0. \tag{4.1.7}$$

In other words, solving (4.1.5), or equivalently (4.1.7), means solving the original equation (3.1.1) on a moving referential mesh with velocity v_i. Assume now that $\{\rho_{i,j}^n\}_{j\in\mathbb{Z}}$, $i = 1,\dots,M$ is an approximate solution of (3.1.1) in the sense of finite volume methods (4.1.1)-(4.1.3) at time $t = t^n$, then a numerical solution $\{\rho_{i,j}^{n+1,-}\}_{j\in\mathbb{Z}}$ of the equation (4.1.7) at time Δt can be naturally computed by

$$\rho_{i,j}^{n+1,-}[\Delta x + (V_{i,j+1/2}^n - V_{i,j-1/2}^n)\Delta t] = \Delta x \rho_{i,j}^n, \quad i = 1,\dots,M, \quad j \in \mathbb{Z}, \tag{4.1.8}$$

since (4.1.8) expresses that the initial mass in the cell $[x_{j-1/2}, x_{j+1/2}]$ at time t^n equals the mass in the modified cell $[\bar{x}_{j-1/2}, \bar{x}_{j+1/2}]$ at time Δt, where $\bar{x}_{j+1/2} = x_{j+1/2} + V_{i,j+1/2}^n \Delta t$ are the new interface positions for all j. We have the following properties.

Lemma 11. *Assume that the time step satisfies the following condition:*

$$\Delta t \leq \left(v_M^{\max} \left\| \psi' \right\|_\infty \| r^n \|_\infty W_0 \right)^{-1}. \tag{4.1.9}$$

If $\{\boldsymbol{\rho}_j^{n+1,-}\}_{j\in\mathbb{Z}}$ *denotes the numerical solution computed by the scheme* (4.1.8)*, then the following bounds hold:*

(*i*) *If* $\rho_{i,j}^n \geq 0$ *for all* $j \in \mathbb{Z}$*, then* $\rho_{i,j}^{n+1,-} \geq 0$ *for all* $j \in \mathbb{Z}$*.*

(*ii*) *In the scalar case* $M = 1$*, the following maximum property holds:*

$$\min\{\rho_j^n, ..., \rho_{j+N}^n\} \leq \rho_j^{n+1,-} \leq \max\{\rho_j^n, ..., \rho_{j+N}^n\} \quad \forall j \in \mathbb{Z}. \tag{4.1.10}$$

Proof. (*i*) Suppose that $\rho_{i,j}^n \geq 0$ for all $j \in \mathbb{Z}$ and $i = 1, ..., M$. From (4.1.8) we have

$$\rho_{i,j}^{n+1,-} = \frac{\rho_{i,j}^n}{1 + \lambda \left(V_{i,j+1/2}^n - V_{i,j-1/2}^n \right)}. \tag{4.1.11}$$

If $V_{i,j+1/2}^n \geq V_{i,j-1/2}^n$ then it is clear that $\rho_{i,j}^{n+1,-} \geq 0$. Consider now the case $V_{i,j+1/2}^n \leq V_{i,j-1/2}^n$. We can compute

$$\begin{aligned} V_{i,j-1/2}^n - V_{i,j+1/2}^n &= -v_i^{\max} \psi'(\xi_{i,j}) \Delta x \left(\sum_{k=1}^{+\infty} \omega_i^k r_{j+k}^n - \sum_{k=1}^{+\infty} \omega_i^k r_{j+k-1}^n \right) \\ &\leq -v_i^{\max} \psi'(\xi_{i,j}) \Delta x \left(\sum_{k=1}^{+\infty} (\omega_i^k - \omega_i^{k+1}) r_{j+k}^n - \omega_i^1 r_j^n \right) \\ &\leq v_i^{\max} \Delta x W_0 \left\| \psi' \right\|_\infty \| r^n \|_\infty, \end{aligned}$$

for some $\xi_{i,j} \in \mathcal{I}\left(\Delta x \sum_{k=1}^{+\infty} \omega_i^k r_{j+k-1}^n, \Delta x \sum_{k=1}^{+\infty} \omega_i^k r_{j+k}^n \right)$, where we have set $\mathcal{I}(a,b) = \left[\min\{a,b\}, \max\{a,b\} \right]$. Therefore $\rho^{n+1,-} \geq 0$ under (4.1.9).

(*ii*) Assume $M = 1$ and set $V_{j+1/2}^n := V_{1,j+1/2}^n$, $\omega^k := \omega_1^k$ and $v^{\max} := v_1^{\max}$. Let us prove the upper bound, the lower one resulting from a symmetric procedure. Define $\bar{\rho}_j = \max\{\rho_j^n, ..., \rho_{j+N}^n\}$. Consider first the case $V_{j+1/2}^n \geq V_{j-1/2}^n$. Then it is clear that

$$\rho_j^{n+1,-} = \frac{\rho_j^n}{1 + \lambda \left(V_{j+1/2}^n - V_{j-1/2}^n \right)} \leq \bar{\rho}_j \,,$$

Consider now the case $V_{j+1/2}^n \leq V_{j-1/2}^n$. We note that

$$\frac{\rho_j^n}{1 + \lambda \left(V_{j+1/2}^n - V_{j-1/2}^n \right)} \leq \bar{\rho}_j \iff \bar{\rho}_j - \rho_j^n + \lambda \bar{\rho}_j \left(V_{j+1/2}^n - V_{j-1/2}^n \right) \geq 0.$$

According with (*i*), we have the estimation

$$V_{j-1/2}^n - V_{j+1/2}^n = -v^{\max} \psi'(\xi_j) \Delta x \left(\sum_{k=1}^{+\infty} \left(\omega^k - \omega^{k+1} \right) \rho_{j+k}^n - \omega^1 \rho_j^n \right)$$

$$\leq v^{\max}\|\psi'\|_\infty \Delta x \left(\omega^1 \bar{\rho}_j - \omega^1 \rho_j\right)$$
$$\leq v^{\max}\|\psi'\|_\infty \Delta x \left(\bar{\rho}_j - \rho_j\right) W_0$$

Finally we obtain that

$$\bar{\rho}_j - \rho_j^n - \lambda \bar{\rho}_j \left(V_{j-1/2}^n - V_{j+1/2}^n\right) \geq \left(\bar{\rho}_j - \rho_j^n\right)\left(1 - \Delta t v^{\max} \bar{\rho}_j \|\psi'\|_\infty W_0\right) \geq 0$$

holds if $\Delta t \leq \left(v^{\max}\|\psi'\|_\infty \|\rho^n\|_\infty W_0\right)^{-1}$.

□

Remark 6. *Due to the lack of uniform* $\mathbf{L}^\infty$ *estimates on approximate solutions [22], the time step should in principle be recomputed at each iteration to comply with (4.1.9). In practice, since the computed solutions stay uniformly bounded in time, it is possible to choose a fixed time step, as we did in Section 4.3. Moreover, we remark that, in the particular case* $M = 1$*, the maximum principle (4.1.10) guarantees that* $\|\rho^n\|_\infty \leq \|\rho^0\|_\infty$ *for all* $n \in \mathbb{N}^*$.

4.1.3 Remap Step: Antidiffusive scheme

After the Lagrangian step, the new value $\rho_{i,j}^{n+1,-}$ represents approximate values of the density of the i-th class on a moved mesh with new cells $[\bar{x}_{j-1/2}, \bar{x}_{j+1/2}]$ for all j. To avoid dealing with moving meshes, a so-called remap step is necessary to define the new approximations ρ_j^{n+1} on the uniform mesh with cells $[x_{j-1/2}, x_{j+1/2}]$. This averaging step can equivalently be reformulated by using the solution of the transport equation (4.1.6) with initial data defined by $\rho_{i,j}^{n+1,-}$ on each cell $[x_{j-1/2}, x_{j+1/2}]$, i.e. we consider a numerical scheme in the form

$$\rho_{i,j}^{n+1} = \rho_{i,j}^{n+1,-} - \bar{V}_{i,j}^n \lambda \left(\rho_{i,j+1/2}^{n+1,-} - \rho_{i,j-1/2}^{n+1,-}\right), \qquad i = 1, \dots, M \quad j \in \mathbb{Z}. \tag{4.1.12}$$

Here, $\bar{V}_{i,j}^n$ is a velocity value, defined in terms of available density, which will be chosen in such a way that the complete scheme (4.1.5) plus (4.1.12) is conservative with respect to (3.1.1). The quantities $\rho_{i,j+1/2}^{n+1,-}$ are numerical fluxes associated with the cell interfaces $x_{j+\frac{1}{2}}$ and will be chosen such that the scheme (4.1.12) has certain stability and consistency properties. In particular, the choice $\rho_{i,j+1/2}^{n+1,-} = \rho_{i,j}^{n+1,-}$ for all $j \in \mathbb{Z}$ produces a diffusive and stable scheme, while $\rho_{i,j+1/2}^{n+1,-} = \rho_{i,j+1}^{n+1,-}$ yields an antidiffusive but unstable scheme. For this reason, we proceed as in [12, 41] and we choose $\rho_{i,j+1/2}^{n+1,-}$ as close to the anti-diffusive value $\rho_{i,j+1}^{n+1,-}$ as possible, subject to the following consistency condition

$$m_{i,j+1/2} := \min\{\rho_{i,j}^{n+1,-}, \rho_{i,j+1}^{n+1,-}\} \leq \rho_{i,j+1/2}^{n+1,-} \leq M_{i,j+1/2} := \max\{\rho_{i,j}^{n+1,-}, \rho_{i,j+1}^{n+1,-}\}, \tag{4.1.13}$$

and maximum principle

$$m_{i,j+1/2} \leq \rho_{i,j}^{n+1} \leq M_{i,j+1/2}, \tag{4.1.14}$$

which resume the properties of the scheme defined by (4.1.12).

Let us now define

$$b_{i,j}^+ := M_{i,j+1/2} + \frac{\rho_{i,j}^{n+1,-} - M_{i,j+1/2}}{\max\{v_{i,j-1/2}^n, v_{i,j+1/2}^n\}\lambda}, \quad B_{i,j}^+ : m_{i,j+1/2} + \frac{\rho_{i,j}^{n+1,-} - m_{i,j+1/2}}{\max\{v_{i,j-1/2}^n, v_{i,j+1/2}^n\}\lambda}$$

and

$$a_{i,j+1/2} := \max\{b^+_{i,j}, m_{i,j+1/2}\}, \qquad A_{i,j+1/2} := \max\{B^+_{i,j}, M_{i,j+1/2}\}.$$

In the next lemma, which is a slight modification of Lemma 4.1 in [15], we summarize the existence and properties of the scheme defined by (4.1.12).

Lemma 12. *Assume that the following CFL condition holds*

$$\Delta t \le \frac{\Delta x}{v_M^{\max}\|\psi\|_\infty}. \tag{4.1.15}$$

Then $a_{i,j+1/2} \le \rho^{n+1,-}_{i,j} \le A_{i,j+1/2}$ *for all* $j \in \mathbb{Z}$, *and for any numerical flux that satisfies*

$$\rho^{n+1,-}_{i,j+1/2} \in [a_{i,j+1/2}, A_{i,j+1/2}], \quad \text{for all } j \in \mathbb{Z}, \tag{4.1.16}$$

the scheme (4.1.12) *is* L^∞*-stable, that is*

$$\rho^{n+1}_{i,j} \in \mathcal{I}(\rho^{n+1,-}_{i,j}, \rho^{n+1,-}_{i,j+1}), \quad \text{for all } j \in \mathbb{Z}, \tag{4.1.17}$$

and TVD, i.e.,

$$\sum_{j\in\mathbb{Z}} \left|\rho^{n+1,-}_{i,j+1} - \rho^{n+1,-}_{i,j}\right| \le \sum_{j\in\mathbb{Z}} \left|\rho^{n}_{i,j+1} - \rho^{n}_{i,j}\right|. \tag{4.1.18}$$

In particular, for each $j \in \mathbb{Z}$, *there exist numbers* $\alpha_{i,j} \in [0,1]$ *such that*

$$\rho^{n+1,-}_{i,j} = \alpha_{i,j}\rho^{n+1,-}_{i,j-1/2} + (1-\alpha_{i,j})\rho^{n+1,-}_{i,j+1/2}. \tag{4.1.19}$$

4.1.4 Choice of numerical flux

In this subsection, we explain how to compute $\rho^{n+1,-}_{i,j+1/2}$ for the scalar case $M = 1$, the procedure can be applied component-wise in the multi-class case $M > 1$. We here proceed as in [15] and consider the so-called U-Bee method proposed in [41] for linear transport equation, which is defined by

$$\rho^{n+1,-}_{j+1/2} := \rho^{n+1,-}_{j} + \frac{1-\bar\lambda_j}{2}\varphi_j(\rho^{n+1,-}_{j+1} - \rho^{n+1,-}_{j}), \tag{4.1.20}$$

where $\bar\lambda_j = \lambda\max\{V^n_{j-1/2}, V^n_{j+1/2}\}$, $\varphi_j := \varphi(R_j, \bar\lambda_j)$, with $R_j := \frac{\rho^{n+1,-}_j - \rho^{n+1,-}_{j-1}}{\rho^{n+1,-}_{j+1} - \rho^{n+1,-}_{j}}$ and

$$\varphi(R,\bar\lambda) := \varphi^{UB}(R,\bar\lambda) = \max\left\{0, \min\left\{\frac{2}{1-\lambda}, \frac{2R}{\lambda}\right\}\right\}. \tag{4.1.21}$$

Similarly, the so-called N-Bee method described, in [12], corresponds to a second-order scheme in space and it is more diffusive that the U-Bee scheme. It is defined as in (4.1.20) with

$$\varphi(R,\bar\lambda) := \varphi^{NB}(R,\bar\lambda) := \max\left\{0, \min\left\{1, \frac{2R}{\lambda}\right\}, \min\left\{R, \frac{2}{1-\bar\lambda}\right\}\right\}. \tag{4.1.22}$$

It is proved in [12] that the numerical flux (4.1.20) for U-Bee and N-Bee methods satisfies the assumptions of Lemma 12.

4.1.5 Lagrangian-Antidiffusive Remap scheme

Assume that $\boldsymbol{\rho}^n = \left(\rho_1^n, \dots, \rho_M^n\right)$ approximates the solution of (3.1.1) at time $t = t^n$ and we wish to advance this solution to $t^{n+1} = t^n + \Delta t$. To this end, two steps are performed successively:

1. *Lagrangian step.* Consider that $\boldsymbol{\rho}^n$ are initial data for (4.1.5). First, we define the intermediate velocities $v^n_{i,j+1/2}$ by using (4.1.3), then we compute the numerical solution $\rho^{n+1,-}_{i,j}$ of equation (4.1.5) after an evolution over a time interval of length Δt, using scheme (4.1.8).

2. *Antidiffusive remap step.* Solve (4.1.6) with initial data $\rho^{n+1,-}_{i,j}$ using an antidiffusive scheme (4.1.12) for a specific choice of $\bar{V}^n_{i,j}$, obtaining a numerical solution $\boldsymbol{\rho}^{n+1}$ which approximates the solution of (3.1.1) a time t^{n+1}.

In the next theorem, the choice of $\bar{V}^n_{i,j}$ is motivated by the existence of a classical conservative update formula for the whole L-AR scheme (4.1.5) plus (4.1.12).

Theorem 12. *Under the stability conditions* (4.1.9) *and* (4.1.15)*, there exists a definition of* $\bar{V}^n_{i,j} \in \mathcal{I}(v^n_{i,j-1/2}, v^n_{i,j+1/2})$ *such that the complete Lagrangian-Antidiffusive remap scheme can be written in the conservative form*

$$\rho^{n+1}_{i,j} = \rho^n_{i,j} - \lambda\left(\rho^{n+1,-}_{i,j+1/2} V^n_{i,j+1/2} - \rho^{n+1,-}_{i,j-1/2} V^n_{i,j-1/2}\right), \qquad j \in \mathbb{Z}. \tag{4.1.23}$$

Proof. Let $\{\rho^{n+1,-}_{i,j}\}_{j\in\mathbb{Z}}$, be a solution of (4.1.5) obtained by scheme (4.1.8). Using this solution we solve (4.1.6) by the scheme (4.1.12), where the value $\bar{V}^n_{i,j}$ still needs to be determined in such a way that the resulting scheme is conservative. Replacing $\rho^{n+1,-}_{i,j}$ in (4.1.12) we obtain

$$\rho^{n+1}_{i,j} = \rho^n_{i,j} - \lambda\left(V^n_{i,j+1/2} - V^n_{i,j-1/2}\right)\rho^{n+1,-}_{i,j} - \bar{V}^n_{i,j}\lambda\left(\rho^{n+1,-}_{i,j+1/2} - \rho^{n+1,-}_{i,j-1/2}\right). \tag{4.1.24}$$

As $\rho^{n+1,-}_{i,j+1/2}$ satisfies the assumptions of Lemma 12, there exist $\alpha_{i,j} \in [0,1]$ satisfying (4.1.19). Setting $\bar{V}^n_{i,j} := \alpha_{i,j} V^n_{i,j-1/2} + (1-\alpha_{i,j}) V^n_{i,j+1/2}$ in (4.1.24), we obtain (4.1.23). □

Note that in the scheme (4.1.23), the numerical flux $F^n_{i,j+1/2} := \rho^{n+1,-}_{i,j+1/2} V^n_{i,j+1/2}$ is consistent with the flux $f_i(\rho) = \rho_i v(r * \omega_i)$ due to (4.1.13). As a consequence of Lemmas 11 and 12, we have the following property.

Lemma 13. (Positivity) *For any* $T > 0$*, under the stability conditions* (4.1.9) *and* (4.1.15)*, the scheme* (4.1.23) *is positivity preserving on* $[0,T] \times \mathbb{R}$.

Moreover, in the scalar case, we have the following estimates.

Lemma 14 (**$\mathbf{L}^\infty$ estimate**, case $M = 1$)**.** *Under conditions* (4.1.15) *and* (4.1.9)*, and as a consequence of* (4.1.10) *and* (4.1.17)*, we have*

$$\rho^{n+1}_j \in \mathcal{I}(\rho^n_{j-1}, \rho^n_{j+1}) \text{ for all } j \in \mathbb{Z}.$$

Lemma 15 (**BV estimates**, case $M = 1$)**.** *Assume* (4.1.15) *and*

$$\Delta t \leq \frac{1}{v^{\max}\|\psi'\|_\infty \|\rho^0\|_\infty W_0}\,. \tag{4.1.25}$$

Let $\boldsymbol{\rho}^{\Delta x}$ *be constructed using* (4.1.23)*. Then for every* $T > 0$ *the following discrete space BV estimate holds*

$$TV(\boldsymbol{\rho}^{\Delta x}(T,\cdot)) \leq e^{v^{\max} W_0 \|\rho^0\|_\infty \left(3\|\psi'\|_\infty + 5\|\psi''\|_\infty \|\rho^0\|_\infty J_1\right) T}\, TV(\rho^0).$$

Proof. Setting $v(\xi) := v^{\max}\psi(\xi)$, from (4.1.8) we recover

$$\rho_{j+1}^{n+1,-} - \rho_j^{n+1,-} = \rho_{j+1}^n - \rho_j^n - \lambda\rho_{j+1}^{n+1,-}\left(V_{j+3/2}^n - V_{j+1/2}^n\right) + \lambda\rho_j^{n+1,-}\left(V_{j+1/2}^n - V_{j-1/2}^n\right).$$

We have

$$- \lambda\rho_{j+1}^{n+1,-}\left(V_{j+3/2}^n - V_{j+1/2}^n\right) + \lambda\rho_j^{n+1,-}\left(V_{j+1/2}^n - V_{j-1/2}^n\right) \tag{4.1.26a}$$

$$= - \lambda\rho_{j+1}^{n+1,-} v'(\xi_{j+1})\Delta x \sum_{k=1}^{+\infty}\omega^k\left(\rho_{j+k+1}^n - \rho_{j+k}^n\right) + \lambda\rho_j^{n+1,-} v'(\xi_j)\Delta x \sum_{k=1}^{+\infty}\omega^k\left(\rho_{j+k}^n - \rho_{j+k-1}^n\right) \tag{4.1.26b}$$

$$= - \Delta t\left[\rho_{j+1}^{n+1,-} - \rho_j^{n+1,-}\right] v'(\xi_{j+1}) \sum_{k=1}^{+\infty}\omega^k\left(\rho_{j+k+1}^n - \rho_{j+k}^n\right) \tag{4.1.26c}$$

$$- \Delta t\rho_j^{n+1,-}\left[v'(\xi_{j+1}) - v'(\xi_j)\right] \sum_{k=1}^{+\infty}\omega^k\left(\rho_{j+k+1}^n - \rho_{j+k}^n\right) \tag{4.1.26d}$$

$$- \Delta t\rho_j^{n+1,-} v'(\xi_j)\left[\sum_{k=1}^{+\infty}\omega^k(\rho_{j+k+1}^n - \rho_{j+k}^n) - \sum_{k=1}^{+\infty}\omega^k(\rho_{j+k}^n - \rho_{j+k-1}^n)\right] \tag{4.1.26e}$$

$$= - \Delta t\left[\rho_{j+1}^{n+1,-} - \rho_j^{n+1,-}\right] v'(\xi_{j+1}) \sum_{k=1}^{+\infty}\omega^k\left(\rho_{j+k+1}^n - \rho_{j+k}^n\right) \tag{4.1.26f}$$

$$- \Delta t\rho_j^{n+1,-}\left[v'(\xi_{j+1}) - v'(\xi_j)\right] \sum_{k=1}^{+\infty}\omega^k\left(\rho_{j+k+1}^n - \rho_{j+k}^n\right) \tag{4.1.26g}$$

$$- \Delta t\rho_j^{n+1,-} v'(\xi_j)\left[\sum_{k=1}^{+\infty}\omega^k(\rho_{j+k+1}^n - \rho_{j+k}^n) - \sum_{k=1}^{+\infty}\omega^k(\rho_{j+k}^n - \rho_{j+k-1}^n)\right] \tag{4.1.26h}$$

This implies

$$\left[1 + \Delta t\, v'(\xi_{j+1}) \sum_{k=1}^{+\infty}\omega^k\left(\rho_{j+k+1}^n - \rho_{j+k}^n\right)\right]\left(\rho_{j+1}^{n+1,-} - \rho_j^{n+1,-}\right) \tag{4.1.27a}$$

$$= \rho_{j+1}^n - \rho_j^n \tag{4.1.27b}$$

$$- \Delta t\rho_j^{n+1,-}\left[v'(\xi_{j+1}) - v'(\xi_j)\right] \sum_{k=1}^{+\infty}\omega^k\left(\rho_{j+k+1}^n - \rho_{j+k}^n\right) \tag{4.1.27c}$$

$$- \Delta t \rho_j^{n+1,-} v'(\xi_j) \left[\sum_{k=1}^{+\infty} \omega^k (\rho_{j+k+1}^n - \rho_{j+k}^n) - \sum_{k=1}^{+\infty} \omega^k (\rho_{j+k}^n - \rho_{j+k-1}^n) \right] \tag{4.1.27d}$$

(4.1.27e)

Observe that

$$1 + \Delta t \, v'(\xi_{j+1}) \sum_{k=1}^{+\infty} \omega^k \left(\rho_{j+k+1}^n - \rho_{j+k}^n \right) \geq 1 - \Delta t \left\| v' \right\|_\infty \left\| \rho^0 \right\|_\infty W_0$$

which is positive if $\Delta t \leq \left(\left\| v' \right\|_\infty \left\| \rho^0 \right\|_\infty W_0 \right)^{-1}$. Moreover, we have that

$$v'(\xi_{j+1}) - v'(\xi_j) = v''(\zeta_{j+1/2})(\xi_{j+1} - \xi_j),$$

with $\zeta_{j+1/2} \in \mathcal{I}\left(\xi_j, \xi_{j+1}\right)$. We can compute

$$\begin{aligned}
\xi_{j+1} - \xi_j =& \vartheta \Delta x \sum_{k=1}^{+\infty} \omega^k \rho_{j+k+1}^n + (1-\vartheta) \Delta x \sum_{k=1}^{+\infty} \omega^k \rho_{j+k}^n \\
& - \mu \Delta x \sum_{k=1}^{+\infty} \omega^k \rho_{j+k}^n - (1-\mu) \Delta x \sum_{k=1}^{+\infty} \omega^k \rho_{j+k-1}^n \\
=& \vartheta \Delta x \sum_{k=2}^{+\infty} \omega^{k-1} \rho_{j+k}^n + (1-\vartheta) \Delta x \sum_{k=1}^{+\infty} \omega^k \rho_{j+k}^n \\
& - \mu \Delta x \sum_{k=1}^{+\infty} \omega^k \rho_{j+k}^n + (1-\mu) \Delta x \sum_{k=0}^{+\infty} \omega^{k+1} \rho_{j+k}^n \\
=& \Delta x \sum_{k=2}^{+\infty} \left[\vartheta \omega^{k-1} + (1-\vartheta)\omega^k - \mu \omega^k - (1-\mu)\omega^{k+1} \right] \rho_{j+k}^n \\
& + \Delta x \left[(1-\vartheta)\omega^1 \rho_{j+1}^n - \mu \omega^1 \rho_{j+1}^n - (1-\mu)\omega^1 \rho_j^n - (1-\mu)\omega^2 \rho_{j+1}^n \right].
\end{aligned}$$

By monotonicity of ω we have

$$\vartheta \omega^{k-1} + (1-\vartheta)\omega^k - \mu \omega^k - (1-\mu)\omega^{k+1} \geq 0.$$

Taking the absolute values we get

$$\begin{aligned}
\left| \xi_{j+1} - \xi_j \right| &\leq \Delta x \left\| \rho^0 \right\|_\infty \left\{ \sum_{k=2}^{+\infty} \left[\vartheta \omega^{k-1} + (1-\vartheta)\omega^k - \mu \omega^k - (1-\mu)\omega^{k+1} \right] + 3\omega^1 \right\} \\
&= \Delta x \left\| \rho^0 \right\|_\infty \left\{ \vartheta \omega^1 + (1-\mu)\omega^2 + 3\omega^1 \right\} \\
&\leq \Delta x \, 5 \left\| \rho^0 \right\|_\infty W_0.
\end{aligned}$$

Taking the absolute values in (4.1.27) we get

$$
\begin{aligned}
&\left(1-\Delta t\left\|v'\right\|_\infty\left\|\rho^0\right\|_\infty W_0\right)\sum_j\left|\rho_{j+1}^{n+1,-}-\rho_j^{n+1,-}\right| \\
&\leq\Bigg[1+\Bigg(\left(\sum_{k=1}^{\infty}\rho_{j-k}^{n+1,-}\left|v'(\xi_{j+1-k})-v'(\xi_{j-k})\right|\omega^k-\rho_{j-k}^{n+1,-}v'(\xi_j)(\omega^k-\omega^{k+1})\right) \\
&\qquad -\rho_j^{n+1,-}v'(\xi_j)\omega^1\Bigg)\Delta t\Bigg]\sum_j\left|\rho_{j+1}^n-\rho_j^n\right| \\
&\leq\left[1+5\Delta t\left\|\rho^0\right\|_\infty^2 W_0\|v''\|\,\Delta x\sum_{k=1}^{\infty}\omega^k+2\,\Delta t\,W_0\left\|\rho^0\right\|_\infty\left\|v'\right\|_\infty\right]\sum_j\left|\rho_{j+1}^n-\rho_j^n\right| \\
&\leq\left[1+\Delta t\left\|\rho^0\right\|_\infty W_0\left(2\left\|v'\right\|_\infty+5\left\|v''\right\|_\infty\left\|\rho^0\right\|_\infty J_1\right)\right]\sum_j\left|\rho_{j+1}^n-\rho_j^n\right|,
\end{aligned}
$$

which, together with the TVD property of the remap step [12, 15], implies

$$
\begin{aligned}
\mathrm{TV}(\rho_{\Delta x}(T,\cdot))&\leq\left(\frac{1+\Delta t\|\rho^0\|_\infty W_0\left(2\left\|v'\right\|_\infty+5\left\|v''\right\|_\infty\|\rho^0\|_\infty J_1\right)}{1-\Delta t\left\|v'\right\|_\infty\left\|\rho^0\right\|_\infty W_0}\right)^{\frac{T}{\Delta t}}\mathrm{TV}(\rho^{\Delta x}(0,\cdot)) \\
&\leq e^{\|\rho^0\|_\infty W_0\left(3\left\|v'\right\|_\infty+5\left\|v''\right\|_\infty\|\rho^0\|_\infty J_1\right)T}\mathrm{TV}(\rho^0).
\end{aligned}
$$

□

Next Theorem follows from Theorem 12 and Lemmas 13, 14 and 15.

Theorem 13 (Convergence to weak solutions, case $M=1$)**.** *Let us consider the Cauchy problem* (3.1.1)-(3.1.5) *with* $M=1$, $\rho^0(x)\in BV(\mathbb{R};[0,1])$, *under the assumptions* **(H1)** - **(H3)**. *If* (4.1.15) *and* (4.1.9) *hold, then the approximate solution* $\rho^{\Delta x}$ *constructed by the scheme* (4.1.23) *converges to a weak solution of* (3.1.1)- (3.1.5).

Proof. Under conditions (4.1.15) and (4.1.9), the approximate solutions $\rho^{\Delta x}$ constructed by the numerical scheme (4.1.23) are uniformly bounded and uniformly bounded total variation. The result follows by standard application of Helly's Theorem. □

4.2 Two simple schemes for the non-local multi-class traffic flow model

In Section 4.3, we consider the following conservative schemes for the multi-class model (3.1.1) in the form

$$
\rho_{i,j}^{n+1}=\rho_{i,j}^n-\lambda\left(F_{i,j+1/2}^n-F_{i,j-1/2}^n\right),\qquad i=1,...,M. \tag{4.2.1}
$$

First, we consider the Godunov-type scheme , which was introduced in [46] in the scalar case and then extended to (3.1.1) in [22] (see chapter 3), with numerical flux

$$F^n_{i,j+1/2} := \rho^n_{i,j} V^n_{i,j+1/2}. \tag{4.2.2}$$

We recall that for scheme (4.2.1)-(4.2.2) the positivity is guaranteed if

$$\lambda \leq \frac{1}{v_M^{\max}\|\psi\|_\infty}.$$

We consider also the approximate solutions constructed via the following adapted Lax-Friedrichs flux, that was used [11, 21] in the scalar case and in [22] for system (3.1.1) (see chapters 1 and 3):

$$F^n_{i,j+1/2} := \frac{1}{2}\left(\rho^n_{i,j} V^n_{i,j-1/2} + \rho^n_{i,j+1} V^n_{i,j-3/2}\right) + \frac{\alpha}{2}\left(\rho^n_{i,j} - \rho^n_{i,j+1}\right), \tag{4.2.3}$$

where $\alpha \geq v_M^{\max}\|\psi\|_\infty$ is the viscosity coefficient and $\lambda\alpha \leq 1$ the CFL condition.

4.2.1 A second-order Godunov scheme

Schemes (4.2.1)-(4.2.2) and (4.2.1)-(4.2.3) being only first-order accurate, we propose here a second-order accuracy scheme, constructed using MUSCL-type variable extrapolation and Runge-Kutta temporal differencing. To implement it, we approximate $\rho_i(x, t^n)$ by a piecewise linear functions in each cell, i.e. $\hat{\rho}_{i,j}(x, t^n) = \rho^n_{i,j} + \sigma^n_{i,j}(x - x_j)$, where the slopes $\sigma^n_{i,j}$ are calculated via the generalized minmod limiter, i.e.

$$\sigma^n_{i,j} = \frac{1}{\Delta x}\text{minmod}(\vartheta(\rho^n_{i,j} - \rho^n_{i,j-1}), \frac{1}{2}(\rho^n_{i,j+1} - \rho^n_{i,j-1}), \vartheta(\rho^n_{i,j+1} - \rho^n_{i,j})),$$

where $\vartheta \in [1, 2]$ and

$$\text{minmod}(a, b, c) := \begin{cases} \text{sgn}(a)\min\{|a|, |b|, |c|\} & \text{if } \text{sgn}(c) = \text{sgn}(b) = \text{sgn}(a) \\ 0 & \text{otherwise.} \end{cases}$$

This extrapolation enables one to define left and right values at the cell interfaces respectively by

$$\begin{aligned} \rho^L_{i,j+1/2,} &:= \hat{\rho}_{i,j}(x_j + \Delta x/2, t^n) = \rho^n_{i,j} + \sigma^n_{i,j}\Delta x/2, \\ \rho^R_{i,j-1/2,} &:= \hat{\rho}_{i,j}(x_j - \Delta x/2, t^n) = \rho^n_{i,j} - \sigma^n_{i,j}\Delta x/2. \end{aligned}$$

In order to define the corresponding velocity approximations, we set

$$\hat{r}^n_{j+k} = \sum_{i=1}^{M} \hat{\rho}^n_{i,j+k} = r^n_{j+k} + \Theta^n_{j+k}(x - x_{j+k}),$$

where $\Theta^n_{j+k} := \sum_{i=1}^{M} \sigma^n_{i,j+k}$, and

$$\hat{V}^n_{i,j+1/2} := v_i((\hat{r} * w_i)(t^n, x_{j+1/2})) = v_i^{\max}\psi\left(\Delta x \sum_{k=1}^{+\infty} \omega_i^k r^n_{j+k} + \Delta x \sum_{k=1}^{+\infty} \tilde{\omega}^k_{i,j}\Theta^n_{j+k}\right) \tag{4.2.4}$$

for $i = 1, \dots, M$, $j \in \mathbb{Z}$, where $\tilde{\omega}^k_{i,j} := \frac{1}{\Delta x} \int_{-\Delta x/2}^{\Delta x/2} y\omega_i(y + (k - 1/2)\Delta x)\, \mathrm{d}y$. The MUSCL version of the i-th flux component thus reads

$$f^n_{i,j+1/2} := \rho^L_{i,j+1/2} \hat{V}^n_{i,j+1/2}.$$

To achieve formal second-order accuracy also in time, we use second-order Runge-Kutta (RK) time stepping. More precisely, if we write our scheme with first-order Euler time difference and second-order spatial difference formally as

$$\boldsymbol{\rho}^{n+1}_j = \boldsymbol{\rho}^n_j - \lambda L_j(\boldsymbol{\rho}^n) := \boldsymbol{\rho}^n_j - \lambda \left(\mathbf{F}^n_{j+1/2} - \mathbf{F}^n_{j-1/2} \right), \tag{4.2.5}$$

then the RK version takes the following two-step form

$$\begin{cases} \boldsymbol{\rho}^{(1)}_j = \boldsymbol{\rho}^n_j - \lambda L_j(\boldsymbol{\rho}^n) \\ \boldsymbol{\rho}^{n+1}_j = \frac{1}{2}(\boldsymbol{\rho}^n_j + \boldsymbol{\rho}^{(1)}_j) - \frac{\lambda}{2} L_j(\boldsymbol{\rho}^{(1)}_j) \end{cases} \tag{4.2.6}$$

Lemma 16. *For any $T > 0$, under the CFL condition*

$$\Delta t \leq \frac{\Delta x}{2 v^{\max}_M \|\psi\|_\infty}, \tag{4.2.7}$$

the scheme (4.2.6) is positivity preserving on $\mathbb{R} \times [0, T]$.

Proof. Let us assume that $\rho^n_{i,j} \geq 0$ for $j \in \mathbb{Z}$ and $i = 1, \dots, M$. The positivity of the reconstructed values $\rho^L_{i,j+1/2}$ and $\rho^L_{i,j+1/2}$ is guaranteed by the positivity preserving property of the chosen limiter [73, 74]. It suffices to prove that $\rho^{n+1}_{i,j} \geq 0$ in (4.2.5). Due to $\rho^n_{i,j} = \frac{1}{2}(\rho^R_{i,j-1/2} + \rho^L_{i,j+1/2})$, the i-th term in (4.2.5) can be written in the form

$$\rho^{n+1}_{i,j} = \frac{1}{2}\rho^R_{i,j-1/2} + \left(\frac{1}{2} - \lambda \hat{V}^n_{i,j+1/2} \right) \rho^L_{i,j+1/2} + \lambda \rho^L_{i,j-1/2} \hat{V}^n_{i,j-1/2} \geq 0,$$

under the CFL condition (4.2.7). □

4.3 Numerical results

In the following numerical tests, we solve (3.1.1) numerically in the intervals $x \in [-1, 1]$ and $t \in [0, T]$, for values of T specified later. We propose several test cases in order to illustrate the behaviour of the Lagrangian-Antidiffusive remap (L-AR) scheme in comparison with first-order Lax-Friedrichs and Godunov (4.2.2) schemes and the second-order Godunov scheme (4.2.6). For each integration, we set Δt to satisfy the most restrictive CFL condition (4.2.7).

Since we cannot compute the exact solution explicitly, we use the second-order Godunov scheme with a refined mesh to obtain a reference solution. The $\mathbf{L^1}$-error for the cell average is given by

$$L^1(\Delta x) = \sum_{i=1}^{M} \left(\frac{1}{N} \sum_{j=1}^{N} |\overline{\rho}_{i,j} - \overline{\rho}^{ref}_{i,j}| \right),$$

where $\overline{\rho}_{i,j}$ and $\overline{\rho}^{ref}_{i,j}$ are the cell averages of the numerical approximation and the reference solution respectively. The Experimental Order of Accuracy (E.O.A.) is naturally defined by

$$\gamma(\Delta x) = \log_2 \left(L^1(\Delta x)/L^1(\Delta x/2) \right).$$

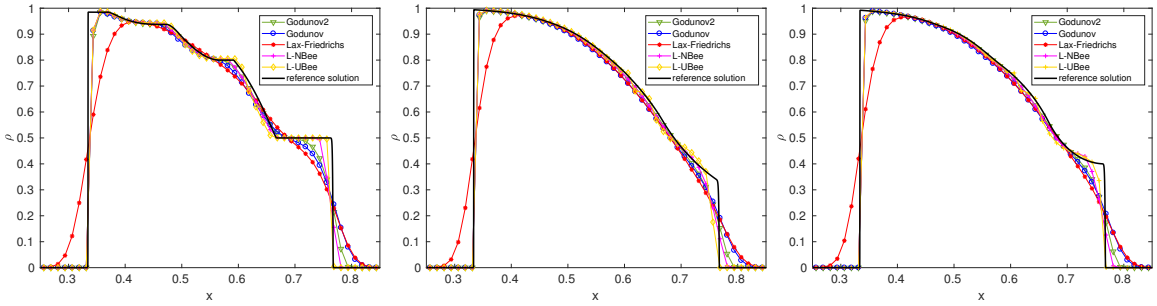

(a) (b) (c)

Figure 4.1: Test 1: Comparison of the numerical solutions at $T = 0.1$ corresponding to the initial condition (4.3.1), computed with $1/\Delta x = 80$ and different kernel functions. (a) $\omega(x) = 1/\eta$, (b) $\omega(x) = 2(\eta - x)/\eta^2$, (c) $\omega(x) = 3(\eta^2 - x^2)/(2\eta^3)$.

4.3.1 Test 1, scalar case

We consider the problem (3.1.1) for $M = 1$, with initial datum

$$\rho_0(x) = \begin{cases} 1, & \text{if } 1/3 \leq x \leq 2/3 \\ 0, & \text{otherwise,} \end{cases} \tag{4.3.1}$$

for $x \in [0, 1]$, with absorbing boundary conditions, and different non-increasing kernel functions with $\eta = 0.1$. In Figure 4.1, we display the numerical approximations obtained with the schemes presented in the previous sections, computed with $1/\Delta x = 80$ at $T = 0.1$. Fig. 4.1a show the result for $\omega(x) = 1/\eta$, Fig. 4.1b for $\omega(x) = 2(\eta - x)/\eta^2$ and Fig. 4.1c for $\omega(x) = 3(\eta^2 - x^2)/(2\eta^3)$. The reference solution is computed with $1/\Delta x = 10240$. The numerical solutions obtained with L-UBee and L-NBee approximate adequately shocks and rarefaction waves according to the theoretical results of Theorem 13. In particular, concerning the shock waves, L-AR schemes capture the reference solution better than the second-order Godunov scheme, whereas the solutions computed with Lax-Friedrichs and Godunov schemes are more diffusive. In the presence of rarefaction waves, L-UBee scheme produces "staircaising" due to the particular choice of the antidiffusive scheme. We can observe the same "staircaising" phenomena also for the linear advection and other equations [12, 15].

Table 4.1 shows the approximate $\mathbf{L^1}$-errors and the numerical orders of accuracy $\gamma(\Delta x)$ for the different schemes. We computed numerical approximations with $1/\Delta x = 40 \times 2^q$ for $q = 1, 2, ..., 5$. Clearly, the error of the L-AR schemes decreases when the mesh is refined and we observe that for each level of refinement, the $\mathbf{L^1}$-error of the L-AR schemes is smaller than the respective errors of Lax-Friedrichs and Godunov schemes. In conclusion, when the solution presents discontinuities, we can compare the performances of the L-AR schemes with those of a second-order scheme.

Now, in order to determine the correct order of accuracy of the L-AR schemes, we consider a smooth initial datum

$$\rho_0(x) = 0.5 + 0.4 \sin(\pi x) \tag{4.3.2}$$

for $x \in [-1, 1]$, with periodic boundary conditions and compute the numerical approximation at $T = 0.15$ for different kernel functions with $\eta = 0.1$. The reference solution is computed

Scheme		$\omega(x) = 1/\eta$		$\omega(x) = 2(\eta - x)/\eta^2$		$\omega(x) = 3(\eta^2 - x^2)/(2\eta^3)$	
	$1/\Delta x$	$\mathbf{L^1}-$ error	EOA	$\mathbf{L^1}-$ error	EOA	$\mathbf{L^1}-$ error	EOA
Godunov	80	1.81e-02	–	1.62e-02	–	1.64e-02	–
	160	1.12e-02	6.98e-01	7.73e-0.3	1.06	8.72e-03	9.11e-01
	320	7.85e-03	5.10e-01	6.15e-03	3.29e-01	6.53e-03	4.19e-01
	640	5.33e-03	5.58e-01	3.43e-03	8.43e-01	4.01e-03	7.04e-01
	1280	3.62e-03	5.58e-01	2.51e-0.3	4.50e-01	2.76e-03	5.39e-01
Lax-F	80	3.48e-02	–	2.89e-02	–	2.94e-02	–
	160	2.50e-02	4.81e-01	1.72e-02	7.50e-01	1.91e-02	6.23e-01
	320	1.86e-02	4.24e-01	1.35 e-02	3.46e-01	1.48e-02	3.67e-01
	640	1.29e-02	5.28e-01	8.94e-03	5.7e-01	1.02e-02	5.38e-01
	1280	8.72e-03	5.64e-01	6.670e-03	4.23e-01	7.30e-03	4.70e-01
L-NBee	80	9.30e-03	–	8.93e-03	–	9.24e-03	–
	160	4.29e-03	1.11	4.78e-03	9.01e-01	4.50e-03	1.03e-01
	320	2.51e-03	7.47e-01	2.52e-03	9.27e-01	2.37e-03	9.25e-01
	640	1.58e-03	1.11	1.15e-03	1.13	1.08e-03	1.13
	1280	6.57e-04	8.17e-01	6.46e-04	8.31e-01	6.19e-04	8.05e-01
L-UBee	80	1.00e-02	–	8.90e-03	–	9.09e-03	–
	160	4.58e-03	1.13	4.40e-03	1.02	4.82e-03	9.16e-01
	320	2.7e-03	7.62e-01	2.87e-03	6.61e-01	2.62e-03	8.80e-01
	640	1.15e-03	1.23	1.38e-03	1.05	1.37e-03	9.30e-01
	1280	9.48e-04	2.76e-01	9.69e-04	5.13e-01	9.00e-04	6.11e-01
Godunov2	80	1.20e-02	–	1.08e-02	–	1.01e-02	–
	160	6.54e-03	8.70e-01	5.5e-03	9.71e-01	5.96e-03	8.86e-01
	320	3.82e-03	7.73e-01	3.35e-03	7.17e-01	3.51e-03	7.64e-01
	640	2.29e-03	7.42e-01	1.76e-03	9.25e-01	1.94e-03	8.53e-01
	1280	1.23e-03	8.89e-01	1.02e-03	7.87e-01	1.08e-03	8.42e-01

Table 4.1: Test 1. Approximate $\mathbf{L^1}$-error and E.O.A. for different numerical schemes and with different kernel functions and $\eta = 0.1$ corresponding to the initial condition (4.3.1).

with $1/\Delta x = 10240$. In Table 4.2 and Figure 4.3 we compute the $\mathbf{L^1}$-error and E.O.A. $\gamma(\Delta x)$. We recover the correct order of accuracy for the second-order Godunov scheme. Instead, we obtain just first-order accuracy for L-AR schemes. However, it is worth underlying that the $\mathbf{L^1}$-error of the L-NBee scheme is smaller than the corresponding error for Lax-Friedrichs and Godunov schemes. For the L-UBee scheme, we obtain first order accuracy and the $\mathbf{L^1}$-error for each level of refinement is bigger than the error of the other first order numerical schemes, due to the antidiffusive property of the UBee scheme.

4.3.2 Test 2. Cars and trucks mixed traffic

In this test case, we consider a stretch of road populated by cars and trucks as in the example proposed in [22, Section 4.2]. The space domain is given by the interval $[-1, 1]$ and we impose absorbing conditions at the boundaries. The dynamics is described by the equation (3.1.1) with $M = 2$, and the following initial conditions and parameter values

$$\begin{aligned} &\rho_1(0,x) = 0.5\chi_{[-0.6,-0.1]}(x), \quad \omega_1(x) = \frac{2}{\eta_1}\left(1 - \frac{x}{\eta_1}\right), \qquad \eta_1 = 0.3, \qquad v_1^{\max} = 0.8, \\ &\rho_2(0,x) = 0.5\chi_{[-0.9,-0.6]}(x), \quad \omega_2(x) = \frac{2}{\eta_2}\left(1 - \frac{x}{\eta_2}\right), \qquad \eta_2 = 0.1, \qquad v_2^{\max} = 1.3. \end{aligned} \tag{4.3.3}$$

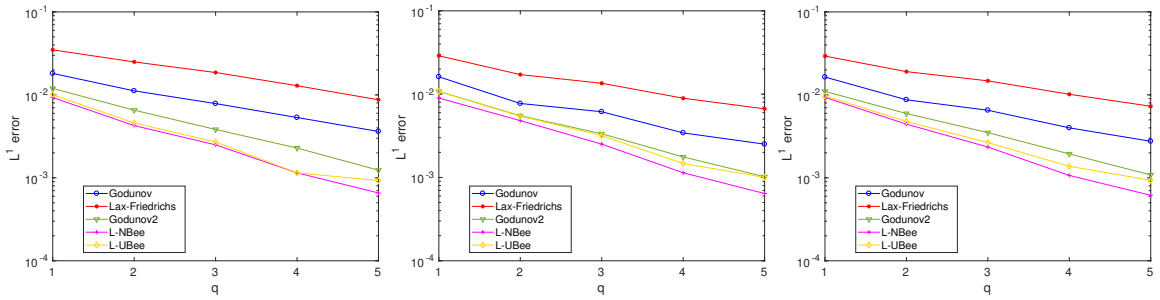

(a) (b) (c)

Figure 4.2: Test 1. Initial condition (4.3.1). Approximate $\mathbf{L^1}$-error for different numerical schemes with: (a) constant kernel function $\omega(x) = 1/\eta$, (b) decreasing kernel function $\omega(x) = 2(\eta - x)/\eta^2$, (c) concave kernel function $\omega(x) = 3(\eta^2 - x^2)/(2\eta^3)$.

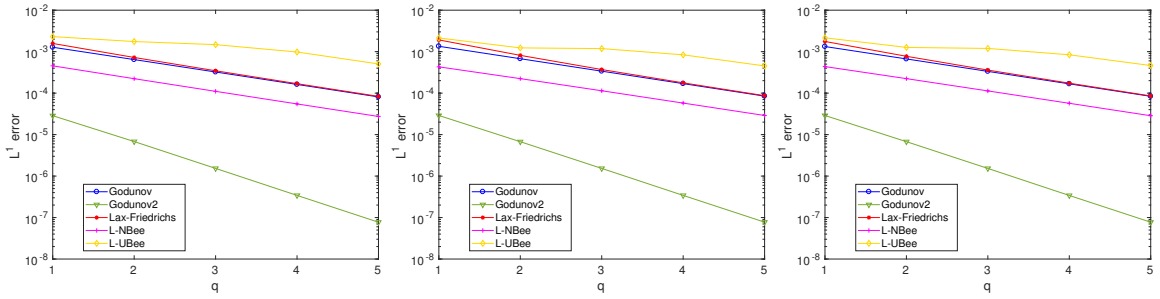

(a) (b) (c)

Figure 4.3: Test 1. Initial condition (4.3.2). Approximate $\mathbf{L^1}$-error for different numerical schemes with: (a) constant kernel function $\omega(x) = 1/\eta$, (b) decreasing kernel function $\omega(x) = 2(\eta - x)/\eta^2$, concave kernel function $\omega(x) = 3(\eta^2 - x^2)/(2\eta^3)$ (c).

In this setting, $\rho_1(t, x)$ and $\rho_2(x, t)$ describe the density of trucks and cars respectively. We have a red traffic light located at $x = -0.1$, which turns green at the initial time $t = 0$. In Figure 4.4, we display the reference solution of equation (3.1.1) with initial conditions and parameters (4.3.3), computed with with $1/\Delta x = 5120$ at increasing time instants ($T = 0.25$ in Fig. 4.4a, $T = 0.5$ in Fig. 4.4b and $T = 1$ in Fig. 4.4c.

In Figure 4.5, we display separately the two density components of the approximate solutions computed using all the considered schemes with $1/\Delta x = 80$, compared to the reference solution of Figure 4.4. The numerical tests indicate that for $M > 1$, the L-AR solutions are anti-diffusive for each class and they keep this anti-diffusive behavior for the whole simulation time. We observe that the L-NBee solution approaches very well the reference solution for each class at different times. Instead, the L-UBee solution shows "stairs" in the presence of rarefaction-waves.

In Table 4.3 and Figure 4.6, we compute the approximate $\mathbf{L^1}$-error and the E.O.A at time $T = 0.5$. We observe that the performance of L-AR schemes are comparable with those of the second order Godunov scheme. In particular, we have that the L-NBee $\mathbf{L^1}$-error is the smallest for each level of refinement.

Scheme		$\omega(x) = 1/\eta$		$\omega(x) = 2(\eta - x)/\eta^2$		$\omega(x) = 3(\eta^2 - x^2)/(2\eta^3)$	
	$1/\Delta x$	$\mathbf{L^1}-$ error	EOA	$\mathbf{L^1}-$ error	EOA	$\mathbf{L^1}-$ error	EOA
Godunov	80	1.28e-03	–	1.33e-03	–	1.33e-03	–
	160	6.44e-04	9.88e-01	6.73e-0.4	9.95e-01	6.68e-04	9.94e-01
	320	3.23e-04	9.94e-01	3.38e-04	9.97e-01	3.34e-04	9.97e-01
	640	1.62e-04	9.97e-01	1.69e-04	9.99e-01	1.67e-04	9.98e-01
	1280	8.11e-05	9.98e-01	8.47e-0.5	9.99e-01	8.38e-05	9.99e-01
Lax-F	80	1.58e-03	–	1.92e-03	–	1.76e-03	–
	160	7.24e-04	1.12	8.14e-04	1.24	7.73e-04	1.18
	320	3.46e-04	1.07	3.70e-04	1.14	3.59e-04	1.10
	640	1.69e-04	1.03	1.77e-04	1.06	1.74e-04	1.05
	1280	8.35e-05	1.02	8.67e-04	1.03	8.55e-05	1.02
L-NBee	80	4.55e-04	–	4.30e-04	–	4.36e-04	–
	160	2.23e-04	1.02	2.24e-04	9.43e-01	2.24e-04	9.65e-01
	320	1.10e-04	1.01	1.14e-04	9.72e-01	1.13e-04	9.83e-01
	640	5.49e-04	1.01	5.76e-05	9.86e-01	5.69e-05	9.92e-01
	1280	2.74e-05	1.00	2.89e-05	9.93e-01	2.85e-05	9.96e-01
L-UBee	80	2.30e-03	–	2.14e-03	–	2.16e-03	–
	160	1.75e-03	3.96e-01	1.23e-03	7.97e-01	1.26e-03	7.72e-01
	320	1.48e-03	2.49e-01	1.18e-03	5.59e-02	1.20e-03	8.05e-02
	640	9.82e-04	5.89e-01	8.39e-04	4.98e-01	8.41e-04	5.09e-01
	1280	5.06e-04	9.56e-01	4.53e-04	8.88e-01	4.63e-04	8.61e-01
Godunov2	80	2.86e-05	–	2.89e-05	–	2.89e-05	–
	160	6.80e-06	2.07	6.74e-06	2.10	6.76e-06	2.09
	320	1.53e-06	2.15	1.53e-06	2.14	1.53e-06	2.14
	640	3.42e-07	2.16	3.42e-07	2.16	3.41e-07	2.16
	1280	7.72e-08	2.15	7.75e-08	2.14	7.73e-08	2.14

Table 4.2: Test 1. Approximate $\mathbf{L^1}$-error and E.O.A., with smooth initial condition (4.3.2) and different kernels function with $\eta = 0.1$.

4.3.3 Test 3. Autonomous and human-driven mixed traffic

The aim of this test is to study the possible impact of the presence of Connected Autonomous Vehicles (CAVs) on road traffic performances, as proposed in [21, Section 4.2]. Let us consider a circular road modeled by the space interval $[-1, 1]$ with periodic boundary conditions at $x = \pm 1$. Autonomous and non-autonomous vehicles have the same maximal speed, but the interaction radius of CAVs is much grater than the one of human-driven cars. Moreover, we can assign a constant convolution kernel to CAVs, since we assume that the degree of accuracy on information they have about surrounding traffic is transmitted through wireless connections and does not depend on distance. We consider the following initial data and parameters

$$\begin{aligned} &\rho_1(0,x) = \beta(0.5 + 0.3\sin(5\pi x)), && \omega_1(x) = \frac{1}{\eta_1}, \quad \eta_1 = 1.0, \quad v_1^{\max} = 1, \\ &\rho_2(0,x) = (1-\beta)\,(0.5 + 0.3\sin(5\pi x)), && \omega_2(x) = \frac{2}{\eta_2}\left(1 - \frac{x}{\eta_2}\right), \quad \eta_2 = 0.05, \quad v_2^{\max} = 1, \end{aligned} \tag{4.3.4}$$

where ρ_1 is the density of autonomous vehicles and ρ_2 the density of human-driven vehicles. The parameter $\beta \in [0, 1]$ gives the penetration rate of autonomous vehicle.

Figure 4.7 displays the reference solution of (3.1.1)-(4.3.4) with $\beta = 0.9$, computed by the

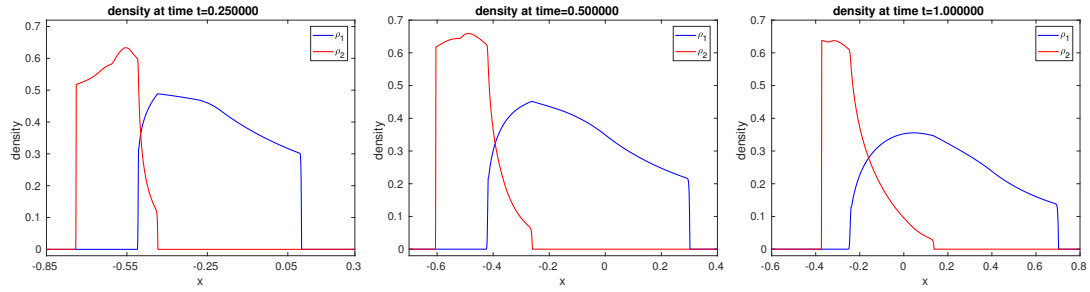

(a) (b) (c)

Figure 4.4: Test 2: Density profiles corresponding to (3.1.1)-(4.3.3), computed by second-order Godunov scheme with $1/\Delta x = 5120$, at different times.

$1/\Delta x$	Godunov		Lax-F		L-NBee		L-UBee		Godunov2	
$1/\Delta x$	$\mathbf{L^1}$-err	$\gamma(\Delta x)$	$\mathbf{L^1}$-err	$\gamma(\Delta x)$	$\mathbf{L^1}$-err	$\gamma(\Delta x)$	$\mathbf{L^1}$-err	$\gamma(\Delta x)$	$\mathbf{L^1}$-err	$\gamma(\Delta x)$
80	2.7e-02	–	4.8e-02	–	5.2e-03	–	1.6e-02	–	8.5e-03	–
160	1.9e-02	0.53	3.4e-02	0.52	2.9e-03	0.83	5.8e-03	1.5	5.5e-03	0.64
320	1.3e-02	0.57	2.3e-02	0.55	1.2e-03	1.3	2.4e-03	1.2	3.0e-03	0.84
640	8.6e-03	0.58	1.6e-02	0.57	5.1e-04	1.3	1.4e-03	0.74	1.7e-03	0.87
1280	5.7e-03	0.59	1.0e-02	0.58	3.6e-04	0.51	9.4e-04	0.63	8.0e-04	1.0

Table 4.3: Test 2. Non-local multi-class LWR model. Initial condition (4.3.3), with decreasing kernel functions, final time $T = 0.5$. The reference solution is computed with $1/\Delta x = 5120$.

second-order Godunov scheme with $1/\Delta x = 10240$ at times $T = 1.5$ in Fig. 4.7a.

In Figure 4.8, we display separately the two classes and we compare the approximate solutions computed by all the considered schemes with $1/\Delta x = 320$, and the reference solution. Again, the numerical solutions obtained using the L-AR schemes are more anti-diffusive than those produced by first-order schemes. We observe a good behavior of the L-NBee scheme. Instead, the L-UBee scheme approaches the reference solution very well in the presence of shock-waves. On the other hand, the usual "stairs" appear in presence of rarefaction-waves.

In Table 4.4 and Figure 4.7b we compute the approximate $\mathbf{L^1}$-error and the E.O.A at time $T = 1.5$. We observe that the performances of L-NBee schemes are comparable with those of the second order Godunov scheme. It is worth pointing out that despite the "staircaising" phenomenon the L-UBee $\mathbf{L^1}$-error is still smaller than the $\mathbf{L^1}$-error of the other first-order schemes.

	Godunov		Lax-F		L-NBee		L-UBee		Godunov2	
$1/\Delta x$	$\mathbf{L^1}$-err	$\gamma(\Delta x)$	$\mathbf{L^1}$-err	$\gamma(\Delta x)$	$\mathbf{L^1}$-err	$\gamma(\Delta x)$	$\mathbf{L^1}$-err	$\gamma(\Delta x)$	$\mathbf{L^1}$-err	$\gamma(\Delta x)$
320	5.2e-02	–	8.5e-02	–	3.0e-03	–	1.3e-02	–	3.1e-03	–
640	3.1e-02	0.76	5.8e-02	0.56	1.4e-03	1.1	5.7e-03	1.3	1.4e-03	1.1
1280	1.7e-02	0.87	3.5e-02	0.73	3.9e-04	1.8	2.8e-03	1.0	3.7e-04	1.9
2560	8.9e-03	0.93	1.9e-02	0.85	1.9e-04	1.0	1.4e-03	1.0	2.0e-04	0.84

Table 4.4: Test 3. Initial condition (4.3.4), with different kernel functions, final time $T = 1.5$. The solutions are computed with $1/\Delta x = 160 \times 2^q$ for $q = 1, ..., 4$.

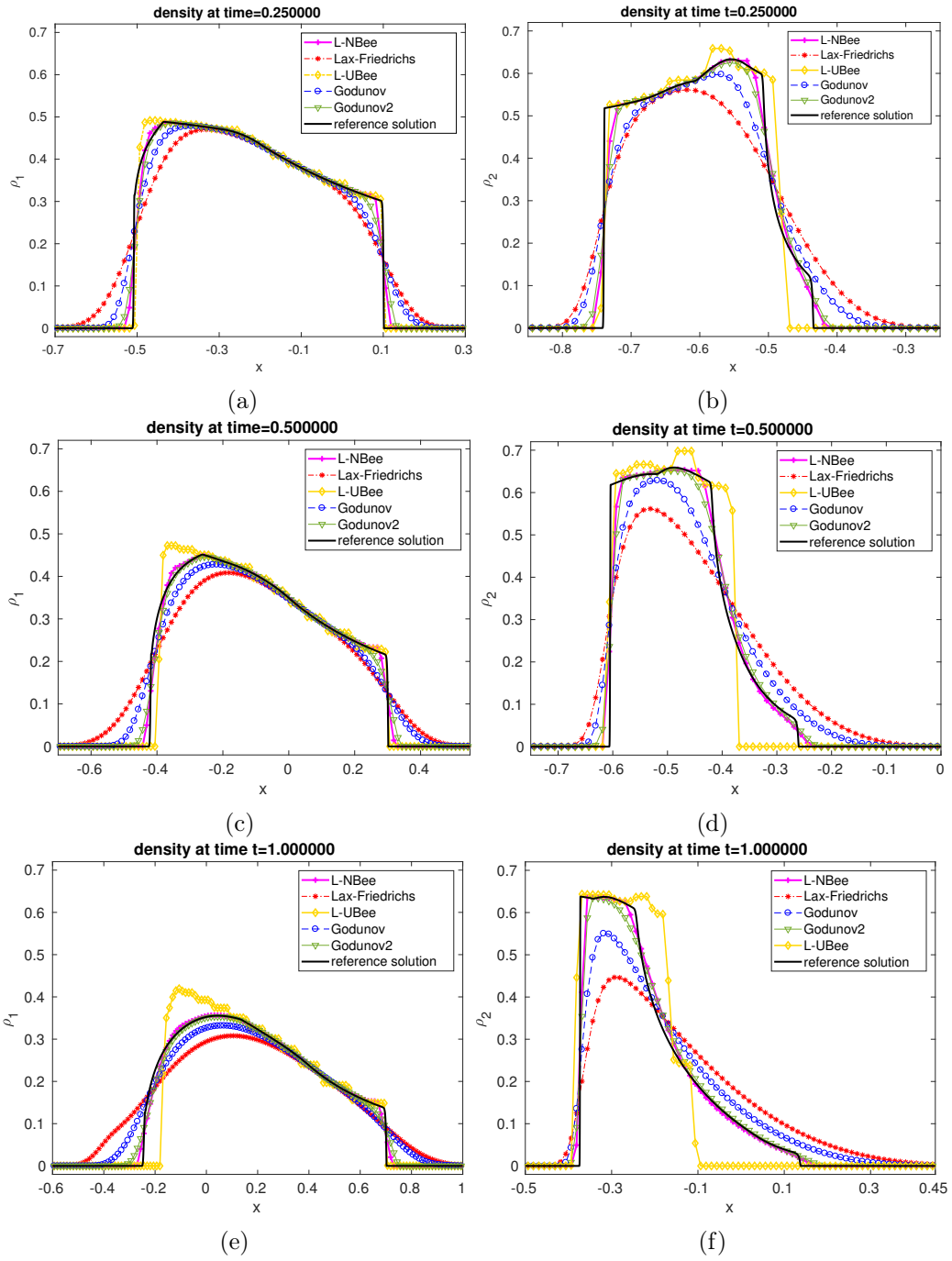

Figure 4.5: Test 2. (a)-(c)-(e) Profile of ρ_1; (b)-(d)-(f) profile of ρ_2 computed with different numerical schemes at different times and $1/\Delta x = 80$.

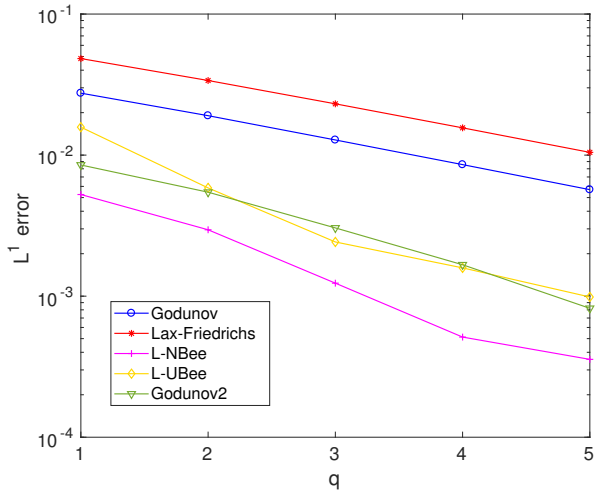

Figure 4.6: Test 2. Approximate total $\mathbf{L^1}$-error for different numerical schemes with the decreasing kernel functions $\omega_1(x) = \omega_2(x) = 2(\eta_{1,2} - x)/\eta_{1,2}^2$, $\eta_1 = 0.3$, $\eta_2 = 0.1$

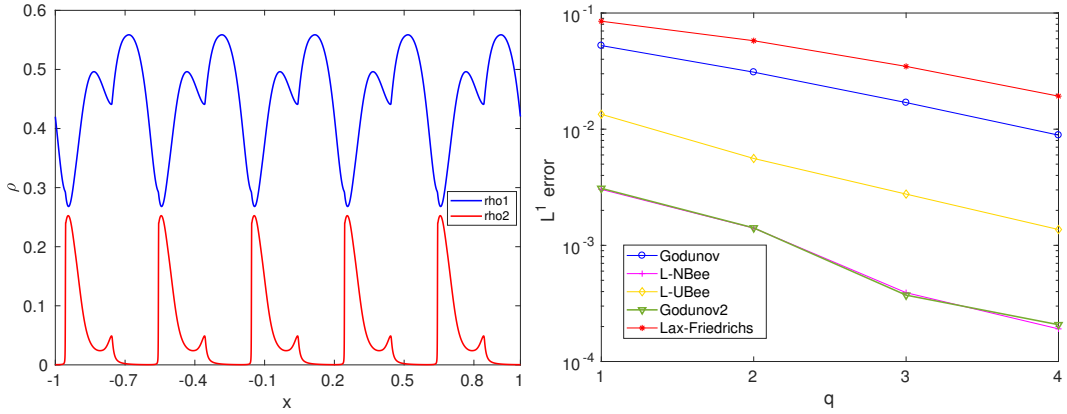

(a) (b)

Figure 4.7: Test 3. (a) Reference solution of Test 3 computed with $1/\Delta x = 10240$. (b) Approximate total $\mathbf{L^1}$-error for different numerical schemes.

4.4 High-order Finite Volume WENO schemes for non-local multi-class traffic flow models

In this section, we solve the non-local system of conservation laws (3.1.1) by using a high-order finite volume WENO scheme [70, 71]. First we consider $\{I_j\}_{j=1}^N$ as a partition of $[-L, L]$ and the points x_j are the center of the cells $I_j = [x_{j-\frac{1}{2}}, x_{j+\frac{1}{2}}]$, with length $|I_j| = \Delta x = \frac{2}{N}$. We denote the unknowns by $\rho_{i,j}(t)$, the cell average of the exact solution $\rho_i(t,\cdot)$ in the cell I_j :

$$\rho_{i,j}(t) := \frac{1}{\Delta x} \int_{I_j} \rho_i(t,x)dx.$$

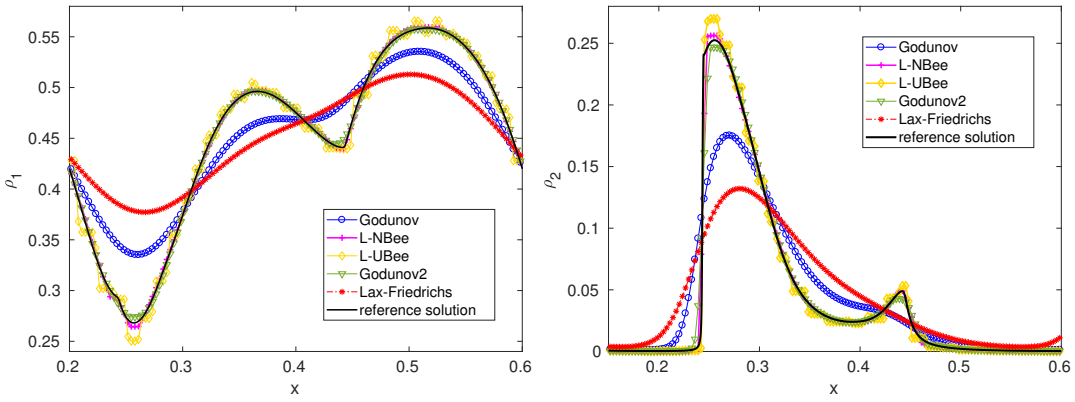

(a) (b)

Figure 4.8: Test 3. (a) Profile of ρ_1; (b) profile of ρ_2, computed with different numerical schemes at time=1.5 and $1/\Delta x = 320$.

We extend $\omega_i(x) = 0$ for $x > \eta_i$, and set

$$\omega_i^k := \frac{1}{\Delta x} \int_{(k-1)\,\Delta x}^{k\,\Delta x} \omega_i(x)\,dx, \qquad k \in \mathbb{N}^*, \tag{4.4.1}$$

so that $\Delta x \sum_{k=1}^{+\infty} \omega_i^k = \int_0^{\eta_i} \omega_i(x)\,dx = J_i$ (the sum is indeed finite since $\omega_i^k = 0$ for $k \geq N_i$ sufficiently large). Moreover, we set $r_j(t) := \sum_{i=1}^{M} \rho_{i,j}(t)$ and define the convolution term in the form $R_i(t,x) := (r * \omega_i)(t,x)$. Integrating (3.1.1) over I_j we obtain

$$\frac{d}{dt}\rho_{i,j}(t) = -\frac{1}{\Delta x}\left(f_i(t, x_{j+1/2}) - f_i(t, x_{j-1/2})\right), \quad i = 1, \dots, M, \quad \forall j \in \mathbb{Z},$$

where $f_i(t, x_{j+1/2}) := \rho_i(t, x_{j+\frac{1}{2}}) v_i(R_i(t, x_{j+\frac{1}{2}}))$. This equation is approximated by the semi-discrete conservative scheme

$$\frac{d}{dt}\rho_{i,j}(t) = -\frac{1}{\Delta x}\left(f_{i,j+\frac{1}{2}} - f_{i,j-\frac{1}{2}}\right), \quad i = 1, \dots, M, \quad \forall j \in \mathbb{Z}, \tag{4.4.2}$$

where $f_{i,j+\frac{1}{2}}$ is a consistent approximation of flux $\rho_i v_i(R_i)$ at interface $x_{j+1/2}$. Here, we consider the multi-class version of the Godunov scheme [22]

$$f_{i,j+\frac{1}{2}} := f(\rho^l_{i,j+\frac{1}{2}}, \rho^r_{i,j+\frac{1}{2}}) = \rho^l_{i,j+\frac{1}{2}} v_i(R^r_{i,j+1/2}), \tag{4.4.3}$$

where $\rho^l_{i,j+\frac{1}{2}}$ and $\rho^r_{i,j+\frac{1}{2}}$ are some left and right high-order WENO reconstructions of $\rho_i(t, x_{j+\frac{1}{2}})$ obtained from the cell averages $\{\rho_{i,j}(t)\}_{j\in\mathbb{Z}}$. In this work, we consider the classical WENO scheme proposed in [70, 71]. $R^r_{i,j+1/2}$ is the right approximation of $R_i(t,x)$ at the interface $x_{j+1/2}$. Since R_i is defined by a convolution, we naturally set $R^r_{i,j+1/2} = R_i(t, x_{j+1/2}) := R_{i,j+1/2}(t)$.

In order to compute the integral $R_{i,j+1/2}$, we use the technique proposed in [19], i.e., we consider a reconstruction of $\rho_i(x,t)$ on I_j by taking advantage of the high-order WENO reconstructions $\rho^r_{i,j-\frac{1}{2}}$ and $\rho^l_{i,j+\frac{1}{2}}$ at the boundaries of I_j, as well as the approximation of the

cell average $\rho_{i,j}^n$. We consider a quadratic polynomial $p_{i,j}(x)$ defined on I_j such that

$$p_{i,j}(x_{j-\frac{1}{2}}) = \rho_{i,j-\frac{1}{2}}^r, \quad p_{i,j}(x_{j+\frac{1}{2}}) = \rho_{i,j+\frac{1}{2}}^l, \quad \frac{1}{\Delta x}\int_{I_j} p_{i,j}(x)dx = \rho_{i,j}^n.$$

In particular, we take

$$p_{i,j}(x) := a_{i,j,0}v^{(0)}(\xi_j(x)) + a_{i,j,1}v^{(1)}\left(\xi_j(x)\right) + a_{i,j,2}v^{(2)}\left(\xi_j(x)\right), \qquad x \in I_j, \tag{4.4.4}$$

with

$$v^{(0)}(y) = 1, \qquad v^{(1)}(y) = y, \qquad v^{(2)}(y) = \frac{1}{2}\left(3y^2 - 1\right), \qquad \xi_j(x) = \frac{x - x_j}{\Delta x/2}.$$

Coefficients in (4.4.4) can be easily computed as

$$a_{i,j,0} = \rho_{i,j}^n, \qquad a_{i,j,1} = \frac{1}{2}\left(\rho_{i,j+\frac{1}{2}}^l - \rho_{i,j-\frac{1}{2}}^r\right), \qquad a_{i,j,2} = \frac{1}{2}\left(\rho_{i,j+\frac{1}{2}}^l + \rho_{i,j-\frac{1}{2}}^r\right) - \rho_{i,j}^n.$$

Now, summing for $i = 1, \ldots, M$, we have

$$P_j(x) := \sum_{i=1}^{M} p_{i,j}(x) = \hat{a}_{j,0}v^{(0)}(\xi_j(x)) + \hat{a}_{j,1}v^{(1)}\left(\xi_j(x)\right) + \hat{a}_{j,2}v^{(2)}\left(\xi_j(x)\right), \qquad x \in I_j,$$

with

$$\hat{a}_{j,0} := \sum_{i=1}^{M} a_{i,j,0} = r_j, \qquad \hat{a}_{j,1} := \sum_{i=1}^{M} a_{i,j,1}, \qquad \hat{a}_{j,2} := \sum_{i=1}^{M} a_{i,j,2}.$$

With this polynomial $P_j(x)$, we can compute $R_{i,j+\frac{1}{2}}$ as

$$\begin{aligned}
R_{i,j+\frac{1}{2}} &= \sum_{k=1}^{M}\int_{I_{j+k}} P_{j+k}(y)\omega_i(y - x_{j+\frac{1}{2}})dy \\
&= \sum_{k=1}^{N}\int_{I_{j+k}} \omega_i(y - x_{j+\frac{1}{2}})\sum_{l=0}^{2}\hat{a}_{j+k,l}v^{(l)}(\zeta_{j+k}(y))dy \\
&= \sum_{k=1}^{M}\sum_{l=0}^{2}\hat{a}_{j+k,l}\int_{I_{j+k}} \omega_i(y - x_{j+\frac{1}{2}})v^{(l)}(\zeta_{j+k}(y))dy \\
&= \sum_{k=1}^{M}\sum_{l=0}^{2}\hat{a}_{j+k,l}\underbrace{\frac{\Delta x}{2}\int_{-1}^{1}\omega_i\left(\frac{\Delta x}{2}y + (k - \frac{1}{2})\Delta x\right)v^{(l)}(y)dy}_{} = \sum_{k=1}^{M}\sum_{l=0}^{2}\hat{a}_{j+k,l}\Gamma_{i,k,l},
\end{aligned} \tag{4.4.5}$$

where the coefficients $\Gamma_{i,k,l}$ are computed exactly or using a high-order quadrature approximation.

The utilization of the quadratic polynomial on each cell to evaluate the convolution term suggests the following algorithm to approach the solution of non-local system (3.1.1):

Algorithm: FV-WENO scheme for non-local multi-class traffic models

Given $\rho_{i,j}^n$ for $j \in \mathbb{Z}$, $i = 1, \dots, M$, approximation of the cell averages of $\rho_i(x,t)$ at t^n.

1. Compute $\rho^l_{i,j+\frac{1}{2}}$ and $\rho^r_{i,j+\frac{1}{2}}$, the left and right high-order WENO approximations for $j \in \mathbb{Z}$ and $i = 1, \dots, M$;
2. Calculate $R_{i,j+\frac{1}{2}}$ for $j \in \mathbb{Z}$ and $i = 1, \dots, M$;
3. Calculate the Godunov numerical flux (4.4.3) for $j \in \mathbb{Z}$ and $i = 1, \dots, M$;
4. Use a high-order accurate Runge-Kutta method to solve the semi-discrete system (4.4.2), with the CFL condition
$$\frac{\Delta t}{\Delta x} v_M^{\max} \|\psi\|_\infty \leq \frac{1}{2}. \tag{4.4.6}$$

In this chapter, we use the WENO method of third (WENO3), fifth (WENO5) and seventh (WENO7) accuracy order proposed by [70, 71]. For the temporal discretization, in order to match the order of spatial accuracy, fifth or seventh explicit Runge-Kutta schemes are used [14].

4.5 Numerical tests

In the following numerical tests, we solve (3.1.1) numerically in the intervals $x \in [-1, 1]$ and $t \in [0, 2]$. We propose two tests in order to illustrate the dynamics of the model (3.1.1) for autonomous and human-driven vehicles, using FV-WENO5 scheme with $1/\Delta x = 400$. For each integration, we set Δt to satisfy the CFL condition (4.4.6).

To test the accuracy order of the proposed method, since we cannot compute the exact solution explicitly, we use a reference solution $\overline{\rho}^{ref}$ obtained using FV-WENO7 on a refined mesh ($1/\Delta x = 6400$). The $\mathbf{L^1}$-error for the cell average is given by

$$L^1(\Delta x) = \sum_{i=1}^{M} \left(\frac{1}{N} \sum_{j=1}^{N} |\overline{\rho}_{i,j} - \overline{\rho}^{ref}_{i,j}| \right),$$

where $\overline{\rho}_{i,j}$ and $\overline{\rho}^{ref}_{i,j}$ are the cell averages of the numerical approximation and the reference solution respectively. The Experimental Order of Accuracy (E.O.A.) is naturally defined by

$$\gamma(\Delta x) = \log_2 \left(L^1(\Delta x)/L^1(\Delta x/2) \right).$$

4.5.1 Test 1, circular road

The aim of this test is to study the possible impact of the presence of Connected Autonomous Vehicles (CAVs) on road traffic performances, as proposed in [22, Section 4.2]. Let us consider a circular road modeled by the space interval $[-1, 1]$ with periodic boundary conditions at $x = \pm 1$. The interaction radius of CAVs is much grater than the one of human-driven cars. Moreover, we can assign a constant convolution kernel to CAVs, since we assume that the information they get about surrounding traffic is transmitted through wireless connections

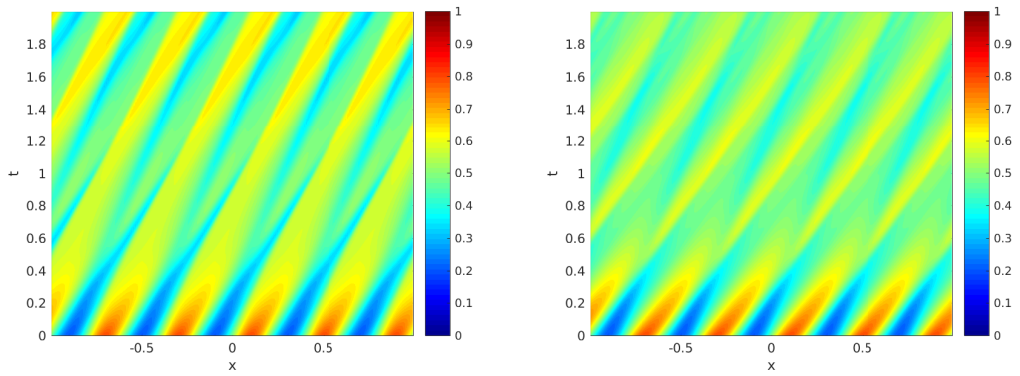

(a) $\alpha = 0.5$, $\beta = 0.3$, $\gamma = 0.2$, (b) $\alpha = 0.5$, $\beta = 0.5$, $\gamma = 0$.

Figure 4.9: $(t, x)-$plots of the total density $r(t, x) = \rho_1(t, x) + \rho_2(t, x) + \rho_3(t, x)$ computed with the FV-WENO5 scheme, corresponding to different penetration rates of autonomous and non-autonomous vehicles: (a) mixed autonomous / human-driven traffic, (b) fully autonomous traffic.

and its degree of accuracy does not depend on distance. We consider the following initial data and parameters

$$\rho_1(0, x) = \alpha p(x), \qquad \omega_1(x) = \frac{1}{\eta_1}, \qquad \eta_1 = 0.3, \qquad v_1^{\max} = 0.8, \tag{4.5.1}$$

$$\rho_2(0, x) = \beta\, p(x), \qquad \omega_2(x) = \frac{1}{\eta_2}, \qquad \eta_2 = 0.3, \qquad v_2^{\max} = 1.2, \tag{4.5.2}$$

$$\rho_3(0, x) = \gamma\, p(x), \qquad \omega_3(x) = \frac{2}{\eta_3}\left(1 - \frac{x}{\eta_3}\right), \qquad \eta_3 = 0.05, \qquad v_3^{\max} = 1.2, \tag{4.5.3}$$

where $p(x) = 0.5 + 0.3\sin(5\pi x)$ is the total initial density, $\alpha, \beta, \gamma \geq 0$ and $\alpha + \beta + \gamma = 1$. Above, ρ_1 represents the density of autonomous trucks, ρ_2 is the density of autonomous cars and ρ_3 is the density of human-driven cars. In Figure 4.9a we consider the penetration rates

$$\alpha = 0.5, \quad \beta = 0.3, \quad \gamma = 0.2,$$

and we can compare the total density $r = \rho_1 + \rho_2 + \rho_3$ with that one in Figure 4.9b where we have no human-driven cars:

$$\alpha = 0.5, \quad \beta = 0.5, \quad \gamma = 0.$$

We observe that oscillations are reduced if only autonomous vehicles are present.

Finally, we compute the E.O.A. for the FV-WENO schemes. We consider parameters $\alpha = 0.5$, $\beta = 0.3$, $\gamma = 0.2$, and compute the $\mathbf{L^1}$-error at $T = 0.2$ in Table 4.4. As expected, we obtain the correct order.

4.5.2 Test 2, stretch of straight road

In this test case, we consider a stretch of road populated by cars and trucks as in the example proposed in [22, Section 4.1]. The space domain is given by the interval $[-1, 1]$ and we impose

	FV-WENO3		FV-WENO5		FV-WENO7	
$1/\Delta x$	L^1-err	$\gamma(\Delta x)$	L^1-err	$\gamma(\Delta x)$	L^1-err	$\gamma(\Delta x)$
100	1.51e-03	–	1.09e-04	–	5.64e-05	–
200	1.38e-04	3.44	9.44e-06	3.53	1.54e-06	5.19
400	1.20e-05	3.53	4.01e-07	4.56	1.58e-08	6.61
800	1.27e-06	3.24	1.26e-08	4.99	1.68e-10	6.55
1600	1.05e-07	3.01	3.60e-10	5.12	4.71e-12	5.15

Table 4.5: E.O.A. Test 1, initial condition (4.5.1)-(4.5.3), with $\alpha = 0.5$, $\beta = 0.3$, $\gamma = 0.2$ and final time $T = 0.2$. The reference solution is computed with FV-WENO7 scheme for $1/\Delta x = 6400$.

absorbing conditions at the boundaries. The dynamics is described by the equation (3.1.1) with $M = 3$, and the following initial conditions and parameter values

$$\rho_1(0,x) = 0.5\chi_{[-0.6,-0.1]}(x), \quad \omega_1(x) = \frac{2}{\eta_1}\left(1 - \frac{x}{\eta_1}\right), \qquad \eta_1 = 0.1, \qquad v_1^{\max} = 0.8, \quad (4.5.4)$$

$$\rho_2(0,x) = \alpha_1\chi_{[-0.9,-0.6]}(x), \quad \omega_2(x) = \frac{1}{\eta_2}, \qquad \eta_2 = 0.5, \qquad v_2^{\max} = 1.3. \quad (4.5.5)$$

$$\rho_3(0,x) = \beta_1\chi_{[-0.9,-0.6]}(x), \quad \omega_3(x) = \frac{2}{\eta_3}\left(1 - \frac{x}{\eta_3}\right), \qquad \eta_3 = 0.05, \qquad v_2^{\max} = 1.3. \quad (4.5.6)$$

In this setting, $\rho_1(t,x)$ describes the density of human-driven trucks, $\rho_2(x,t)$ the density of autonomous cars and $\rho_3(x,t)$ is density of human driven cars. We have a red traffic light located at $x = -0.1$, which turns green at the initial time $t = 0$.

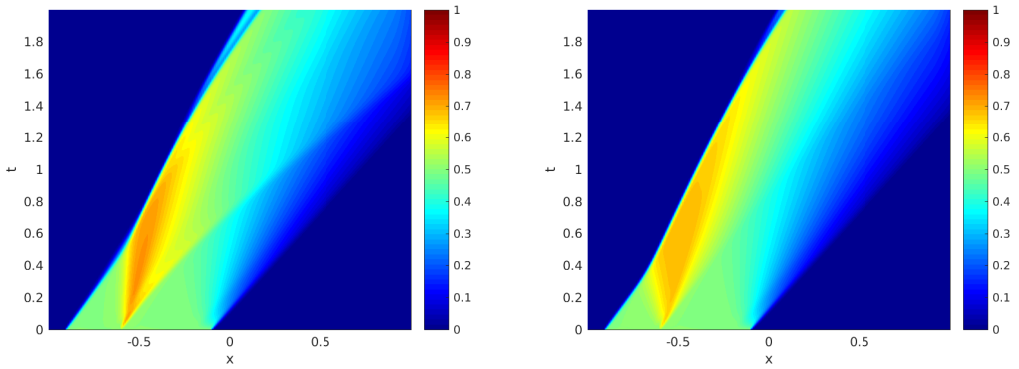

(a) $\alpha_1 = 0.25$, $\beta_1 = 0.25$, (b) $\alpha_1 = 0$, $\beta_1 = 0.5$.

Figure 4.10: $(t,x)-$plots of the total density $r(t,x) = \rho_1(t,x) + \rho_2(t,x) + \rho_3(t,x)$ computed with FV-WENO5 scheme, corresponding to different penetration rates of cars and trucks.

In Figure 4.10a we consider the rates

$$\alpha_1 = 0.25, \quad \beta_1 = 0.25,$$

and we can compare the space-time evolution of the total density $r = \rho_1 + \rho_2 + \rho_3$ with the one in Figure 4.10b, where

$$\alpha_1 = 0, \quad \beta_1 = 0.5.$$

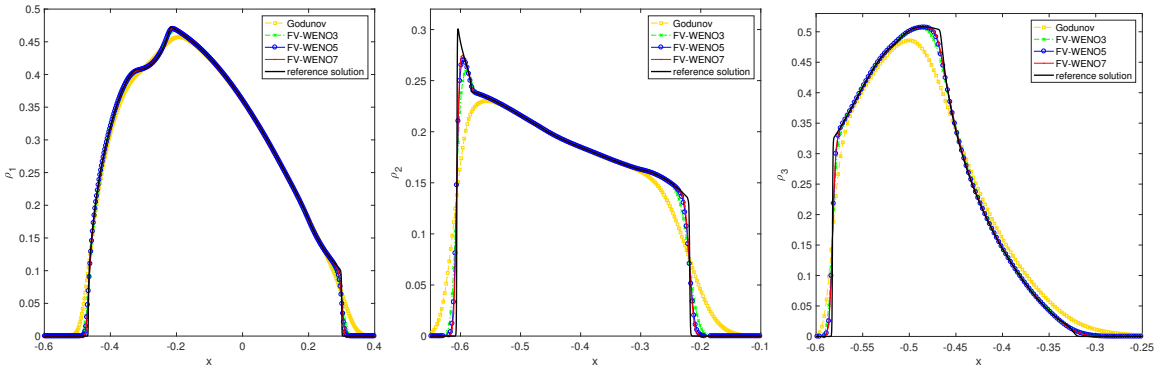

(a) (b) (c)

Figure 4.11: Test 2(a). (a) Profile of ρ_1; (b) profile of ρ_2, (c) profile of ρ_3 computed with different numerical schemes at time=0.5 and $1/\Delta x = 400$. The reference solution is computed with $1/\Delta x = 3200$.

In this case, the presence of autonomous cars in a heterogeneous traffic of human-driven vehicles induces higher vehicle densities during the overtaking phase, but for shorter time. In Figure 4.11 we display the density profiles of ρ_1, ρ_2 and ρ_3 computed with different FV-WENO schemes at time $t = 0.5$ in the same setting of Test 2(a). We can appreciate the efficiency of FV-WENO schemes in presence of discontinuities in comparison with the finite volume Godunov type scheme.

Chapter 5

A non-local traffic flow model for 1-to-1 junctions

In this chapter, we propose the study detailed in [20].
In this non-local scalar model, the flux function may involve different velocity functions on different parts of the road. The model focuses on a non-local mean downstream velocity and can therefore describe the behavior of drivers travelling on a road changing maximal velocity and capacity at a given point, without violating the maximal density constraint on each road segment. In Section 5.1, we present our model and the main result of this work. In Section 5.2, we prove the Lipschitz continuous dependence of weak entropy solutions with respect to the initial data, which implies their uniqueness. In Section 5.3, we introduce an adapted upwind type scheme and derive important properties: the maximum principle, uniform total variation (BV) estimates and a discrete entropy inequality. Afterwards, we prove the convergence of the scheme and the main theorem in Section 5.4. In the last Section 5.3, we show numerical simulations fixing the support of the kernel function that appears in the non-local flux and we present some results regarding the limit model as the support tends to zero.

5.1 Modeling

Based on the model presented in [46] we consider the following conservation law

$$\partial_t \rho(t,x) + \partial_x f(t,x,\rho) = 0, \quad x \in \mathbb{R},\, t > 0, \tag{5.1.1}$$

where

$$f(t,x,\rho) := \rho(t,x) V_1(t,x) + g(\rho(t,x)) V_2(t,x), \tag{5.1.2}$$

with

$$g(\rho) := \min\{\rho, \rho_{\max}^2\}, \tag{5.1.3}$$

$$V_1(t,x) := \int_{\min\{x,0\}}^{\min\{x+\eta,0\}} v_1(\rho(t,y))\omega_\eta(y-x)dy, \tag{5.1.4}$$

$$V_2(t,x) := \int_{\max\{x,0\}}^{\max\{x+\eta,0\}} v_2(\rho(t,y))\omega_\eta(y-x)dy, \tag{5.1.5}$$

for any $\eta > 0$. We couple the equation (5.1.1) with the initial datum

$$\begin{aligned} &\rho(0,x) = \rho_0(x) \in \mathrm{BV}(\mathbb{R}), \\ &\text{s.t. } \rho_0(x) \in [0, \rho_{\max}^1] \text{ for } x < 0 \text{ and } \rho_0(x) \in [0, \rho_{\max}^2] \text{ for } x > 0. \end{aligned} \tag{5.1.6}$$

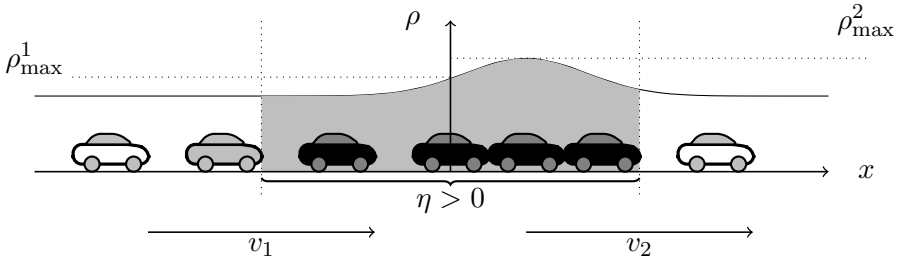

Figure 5.1: Illustration of the non-local traffic flow model (5.1.1) and (5.1.6) for different parameters on each road segment

The model assumes that drivers adapt their speed based on a weighted mean of downstream velocities. In the considered setting, changes in road characteristics at $x = 0$ may translate in different velocity functions, v_1 and v_2, and in different road capacities, $\rho^1_{\max}$ and $\rho^2_{\max}$, for $x < 0$ and $x > 0$ respectively. In (5.1.2), the flux also accounts for the maximum capacity of the second road segment. An illustration of the model can be seen in Figure 5.1.

The special structure of the flux function (5.1.2) does not fit into the framework proposed in e.g. [21, 46, 55]. Only for $v_1 \equiv v_2$ and therefore $\rho^1_{\max} = \rho^2_{\max}$ the model coincides with the one presented in [46]. Therefore, we have to investigate its well-posedness in the general case.

We impose the following reasonable hypotheses on $v_i,\ i \in \{1, 2\}$ and ω_η:

$$\begin{aligned} v_i \in C^2([0, \rho^i_{\max}]; \mathbb{R}^+) &: v_i' \leq 0,\ v_i(\rho^i_{\max}) = 0, \\ \omega_\eta \in C^1([0, \eta]; \mathbb{R}^+) &: \omega_\eta' \leq 0,\ \int_0^\eta \omega_\eta(x)dx = 1\ \forall \eta > 0, \end{aligned} \tag{5.1.7}$$

where η represents the look-ahead distance of the drivers.

Since the flux function (5.1.2) is continuous in x, entropy weak solutions of (5.1.1), (5.1.6) are intended in the following way:

Definition 4 (Entropy weak solution (see [59]))**.** *A measurable function*

$$\rho : \Pi_T := [0, T[\times \mathbb{R} \to [0, \max\{\rho^1_{\max}, \rho^2_{\max}\}]$$

is an entropy weak solution of the initial value problem (5.1.1)–(5.1.6) *if for any test function* $\varphi \in C^1_c(\Pi_T; \mathbb{R}^+)$ *and for any constant* $c \in \mathbb{R}$,

$$\begin{aligned} \iint_{\Pi_T} \left(|\rho - c|\varphi_t + \operatorname{sgn}(\rho - c)(f(t, x, \rho) - f(t, x, c))\varphi_x - \operatorname{sgn}(\rho - c) f(t, x, c)_x \varphi \right) dxdt \\ + \int_{-\infty}^{\infty} |\rho_0(x) - c|\varphi(0, x)\, dx \geq 0. \end{aligned} \tag{5.1.8}$$

The main result of this chapter is the following theorem:

Theorem 14. *Let* $\rho_0 \in BV(\mathbb{R}; [0, \max\{\rho^1_{\max}, \rho^2_{\max}\}])$ *such that* $\rho_0(x) \leq \rho^1_{\max}$ *for* $x < 0$ *and* $\rho_0(x) \leq \rho^2_{\max}$ *for* $x \geq 0$*, and hypotheses* (5.1.7) *hold. Then the Cauchy problem*

$$\begin{cases} \partial_t \rho(t, x) + \partial_x f(t, x, \rho) = 0, & x \in \mathbb{R},\ t > 0, \\ \rho(0, x) = \rho_0(x), & x \in \mathbb{R}, \end{cases}$$

admits a unique entropy weak solution in the sense of Definition 4 and

$$\begin{aligned} 0 \le \rho(t,x) \le \rho^1_{\max} \quad & \text{for a.e. } x<0,\ t>0,\\ 0 \le \rho(t,x) \le \rho^2_{\max} \quad & \text{for a.e. } x\ge 0,\ t>0. \end{aligned}$$

Theorem 14 is proved at the end of Section 5.4.

5.2 Uniqueness

Let us start to prove the Lipschitz continuous dependence of weak entropy solutions with respect to the initial data, which ensures the uniqueness of entropy solutions of the model (5.1.1)–(5.1.6). We follow [11, 21, 46], using Kružkov's doubling of variables technique [59].

Theorem 15. *Under hypotheses (5.1.7), let ρ and $\tilde\rho$ be two entropy solutions of (5.1.1) with initial datum ρ_0 and $\tilde\rho_0$, respectively. Then, for any $T>0$, there holds*

$$\left\|\rho(t,\cdot)-\tilde\rho(t,\cdot)\right\|_{L^1} \le \exp(KT)\|\rho_0-\tilde\rho_0\|_{L^1} \quad \forall t\in[0,T], \tag{5.2.1}$$

with K given by (5.2.7).

Proof. The functions ρ and $\tilde\rho$ are weak entropy solutions of

$$\begin{aligned} &\partial_t\rho(t,x)+\partial_x\left(\rho(t,x)V_1(t,x)+g(\rho)V_2(t,x)\right)=0, \quad \rho(0,x)=\rho_0(x),\\ &\partial_t\tilde\rho(t,x)+\partial_x\left(\tilde\rho(t,x)\tilde V_1(t,x)+g(\tilde\rho)\tilde V_2(t,x)\right)=0, \quad \tilde\rho(0,x)=\tilde\rho_0(x), \end{aligned}$$

respectively. V_i, $\tilde V_i$ for $i=1,2$ are defined as in (5.1.4) and (5.1.5), where the convolution is computed over the velocity of ρ and $\tilde\rho$, respectively. They are bounded measurable functions and Lipschitz continuous w.r.t. x since ρ, $\tilde\rho\in\left(L^1\cap L^\infty\cap \mathrm{BV}\right)(\mathbb{R}^+\times\mathbb{R};\mathbb{R})$.
Using the classical doubling of variables technique, see [52, 59], we get the following inequality:

$$\begin{aligned} \left\|\rho(t,\cdot)-\tilde\rho(t,\cdot)\right\|_{L^1} \le & \|\rho_0-\tilde\rho_0\|_{L^1} + \int_0^T\int_{\mathbb{R}} \left|\partial_x\rho(t,x)\right|\left|V_1(t,x)-\tilde V_1(t,x)\right|dxdt\\ &+\int_0^T\int_{\mathbb{R}} \left|\partial_x\rho(t,x)\right|\left|V_2(t,x)-\tilde V_2(t,x)\right|dxdt\\ &+\int_0^T\int_{\mathbb{R}} |\rho|\left|\partial_x V_1-\partial_x\tilde V_1\right|dxdt+\int_0^T\int_{\mathbb{R}} \left|g(\rho)\right|\left|\partial_x V_2-\partial_x\tilde V_2\right|dxdt, \end{aligned} \tag{5.2.2}$$

where $\partial_x\rho$ must be understood in the sense of measures. Applying the mean value theorem and using the properties of the kernel function, we deduce

$$\left|V_i(t,x)-\tilde V_i(t,x)\right| \le \omega_\eta(0)\left\|v_i'\right\|_\infty\left\|\rho(t,\cdot)-\tilde\rho(t,\cdot)\right\|_{L^1}, \quad \text{for } i=1,2. \tag{5.2.3}$$

Using the Leibniz integral rule and again the mean value theorem, we can also obtain for a.e. $x \in \mathbb{R}$

$$\begin{aligned}\left|\partial_x V_1(t,x) - \partial_x \tilde{V}_1(t,x)\right| = &\begin{cases} 0, & \text{if } x > 0, \\ \Big|\int_x^0 (v_1(\rho(t,y)) - v_1(\tilde{\rho}(t,y)))\omega_\eta'(y-x)dy \\ + \left(v_1(\tilde{\rho}(t,x)) - v_1(\rho(t,x))\right)\omega_\eta(0)\Big|, & \text{if } -\eta < x < 0, \\ \Big|\int_x^{x+\eta} (v_1(\rho(t,y)) - v_1(\tilde{\rho}(t,y)))\omega_\eta'(y-x)dy \\ + \left(v_1(\tilde{\rho}(t,x+\eta)) - v_1(\rho(t,x+\eta))\right)\omega_\eta(\eta) \\ + \left(v_1(\tilde{\rho}(t,x)) - v_1(\rho(t,x))\right)\omega_\eta(0)\Big|, & \text{if } x < -\eta \end{cases} \\ \leq &\left\|\omega_\eta'\right\|_\infty \|v_1'\|_\infty \|\rho(t,\cdot) - \tilde{\rho}(t,\cdot)\|_{L^1} \\ &+ \omega_\eta(0)\|v_1'\|_\infty \left(|\rho - \tilde{\rho}|(t,x+\eta) + |\rho - \tilde{\rho}|(t,x)\right). \end{aligned} \tag{5.2.4}$$

Similarly, we obtain

$$\left|\partial_x V_2(t,x) - \partial_x \tilde{V}_2(t,x)\right| \leq \left\|\omega_\eta'\right\|_\infty \|v_2'\|_\infty \|\rho(t,\cdot) - \tilde{\rho}(t,\cdot)\|_{L^1} \tag{5.2.5}$$

$$+ \omega_\eta(0)\|v_2'\|_\infty \left(|\rho - \tilde{\rho}|(t,x+\eta) + |\rho - \tilde{\rho}|(t,x)\right). \tag{5.2.6}$$

Plugging (5.2.3), (5.2.4), (5.2.5) into (5.2.2), we obtain

$$\begin{aligned}&\|\rho(t,\cdot) - \tilde{\rho}(t,\cdot)\|_{L^1} \leq \|\rho_0 - \tilde{\rho}_0\|_{L^1} \\ &+ \max_{i=1,2}\left\{\|v_i'\|_\infty\right\} \int_0^T \|\rho(t,\cdot) - \tilde{\rho}(t,\cdot)\|_{L^1} dt \left[2\omega_\eta(0) \sup_{t\in[0,T]} \|\rho(t,\cdot)\|_{\mathrm{BV}(\mathbb{R})}\right. \\ &\qquad \left. + \left\|\omega_\eta'\right\|_\infty \left(\sup_{t\in[0,T]} \|\rho(t,\cdot)\|_{L^1} + \sup_{t\in[0,T]} \|g(\rho(t,\cdot))\|_{L^1}\right)\right] \\ &+ \max_{i=1,2}\left\{\|v_i'\|_\infty\right\} \omega_\eta(0) \left(\sup_{t\in[0,T]} \|\rho(t,\cdot)\|_\infty + \sup_{t\in[0,T]} \|g(\rho(t,\cdot))\|_\infty\right) \\ &\qquad \int_0^T \int_{\mathbb{R}} \left(|\rho - \tilde{\rho}|(t,x+\eta) + |\rho - \tilde{\rho}|(t,x)\right) dxdt \\ \leq &\|\rho_0 - \tilde{\rho}_0\|_{L^1} + K \int_0^T \|\rho(t,\cdot) - \tilde{\rho}(t,\cdot)\|_{L^1} dt, \end{aligned}$$

with

$$\begin{aligned}K := \max_{i=1,2}\left\{\|v_i'\|_\infty\right\} &\left[2\omega_\eta(0) \sup_{t\in[0,T]} \|\rho(t,\cdot)\|_{\mathrm{BV}(\mathbb{R})}\right. \\ &+ \left\|\omega_\eta'\right\|_\infty \left(\sup_{t\in[0,T]} \|\rho(t,\cdot)\|_{L^1} + \sup_{t\in[0,T]} \|g(\rho(t,\cdot))\|_{L^1}\right) \\ &\left. + 2\omega_\eta(0) \left(\sup_{t\in[0,T]} \|\rho(t,\cdot)\|_\infty + \sup_{t\in[0,T]} \|g(\rho(t,\cdot))\|_\infty\right)\right]. \end{aligned} \tag{5.2.7}$$

By Gronwall's lemma we get the statement and for $\rho_0 = \tilde{\rho}_0$ the uniqueness of entropy solutions. □

Remark 7. *Note that we cannot directly apply previous results in the literature [23, 34, 52] to the present model, because it does not fit precisely the assumptions therein. Moreover, direct computations allow to recover sharper estimates on the coefficients.*

5.3 Numerical scheme

In order to prove the well-posedness of model (5.1.1)–(5.1.6), we prove the existence of solutions via a numerical scheme which is based on the scheme from [46]. Even though this scheme has been introduced in [46] as a Godunov type scheme, it reduces to an upwind type scheme.
For $j \in \mathbb{Z}$ and $n \in \mathbb{N}$, let $x_{j-1/2} = j\Delta x$ be the cell interfaces, $x_j = (j+1/2)\Delta x$ the cells centers, corresponding to a space step Δx such that $\eta = N_\eta \Delta x$ for some $N_\eta \in \mathbb{N}$, and let $t^n = n\Delta t$ be the time mesh. In particular, $x = x_{-1/2} = 0$ is a cell interface. We aim at constructing a finite volume approximate solution $\rho^{\Delta x}$ such that $\rho^{\Delta x}(t,x) = \rho_j^n$ for $(t,x) \in [t^n, t^{n+1}[\times [x_{j-1/2}, x_{j+1/2}[$. To this end, we approximate the initial datum ρ_0 with the piecewise constant function

$$\rho_j^0 = \frac{1}{\Delta x} \int_{x_{j-1/2}}^{x_{j+1/2}} \rho_0(x)dx, \qquad j \in \mathbb{Z}.$$

Following [46], we consider the numerical flux function

$$F_{j+1/2}^n(\rho_j^n) := \rho_j^n V_j^{1,n} + g(\rho_j^n) V_j^{2,n} \tag{5.3.1}$$

with

$$V_j^{1,n} = \sum_{k=0}^{\min\{-j-2, N_\eta - 1\}} \gamma_k v_1(\rho_{j+k+1}^n), \qquad V_j^{2,n} = \sum_{k=\max\{-j-1,0\}}^{N_\eta - 1} \gamma_k v_2(\rho_{j+k+1}^n), \tag{5.3.2}$$

$$\gamma_k = \int_{k\Delta x}^{(k+1)\Delta x} \omega_\eta(x)dx, \qquad k = 0, \dots, N_\eta - 1, \tag{5.3.3}$$

where we set, with some abuse of notation $\sum_{k=a}^b = 0$ whenever $b < a$. In this way we can define the following finite volume numerical scheme

$$\rho_j^{n+1} = \rho_j^n - \lambda \left(F_{j+1/2}^n(\rho_j^n) - F_{j-1/2}^n(\rho_{j-1}^n) \right) \text{ with } \lambda := \frac{\Delta t}{\Delta x}. \tag{5.3.4}$$

Note that, due to the accurate calculation of the integral in (5.3.3) and the definition of the convoluted velocities in (5.3.2), there holds

$$0 \le V_j^{1,n} \le v_{\max}^1, \quad 0 \le V_j^{2,n} \le v_{\max}^2, \quad 0 \le V_j^{1,n} + V_j^{2,n} \le \max\{v_{\max}^1, v_{\max}^2\}, \ \forall\, j \in \mathbb{Z}, \ n \in \mathbb{N}.$$

We set

$$\|v\| := \max\{\|v_1\|_\infty, \|v_2\|_\infty\}, \quad \|v'\| := \max\{\|v_1'\|_\infty, \|v_2'\|_\infty\}, \quad \|\rho\| := \max\{\rho_{\max}^1, \rho_{\max}^2\}$$

and consider the following CFL condition:

$$\lambda \leq \frac{1}{\gamma_0 \|v'\| \|\rho\| + \|v\|}. \tag{5.3.5}$$

We will show that, under this CFL condition, the numerical scheme (5.3.1)–(5.3.4) satisfies a maximum principle, uniform BV estimates and a discrete entropy inequality. Equipped with these properties, we will show in Section 5.4 that the sequence of approximate solutions $\left\{\rho^{\Delta x}\right\}$ converges towards the entropy solution of (5.1.1)–(5.1.6). Note that, for $v_1 \equiv v_2$, the scheme (5.3.1)–(5.3.4) coincides with the scheme in [46].

In the following proofs, we will omit the dependence on n of the flux function and the velocity whenever possible, in order to simplify the notation.

5.3.1 Maximum principle

The solutions generated by the numerical scheme (5.3.4) stay always positive and they are bounded by the maximum road capacity of each road segment as stated by the following lemma.

Lemma 17. *Under hypothesis (5.1.6) and the CFL condition (5.3.5), the sequence generated by the numerical scheme (5.3.1)–(5.3.4) satisfies the following maximum principle:*

$$0 \leq \rho_j^n \leq \rho_{\max}^1 \quad \textit{for} \quad j \leq -1 \qquad \textit{and} \qquad 0 \leq \rho_j^n \leq \rho_{\max}^2 \quad \textit{for} \quad j \geq 0, \qquad \forall n \in \mathbb{N}.$$

Proof. We start by showing the positivity. We directly obtain

$$\rho_j^{n+1} = \rho_j^n - \lambda \left(F^n_{j+\frac{1}{2}}(\rho_j^n) - F^n_{j-\frac{1}{2}}(\rho_{j-1}^n) \right) \geq \rho_j^n - \lambda F^n_{j+\frac{1}{2}}(\rho_j^n) \geq \rho_j^n - \lambda \|v\| \rho_j^n \geq 0.$$

Here we used the CFL condition (5.3.5) and $g(\rho_j^n) \leq \rho_j^n$.
The rest of the proof follows closely the proof of [46, Theorem 3.1]. Therefore, we compute the differences of the velocities and obtain

$$V^{1,n}_{j-1} - V^{1,n}_j = \begin{cases} \sum_{k=1}^{N_\eta - 1} (\gamma_k - \gamma_{k-1}) v_1(\rho^n_{j+k}) - \gamma_{N_\eta - 1} v_1(\rho^n_{j+N_\eta}) + \gamma_0 v_1(\rho^n_j), & j \leq -N_\eta - 1, \\ \sum_{k=1}^{-j-1} (\gamma_k - \gamma_{k-1}) v_1(\rho^n_{j+k}) + \gamma_0 v_1(\rho^n_j), & -N_\eta \leq j \leq -2, \\ \gamma_0 v_1(\rho^n_{-1}), & j = -1, \\ 0, & j \geq 0, \end{cases} \tag{5.3.6}$$

and

$$V^{2,n}_{j-1} - V^{2,n}_j = \begin{cases} 0, & j \leq -N_\eta - 1, \\ -\gamma_{N_\eta - 1} v_2(\rho^n_0), & j = -N_\eta, \\ \sum_{k=-j}^{N_\eta - 1} (\gamma_k - \gamma_{k-1}) v_2(\rho^n_{j+k}) - \gamma_{N_\eta - 1} v_2(\rho^n_{j+N_\eta}), & -N_\eta + 1 \leq j \leq -1, \\ \sum_{k=1}^{N_\eta - 1} (\gamma_k - \gamma_{k-1}) v_2(\rho^n_{j+k}) - \gamma_{N_\eta - 1} v_2(\rho^n_{j+N_\eta}) + \gamma_0 v_2(\rho^n_j), & j \geq 0. \end{cases} \tag{5.3.7}$$

It is easy to see that the following estimates hold:

$$V_{j-1}^{1,n} - V_j^{1,n} \leq \begin{cases} \gamma_0 v_1(\rho_j^n) & j \leq -1, \\ 0, & j \geq 0, \end{cases}$$

$$V_{j-1}^{2,n} - V_j^{2,n} \leq \begin{cases} 0 & j \leq -1, \\ \gamma_0 v_2(\rho_j^n), & j \geq 0. \end{cases}$$

Using $v_1(\rho_{\max}^1) = v_2(\rho_{\max}^2) = 0$ and the mean value theorem we get

$$V_{j-1}^{1,n} - V_j^{1,n} \leq \begin{cases} \gamma_0 \|v'\|(\rho_{\max}^1 - \rho_j^n) & j \leq -1, \\ 0, & j \geq 0, \end{cases}$$

$$V_{j-1}^{2,n} - V_j^{2,n} \leq \begin{cases} 0 & j \leq -1, \\ \gamma_0 \|v'\|(\rho_{\max}^2 - \rho_j^n), & j \geq 0. \end{cases}$$

Now we consider the case $j \leq -1$ and multiply the first inequality by $\rho_{\max}^1$, subtract $V_j^{1,n}\rho_j^n$ and we get

$$V_{j-1}^{1,n}\rho_{\max}^1 - V_j^{1,n}\rho_j^n \leq \left(\gamma_0 \|v'\|\|\rho\| + V_j^{1,n}\right)(\rho_{\max}^1 - \rho_j^n).$$

Similarly, we get

$$V_{j-1}^{2,n} g(\rho_{\max}^1) - V_j^{2,n} g(\rho_j^n) \leq V_j^{2,n}\left(g(\rho_{\max}^1) - g(\rho_j^n)\right) \leq V_j^{2,n}(\rho_{\max}^1 - \rho_j^n).$$

Adding the last two inequalities we obtain,

$$V_{j-1}^{1,n}\rho_{\max}^1 - V_j^{1,n}\rho_j^n + V_{j-1}^{2,n} g(\rho_{\max}^1) - V_j^{2,n} g(\rho_j^n) \leq \left(\gamma_0 \|v'\|\|\rho\| + \|v\|\right)(\rho_{\max}^1 - \rho_j^n).$$

Due to the CFL condition (5.3.5), we have for $j \leq -1$

$$\rho_j^{n+1} \leq \rho_j^n + \lambda\left(V_{j-1}^{1,n}\rho_{\max}^1 - V_j^{1,n}\rho_j^n + V_{j-1}^{2,n} g(\rho_{\max}^1) - V_j^{2,n} g(\rho_j^n)\right) \leq \rho_{\max}^1.$$

For $j \geq 0$ the bound

$$V_{j-1}^{2,n}\rho_{\max}^2 - V_j^{2,n}\rho_j^n \leq \left(\gamma_0 \|v'\|\|\rho\| + \|v\|\right)(\rho_{\max}^2 - \rho_j^n)$$

follows analogously to above. Note that $V_j^{1,n} = 0$ for $j \geq -1$. Since $g(\rho_{j-1}^n) \leq \rho_{\max}^2$ holds even for $j = 0$ and $g(\rho_j^n) = \rho_j^n$ for $j \geq 0$, we obtain

$$\rho_j^{n+1} \leq \rho_j^n + \lambda\left(V_{j-1}^{2,n}\rho_{\max}^2 - V_j^{2,n}\rho_j^n\right) \leq \rho_{\max}^2.$$

This concludes the proof. □

Remark 8. *The role of the limiter g given by (5.1.3) in the flux function (5.1.2) is essential for the maximum principle above. Indeed, let us consider for example an approximate initial datum $\rho_j^0 = \rho_{\max}^1$ for $j \leq -1$, $\rho_0^0 = \rho_{\max}^2$ in the first cell on the right of $x = 0$ and $\rho_j^0 = 0$ for $j \geq 1$. The flux entering the cell $j = 0$ is given by $(1 - \gamma_0)v_{\max}^2\rho_{\max}^1$ and the flux leaving this cell is given by $v_{\max}^2\rho_{\max}^2$. Obviously, choosing $\rho_{\max}^1 > \rho_{\max}^2/(1 - \gamma_0)$ results in a violation of the maximum principle in the cell $j = 0$ (as long as $\eta > \Delta x$).*

5.3.2 BV estimate

In addition to the L^∞ bound, we also need a uniform estimate on the total variation of the sequence of approximate solutions. The crucial part here lies in the presence of the limiter g at $x = 0$.

Lemma 18. *Let $\rho^{\Delta x}$ be constructed by (5.3.1)–(5.3.4) and let the CFL condition (5.3.5) hold, then for every $T > 0$ the following discrete space BV estimate is satisfied:*

$$TV(\rho^{\Delta x}(T,\cdot)) \leq \exp\Big(Tw_\eta(0)\left(2\|v\| + \|v'\|\|\rho\|\right)\Big)\left(TV(\rho_0) + T2\omega_\eta(0)\|v\|\|\rho\|\right) =: K(T). \tag{5.3.8}$$

Proof. We set

$$\Delta_j^n := \rho_{j+1}^n - \rho_j^n.$$

In the following we consider a regularization of the function g defined in (5.1.3), namely

$$g_\varepsilon(\rho) = \frac{1}{2}\left(\rho + \rho_{\max}^2 - \sqrt{(\rho - \rho_{\max}^2)^2 + \varepsilon}\right), \qquad \varepsilon > 0. \tag{5.3.9}$$

The function g_ε is differentiable for every $\varepsilon > 0$ with $\|g_\varepsilon'\| \leq 1$ for all $\varepsilon > 0$. This will allow us to use the mean value theorem in the following computations. In particular, we will denote by ξ_j^n a value between ρ_j^n and ρ_{j+1}^n such that $g_\varepsilon'(\xi_j^n)\Delta_j^n = g_\varepsilon(\rho_{j+1}^n) - g_\varepsilon(\rho_j^n)$ holds. We obtain:

$$\begin{aligned}
\Delta_j^{n+1} =& \Delta_j^n - \lambda\left(F_{j+\frac{3}{2}}^n(\rho_{j+1}^n) - 2F_{j+\frac{1}{2}}^n(\rho_j^n) + F_{j-\frac{1}{2}}^n(\rho_{j-1}^n)\right)\\
=& \Delta_j^n - \lambda\Big(\left(V_{j+1}^{1,n} + g_\varepsilon'(\xi_j^n)V_{j+1}^{2,n}\right)\Delta_j^n - \left(V_{j-1}^{1,n} + g_\varepsilon'(\xi_{j-1}^n)V_{j-1}^{2,n}\right)\Delta_{j-1}^n\\
&+\rho_j^n\left(V_{j+1}^{1,n} - 2V_j^{1,n} + V_{j-1}^{1,n}\right) + g_\varepsilon(\rho_j^n)\left(V_{j+1}^{2,n} - 2V_j^{2,n} + V_{j-1}^{2,n}\right)\Big).
\end{aligned}$$

Let us now consider the differences of the velocities. With the differences already computed in (5.3.6) and (5.3.7) and the help of the mean value theorem, where ζ_j^n is a value between ρ_j^n and ρ_{j+1}^n for which $v_i'(\zeta_j^n)\Delta_j^n = v_i(\rho_{j+1}^n) - v_i(\rho_j^n)$ for $i \in \{1,2\}$ holds, we derive

$$V_{j+1}^{1,n} - 2V_j^{1,n} + V_{j-1}^{1,n} =$$
$$\begin{cases}
\sum_{k=1}^{N_\eta-1}(\gamma_{k-1}-\gamma_k)v_1'(\zeta_{j+k}^n)\Delta_{j+k}^n + \gamma_{N_\eta-1}v_1'(\zeta_{j+N_\eta}^n)\Delta_{j+N_\eta}^n - \gamma_0 v_1'(\zeta_j^n)\Delta_j^n, & j \leq -N_\eta - 2,\\
\sum_{k=1}^{N_\eta-1}(\gamma_{k-1}-\gamma_k)v_1'(\zeta_{j+k}^n)\Delta_{j+k}^n - \gamma_{N_\eta-1}v_1(\rho_{-1}^n) - \gamma_0 v_1'(\zeta_j^n)\Delta_j^n, & j = -N_\eta - 1,\\
\sum_{k=1}^{-j-2}(\gamma_{k-1}-\gamma_k)v_1'(\zeta_{j+k}^n)\Delta_{j+k}^n + (\gamma_{-j-1}-\gamma_{-j-2})v_1(\rho_{-1}^n) - \gamma_0 v_1'(\zeta_j^n)\Delta_j^n, & -N_\eta \leq j \leq -3,\\
(\gamma_1-\gamma_0)v_1(\rho_{-1}^n) - \gamma_0 v_1'(\zeta_j^n)\Delta_j^n, & j = -2,\\
\gamma_0 v_1(\rho_{-1}^n), & j = -1,\\
0, & j \geq 0,
\end{cases}$$

and

$$V_{j+1}^{2,n} - 2V_j^{2,n} + V_{j-1}^{2,n} =$$

$$\begin{cases} 0, & j \le -N_\eta - 2, \\ \gamma_{N_\eta-1} v_2(\rho_0^n), & j = -N_\eta - 1, \\ \gamma_{N_\eta-1} v_2'(\zeta_{j+N_\eta}^n)\Delta_{j+N_\eta}^n + (\gamma_{N_\eta-1} - \gamma_{N_\eta}) v_2(\rho_0^n), & j = -N_\eta, \\ \sum_{k=-j}^{N_\eta-1}(\gamma_{k-1} - \gamma_k) v_2'(\zeta_{j+k}^n)\Delta_{j+k}^n & \\ \qquad + \gamma_{N_\eta-1} v_2'(\zeta_{j+N_\eta}^n)\Delta_{j+N_\eta}^n + (\gamma_{-j-2} - \gamma_{-j-1}) v_2(\rho_0^n), & -N_\eta + 1 \le j \le -2, \\ \sum_{k=1}^{N_\eta-1}(\gamma_{k-1} - \gamma_k) v_2'(\zeta_{j+k}^n)\Delta_{j+k}^n & \\ \qquad + \gamma_{N_\eta-1} v_2'(\zeta_{j+N_\eta}^n)\Delta_{j+N_\eta}^n - \gamma_0 v_2(\rho_0^n), & j = -1, \\ \sum_{k=1}^{N_\eta-1}(\gamma_{k-1} - \gamma_k) v_2'(\zeta_{j+k}^n)\Delta_{j+k}^n & \\ \qquad + \gamma_{N_\eta-1} v_2'(\zeta_{j+N_\eta}^n)\Delta_{j+N_\eta}^n - \gamma_0 v_2'(\zeta_j^n)\Delta_j^n, & j \ge 0. \end{cases}$$

Putting everything together we have

$$\begin{aligned} \Delta_j^{n+1} = &\left(1 - \lambda\left(V_{j+1}^{1,n} + g_\varepsilon'(\xi_j^n) V_{j+1}^{2,n} - \gamma_0 a_j^n\right)\right)\Delta_j^n + \lambda\left(V_{j-1}^{1,n} + g_\varepsilon'(\xi_{j-1}^n) V_{j-1}^{2,n}\right)\Delta_{j-1}^n \\ &+ \lambda \sum_{k=1}^{N_\eta-1} (\gamma_{k-1} - \gamma_k) b_{j+k}^n \Delta_{j+k}^n + \lambda \gamma_{N_\eta-1} c_{j+N_\eta}^n \Delta_{j+N_\eta}^n \\ &+ \lambda d_j^n \left(\rho_j v_1(\rho_{-1}^n) - g_\varepsilon(\rho_j^n) v_2(\rho_0^n)\right), \end{aligned} \tag{5.3.10}$$

where

$$a_j^n = \begin{cases} v_1'(\zeta_j^n)\rho_j^n, & j \le -2, \\ 0, & j = -1, \\ v_2'(\zeta_j^n)\rho_j^n, & j \ge 0, \end{cases} \qquad b_{j+k}^n = \begin{cases} -v_1'(\zeta_{j+k}^n)\rho_j^n, & j+k \le -2, \\ 0, & j+k = -1, \\ -v_2'(\zeta_{j+k}^n) g_\varepsilon(\rho_j^n), & j+k \ge 0, \end{cases}$$

$$c_{j+N_\eta}^n = \begin{cases} -v_1'(\zeta_{j+N_\eta}^n)\rho_j^n, & j \le -N_\eta - 2, \\ 0, & j = -N_\eta - 1, \\ -v_2'(\zeta_{j+N_\eta}^n) g_\varepsilon(\rho_j^n), & j \ge -N_\eta, \end{cases} \qquad d_j^n = \begin{cases} 0, & j \le -N_\eta - 2, \\ \gamma_{N_\eta-1}, & j = -N_\eta - 1, \\ \gamma_{-j-2} - \gamma_{-j-1}, & -N_\eta \le j \le -2, \\ -\gamma_0, & j = -1, \\ 0, & j \ge 0. \end{cases}$$

Since the coefficients in (5.3.10) are positive due to the CFL condition (5.3.5), we take absolute values, sum over j and rearrange the indices, which gives us

$$\begin{aligned} \sum_j |\Delta_j^{n+1}| \le \sum_j \Bigg[&\left(1 - \lambda\left(V_{j+1}^{1,n} + g_\varepsilon'(\xi_j^n) V_{j+1}^{2,n} - \gamma_0 a_j^n\right)\right)|\Delta_j^n| \\ &+ \lambda\left(V_{j-1}^{1,n} + g_\varepsilon'(\xi_{j-1}^n) V_{j-1}^{2,n}\right)|\Delta_{j-1}^n| \\ &+ \lambda \sum_{k=1}^{N_\eta-1} (\gamma_{k-1} - \gamma_k) b_{j+k}^n |\Delta_{j+k}^n| + \lambda \gamma_{N_\eta-1} c_{j+N_\eta}^n |\Delta_{j+N_\eta}^n| \\ &+ \lambda |d_j^n| \left|\rho_j v_1(\rho_{-1}^n) - g_\varepsilon(\rho_j^n) v_2(\rho_0^n)\right| \Bigg] \end{aligned}$$

$$
\begin{aligned}
&= \sum_j \Bigg[1 - \lambda \left(V_{j+1}^{1,n} + g_\varepsilon'(\xi_j^n) V_{j+1}^{2,n} - V_j^{1,n} - g_\varepsilon'(\xi_j^n) V_j^{2,n} \right) \\
&\quad + \lambda \left(\gamma_0 a_j^n + \sum_{k=1}^{N_\eta - 1} (\gamma_{k-1} - \gamma_k) b_j^n + \gamma_{N_\eta - 1} c_j^n \right) \Bigg] |\Delta_j^n| \\
&\quad + \sum_j \lambda |d_j^n| \left| \rho_j v_1(\rho_{-1}^n) - g_\varepsilon(\rho_j^n) v_2(\rho_0^n) \right|.
\end{aligned}
$$

Now we use that $V_j^{i,n} - V_{j+1}^{i,n} \leq \gamma_0 \|v\|$ and $\|g_\varepsilon'\| \leq 1$ for the first term and for the second term we have $a_j^n \leq 0$ and $b_j^n, c_j^n \leq \|v'\| \|\rho\|$, which gives us

$$
\begin{aligned}
\sum_j |\Delta_j^{n+1}| &\leq \left(1 + \lambda \gamma_0 \left(2\|v\| + \|v'\| \|\rho\| \right) \right) \sum_j |\Delta_j^n| \\
&\quad + \sum_j \lambda |d_j^n| \left| \rho_j v_1(\rho_{-1}^n) - g_\varepsilon(\rho_j^n) v_2(\rho_0^n) \right|.
\end{aligned}
$$

Since $\sum_j |d_j^n| = 2\gamma_0$ holds, using also $\lambda \gamma_0 \leq \Delta t \omega_\eta(0)$ we finally obtain

$$
\sum_j |\Delta_j^{n+1}| \leq \left(1 + \Delta t \omega_\eta(0) \left(2\|v\| + \|v'\| \|\rho\| \right) \right) \sum_j |\Delta_j^n| + \Delta t 2 \omega_\eta(0) \|v\| (\|\rho\| + \frac{\sqrt{\varepsilon}}{2}).
$$

This estimate holds for any $\varepsilon > 0$ and for $\varepsilon \to 0$ we obtain the following estimate for the total variation

$$
\begin{aligned}
TV(\rho(T, \cdot)) &\leq \left(1 + \Delta t \omega_\eta(0) \left(2\|v\| + \|v'\| \|\rho\| \right) \right)^{T/\Delta t} \left(TV(\rho_0) + T 2 \omega_\eta(0) \|v\| \|\rho\| \right) \\
&\leq \exp \left(\omega_\eta(0) \left(2\|v\| + \|v'\| \|\rho\| \right) T \right) \left(TV(\rho_0) + T 2 \omega_\eta(0) \|v\| \|\rho\| \right).
\end{aligned}
$$

□

To finally apply Helly's Theorem we also need an estimate for the discrete total variation in space and time, which we are now able to provide.

Lemma 19. *Let $\rho^{\Delta x}$ be constructed by (5.3.1)–(5.3.4) and let the CFL condition (5.3.5) hold, then for every $T > 0$ the following discrete space and time total variation estimate is satisfied:*

$$
TV(\rho^{\Delta x}; \mathbb{R} \times [0, T]) \leq T K(T) (1 + \|v'\| \|\rho\| + \|v\|)
$$

with $K(T)$ defined as in (5.3.8).

Using the regularization of g given by (5.3.9), the proof is entirely analogous to the one of [46, Theorem 3.3].

5.3.3 Discrete Entropy Inequality

In the following, we use the notation $a \wedge b = \max\{a, b\}$, $a \vee b = \min\{a, b\}$ and follow [5, 21, 46].

Lemma 20. *Let $\rho^{\Delta x}$ be constructed by (5.3.1)–(5.3.4). If the CFL condition (5.3.5) holds, then for $c \in \mathbb{R}$ we have the following discrete entropy inequality*

$$\begin{aligned}\left|\rho_j^{n+1} - c\right| \le \left|\rho_j^n - c\right| &- \lambda\left(H_{j+1/2}^n(\rho_j^n) - H_{j-1/2}^n(\rho_{j-1}^n)\right) \\ &- \lambda \operatorname{sgn}(\rho_j^{n+1} - c)\left(F_{j+1/2}^n(c) - F_{j-1/2}^n(c)\right),\end{aligned} \tag{5.3.11}$$

where

$$H_{j+1/2}^n(u) = F_{j+1/2}^n(u \wedge c) - F_{j+1/2}^n(u \vee c).$$

Proof. Let

$$G_j^n(u, w) = w - \lambda(F_{j+1/2}^n(w) - F_{j-1/2}^n(u)).$$

Under the CFL condition (5.3.5) and using the regularization (5.3.9) of g, G_j is monotone in both its arguments, since we obtain

$$\frac{\partial G_j^n}{\partial w} = 1 - \lambda(V_{j+\frac{1}{2}}^{1,n} + g_\varepsilon'(w)V_{j+\frac{1}{2}}^{2,n}) \ge 0, \quad \frac{\partial G_j^n}{\partial u} = \lambda(V_{j-\frac{1}{2}}^{1,n} + g_\varepsilon'(u)V_{j-\frac{1}{2}}^{2,n}) \ge 0.$$

The monotonicity implies that

$$G_j^n(\rho_{j-1}^n \wedge c, \rho_j^n \wedge c) \ge G_j^n(\rho_{j-1}^n, \rho_j^n) \wedge G_j^n(c, c) \tag{5.3.12}$$

$$G_j^n(\rho_{j-1}^n \vee c, \rho_j^n \vee c) \le G_j^n(\rho_{j-1}^n, \rho_j^n) \vee G_j^n(c, c). \tag{5.3.13}$$

Subtracting (5.3.13) from (5.3.12), we obtain

$$\left|G_j^n(\rho_{j-1}^n, \rho_j^n) - G_j^n(c, c)\right| \le \left|\rho_j^n - c\right| - \lambda\left(H_{j+1/2}^n(\rho_j^n) - H_{j-1/2}^n(\rho_{j-1}^n)\right). \tag{5.3.14}$$

The left side of (5.3.14) is $\left|\rho_j^{n+1} - c + \lambda(F_{j+1/2}^n(c) - F_{j-1/2}(c))\right|$, and we get

$$\begin{aligned}&\left|\rho_j^{n+1} - c + \lambda(F_{j+1/2}^n(c) - F_{j-1/2}^n(c))\right| \\ &\qquad \ge \operatorname{sgn}(\rho_j^{n+1} - c)\left(\rho_j^{n+1} - c + \lambda(F_{j+1/2}^n(c) - F_{j-1/2}^n(c))\right) \\ &\qquad = \left|\rho_j^{n+1} - c\right| + \lambda \operatorname{sgn}(\rho_j^{n+1} - c)\left(F_{j+1/2}^n(c) - F_{j-1/2}^n(c)\right).\end{aligned} \tag{5.3.15}$$

The proof is completed by combining (5.3.14) and (5.3.15). □

5.4 Convergence

Lemma 21. *Let $\rho = \rho(t, x) \in L^1 \cap L^\infty \cap BV(\mathbb{R}^+ \times \mathbb{R}; [0, \max\{\rho_{\max}^1, \rho_{\max}^2\})$ be the L_{loc}^1-limit of approximations $\rho^{\Delta x}$ generated by the upwind scheme (5.3.4) and let $c \in \mathbb{R}$, $\varphi \in C_c^1(\Pi_T)$. Then ρ satisfies the entropy inequality given by (5.1.8).*

Proof. Let $\varphi \in C_c^1(\Pi_T)$ and set $\varphi_j^n = \varphi(t^n, x_j)$. We multiply the discrete entropy inequality (5.3.11) by $\varphi_j^n \Delta x$, and then apply summation by parts to get

$$\Delta x \Delta t \sum_{n \ge 0} \sum_{j \in \mathbb{Z}} \left|\rho_j^{n+1} - c\right| (\varphi_j^{n+1} - \varphi_j^n)/\Delta t + \Delta x \sum_j \left|\rho_j^0 - c\right| \varphi_j^0 \tag{5.4.1}$$

$$+\Delta x\Delta t\sum_{n\geq 0}\sum_{j\in\mathbb{Z}} H^n_{j-1/2}(\varphi^n_j-\varphi^n_{j-1})/\Delta x \tag{5.4.2}$$

$$-\Delta x\Delta t\sum_{n\geq 0}\sum_{j\in\mathbb{Z}}\operatorname{sgn}(\rho^{n+1}_j-c)\left(F^n_{j+1/2}(c)-F^n_{j-1/2}(c)\right)\varphi^n_j/\Delta x\geq 0. \tag{5.4.3}$$

By Lebesgue's dominated convergence theorem, as $\Delta x\to 0$, we have

$$(5.4.1)\to\iint_{\Pi_T}|\rho-c|\varphi_t dxdt+\int_{-\infty}^{\infty}|\rho_0(x)-c|\varphi(0,x)dx.$$

As $\Delta x\to 0$, the sums in (5.4.2) converge by standard arguments, see [10], [11, Sec. 4 Proof of Theorem 1], [53], to

$$\iint_{\Pi_T}\operatorname{sgn}(\rho-c)(f(t,x,\rho)-f(t,x,c))\varphi_x\,dxdt.$$

Now let us study the sum (5.4.3) and we have

$$\begin{aligned}
(5.4.3)=&-\Delta x\Delta t\sum_{n\geq 0}\sum_{j\in\mathbb{Z}}\operatorname{sgn}(\rho^{n+1}_j-c)\left(cV^1_j+g(c)V^2_j-cV^1_{j-1}-g(c)V^2_{j-1}\right)\varphi^n_j/\Delta x\\
=&-\Delta x\Delta t\sum_{n\geq 0}\sum_{j\in\mathbb{Z}}\operatorname{sgn}(\rho^{n+1}_j-c)\left(c\frac{V^1_j-V^1_{j-1}}{\Delta x}+g(c)\frac{V^2_j-V^2_{j-1}}{\Delta x}\right)\varphi^n_j\\
=&-\Delta x\Delta t\sum_{n\geq 0}\sum_{j\in\mathbb{Z}}(\operatorname{sgn}(\rho^{n+1}_j-c)-\operatorname{sgn}(\rho^n_j-c))\left(c\frac{V^1_j-V^1_{j-1}}{\Delta x}+g(c)\frac{V^2_j-V^2_{j-1}}{\Delta x}\right)\varphi^n_j\\
&-\Delta x\Delta t\sum_{n\geq 0}\sum_{j\in\mathbb{Z}}\operatorname{sgn}(\rho^n_j-c)\left(c\frac{V^1_j-V^1_{j-1}}{\Delta x}+g(c)\frac{V^2_j-V^2_{j-1}}{\Delta x}\right)\varphi^n_j.
\end{aligned}$$

The second term in the last equality clearly converges to

$$-\int_0^T\int_{-\infty}^{-\eta}\operatorname{sgn}(\rho-c)\left(c(V_1)_x+g(c)(V_2)_x\right)\varphi)dxdt.$$

We will show now that the first term vanishes as $\Delta x\to 0$. We follow here [10, 11] and we perform a summation by parts, which gives us:

$$\begin{aligned}
&\Delta t\sum_{n\geq 0}\sum_{j\in\mathbb{Z}}\operatorname{sgn}(\rho^{n+1}_j-c)\varphi^n_j\left[c\left[\left(V^{1,n+1}_j-V^{1,n+1}_{j-1}\right)-\left(V^{1,n}_j-V^{1,n}_{j-1}\right)\right]\right.\\
&\left.+g(c)\left[\left(V^{2,n+1}_j-V^{2,n+1}_{j-1}\right)-\left(V^{2,n}_j-V^{2,n}_{j-1}\right)\right]\right]\\
&+\Delta t\Delta t\Delta x\sum_{n\geq 0}\sum_{j<0}\operatorname{sgn}(\rho^{n+1}_j-c)\\
&\qquad\times\left[c\frac{\left(V^{1,n+1}_j-V^{1,n+1}_{j-1}\right)}{\Delta x}+g(c)\frac{\left(V^{2,n+1}_j-V^{2,n+1}_{j-1}\right)}{\Delta x}\right]\frac{\left(\varphi^{n+1}_j-\varphi^n_j\right)}{\Delta t}.
\end{aligned}$$

As can be seen in (5.3.6) and (5.3.7) $V_j^{i,n+1} - V_{j-1}^{i,n+1} \leq \Delta x \omega_\eta(0)\|v\|$ holds and due to the compactness of the support function the second term vanishes as $\Delta x, \Delta t \to 0$. For the first term we first obtain that

$$\begin{aligned}
&\left(V_j^{1,n+1} - V_{j-1}^{1,n+1}\right) - \left(V_j^{1,n} - V_{j-1}^{1,n}\right) \\
&= \begin{cases}
\sum_{k=1}^{N_\eta - 1} (\gamma_{k-1} - \gamma_k)(v_1(\rho_{j+k}^{n+1} - v_1(\rho_{j+k}^n)) & \\
+ \gamma_{N_\eta - 1}(v_1(\rho_{j+N_\eta}^{n+1}) - v_1(\rho_{j+N_\eta}^n)) - \gamma_0(v_1(\rho_j^{n+1}) - v_1(\rho_j^n)), & j \leq -N_\eta - 1, \\
\sum_{k=1}^{-j-1} (\gamma_{k-1} - \gamma_k)(v_1(\rho_{j+k}^{n+1}) - v_1(\rho_{j+k}^n)) - \gamma_0(v_1(\rho_j^{n+1}) - v_1(\rho_j^n)), & -N_\eta \leq j \leq -2, \\
\gamma_0(v_1(\rho_{-1}^{n+1}) - v_1(\rho_{-1}^n)), & j = -1,
\end{cases}
\end{aligned}$$

and

$$\begin{aligned}
&\left(V_j^{2,n+1} - V_{j-1}^{2,n+1}\right) - \left(V_j^{2,n} - V_{j-1}^{2,n}\right) \\
&= \begin{cases}
0, & j \leq -N_\eta - 1, \\
\gamma_{N_\eta - 1}(v_2(\rho_{j+N_\eta}^{n+1}) - v_2(\rho_{j+N_\eta}^n)), & j = -N_\eta, \\
\sum_{k=-j}^{N_\eta - 1}(\gamma_{k-1} - \gamma_k)(v_2(\rho_{j+k}^{n+1}) - v_2(\rho_{j+k}^n)) & \\
\qquad + \gamma_{N_\eta - 1}(v_2(\rho_{j+N_\eta}^{n+1}) - v_2(\rho_{j+N_\eta}^n)), & -N_\eta + 1 \leq j \leq -1.
\end{cases}
\end{aligned}$$

Now we use the compact support of the test function. There exist $T > 0$ and $R > 0$ such that $\varphi(t,x) = 0$ for $t > T$ and $|x| > R$. Let $n_T \in \mathbb{N}$ and $j_0, j_1 \in \mathbb{Z}$ be such that $T \in]n_T \Delta t, (n_T + 1)\Delta t]$, $-R \in]x_{j_0 - \frac{1}{2}}, x_{j_0 + \frac{1}{2}}]$, $R \in]x_{j_1 - \frac{1}{2}}, x_{j_1 + \frac{1}{2}}]$. We only consider $j_0 < 0$, since otherwise the term is already 0. In addition, similar to [46, Theorem 3.3], the following estimate is derived during the proof of Lemma 19:

$$\sum_{n=0}^{N_T} \sum_j \Delta x |\rho_j^{n+1} - \rho_j^n| \leq \tilde{K},$$

By plugging in the equality obtained before, using the mean value theorem, the above mentioned estimate and $g(c) \leq c$ we obtain

$$\begin{aligned}
&\Delta t \sum_{n \geq 0} \sum_{j < 0} \operatorname{sgn}(\rho_j^{n+1} - c)\varphi_j^n \left[c \left(\left(V_j^{1,n+1} - V_{j-1}^{1,n+1}\right) - \left(V_j^{1,n} - V_{j-1}^{1,n}\right) \right) \right. \\
&\left. + g(c) \left(\left(V_j^{2,n+1} - V_{j-1}^{2,n+1}\right) - \left(V_j^{2,n} - V_{j-1}^{2,n}\right) \right) \right] \\
&\leq \frac{\Delta t}{\Delta x} \|\varphi\| \|v'\| c \left[\gamma_{N_\eta - 1} \sum_{n=0}^{N_T} \sum_{j=j_0}^{\min\{-1, j_1\}} \Delta x |\rho_{j+N_\eta}^{n+1} - \rho_{j+N_\eta}^n| + \right. \\
&\left. \sum_{k=1}^{N_\eta - 1} (\gamma_{k-1} - \gamma_k) \sum_{n=0}^{N_T} \sum_{j=j_0}^{\min\{-1, j_1\}} \Delta x |\rho_{j+k}^{n+1} - \rho_{j+k}^n| + \gamma_0 \sum_{n=0}^{N_T} \sum_{j=j_0}^{\min\{-1, j_1\}} \Delta x |\rho_j^{n+1} - \rho_j^n| \right]
\end{aligned}$$

$$\leq \Delta t \|\varphi\| \|v'\| c\tilde{K} 2\omega_\eta(0),$$

which goes to zero as $\Delta x \to 0$ (and then $\Delta t \to 0$). This concludes the proof. □

Proof of Theorem 14.
Similar to [21, Theorem 1], [46, Theorem 2.3] or [11, Theorem 1], the convergence of the approximate solutions constructed by the upwind scheme (5.3.4) to the unique weak entropy solution can be proven by applying Helly's theorem, see [44, Lemma 5.6]. Due to Lemma 17 and Lemma 19, there exists a sub-sequence of approximate solutions that converges to some $\rho \in (L^1 \cap L^\infty \cap \mathrm{BV})(\mathbb{R}^+ \times \mathbb{R}; [0, \max\{\rho^1_{\max}, \rho^2_{\max}\}])$. Lemma 21 shows that the limit function ρ is a weak entropy solution of (5.1.1)–(5.1.6) in the sense of Definition 4. Adding the uniqueness result in Theorem 15, we conclude the proof of Theorem 14. □

5.5 Numerical simulations

The aim of this section is to give some numerical examples to show our model's behaviour. To this end, we will consider Riemann initial data of the type

$$\rho_0(x) = \begin{cases} \rho_L, & \text{if } x < 0, \\ \rho_R, & \text{if } x > 0. \end{cases} \tag{5.5.1}$$

We take a spatial step size of $\Delta x = 10^{-3}$. The time step size Δt is given by the CFL condition (5.3.5).
We divide this section into three parts. In the first part we analyze how our model behaves for a fixed look ahead distance $\eta > 0$. For non-local conservation laws, it is still an open question whether the model tends to the corresponding local equation for η tending to zero (see for example [26] for a recent overview). For this reason, we will investigate the limit question as $\eta \to 0$ from the numerical point of view in Section 5.5.2. Overall, we will consider the following settings:

Test 1: $v_i(\rho) = v^i_{\max}\left(1 - \left(\frac{\rho}{\rho^i_{\max}}\right)^2\right)$ for $i \in \{1,2\}$, with $v^1_{\max} = 1,\ v^2_{\max} = 2,\ \rho^1_{\max} = \rho^2_{\max} = 1,\ \rho_L = 0.75,\ \rho_R = 0.5$;

Test 2: as in Test 1, but with $v^1_{\max} = 2,\ v^2_{\max} = 1$;

Test 3: $v_i(\rho) = v^i_{\max}\left(1 - \frac{\rho}{\rho^i_{\max}}\right)$ for $i \in \{1,2\}$, with $v^1_{\max} = 2,\ v^2_{\max} = 1,\ \rho^1_{\max} = 0.5,\ \rho^2_{\max} = 1,\ \rho_L = 0.25,\ \rho_R = 0.5$;

Test 4: v_i as in Test 3, but with $v^1_{\max} = 1,\ v^2_{\max} = 2,\ \rho^1_{\max} = 1,\ \rho^2_{\max} = 0.5,\ \rho_L = 0.5,\ \rho_R = 0.25$.

The first two settings are used to show that the obtained solutions are reasonable also for non-linear velocity functions, while the last two settings turn out to be interesting in Section 5.5.2. For all the tests, the kernel function is given by $\omega_\eta(x) = 2(\eta - x)/\eta^2$ and the final simulation time is $T = 1$.
Finally, in Section 5.5.3, we will show that our model can be easily extended to more than two stretches and therefore to a sequence of 1-to-1 junctions to simulate traffic.

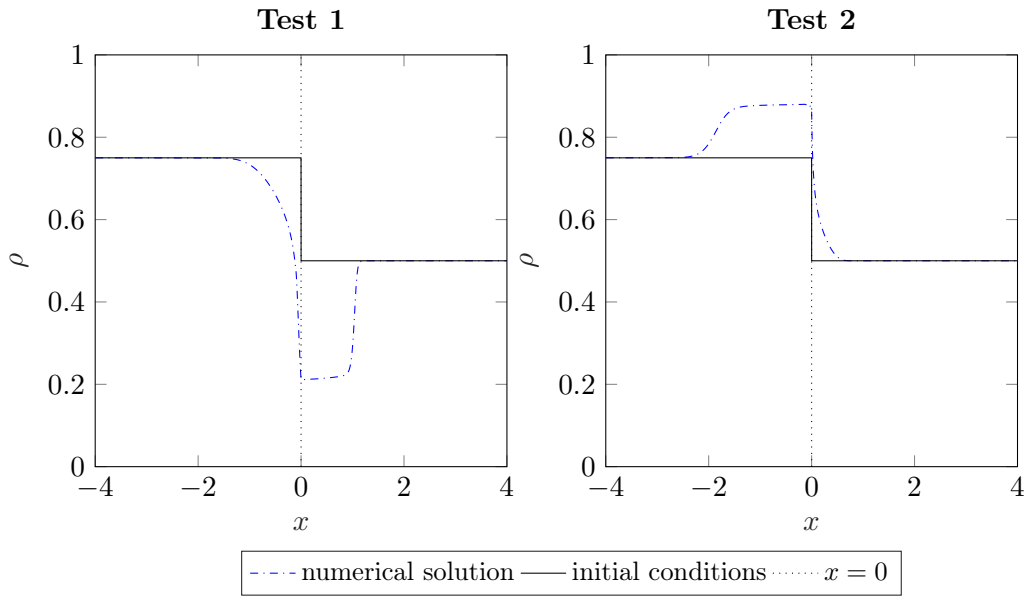

Figure 5.2: Numerical solutions at $T = 1$ corresponding to Test 1 (left) and Test 2 (right).

5.5.1 Fixed look-ahead distance

We set the look-ahead distance $\eta = 0.1$. Let us consider the first test. Here we start with a congested situation on the first road segment. In addition, the maximum velocity on the first road is lower than the one on the second road segment. Therefore, the traffic jam resolves over time as can be seen in Figure 5.2, left. In contrast to Test 1, Test 2 presents the opposite situation: the velocity on the first road segment is now higher than the second one. Hence, the traffic jam can not resolve and we get a backward traveling increase of the density (see Figure 5.2, right).

In the last two settings we can see that the presence of the look ahead distance results in a smoothing of the density close to the end of the first and the beginning of the second road segment, see Figure 5.3.

5.5.2 Look-ahead distance tending to zero

As mentioned above, the behaviour of solutions for η tending to zero is of special interest for non-local conservation laws. Concerning non-local LWR traffic flow models as in [21, 46], or model (5.1.1) with $v_1 \equiv v_2$, so far the convergence to the classical LWR traffic flow model [65, 67] can only be proven for monotone initial data (see [26, 56]), since the solution is monotonicity preserving and therefore has a strict maximum principle and a bounded total variation, uniformly in η. Unfortunately, similar results do not hold for model (5.1.1) with $v_1 \neq v_2$, since the model is, in general, not monotonicity preserving even for constant initial data. Therefore, we just investigate the limit numerically.

The local (discontinuous) conservation law corresponding to model (5.1.1) is given by:

$$\rho_t + f(x,\rho)_x = 0, \quad \text{with } f(x,\rho) := H(-x)\rho v_1(\rho) + H(x)\rho v_2(\rho), \tag{5.5.2}$$

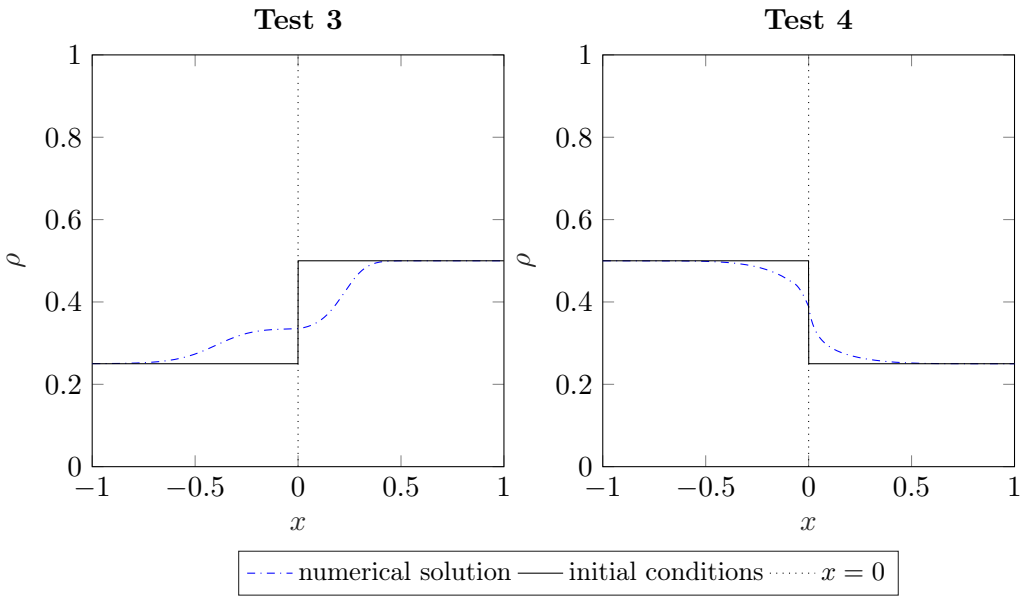

Figure 5.3: Numerical solutions at $T = 1$ for the Test 3 (left) and Test 4 (right).

where $H(x)$ is the Heaviside function. As pointed out in [1, 18], (5.5.2) admits many L^1 contraction semigroups, one for each so-called (A, B)-*connection*. The two most common connections are the one corresponding to the supply-demand approach [61], and the vanishing viscosity solution (see [54, Definition 3.1]), which is a weak solution satisfying, besides the Kruzkov entropy inequalities for $x < 0$ and $x > 0$, the Γ-condition of [42, 43], see also [54, Definition 3.1] and [6].
For instance, the vanishing viscosity solution can be obtained by a Godunov scheme considering a grid where $x = 0$ is a cell midpoint, see [54]. In the following, we will consider $\eta \in \{50\Delta x, 10\Delta x, 2\Delta x\}$ and compare it to the solution of (5.5.2)–(5.5.1), which will be computed by the Godunov scheme as presented in [54], since we are interested in the vanishing viscosity solution. Note that, due to the different grids, we do not compute L^1-errors between the different solutions. We will now investigate the previous four test cases. In the first two settings, as $\eta \to 0$ the solution of (5.1.1) with initial conditions (5.5.1) is very similar to the vanishing viscosity solution of the corresponding local problem, see Figure 5.4. We also remark that, in the parameters settings Test 1 and Test 2, the solution obtained by the supply-demand approach is equal to the vanishing viscosity solution.

Let us now consider Tests 3 and 4. The initial datum in both of them is exactly the density corresponding to the maximum fluxes attainable on each road segment. Therefore, the solution of the supply and demand approach is given by a stationary discontinuity coinciding with the initial datum. As can be seen in Figure 5.5, in both tests the limit of model (5.1.1) behaves as the vanishing viscosity solution. In Test 4, the numerical results also coincide with supply-demand solution. The most interesting case is Test 3. For these parameters, the vanishing viscosity solution differs from the supply-demand solution and, as can be seen in Figure 5.5 (left picture) the solution of the model (5.1.1) seems to converge to the vanishing viscosity

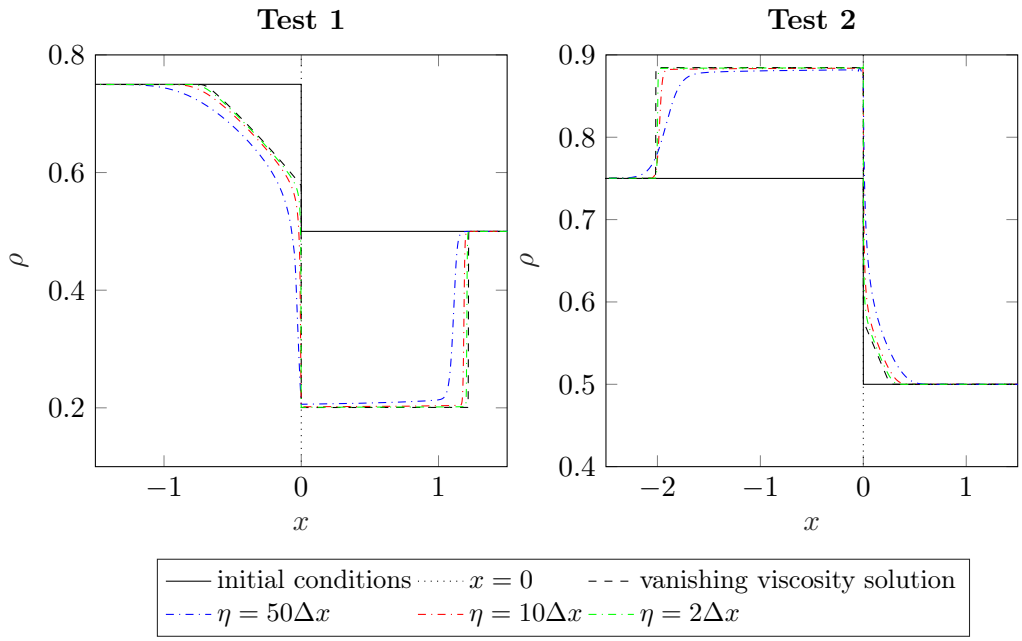

Figure 5.4: Numerical solutions at $T = 1$ corresponding to Test 1 (left) and Test 2 (right) and different values of η.

solution for η tending to zero.

5.5.3 Linear network scenario

Finally, we show that the model can be extended to more than two stretches of a road. We consider the case of road works on a highway, modeled by the segment $[0, L]$, with $L = 2$, where the road capacity and the maximal speed are smaller. Therefore, we have three different road segments, $]-\infty, 0[$, $[0, L[$ and $[L, \infty[$, and we consider the linear velocity function as in Test 3, with $v^1_{\max} = v^3_{\max} = \rho^1_{\max} = \rho^3_{\max} = 1$ before and after the road works, and $v^2_{\max} = 0.5$ and $\rho^2_{\max} = 0.8$ for $x \in [0, L]$. We start with a higher density on the segment with the road works, i.e.

$$\rho_0(x) = \begin{cases} 0.4, & \text{if } x < 0, \\ 0.5, & \text{if } 0 < x < L, \\ 0.4, & \text{if } L < x \end{cases} \tag{5.5.3}$$

As in Section 5.5.1, the look ahead distance is $\eta = 0.1$, and as in Section 5.5.2 we also present the vanishing viscosity solution obtained by the Godunov scheme of [54] to get an impression of the corresponding local problem. As can be seen in Figure 5.6, the presence of the road works results in a traffic jam upstream and a decrease of the density downstream. As noticed in Section 5.5.2, the numerical solution of the non-local problem tends for small η towards the vanishing viscosity solution.

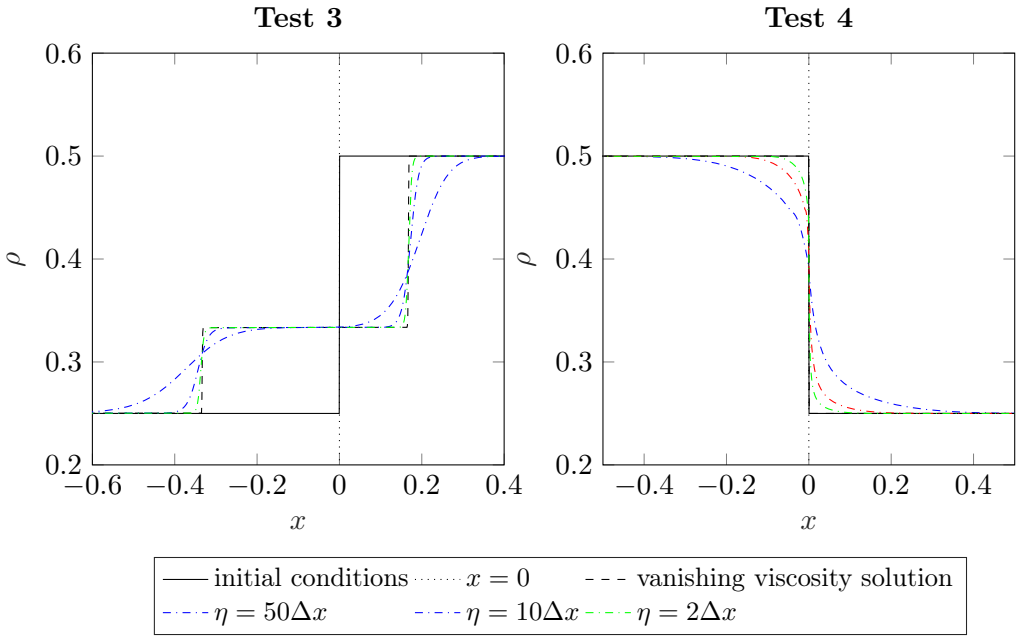

Figure 5.5: Numerical solutions at $T = 1$ corresponding to Test 3 (left) and Test 4 (right) and different values of η

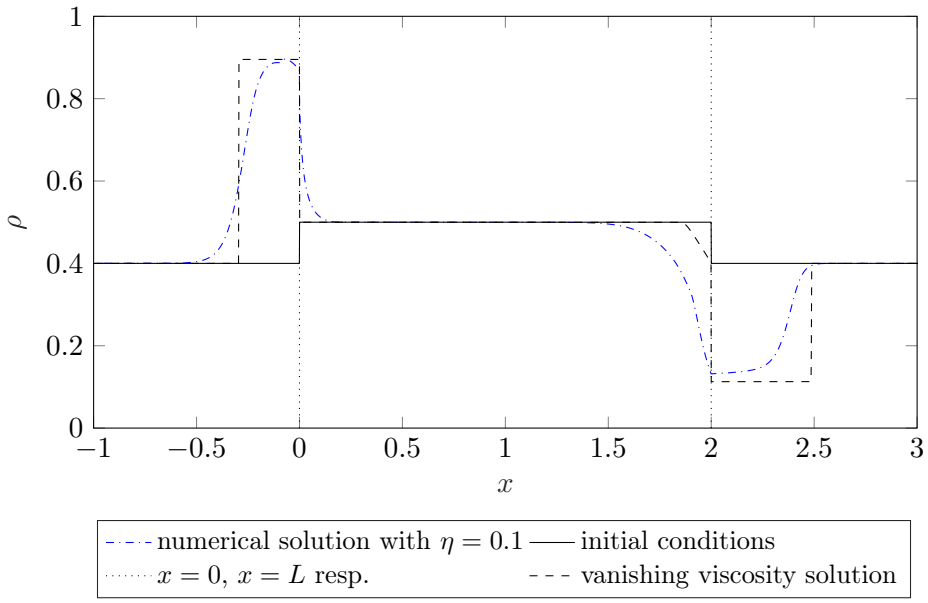

Figure 5.6: Numerical solution for three road segments at $T = 1$

Conclusions and perspectives

In this work, we introduced and studied non-local traffic flow models and different schemes to numerically approximate their solutions. In particular, we presented a scalar non-local traffic flow model, proving its well-posedness through a Lax-Friedrichs type numerical scheme and analyzing the limit model as the support of the kernel function tends to infinity. Moreover, under higher regularity assumptions, we showed the stability with respect to the kernel function, the velocity and the initial datum. Then, we presented a non-local multi-class traffic flow model taking into account the behaviour of different classes of vehicles or drivers. We extended the L-AR schemes proposed in [15, 16] to compute approximate solutions of this multi-class system. The proposed numerical tests indicate that these schemes are competitive with the first and second-order schemes proposed in the literature, in particular when more than one class are involved. If the initial datum has jump discontinuities, the performance of L-AR schemes are comparable with those of the second-order Godunov scheme. We also applied high-order finite volume WENO schemes to the non-local multi-class traffic flow model proposed in [22]. Finally, we presented a non-local flux model, which can handle changes of velocities and maximum capacities on the road and therefore can model a 1-to-1 junction. Numerical examples suggest that the solution tends to the vanishing viscosity solution of the corresponding local conservation law as the look-ahead distance goes to 0. The above mentioned results open several perspectives for future research. We intend to further investigate the analytical limit model question in future work for all the non-local models presented in this thesis. In addition, the model based on the mean downstream velocity may be extended to more general junctions to model traffic flow on networks. Hence, in the future, we aim to extend this model from the current simple network structure to a more general network formulation. Another perspective is the study of other high-order numerical schemes for these non-local equations. It could be interesting to also analyze the validation and calibration of all these non-local models, if appropriate data will be available. Optimal control of traffic flow is a powerful subject and we could also work in this setting to improve performances. Other open problems are the analysis of non-local space-discontinuous models, the description of other non-local models for pedestrian traffic, a second-order non-local traffic flow model, micro-macro limits and other studies of the initial boundary value problem for non-local conservation laws.

Bibliography

[1] Adimurthi, S. Mishra, and G. V. Gowda. Optimal entropy solutions for conservation laws with discontinuous flux-functions. *J. Hyperbolic Differ. Equ.*, 2(04):783–837, 2005. (Cited on page 118.)

[2] A. Aggarwal, R. M. Colombo, and P. Goatin. Nonlocal systems of conservation laws in several space dimensions. *SIAM J. Numer. Anal.*, 53(2):963–983, 2015. (Cited on pages 2, 6, 7, 46 and 54.)

[3] D. Amadori and W. Shen. An integro-differential conservation law arising in a model of granular flow. *J. Hyperbolic Differ. Equ.*, 9(1):105–131, 2012. (Cited on page 1.)

[4] P. Amorim. On a nonlocal hyperbolic conservation law arising from a gradient constraint problem. *Bull. Braz. Math. Soc. (N.S.)*, 43(4):599–614, 2012. (Cited on page 1.)

[5] P. Amorim, R. Colombo, and A. Teixeira. On the numerical integration of scalar nonlocal conservation laws. *ESAIM M2AN*, 49(1):19–37, 2015. (Cited on pages 2, 3, 4, 6, 13, 14, 24, 25, 31, 32, 46, 54 and 112.)

[6] B. Andreianov, K. H. Karlsen, and N. H. Risebro. A theory of L^1-dissipative solvers for scalar conservation laws with discontinuous flux. *Arch. Ration. Mech. Anal.*, 201(1):27–86, 2011. (Cited on page 118.)

[7] A. Aw and M. Rascle. Resurrection of "second order" models of traffic flow. *SIAM J. Appl. Math.*, 60(3):916–938 (electronic), 2000. (Cited on page 1.)

[8] S. Benzoni-Gavage and R. M. Colombo. An n-populations model for traffic flow. *European J. Appl. Math.*, 14(5):587–612, 2003. (Cited on pages 7, 53, 57 and 65.)

[9] F. Berthelin and P. Goatin. Regularity results for the solutions of a non-local model of traffic flow. *Discrete and Continuous Dynamical Systems A*, 39(1078-0947 2019 6 3197):3197, 2019. (Cited on page 5.)

[10] F. Betancourt, R. Bürger, K. H. Karlsen, and E. M. Tory. On nonlocal conservation laws modelling sedimentation. *Nonlinearity*, 24(3):855–885, 2011. (Cited on pages 1, 2, 6, 13, 15, 31, 44 and 114.)

[11] S. Blandin and P. Goatin. Well-posedness of a conservation law with non-local flux arising in traffic flow modeling. *Numer. Math.*, 132(2):217–241, 2016. (Cited on pages 1, 2, 3, 5, 6, 7, 13, 14, 15, 17, 24, 25, 26, 27, 46, 53, 54, 63, 88, 105, 114 and 116.)

[12] O. Bokanowski and H. Zidani. Anti-dissipative schemes for advection and application to Hamilton–Jacobi–Bellmann equations. *J. Sci. Comput.*, 30(1):1–33, 2007. (Cited on pages 80, 82, 83, 87 and 90.)

[13] F. Bouchut and B. Perthame. Kružkov's estimates for scalar conservation laws revisited. *Trans. Amer. Math. Soc.*, 350(7):2847–2870, 1998. (Cited on page 37.)

[14] P. Buchmüller and C. Helzel. Improved accuracy of high-order weno finite volume methods on cartesian grids. *J. Sci. Comput.*, 61(2):343–368, 2014. (Cited on page 99.)

[15] R. Bürger, C. Chalons, and L. M. Villada. Antidiffusive and random-sampling lagrangian-remap schemes for the multiclass Lighthill-Whitham-Richards traffic model. *SIAM J. Sci. Comput.*, 35(6):B1341–B1368, 2013. (Cited on pages 7, 79, 83, 87, 90 and 121.)

[16] R. Bürger, C. Chalons, and L. M. Villada. Antidiffusive Lagrangian-remap schemes for models of polydisperse sedimentation. *Numer. Methods Partial Differential Equations*, 32(4):1109–1136, 2016. (Cited on pages 7, 79 and 121.)

[17] R. Bürger, A. García, K. Karlsen, and J. Towers. A family of numerical schemes for kinematic flows with discontinuous flux. *J. Engrg. Math.*, 60(3-4):387–425, 2008. (Cited on page 7.)

[18] R. Bürger, K. H. Karlsen, and J. D. Towers. An Engquist-Osher-type scheme for conservation laws with discontinuous flux adapted to flux connections. *SIAM J. Numer. Anal.*, 47(3):1684–1712, 2009. (Cited on page 118.)

[19] C. Chalons, P. Goatin, and L. M. Villada. High-order numerical schemes for one-dimensional nonlocal conservation laws. *SIAM J. Sci. Comput.*, 40(1):A288–A305, 2018. (Cited on pages 2, 7 and 97.)

[20] F. A. Chiarello, J. Friedrich, P. Goatin, S. Göttlich, and O. Kolb. A non-local traffic flow model for 1-to-1 junctions. *European J. Appl. Math.*, pages 1–21, 2019. (Cited on page 103.)

[21] F. A. Chiarello and P. Goatin. Global entropy weak solutions for general non-local traffic flow models with anisotropic kernel. *ESAIM: M2AN*, 52(1):163–180, 2018. (Cited on pages 6, 7, 13, 53, 88, 93, 104, 105, 112, 116 and 117.)

[22] F. A. Chiarello and P. Goatin. Non-local multi-class traffic flow models. *Netw. Heterog. Media*, 14(2):371 – 387, 2019. (Cited on pages 7, 53, 79, 82, 88, 91, 97, 99, 100 and 121.)

[23] F. A. Chiarello, P. Goatin, and E. Rossi. Stability estimates for non-local scalar conservation laws. *Nonlinear Anal. Real World Appl.*, 45:668–687, 2019. (Cited on pages 31 and 107.)

[24] F. A. Chiarello, P. Goatin, and L. M. Villada. High-order Finite Volume WENO schemes for non-local multi-class traffic flow models. *Proc. XVII International Conference on Hyperbolic Problems Theory, Numerics, Applications*, 2019. (Cited on page 79.)

[25] F. A. Chiarello, P. Goatin, and L. M. Villada. Lagrangian-antidiffusive remap schemes for non-local multi-class traffic flow models. *Comput. Appl. Math.*, 2020. (Cited on page 79.)

[26] M. Colombo, G. Crippa, M. Graffe, and L. V. Spinolo. Recent results on the singular local limit for nonlocal conservation laws. *arXiv:1902.06970*, 2019. (Cited on pages 3, 116 and 117.)

[27] M. Colombo, G. Crippa, and L. V. Spinolo. On the singular local limit for conservation laws with nonlocal fluxes. *arXiv e-prints*, page arXiv:1710.04547, Oct 2017. (Cited on page 3.)

[28] R. M. Colombo, M. Garavello, and M. Lécureux-Mercier. A class of nonlocal models for pedestrian traffic. *Math. Models Methods Appl. Sci.*, 22(04):1150023, 2012. (Cited on pages 4 and 6.)

[29] R. M. Colombo, P. Goatin, and M. D. Rosini. On the modelling and management of traffic. *ESAIM Math. Model. Numer. Anal.*, 45(5):853–872, 2011. (Cited on page 48.)

[30] R. M. Colombo and A. Groli. Minimising stop and go waves to optimise traffic flow. *Appl. Math. Lett.*, 17(6):697–701, 2004. (Cited on pages 48, 49 and 67.)

[31] R. M. Colombo, M. Herty, and M. Mercier. Control of the continuity equation with a non local flow. *ESAIM Control Optim. Calc. Var.*, 17(2):353–379, 2011. (Cited on pages 1, 2 and 4.)

[32] R. M. Colombo and M. Lécureux-Mercier. Nonlocal crowd dynamics models for several populations. *Acta Math. Sci. Ser. B Engl. Ed.*, 32(1):177–196, 2012. (Cited on pages 1 and 4.)

[33] R. M. Colombo and F. Marcellini. Nonlocal systems of balance laws in several space dimensions with applications to laser technology. *J. Differential Equations*, 259(11):6749–6773, 2015. (Cited on page 6.)

[34] R. M. Colombo, M. Mercier, and M. D. Rosini. Stability and total variation estimates on general scalar balance laws. *Commun. Math. Sci.*, 7(1):37–65, 2009. (Cited on pages 6 and 107.)

[35] R. M. Colombo and E. Rossi. Hyperbolic predators vs. parabolic prey. *Commun. Math. Sci.*, 13(2):369–400, 2015. (Cited on page 6.)

[36] R. M. Colombo and E. Rossi. Rigorous estimates on balance laws in bounded domains. *Acta Math. Sci. Ser. B Engl. Ed.*, 35(4):906–944, 2015. (Cited on pages 37, 38, 39 and 40.)

[37] R. M. Colombo and E. Rossi. IBVPs for scalar conservation laws with time discontinuous fluxes. *Math. Methods Appl. Sci.*, 41(4):1463–1479, 2018. (Cited on pages 48 and 49.)

[38] R. M. Colombo and E. Rossi. Nonlocal conservation laws in bounded domains. *SIAM J. Math. Anal.*, 50(4):4041–4065, 2018. (Cited on page 2.)

[39] G. Crippa and M. Lécureux-Mercier. Existence and uniqueness of measure solutions for a system of continuity equations with non-local flow. *NoDEA Nonlinear Differential Equations Appl.*, pages 1–15, 2012. (Cited on page 4.)

[40] C. DeFilippis and P. Goatin. The initial boundary value problem for general non-local scalar conservation laws in one space dimension. *Nonlinear Analysis*, 161:131 – 156, 2017. (Cited on page 2.)

[41] B. Després and F. Lagoutière. Contact discontinuity capturing schemes for linear advection and compressible gas dynamics. *J. Sci. Comput.*, 16(4):479–524, 2001. (Cited on pages 82 and 83.)

[42] S. Diehl. On scalar conservation laws with point source and discontinuous flux function. *SIAM J. Math. Anal.*, 26(6):1425–1451, 1995. (Cited on page 118.)

[43] S. Diehl. A uniqueness condition for nonlinear convection-diffusion equations with discontinuous coefficients. *J. Hyperbolic Differ. Equ.*, 6(01):127–159, 2009. (Cited on page 118.)

[44] R. Eymard, T. Gallouët, and R. Herbin. Finite volume methods. In *Handbook of numerical analysis, Vol. VII*, Handb. Numer. Anal., VII, pages 713–1020. North-Holland, Amsterdam, 2000. (Cited on pages 2, 22 and 116.)

[45] J. Friedrich and O. Kolb. Maximum principle satisfying CWENO schemes for nonlocal conservation laws. *SIAM J. Sci. Comput.*, 41(2):A973–A988, 2019. (Cited on page 2.)

[46] J. Friedrich, O. Kolb, and S. Göttlich. A Godunov type scheme for a class of LWR traffic flow models with non-local flux. *Netw. Heterog. Media*, 13(4):531 – 547, 2018. (Cited on pages 2, 6, 7, 8, 54, 55, 88, 103, 104, 105, 107, 108, 112, 115, 116 and 117.)

[47] P. Goatin and E. Rossi. Well-posedness of IBVP for 1D scalar non-local conservation laws. *ZAMM Z. Angew. Math. Mech.*, 0(0):e201800318, 2019. (Cited on pages 2 and 3.)

[48] P. Goatin and S. Scialanga. The Lighthill-Whitham-Richards traffic flow model with non-local velocity: analytical study and numerical results. Research Report RR-8685, Inria Sophia Antipolis ; INRIA, Feb. 2015. (Cited on pages 21 and 26.)

[49] P. Goatin and S. Scialanga. Well-posedness and finite volume approximations of the LWR traffic flow model with non-local velocity. *Netw. Heterog. Media*, 11(1):107–121, 2016. (Cited on pages 2, 5, 6, 13, 15, 24 and 53.)

[50] E. Godlewski and P. Raviart. Numerical approximation of hyperbolic systems of conservation laws, apl. *Math. Sci*, 118, 1996. (Cited on page 80.)

[51] S. Göttlich, S. Hoher, P. Schindler, V. Schleper, and A. Verl. Modeling, simulation and validation of material flow on conveyor belts. *Appl. Math. Model.*, 38(13):3295 – 3313, 2014. (Cited on pages 1, 4 and 6.)

[52] K. H. Karlsen and N. H. Risebro. On the uniqueness and stability of entropy solutions of nonlinear degenerate parabolic equations with rough coefficients. *Discrete Contin. Dyn. Syst.*, 9(5):1081–1104, 2003. (Cited on pages 6, 31, 34, 37, 105 and 107.)

[53] K. H. Karlsen, N. H. Risebro, and J. D. Towers. L^1 stability for entropy solutions of nonlinear degenerate parabolic convection-diffusion equations with discontinuous coefficients. *Skr. K. Nor. Vidensk. Selsk.*, (3):1–49, 2003. (Cited on page 114.)

[54] K. H. Karlsen and J. D. Towers. Convergence of a Godunov scheme for conservation laws with a discontinuous flux lacking the crossing condition. *J. Hyperbolic Differ. Equ.*, 14(04):671–701, 2017. (Cited on pages 118 and 119.)

[55] A. Keimer and L. Pflug. Existence, uniqueness and regularity results on nonlocal balance laws. *J. Differential Equations*, 263(7):4023–4069, 2017. (Cited on pages 2, 5 and 104.)

[56] A. Keimer and L. Pflug. On approximation of local conservation laws by nonlocal conservation laws. *J. Appl. Math. Anal. Appl.*, 475(2):1927 – 1955, 2019. (Cited on pages 3 and 117.)

[57] A. Keimer, L. Pflug, and M. Spinola. Existence, uniqueness and regularity of multidimensional nonlocal balance laws with damping. *J. Math. Anal. Appl.*, 466(1):18 – 55, 2018. (Cited on page 2.)

[58] A. Keimer, L. Pflug, and M. Spinola. Nonlocal scalar conservation laws on bounded domains and applications in traffic flow. *SIAM J. Math. Anal.*, 50(6):6271–6306, 2018. (Cited on page 2.)

[59] S. N. Kružkov. First order quasilinear equations with several independent variables. *Mat. Sb. (N.S.)*, 81 (123):228–255, 1970. (Cited on pages 6, 13, 14, 15, 34, 36, 37, 104 and 105.)

[60] A. Kurganov and A. Polizzi. Non-oscillatory central schemes for a traffic flow model with arrehenius look-ahead dynamics. *Netw. Heterog. Media*, 4(3):431–451, 2009. (Cited on page 27.)

[61] J. P. Lebacque. The Godunov scheme and what it means for first order traffic flow models. *Proc. 13th Intrn. Symp. Transportation and Traffic Theory*, 1996. (Cited on page 118.)

[62] M. Lécureux-Mercier. Improved stability estimates for general scalar conservation laws. *J. Hyperbolic Differ. Equ.*, 08(04):727–757, 2011. (Cited on pages 6 and 44.)

[63] R. J. LeVeque. Finite volume methods for hyperbolic problems. *Cambridge Texts in Applied Mathematics*, pages xx+558, 2002. (Cited on pages 7, 54 and 63.)

[64] D. Li and T. Li. Shock formation in a traffic flow model with Arrhenius look-ahead dynamics. *Netw. Heterog. Media*, 6(4):681–694, 2011. (Cited on pages 5, 6, 13 and 26.)

[65] M. J. Lighthill and G. B. Whitham. On kinematic waves. II. A theory of traffic flow on long crowded roads. *Proc. Roy. Soc. London. Ser. A.*, 229:317–345, 1955. (Cited on pages 1, 27 and 117.)

[66] H. Payne. *Models of Freeway Traffic and Control*. Simulation Councils, Incorporated, 1971. (Cited on page 1.)

[67] P. I. Richards. Shock waves on the highway. *Oper. Res.*, 4:42–51, 1956. (Cited on pages 1, 27 and 117.)

[68] J. Ridder and W. Shen. Traveling waves for nonlocal models of traffic flow. *Discrete Contin. Dyn. Syst.*, 39(1078-0947 2019 7 4001):4001, 2019. (Cited on page 3.)

[69] W. Shen. Traveling Waves for Conservation Laws with Nonlocal Flux for Traffic Flow on Rough Roads. *arXiv e-prints*, page arXiv:1809.02998, Sep 2018. (Cited on page 3.)

[70] C.-W. Shu. Essentially non-oscillatory and weighted essentially non-oscillatory schemes for hyperbolic conservation laws. In *Advanced numerical approximation of nonlinear hyperbolic equations*, pages 325–432. Springer, 1998. (Cited on pages 96, 97 and 99.)

[71] C.-W. Shu and S. Osher. Efficient implementation of essentially non-oscillatory shock-capturing schemes. *J. Comput. Phys.*, 77(2):439–471, 1988. (Cited on pages 96, 97 and 99.)

[72] A. Sopasakis and M. A. Katsoulakis. Stochastic modeling and simulation of traffic flow: asymmetric single exclusion process with Arrhenius look-ahead dynamics. *SIAM J. Appl. Math.*, 66(3):921–944 (electronic), 2006. (Cited on pages 1, 4, 5, 6, 13 and 26.)

[73] P. K. Sweby. High resolution schemes using flux limiters for hyperbolic conservation laws. *SIAM J. Numer. Anal.*, 21(5):995–1011, 1984. (Cited on page 89.)

[74] B. Van Leer. Towards the ultimate conservative difference scheme. v. a second-order sequel to Godunov's method. *J. Comput. Phys.*, 32(1):101–136, 1979. (Cited on page 89.)

[75] G. Whitham. *Linear and nonlinear waves*. Pure and applied mathematics. Wiley, 1974. (Cited on page 1.)

[76] H. Zhang. A non-equilibrium traffic model devoid of gas-like behavior. *Transportation Research Part B: Methodological*, 36(3):275 – 290, 2002. (Cited on page 1.)

[77] K. Zumbrun. On a nonlocal dispersive equation modeling particle suspensions. *Quart. Appl. Math.*, 57(3):573–600, 1999. (Cited on pages 3 and 6.)